A FRAMEWORK FOR OPTIMIZING PUBLIC TRANSIT BUS FLEET CONVERSION TO ALTERNATIVE FUELS

A Dissertation
Presented to
The Academic Faculty

by

Hanyan Li

In Partial Fulfillment
of the Requirements for the Degree
Doctor of Philosophy in the
School of Civil and Environmental Engineering

Georgia Institute of Technology
December, 2019

A FRAMEWORK FOR OPTIMIZING PUBLIC TRANSIT BUS FLEET CONVERSION TO ALTERNATIVE FUELS

Approved by:

Dr. Randall Guensler, Advisor
School of Civil and Environmental Engineering
Georgia Institute of Technology

Dr. Haobing Liu
School of Civil and Environmental Engineering
Georgia Institute of Technology

Dr. Michael O. Rodgers
School of Civil and Environmental Engineering
Georgia Institute of Technology

Dr. Enlu Zhou
H. Milton School of Industrial and Systems Engineering
Georgia Institute of Technology

Dr. Kari Watkins
School of Civil and Environmental Engineering
Georgia Institute of Technology

Dr. Oscar Delgado
International Council on Clean Transportation

Date Approved: [August 7, 2019]

Dedicated to my beloved

parents (Ge Zhang and Qing Li)

and husband (Cody Wang).

ACKNOWLEDGEMENTS

I would like to express my deepest appreciation to my advisor, Dr. Randall Guensler, who has always been supportive, encouraging, and considerate, and has given me the freedom to pursue various projects. I would also like to extend my deepest gratitude to Dr. Haobing Liu, who has enlightened me not only from his knowledge but also from his continuous passions and motivation with research.

I would like to extend my sincere thanks to the rest of my thesis committee members, Dr. Michael O. Rodgers, Dr. Kari Watkins, Dr. Enlu Zhou, and Dr. Oscar Delgado, for the invaluable guidance through this process. I would also like to thank Dr. Hangbin Wu and Dr. Yi-Chang James Tsai for initiating my research journey, Dr. Yanzhi Ann Xu for her research guidance, and Majorie Jorgenson for her timely help.

I would like to express my thanks to my lab mates: Dr. Alper Akanser, Dr. Alice Grossman, Dr. Cody Wang, Xiaodan Xu, Yingping Zhao, Daejin Kim, Hongyu Lu, Diyi Liu, Daniel Walls, Deep Patel, and Chris Chang. My gratitude also goes to the friends I made at Georgia Tech: Dr. Tianlong Xu, Atiyya Shaw, Xi Liu, Judy Cruz, Jonathan and Katelyn DiGioia, Dr. Chengbo Ai, Dr. Ross Wang, Dr. Fangru Wang, Li Yi, Dr. Dan Sun, Glenn and Mary Rowan, Dr. Erin Garcia, Dr. Amy Musselman, Dr. Amy Moore, to name a few.

Last but not least, I am profoundly thankful to my parents and my husband for their unconditional love and support. Thank you for making me feel great every single day.

I have been dreaming of writing this page for years, and finally my dream has just come true. So many thanks to the people who have trusted in me and helped me walk this unforgettable journey.

TABLE OF CONTENTS

LIST OF TABLES

LIST OF FIGURES

LIST OF SYMBOLS AND ABBREVIATIONS

BEV	Battery-electric vehicle
CNG	Compressed natural gas
DEM	Digital elevation model
DGE	Diesel gallon equivalent
GHG	Greenhouse gas
GPS	Global positioning system
GREET	Greenhouse gases, Regulated Emissions, and Energy use in Transportation
GTFS	General Transit Feed Specification
HEV	Hybrid-electric vehicle
KNN	K-nearest neighbor
LNG	Liquefied natural gas
MAPE	Mean absolute percentage error
MARTA	Metropolitan Atlanta Rapid Transit Authority
MILP	Mixed integer linear programming
MOVES	Motor Vehicle Emission Simulation
MPDGE	Miles per diesel gallon equivalent
NASEM	National Academies of Sciences, Engineering, and Medicine
NTD	National Transit Database
SOC	State of charge
STP	Scaled Tractive Power in MOVES
VSP	Vehicle-Specific Power in MOVES
XGBoost	Extreme gradient boosting

SUMMARY

Public transit service using alternative fuel buses has a great potential to reduce lifecycle energy use and criteria pollutant emissions. However, a number of barriers and concerns discourage switching from traditional diesel buses to alternative fuels. The goal of this study is to develop an analytical framework for optimizing public transit bus fleet conversion to alternative fuels, which will help achieve sustainable transportation. The alternative fuel options included in this model are compressed natural gas (CNG), hybrid-electric, and battery-electric vehicles. The modeling framework will help transit agencies obtain reasonable estimates of reductions in fuel use, operating cost, and lifecycle CO_2 emissions based on fleet-specific features, route characteristics, vehicle constraints, and on-road operating conditions. Then the most economically-efficient and energy-efficient plan will be identified in terms of fleet turnover, vehicle-route assignment, vehicle-depot assignment, charging scheduling, and charging station/depot location selection.

In the framework, four sets of models are proposed, including one set of machine learning models for predicting energy use and three sets of mixed integer programming models for optimizing on-road fleet operations and fleet turnover. The equations formulated for each model and then applied to the local transit network in Atlanta, Georgia, to demonstrate the model capabilities. Results are compared with the baseline scenarios to showcase the potential energy and emissions benefits associated with changes in fleet operations and fleet conversion to alternative fuels.

The first set of models consists of energy use prediction models that predict energy use at the micro-trip level. Eight models are trained and then applied to predict energy use

for four vehicle types (i.e. conventional diesel, CNG, hybrid-electric, and battery-electric) and two facility types (i.e. highways and local roads). Energy use is simulated using advanced modeling tools based on real-world second-by-second on-road operating conditions. Machine learning models, applying five algorithms, are developed from vehicle-specific and operation-related features. The model with the best performance is selected and used assess the fleet-wide energy use of different fuel technologies.

The second set of models optimizes the on-road operations of existing mixed fuel fleets to minimize fleet-wide operating costs through optimized depot, trip, and route assignment. The four models include: 1) a deadheading minimization model, 2) a bus-to-tour assignment model, 3) a tour design model, and 4) a combined model. Operating cost metrics are formulated for CO_2 emissions, operating monetary cost, and on-road energy use.

The third set of models optimizes overall fleet operations as newly-procured electrified sub-fleets are added to the existing fleet. This model set optimizes decisions about vehicle-to-tour assignment, charging facility placement for the new buses, and charging schedules for the new sub-fleets. Three models include: 1) an electrification cost model, which aims to minimize the total cost (vehicle capital, charging facility, utility, and operator) when electrifying a set of tours; 2) an operation optimization model for depot-charged electric vehicle sub-fleets, which aims to minimize the operating cost in a mixed fleet with both electrified and non-electrified vehicles; and 3) a budget-constrained sub-fleet electrification optimization model, which aims to maximize the benefits of reducing lifecycle CO_2 emissions when new electrified sub-fleets are procured (while simultaneously satisfying user-prescribed budget constraints).

The fourth set of models is designed to optimize the conversion of large fleets to alternative fuel over time, given capital purchase budget constraints. The goal is to minimize the fleet-wide lifecycle CO_2 emissions, or maximize the benefits of reducing lifecycle CO_2 emissions, compared to the baseline fleet. Within the planning horizon, models generate annual vehicle procurement decisions, vehicle-to-tour assignment, charging facility placement, and charging schedules. The two models include: 1) fleet conversion without salvage, which focuses on the additional monetary costs and reductions in lifecycle CO_2 emissions from adopting new fleets with alternative fuels, compared to the baseline fleet; and 2) fleet conversion with salvage, which aims to minimize the fleet-wide life-cycle CO_2 emissions by explicitly determining fleet composition and operations of both new and existing fleets.

The models developed for this dissertation work are open source, available for local transit agency use, and readily customized for each agency's fleet and operations. These modeling tools reduce the technological uncertainty associated with the assessment of alternative fuel vehicle energy and emissions impacts and are deigned to assist policy-makers in making rational fleet management and fleet procurement decisions.

CHAPTER 1. INTRODUCTION

To reduce greenhouse gas emissions, four major areas are commonly considered: activities, mode share, fuel intensity, and fuel type (*Li, et al., 2018b; Xu et al., 2017; Xu, et al., 2015; Zegras, 2007*). In metropolitan areas, public transit service using alternative fuel buses (hybrid-electric, battery-electric, compressed natural gas, etc.) have great potentials to reduce life-cycle energy use and criteria pollutant emissions. This is because of the lower greenhouse gas emissions per passenger (*Eudy, et al., 2014; Mahmoud, et al., 2016*) and better fuel efficiency as compared with traditional diesel buses. The Greenhouse Gas and Energy Reduction Program, which provides funds to transit agencies to reduce energy use and/or greenhouse gas (GHG) emissions reports that emissions can be reduced by up to 70% (*Eudy, et al., 2014*).

1.1 Transit Fleets in the U.S.

Over the past 15 years, the amount of transit bus service in the U.S. has remained relatively stable. According to the 2017 National Transit Database (NTD), total transit mileage driven increased by 2.4% between 2002 and 2017, while the number of transit buses has increases by 14.7% (*NTD, 2017*). Figure 1 shows the annual fleet inventory by fuel technologies. The "Other" category includes liquefied natural gas (LNG), fuel cell, dual fuel, and battery-electric vehicles (BEV). Even though the percentage of conventional diesel buses has dropped from 88% in 2002 to 62% in 2017, diesel remains the dominant fuel type in transit fleets. Compressed natural gas (CNG) and hybrid-electric vehicles (HEV) are the two most popular types of alternative fuel/powertrain technologies, with 2017 fleet penetration rates of 20% and 12% respectively. In this dataset, the market

penetration of battery-electric vehicles has remained very low, with only 260 vehicles (0.4% of the fleet) in 2017. The NTD only reports active, in-use vehicles (excludes planned vehicle purchases), operated by public transit agencies (excludes university nd private fleets). The survey conducted by National Academies of Sciences, Engineering, and Medicine (NASEM) reports that the total number of vehicles awarded, contracted, and/or sold in 2016 included 582 battery-electric buses and 76 for fuel cell buses in the U.S. (*NASEM, 2018*). Currently, more than 70 transit agencies have deployed one or more battery-electric buses.

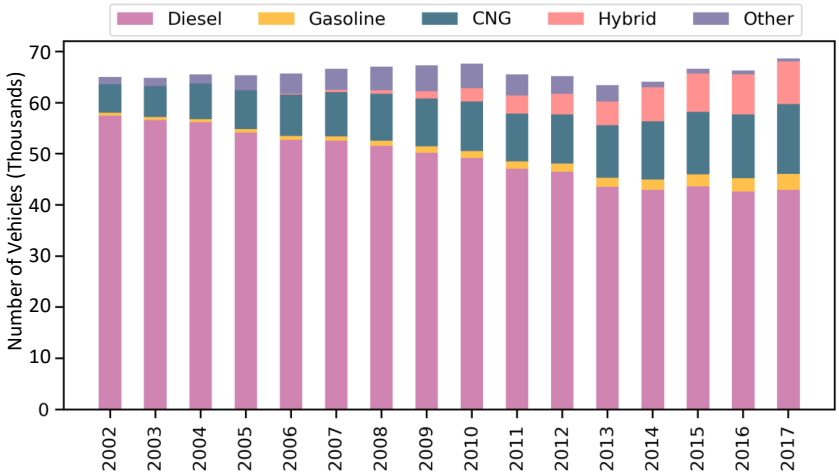

Figure 1 – Annual Transit Fleet Inventory in the U.S.

Figure 2 shows the 2017 fleet composition by fuel type for vehicle model years (MYs) 2010 and later, excluding battery-electric and fuel cell vehicles due to the small market penetration. This represents the newly purchased vehicles in recent years. Conventional diesel is still the most popular fuel type, penetrating over half of the market. CNG vehicle purchases have recently increased, whereas the percentage of hybrid-electric vehicles has decreased.

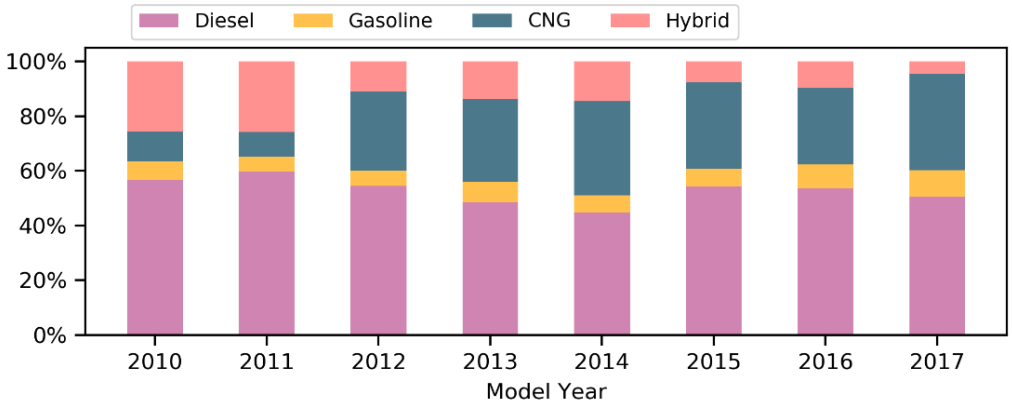

Figure 2 – 2017 Transit Fleet Composition by Model Year in the U.S.

1.2 Concerns of Transitioning to Alternative Fuels

There are several main concerns and challenges for transit agencies in adopting alternative fuel vehicles. However, qualitative investigations of the decision-making process associated with procurement and deployment of alternative fuel buses from the service provider perspective are very rare (*Mohamed, et al., 2018*). Four main procurement and deployment concerns summarized below.

Procurement and Operating Costs - The higher capital expenses for adopting alternative fuel buses, need to be offset by fuel-savings. Compared with conventional diesel buses, alternative fuel buses have higher procurement cost and require additional costs of building refueling and recharging infrastructure, which serve as primary market barriers to entry (*Lajunen, 2018*). Vehicle maintenance cost can be higher, too. For example, hybrid-electric buses have more parts to fix than diesel buses. Also, some transit providers argue that additional training period and trained mechanics are needed because electric buses require different skill sets. Hence, fleet management can be more costly and time consuming (*Mohamed, et al., 2018*).

Technology Uncertainty - Alternative fuel bus technologies are relatively new, and vehicle durability and operating performance are essential concerns to potential transit fleet agencies and governmental stakeholders (*He, et al., 2018*). Discrepancies between the claimed fuel economy and real-world performance under variable and diverse traffic conditions, roadway configurations, and designated routings contribute to economic uncertainty. Durability under extreme weather conditions can be a challenge to ensure operation range for electrified fleets.

On-road Vehicle Performance - Electrified fleets result complicate the decision-making process because charging activities must be embedded with existing bus scheduling. Conventional diesel buses cannot be directly replaced with electric buses if BEV range or performance is insufficient to meet route and schedule demands. Driving range for battery electric buses is 25-65% less than that of diesel buses, which is difficult to operate continuously without recharging and thus needs additional charging infrastructure (*Wang, et al., 2017)*. This means that there may be trade-offs between adopting high-capacity batteries for longer range and building more fast charging stations for more frequent charging opportunities. Either case will cause additional expenses. Uncertainties exist in different operating contexts as the electrification feasibility in terms of the whole transit network vary significantly (*Mohamed, et al., 2018*). Moreover, layover time at end stations may not be sufficient for recharging, especially when delay occurs. It may be impossible to maintain the existing bus scheduling, requiring additional operations adjustments.

Fleet Scalability - Scaling up electrified fleets introduces a new set of issues. Currently, battery-electric vehicles are still at the early stage, and in-service fleet size is

mostly below 10 in the U.S. There are no well-documented practices and models readily available to agencies that are designed to assess and optimize any increase in the size of their electrified fleet. The adoption of additional battery-electric vehicles typically requires the installation of additional chargers, which may not be feasible for agencies with depot space and grid power limits. This can also be a challenge when maintaining fleet operability during power outages. Maintaining additional charging facilities also requires additional staffing. In the survey conducted by the NASEM (*2018*), 39% of the agencies focused only on their initial deployment and do not necessarily plan on scaling up the fleets, and 50% of the respondents anticipate issues with inadequate charging opportunities in scaling up their system.

1.3 Research Gaps

Although transit fleet turnover planning in general is not a new research topic, there are some significant research gaps that must be resolved before transit agencies can develop long-range plans for electrification of their fleets. First, current estimations of fuel-saving benefits from electrification are over-simplified and may not properly reflect the real-world practice. Some studies have quantified fuel-savings by using fuel economy per vehicle type, simulated by using standard drive cycles, or constructed drive cycles (*Suzuki and Pautsch, 2005; Feng and Figliozzi., 2012; Figliozzi, et al, 2013*). However, such generalized results are not directly applicable to the on-road operations specific fleets, given the diversity of vehicle operating characteristics across different transit agencies (*Huang, et al., 2017; Xu, et al., 2017; Ho, et al., 2014; Xu, et al., 2013; Lee, et al., 2011; Wang, et al., 2008; Hung, et al., 2007; Yoon, et al., 2004*). In particular, even for the same fleet, the energy use and battery state of charge (SOC) may differ significantly across

laboratory cycles, simulation cycles, and real world operating cycles, which adds more uncertainty to energy and emissions modeling. It is essential to evaluate the fuel-saving benefits using real-world operating conditions (which include on-road speed/acceleration conditions and grade), which are a function of roadway configuration, traffic conditions, and vehicle routing.

Few studies link fleet turnover, vehicle-to-route assignment, and refueling facility design and placement. However, minimizing total life-cycle costs of operation requires that these decisions be made concurrently. Transit agencies currently lack a framework that can account for on-road operating conditions, fuel efficiency, refueling/recharging scheduling, charging station location, and charging station availability (all of which are required for proper scaling over the long term).

1.4 Research Scope

The scope of this study is the fixed-route transit system, the most common form of public transportation in the U.S. In the system, buses operate on predetermined routes according to the predetermined schedule. Transit vehicles are dispatched to serve tours, consisting of sequential trips that include both revenue and deadheading operations. Revenue service means a bus is "available to the general public and there is an expectation of carrying passengers" (*NTD, 2017*). In fixed route service, revenue routes are pre-determined, and each fixed route revenue trip serves the same origins and destinations. Deadheading means that a vehicle travels when out of revenue service, including: 1) depot pull-in and pull-out, i.e. leaving or returning to the garage; 2) interlining, i.e. changing from one bus route to another; and 3) when there is no expectation of carrying revenue

passengers, which may occur when vehicle travel to a refueling station or to a third-party maintenance shop. Among the 409 transit agencies that provide their annual mileage information, the average percentage of deadheading mileage is 8% (*NTD, 2017*).

A bus tour is typically defined as the series of operations that begins with a departure from a depot, followed by a series of chained revenue trips which are connected through interlining, and terminates with pulling the bus back to the same depot. A tour is also referred to as a block, a task, or an assignment. Transit operators typically refuel buses when they return to a depot from a tour. Once refueled, the bus may be dispatched to serve another tour. When chaining revenue trips, the general rule is to provide enough layover time for the driver to rest while minimizing the efforts when interlining, i.e. driving from one route to another. Tours vary across weekdays and weekends, by seasons, and for holidays. Most transit agencies schedule more frequent service with shorter headways on weekdays than on weekends, corresponding to the ridership demand.

Figure 3 shows an example of a tour, including nine revenue trips (three different revenue routes), two depot pull-in/pull-out trips, and eight interlining trips. Revenue trips are color-coded based on its Route ID (1, 2, and 3). Solid lines represent one direction (ID=0) and dashed line represents the return direction (ID=1). The interlining layover time ranges from 10 minutes (between Trip 3 and Trip 4) to 45 minutes (between Trip 4 and Trip 5).

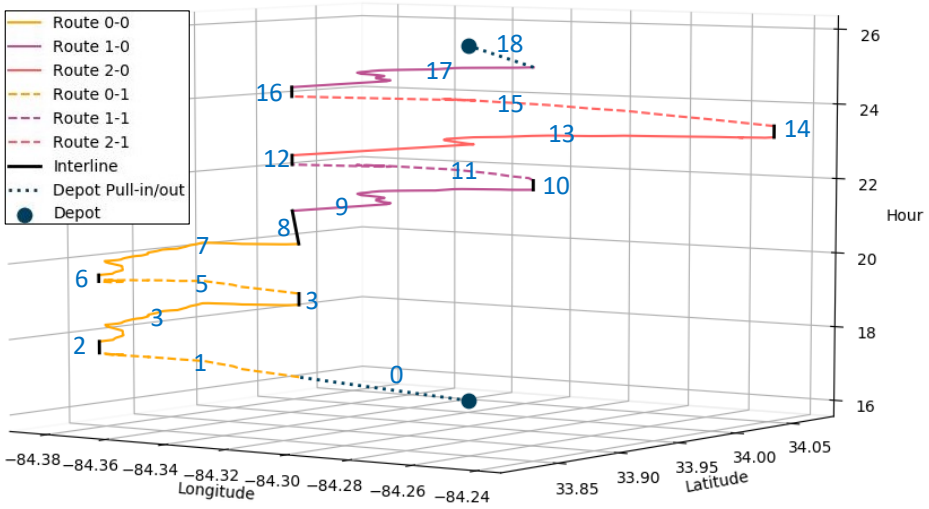

Figure 3 - Tour Example

1.5 Research Objectives and Tasks

The goal of this study is to develop an analytical framework for optimizing public transit bus fleet conversion to alternative fuels (i.e., designed to support sustainable transportation decision making). The vehicle fuel options include traditional diesel as well as three alternatives: CNG, hybrid-electric, and battery-electric vehicles. [The other fuel options, such as liquefied natural gas, biodiesel, and fuel cell, are not included in the analysis, but the framework can be adjusted to incorporate these fuel options in the future.] The framework will help transit agencies obtain reasonable estimation of reductions in fuel use, life-cycle operating costs, and life-cycle CO_2 emissions, based on fleet-specific features, route characteristics, vehicle constraints, and on-road operating conditions. The modeling tools will be capable of identifying the most economically efficient and energy-efficient plans for fleet electrification, vehicle-route assignment, vehicle-depot assignment, charge scheduling, and charge station/depot location selection. Four main models proposed in the framework are described in the subsections that follow.

1.5.1 Energy Use Prediction Model

The Energy Use Prediction Model predicts the energy use of different vehicle fuel technologies at the micro-trip level. Vehicle types include conventional diesel, CNG, hybrid-electric, and battery-electric transit buses. Energy use is simulated using advanced modeling tools based on real-world second-by-second operating cycles. Five machine learning models are developed from vehicle-specific and on-road operation features. The model with the best performance is selected, and applied to assess the fleet-wide energy use of different fuel technologies.

1.5.2 Operation Optimization for Existing Mixed Fuel Fleets

The goal of the Operation Optimization for Existing Mixed Fuel Fleets suite of models is to minimize current fleet operating costs by optimizing the assignment of vehicles to depots, tours, and routes. Four models are proposed:

1) Deadheading Minimization Model - Reduces depot pull-in/pull-out cost by re-assigning buses to depots in a multi-depot network;
2) Bus-to-tour Assignment Model - Reduces tour cost by re-assigning buses to depot-based tours (combinations of routes) accounting for the fact that fuel efficiency differs across transit routes;
3) Tour Design Model - Minimizes tour cost by re-chaining revenue trips to transit tours;
4) Combined Model - Reduces operating costs by combining the deadheading minimization model with the bus-to-tour or the tour design model.

1.5.3 Fleet Electrification

The goal of the Fleet Electrification suite of models is to optimize operations when introducing electrified sub-fleets to the existing fleet. The optimized decisions consist of vehicle procurement, vehicle-to-tour assignment, charging facility location selection, and charging schedules. Three models are developed:

1) Electrification Cost Model - Minimizes the total cost (vehicle capital, charging facility, utility, and operator) when electrifying a set of tours;
2) Operation Optimization Model - Minimizes the operating cost in a mixed fleet with both electrified and non-electrified vehicles by properly pairing depot-charged electric vehicle sub-fleets with tours;
3) Budget-constrained Sub-fleet Electrification Optimization Model - Minimizes life-cycle CO_2 emissions when introducing electrified fleets while simultaneously satisfying pre-defined budget constraints.

1.5.4 Fleet Conversion

The Fleet Conversion suite of models optimizes the conversion of large fleets to alternative fuels over time under pre-defined capital purchase budget constraints. The goal is to minimize the fleet-wide life-cycle CO_2 emissions, or maximize the benefits of reducing life-cycle CO_2 emissions, compared with the baseline fleet. Within the planning horizon, models generate decisions in terms of vehicle procurement, vehicle-to-tour assignment, charging facilities, and charging schedules per year. Two models are proposed:

1) Fleet Conversion Model without Salvage - Focuses on the additional monetary costs and reductions of life-cycle CO_2 emissions from adopting new fleets with alternative fuels, compared with the baseline fleet.
2) Fleet Conversion Model with Salvage - aims to minimize fleet-wide life-cycle CO_2 emissions by explicitly addressing fleet composition and operations for both the new and existing fleets.

1.6 Dissertation Outline

Chapter 2 reviews the previous studies in terms of fleet replacement models, transit vehicle energy modeling, new topics raised for electrified fleets, and fleet electrification costs. Chapter 3 describes the study scope, data inputs, and data pre-processing methods. Chapter 4 describes the process of simulating energy use of the four types of vehicles (diesel, CNG, hybrid-electric, and battery-electric vehicles), based on machine learning models developed and applied to evaluate fleet-wide energy use. Chapter 5, Chapter 6, and Chapter 7 describe the model formulation and implementation results for the three sets of optimization models: operation optimization of existing mixed fuel fleet, fleet electrification, and fleet conversion under budget constraints. Chapter 8 summarizes the main findings and limitations of the study.

CHAPTER 2. LITERATURE REVIEW

2.1 Fleet Replacement Models

Transit fleet replacement is essentially an equipment replacement optimization problem, which has historically been tackled using homogeneous and heterogeneous models. In homogeneous models, buses of the same type and age are replaced at the same time, which is commonly solved with dynamic programming approaches (*Oakford, et al., 1984; Hartman, 2001*). Bellman (*1955*) proposed an optimization model using dynamic programming to determine the procedure of replacing old equipment with new ones. However, dynamic programming has its limitations. For example, equipment is assumed to be replaced when reaching maximum service life (*Hartman and Tan, 2014*). In practical settings, buses of the same type and model year may not be replaced simultaneously, due to budget constraints; hence, heterogeneous models are introduced, mostly solved by integer programming (*Karabakal, et al., 1994; Hartman, 1999*). In the transit field, numerous studies have been conducted to optimize fleet replacement, but the increasing popularity of alternative fuel vehicles results in additional complexity and challenge in generating an optimal replacement plan. The following sections provide a comprehensive review of previous studies related to transit bus fleet replacement models, organized based on the different sub-areas that are used as constraints or objective functions in different studies.

2.1.1 Monetary Costs

Most studies focus on minimizing monetary costs, consisting of vehicle purchase costs, operating costs, maintenance costs, and salvage revenue (negative costs). Keles and Hartman (*2004*) propose a 30-year bus replacement period for a transit fleet with more than 600 buses in a European city. The constraints include a constant annual budget and service demand, represented by the number of in-use vehicles, with a fixed increasing rate annually. They also include a fixed charge per purchase period to mimic the concept of economies of scale, where volume discounts are incurred in the total package price. Vehicle purchase cost is the most influential factor in fleet replacement, as operations across buses are usually fairly similar.

The cost-minimizing model proposed by Parthanadee, et al. (*2012*) considers a vehicle utilization pattern, where average utilization decreases as vehicles age, instead of the widely-used constant utilization assumption. In the long-term mixed fleet optimization model proposed by Stasko and Gao (*2010*), cost including infrastructure, operations, and maintenance is used for both of their objective function as well as budget constraints. Decisions for long-term and short-term horizons are compared, and the former shows greater benefits because high-cost depot modifications to refuel and maintain CNG buses are initiated earlier. A similar cost-minimization model is proposed by Feng and Figliozzi (*2012*), which optimizes a mixed fleet consisting of diesel and hybrid electric vehicles. They also discuss the breakeven values of government subsidies for hybrid vehicles to make them economically competitive. The model does not consider bus-to-route assignment; instead, travel demand (annual mileage) is used as a constraint.

Ercan, et al. (*2015*) propose a mixed fleet optimization model, with the fuel choices of diesel, hybrid, battery-electric, B20, CNG and LNG. Their objective function incorporates system-wise life-cycle cost, consisting of fuel use, maintenance, battery replacement, refueling infrastructure, and insurance cost, with cost data generated from the Department of Energy's Greenhouse gases, Regulated Emissions, and Energy use in Transportation (GREET) model. Li, et al. (*2018a*) propose a multi-year mixed fleet management model. The model outputs early retirement, extra bus purchase, and vehicle routing decisions to minimize additional monetary cost and maximize external benefits. An annual budget is used as an important constraint in the model. Ke, et al. (*2016*) propose a fleet replacement model with the goal of the minimizing the cost of vehicles, battery, chargers, and electricity. The battery cost is estimated proportionally, based on the battery capacity. Wang, et al. (*2017*) propose a model to optimize the charging scheduling of a full battery-electric transit fleet with the objective of minimizing the annual system cost, consisting of additional deadhead cost from traveling to the charging center, charging cost, and charger and charging station infrastructure cost. A charging waiting penalty is included to generate more centralized charging activities.

2.1.2 Environmental Performance

Environmental performance plays an essential role in transit fleet replacement because emissions reductions and energy efficiency usually requires a trade-off with increased capital costs and sometimes increased operating expenses. Hence, optimizing environmental performance may come with increased capital facility and maintenance costs. However, environmental objectives have largely been ignored in previous transit network studies (*Farahani, et al., 2013*). Numerous studies can be found to optimize bus

operations with the conventional criteria such as cost, ridership, and accessibility, but so far little attention has been paid to environmental performance (*Jiménez and Román, 2016*). When introducing environmental costs to transit optimization models, a common approach is to monetize the emissions (*Stevens, et al., 2005*). Fusco, et al. (*2013*) monetized pollutant emissions as environmental costs so that these costs could be combined with capital, infrastructure, operating, and maintenance costs and evaluated under different fleet mix and charging strategies. Feng and Figliozzi (*2012*) applied a tailpipe GHGemissions rate (kg/mile) to the objective function to minimize the total costs. Buses of two fuel types, conventional diesel and hybrid diesel, are included in their 100-year fleet purchase plan, based on King County Metro fleet data. Stasko and Gao (*2010*) used both operating cost and a $PM_{2.5}$ emissions penalty in their objective function. They also included the additional infrastructure cost for CNG buses, i.e. depot modification and refueling station installation. To evaluate the impact of carbon pricing on fleet purchase, Stasko and Gao (2010) conducted a sensitivity analysis and included a wide range of GHG emissions penalties. They found that CNG buses are less beneficial when CO_2 costs exceed $1,550/ton; however, the penalty cost is beyond the range of previous estimates for carbon sequestration. In their follow-up study, they propose an approximate dynamic programming approach to incorporate stochastic vehicle breakdowns instead of previous deterministic settings of vehicle maintenance and repairs to further represent the reality (*Stasko and Gao, 2012*).

Xylia, et al. (*2017*) developed two scenarios to optimize the mixed fleet with biofuel and electric buses. One scenario minimizes the monetary cost of the entire system and the other minimizes the on-road GHG emissions by applying distance-based emission rates.

Li, et al. (*2015*) proposed the approach remaining life additional benefit-cost analysis for fleet optimization. In their objective function, additional benefits come from emissions reductions through vehicle replacement and retrofitting, and additional costs consist of the price difference of early purchase due to price inflation, loss of residual value from early retirement, and the corresponding operating cost difference. In their follow-up study, they expanded the scope to a mixed fleet by including alternative fuel vehicles. They used new additional life instead of remaining life as the planning time horizon because adopting new buses with high purchase costs will be disadvantaged unless life extension after replacement is considered (*Li, et al., 2018a*). They point out that the inclusion of emissions cost does not impact the scheduling and routing of the transit fleet because of the dominance of operating cost.

To solve the optimization problem of wireless charger deployment for electric bus networks, Bi, et al. (*2018*) use a single-objective model to minimize life-cycle energy use, GHG emissions, and cost individually. Then they pair two objectives and identify the trade-off zones that range from achieving one optimum objective to achieveing the optimum for the other.

In addition, some studies use fleet-wide total emissions as constraints in their optimization models (*Gao and Stasko, 2009; Gong and Wu, 2011*). Gao and Stasko (*2009*) propose a cost-minimizing model while achieving emissions reductions by choosing the treatment strategy, retrofitting or replacement. Gong and Wu (*2011*) use a model to minimize the total operating and vehicle depreciation costs through replacing the fleet with three types of vehicles, i.e. diesel, CNG, and hybrid-electric. Annual total NOx and PM emissions limits are used as environmental constraints. Li and Head (*2009*) solve the bus-

scheduling problem with replacement of alternative fuel vehicles in a multi-depot context. The objective of the model is to minimize operating cost, which consists of fuel cost for revenue trips, and fuel cost as well as wasted time cost for deadhead trips. Li and Head (2009) use capital cost and air pollutant emissions as constraints. Because solutions cannot always be found under some strict constraints, they use an elastic formulation, allowing violation of the emissions constraint and adding penalty costs (*Brown, et al., 1990*).

Durango-Cohen and McKenzie (*2018*) solve the mixed bus fleet problem by minimizing the life-cycle cost, while satisfying environmental constraints and passenger demands. They also report the shadow price to show the trade-offs between environmental impacts and level of service for hydrogen fuel cell, diesel, CNG, and hybrid-electric buses. The decision variables of the optimization model are continuous rather than discrete; hence, the results are not easily translated to real-world fleets.

Even though environmental performance is not included in the optimization model, some transit-fleet optimization studies still discuss the environmental impact after the optimization. Wang, et al. (*2017*) compare the total transit network cost in five scenarios with different electrification rate by incorporating environmental impact as social cost. They show that higher electrification rate corresponds to the lower total cost.

2.1.3 Health Impacts

Some studies incorporate health impacts into their fleet optimization models. Optimizing operating costs or tailpipe emissions alone may result in the increase of health risks by 49% (*Gouge, et al., 2013*). Ercan, et al. (*2015*) consider both tailpipe and upstream emissions-related health damage in their transit fleet optimization model, generating

multiple scenarios by assigning different weights to cost, environmental impact, and health damage. This is consistent with the practical world, because transit agencies tend to give different priority to these three components.

2.1.4 Vehicle Routing and Scheduling

The studies above optimize the fleet replacement strategy by determining the optimal number of buses and their types to purchase and salvage each year. However, none of the research above takes vehicle routing into account. Transit vehicle routing essentially includes two aspects: 1) designing transit routes and their schedules, and 2) assigning vehicle to routes. Vehicle routing cannot be ignored in the fleeting arena for five main reasons:

- First, energy use and emissions can vary significantly across routes (*Xu, et al., 2017; Yoon, et al., 2004*). In a study of optimizing vehicle assignment of a mixed fleet of diesel and CNG buses, the worst case can double the $PM_{2.5}$ emissions of the optimal case (*Gouge, et al., 2013*).

- Second, it may not be feasible to directly switch from conventional diesel vehicles to battery-electric vehicles and maintain the current schedule because battery-electric vehicles have range limits. Different characteristics of the timetabled trips lead to different results in terms of whether or not purchase additional vehicles are needed. Li (*2014*) shows that switching to electric fleet does not lead to a notable increase of the number of buses if battery swapping or fast charging are used in the case study.

- Third, introducing electrified and CNG vehicles requires the construction of charging and refueling infrastructure; thus, the selection and location of the additional infrastructure, transit scheduling and routing, and selection of bus types should be analyzed jointly. The reason behind this is to consider the particularities of each bus type, e.g. battery capacity and charging needs, and ensure a viable transit operating system (*Ostadi and Kazerani, 2015; Rogge, et al., 2018; Teoh, et al., 2018*). For example, when evaluating electrification potentials without changing existing bus schedules, it is necessary to focus on the entire vehicle schedules instead of individual transit trips because opportunity charging requires sufficient layover time between trips (*Rogge, et al., 2015*).

- Fourth, passenger capacity (i.e. number of seats) varies by vehicle type. During peak periods, more buses may be needed if lower-capacity buses replace large diesel buses (*Durango-Cohen and McKenzie, 2018*).

- Fifth, energy demand of electric buses and their charging schedules jointly influence electricity grid load and should be taken into account to ensure the stability of the local electricity grid (*Rogge, et al., 2015*). Also, charging activities of electric vehicles may result in higher peak demand, and thus higher electricity rate charges. Demand charges can be as much as 30% of a typical electricity bill for commercial and industrial buildings, but have always been overlooked by the previous fleet replacement optimization models (*Qin, et al., 2016*).

Most studies tackle the problem of optimizing the mixed transit fleet without considering vehicle routing (*Rogge, et al., 2018*). In fact, vehicle routing and scheduling is rather a complex problem (*Ceder, 2011*). Instead of assigning vehicles to individual routes, Gouge, et al. (*2013*) conduct the optimization through assigning vehicles of different types to blocks, consisting of several linked routes. Stasko and Gao (*2010*) propose an aggregated level approach, called assignment task, which is generated based on the percentage of two typical duty cycles, due to the difficulty of predicting future vehicle routing details. Li, et al. (*2018a*) include bus routing and charging into their long-term fleet replacement model. In this model, the service time of a day is divided into multiple periods, constrained by electric bus ranges, and a routing plan is generated within each time period. This multi-period approach is more realistic than the single-period routing approach, which simplifies the charging practice by spreading the charging time to different trips based on the travel distance. Li, et al. (2018a) also consider bus interlining in their routing model, as this significantly reduces operating cost. Jiménez and Román (*2016*) formulate a vehicle-to-route assignment model by minimizing the weighted sum of pollutant emissions under two scenarios. One is to minimize emissions without constraints, and the other is to minimize total emissions while avoiding an increase of certain pollutants. To capture the operational characteristics of each route, they cluster vehicle routes based on kinematic features and construct a driving cycle for each cluster to calculate the emissions for each route. Route-depot assignment is predetermined, alternative fuel vehicles can only be refueled in certain depots, and a limited set of route options are available for these vehicles. They also evaluate the difference of emissions between inter-depot and within-depot assignment of buses to routes.

Li and Head (*2009*) adopt the station-based time-space network approach to solve the bus-scheduling problem in a mixed fleet of hybrid, diesel, and CNG buses. The underlying idea is to aggregate trips with the same starting and ending stations through latest-first matching, which is said to significantly reduce the number of arcs in the network because the number of stations is much fewer than the number of trips (*Kliewer, et al., 2006*). Paul and Yamada (*2014*) propose a k-Greedy Algorithm to generate bus scheduling and charging plans when operating a mixed fleet of diesel and electric buses. By varying the number of electric buses, they calculate the minimum number of diesel buses required and find the best electric bus travel distance to reduce the fuel use and CO_2 emissions.

Ke, et al. (*2016*) used Generic Algorithm to solve the problem of fully converting the conventional transit bus fleet to electric buses by maintaining the existing transit routes and scheduling. Their goal is to minimize the construction cost, including vehicle purchase, battery, charger and electricity cost. The full-electrified transit network has the daytime and nighttime charging options and maintains the existing route scheduling by either using high-capacity battery or dispatching additional buses. The optimized variables include battery capacity, number of buses, and daytime charging time. However, the number of chargers is simplified such that the same number of chargers as buses are procured. Wang and Shen (*2007*) solve the transit scheduling and routing problem with a range constraint, set as a maximum travel time after the vehicle is recharged. The scenario employs a homogenous fleet with multiple depots, and charging can only occur at depots. They use multiple ant colony algorithm to solve this problem, with two hierarchical objectives: minimize the total number of vehicles, and minimize the total deadhead time. Wei, et al. (*2010*) later expanded the horizon to multiple-vehicle types and included a

waiting time cost in the objective function. These two previous studies did not require buses to return to the same depot, which may not be practical, because it causes inconvenience in fleet management. Hao, et al. (*2012*) further expand the model by adding the constraint that vehicles should return to the same depot.

2.1.5 Infrastructure Location Selection

Location selection for infrastructure is often ignored or simplified in transit fleet planning problems; however, spatial location is a necessary component to reduce deadheading and optimize charger siting. New modeling approaches to reduce energy use and enhancing sustainability performance of transit fleets include spatial allocation of chargers as an explicit optimization element (*Li, et al., 2016; Bi, et al., 2018*). In particular, when adopting electric vehicles in the transit system, charging station placement should be considered in relation to battery capacity, bus routes, and operating cost (*Hu, et al., 2013; Ke, et al., 2016; Sinhuber, et al., 2010; and Zhu, et al., 2013*).

Location selection for transit depots directly relates to the deadheading operations, which can be costly if the distance between starting/ending termini of revenue routes and depot is long. Sharma and Prakash (*1986*) proposed a deadhead mileage optimization model to achieve two objectives, one to minimize the total deadhead mileage of all buses, and the other to minimize the maximum deadhead mileage for each bus. Total deadhead duration coming from interlining among different bus routes is one of the two objectives in the scheduling problem solved by Wang and Shen (*2007*). Interlining can reduce the fleet size, and plays an essential part for battery-electric transit fleet with range constraints. Re-assigning buses to depots can reduce fuel use by 6% without additional expenditures in

the case study of Atlanta, Georgia (*Li, et al., 2016*). In the case study by Jiménez and Román (*2016*), inter-depot reorganization can reduce CO_2 emissions by 3% and PM emissions by 20.5% in their optimal vehicle-to-route assignment plan. Djiba, et al. (*2012*) proposed an optimization model to minimize cumulative deadhead distance. Bus-to-depot assignment is determined separately for pull-in and pull-out trips.

To achieve high energy and cost efficiency, introducing electric vehicles into transit operations brings in the additional considerations of charging method and bus configuration (i.e. the battery pack) because of the limitations of the electrical energy storage (*Göhlich, 2014; Lajunen, 2018*). Charging strategy includes two main types, slow overnight charging and fast charging. Overnight charging commences after daytime operations are complete, and is beneficial to battery life because the charging power is moderate. However, overnight charging has drawbacks in terms of increase energy use from additional vehicle weight (to obtain the range required to support a full-day's operation), battery aging due to high depth of discharge, and overall higher battery cost (*Rothgang, et al., 2015*). Fast charging allows the agency to recharge a battery on-route, and the battery may only be partially charged at each connection. This allows the agency to partially charge the battery at multiple locations, depending on time available on the schedule between arrival and departure. Fast charging can be further classified into: 1) opportunity charging at the intermediate transit stops, and 2) end station charging at the route termini. Usually, charge time duration at an end station is longer than opportunity charging on-route. Fast charging strategies feature smaller dimensioned batteries with lower capacity, lower vehicle weight, and lower battery cost, which current models identify as a cost-competitive advantage (*Kunith, et al., 2017; Lajunen and Tammi, 2016*).

Charging infrastructure and strategy should be accustomed to local context by considering the fleet-specific operating situations and requirements (*Rothgang, et al., 2015*). However, charging infrastructure is predetermined in most mixed fleet replacement optimization problems, and thus charger optimization is typically excluded from fleet planning (*Rogge, et al., 2018*). Lajunen (*2018*) developed a simulation tool to evaluate the energy use and cost for a given charging strategy and route, through which end station charging is shown to minimize cost. However, because each route is simulated individually, sharing f charging infrastructure is not included, which could have significantly reduced the infrastructure cost for large, complex transit networks. Sebastiani, et al. (*2016*) use genetic algorithm to achieve two objectives: 1) minimize the number of charging stations, and 2) minimizing the average extra time used for opportunity charging. This simulation optimization approach is applied to a real-world transit system and the results indicate that charging stations can be viably shared by different routes, decreasing the total number of required charging stations. Kunith, et al. (*2017*) propose a cost-minimizing model in a fully electrified transit system without changing current schedules. The model jointly determines the battery sizing and the number of charging stations and their locations. They consider the cost savings from sharing charging stations, which is possible when multiple transit routes go through the same bus stop (such as a connection point between bus lines at a rail station). However, bus interlining is not included in the model, due to the assumption that one bus serves one transit route.

Wang, et al. (*2017*) propose a model for making concurrent decisions on the number and location of fast-charging infrastructure, as well as the charging schedules. The model is applied to replace diesel fleet with a fully electrified fleet while maintaining the current

schedule and vehicle-to-route assignment. They use equal charging duration per charge and analyze the impact of various charging durations. The total operating cost decreases as the duration increases because of fewer charging activities incurred; however, the decrease is trivial after the duration reaches a certain level. Bi, et al. (*2018*) propose an optimization model to select wireless charging infrastructure as well as charging schedules in an electric fleet, without changing the current transit routing and schedule. Rogge, et al. (*2018*) propose a cost-minimization model by determining vehicle composition and their charging schedules, with the option of rescheduling charging events. However, the only charging approach included in the model is the overnight charging at depot. Adjusting schedules can reduce the number of chargers and overall power requirements at the bus depot, and the time-shift can be represented as monetary penalties to the objective function.

When modeling energy use of transit buses, most studies consider the additional weight of batteries of electric vehicles, but do not consider dynamic vehicle load coming from ridership at different demand periods and different stops. Goeke and Schneider (*2015*) find that actual passenger load (especially in the peak period) strongly impacts the optimization results for a mixed fleet.

2.2 Vehicle Energy and Emissions Modeling

This section first reviews the previous studies about modeling the tailpipe energy consumption and emissions of alternative fuel transit buses. Three techniques are used: 1) applying distance-based energy use and tailpipe emission rates, 2) using a conversion factor based upon conventional fuel bus counterparts, and 3) using kinematic characteristics and roadway topology. Previous studies on life-cycle cost-effectiveness of alternative fuel

vehicles are then discussed. Finally, the vehicle energy/emissions modeling tools used in this study are described.

2.2.1 On-road Energy and Emissions Modeling

Some studies apply distance-based energy use and tailpipe emission rates to quantify fleet-wide environmental impact. The distance-based energy consumption and tailpipe emission rates generated by the COPERT model (*Ntziachristos, et al., 2009*) were used to quantify the operational cost and environmental impact in several fleet optimization models (*Fusco, et al., 2013; Li, et al., 2015; and Li, et al., 2018a*). Even though battery-electric buses have zero tailpipe emissions, Li, et al. (*2018a*) include CO_2 emissions associated with power generation. Feng and Figliozzi (*2012*) use CO_2 emissions rates on a per-mile base, i.e. 2.504 kg/mile for hybrid buses and 3.407 kg/mile for diesel buses, based on the study from Clark, et al. (*2007*). Ke, et al. (*2016*) use distance-based energy use rates in their optimization model of the transit fleet conversion to electric buses. They use different values for large and medium-sized buses, and also consider the difference between running empty and full loads. Similarly, Bi, et al. (*2018*) use the distance-based energy use when optimizing wireless charger deployment. Bi, et al. (*2015*) also use a light-weighting correlation factor to adjust the energy use rate based on route-based ridership and downsized battery. Xylia, et al. (*2017*) use distance-based energy use and on-road GHG emissions factors for their two-scenario optimization model, consisting of a mixed fleet with biofuel and electric buses. In addition to using a fixed energy consumption factor, they also conduct a sensitivity analysis for energy consumption ranging, from 40% to 160% of the reference values, to examine variations of different traffic and roadway characteristics. Wang, et al. (*2017*) analyze the energy use of electric bus based on driving

range. Each fully-charged electric bus is assumed to have a 120km range, with a 150km initial range and a minimum retention range of 30km, or 20% of the maximum driving range. Durango-Cohen and McKenzie (*2018*) use the emission rates for diesel, CNG, hybrid, and hydrogen fuel cell vehicles to solve the mixed fleet cost-minimization problem. The emission rates are calculated by averaging the results from previous NREL demonstration projects (*Barnitt and Chanler, 2005; Chandler and Eberts, 2006; Chandler and Eudy, 2008; Chandler and Eudy, 2008a; and Chandler and Eudy, 2009b*).

Some studies use scaling factors to obtain the energy use for alternative fuel buses based upon conventional fuel bus counterparts. When evaluating different transit fleet charging strategies for a mixed transit fleet, Fusco, et al. (*2013*) started with the factors from the COPERT model for internal combustion engines and applied a conversion function to calibrate the energy use of electric buses based on the diesel counterparts. They also assumed a simplifying assumption of linear dependence between energy use and battery weight when evaluating the operational performance of electric buses with different battery capacities.

Some studies include both kinematic characteristics and roadway topology. Jiménez and Román (*2016*) apply the regression model proposed by INSIA-UPM (*2010*), to solve the fleet-to-route assignment problem. The model takes route-average speed, operation and acceleration durations, as well as average road grade as inputs and predicts route-based emissions. In the transit fleet optimization model proposed by Ercan, et al. (*2015*), on-road emissions for diesel, CNG and LNG buses are estimated based on the Motor Vehicle Emission Simulation (*MOVES*), developed by the U.S. Environmental Protection Agency (USEPA, 2015). Second-by-second speed and acceleration traces

represent the vehicle operations. Hybrid electric buses and B20 buses are estimated using conversion factors from the Alternative Fuel Life-Cycle Environmental and Economic Transportation tool (*AFLEET website*). Upstream emissions associated with energy production are calculated in the same manner, with the addition of battery cost for electrified buses, using the GREET model.

2.2.2 Lifecycle Analysis

Lifecycle analysis is necessary when evaluating environmental and economic performances of transit fleets. Instead of focusing on one individual component, a comprehensive analysis that incorporates the interdependencies among processes, services, and products will have a greater impact (*Chester and Horvath, 2009*). Bicer and Dincer *(2018*) evaluate the well-to-wheel environmental impacts of seven types of buses, including conventional fuel, alternative fuel and advanced powertrain configurations using the GREET 2015 model. They find hydrogen vehicles are the most benign option; although electric vehicles do not emit direct CO_2 during operations, the production and disposal of have significant consequences, as maintenance and manufacturing phases contribute more than 80% of the overall impact.

Wang, et al. (*2015*) compare the well-to-wheel emissions and energy use of buses with different fuel types at a regional level in China. They find that only hybrid-electric buses show benefits of reducing both energy use and pollutant emissions at the same time. However, they do not specify real-world operating conditions. Similar results are shown in another life-cycle analysis in Argentina by Correa, et al. (*2017*), in which they use the GREET model for evaluating upstream energy and emissions with fuel pathways

customized to Argentina, and the simulated the on-road sectors using ADVISOR (*Markel, et al., 2002*). Hybrid electric transit vehicles show the best performance among all five alternative fuel and advanced powertrain configurations in both 2018 and 2030 scenarios, and battery-electric vehicles for short ranges are projected to be competitive with higher generation of renewable energy in the 2030 scenario.

Xu, et al. (*2015*) incorporate second-by-second bus operating cycles to conduct the comparison by using the Fuel and Emissions Calculator. They find that the on-road GHG and criteria pollutants emissions dominant the life-cycle emissions of conventional vehicles, whereas electric buses have zero on-road emissions. However, electric buses have comparable or higher upstream emissions with conventional diesel buses. Zhou, et al. (*2016*) compare the well-to-wheel energy use between battery-electric and conventional diesel buses on a test route by using second-by-second operations data collected from on-board diagnostics. He, et al. (*2018*) compare the well-to-wheel energy use and emissions of conventional diesel, CNG, hybrid diesel, battery electric under complex real-world operating conditions. They use an operating mode binning method to calculate on-road energy use and find that traffic conditions, loading mass, and AC usage greatly impacts energy use (*Zhang, et al., 2014*). For example, under congested driving conditions, battery-electric buses are more beneficial in terms of energy efficiency than conventional diesel and hybrid diesel counterparts.

2.3 Modeling Tools

In this section, we describe and vehicle energy/emissions modeling tools the optimization models used this study.

2.3.1 Energy Modeling

2.3.1.1 Autonomie®

Autonomie® is the state-of-the-art for automotive control-system design, and simulating vehicle energy consumption and performance. Previously known as PSAT, Autonomie® is developed by Argonne National Laboratory (ANL) in collaboration with General Motors. It is the primary vehicle simulation tool selected by the United States Department of Energy (USDOE) to support its U.S. DRIVE Program and Vehicle Technologies Office (VTO) research projects. Autonomie® runs in a Matlab® software environment and can be easily integrated into third-party tools, including economic, component cost, and environmental models like LCOD and GREET.

Autonomie® can incorporate a variety of vehicle classes (light-duty vehicles and heavy-duty vehicles), and powertrain configurations (conventional, start-stop, battery electric vehicles, parallel hybrid electric vehicles, series hybrid electric vehicles, fuel cell hybrid electric vehicles, etc.). It also covers a variety of fuel types, such as gasoline, diesel, E-85, CNG, hydrogen, and electricity. Autonomie® is user-friendly and offers many customizable settings including environment, driver, vehicle propulsion architecture, vehicle propulsion controller for advanced powertrain vehicles, etc. Additionally, data can be readily visualized and/or post-processed in Matlab®. Autonomie® can output high-resolution energy consumption data for each second of a trip for the entire vehicle, and/or the component parts, such as the engine and tires. Many recent published studies looking at heavy-duty fuel consumption have relied on Autonomie® for simulation purposes; Daw, et al. (*2013*) simulate fuel economy and emissions performance of heavy-duty hybrid

trucks during city and interstate driving; Delgado and Lutsey (*2017*) look at potential efficiency of advanced tractor-trailers in the 2020–2030 timeframe; Delgado, et al. (*2016*) use Autonomie® to estimate the fuel efficiency technology potential of heavy-duty trucks in major markets around the world; Delgado and Li (*2017*) analyze the fuel efficiency technology potential of heavy-duty vehicles in the Chinese market; and Xu, et al. (2019) assess fleet-wide energy consumption of light-duty hybrid electric vehicles. In this study, Autonomie® is used to simulate the energy use of diesel, hybrid-electric, and battery-electric vehicles, which will be described in detail in Section 4.2.2.

2.3.1.2 MOVES-Matrix

MOVES-Matrix (*Guensler, et al., 2016*) is constructed from more than 146,000 MOVES runs for each modeling region in the United States. MOVES runs are iterated across all input variables that affect output emission rates, and each iteration yields a set of pollutant emission rates by vehicle source type, model year (age group), vehicle fuel type (gasoline, diesel, CNG, etc.), specific on-road operating condition (average speed and road type, or on-road vehicle specific power (VSP) operating mode bins for light-duty vehicles or scaled tractive power (STP) operating mode bins for heavy-duty vehicles), and temperature and humidity conditions, for each calendar year and applicable set of regional regulatory parameters (fuels properties, I/M program parameters). Once the 90 billion individual energy use and emission rates derived from the iterative MOVES run sare compiled by MOVES-Matrix, users can query the into the working matrix to obtain applicable emission rates for any vehicle fleet and set of environment and operating conditions without ever having to launch MOVES or transfer MOVES outputs into the

analyses (*Liu, et al., 2019)*. In this study, MOVES-Matrix is used to simulate the energy use of diesel and CNG vehicles, which will be described in detail in Section 4.2.3.

2.3.2 Optimization

In Chapter 5-Chapter 7, optimization models are developed by formulating mixed integer linear programming (MILP) models, where no quadratic terms are involved and in the solution set, some of the decision variables are constrained to be integers and some can be continuous variables. MILP problems are non-convex and must be solved by exhaustive search. These problems are generally solved by using Branch and Bound algorithm, which starts with finding the optimal solution without the integer constraints. Then the integer variables whose solutions are not integral will "branch" by creating two sub-problems with tighter constraints and then will be solved. The process repeats until all integer constraints are satisfied.

Per proposed optimization model, the mathematical formulation includes (1) the decision variables as well as their types, (2) the objective function, minimizing cost or maximizing benefits, and (3) the constraints, to ensure the requirements are met in terms of fleet service demand, battery energy levels, facility requirements, etc. For model implementation, the formulated models are programmed in Python environment and solved using the commercial solver CPLEX 12.8 (*CPLEX Optimizer*). CPLEX solver has been widely used in solving MILP problems in transit fleet optimization (*Li, et al., 2018; Kunith, et al., 2017; Wang, et al., 2017; Xylia, et al., 2017*). All numerical experiments are run on a desktop with 32 GB of RAM and 3.40 GHz of CPU under a Windows 10 environment.

2.4 Transition to Electrified Fleets in the U.S.

Because battery-electric vehicles are at the early stage, this section is structured around the new topics and problems raised when adopting battery-electric transit fleets. For each topic, common practices in the U.S. are described.

2.4.1 Grants and Incentive Programs

The capital costs for hybrid and battery electric buses are much higher than the costs of conventional diesel buses. In the U.S., federal grants and incentive programs help offset up-front vehicle investment and motivate transit agencies to adopt battery-electric vehicles. Examples of federal programs are Low or No Emission Vehicle Deployment Program (Low-No), Transit Investments for Greenhouse Gas and Energy Reduction (TIGGER), Congestion Mitigation and Air Quality (CMAQ) Improvement Program, Transportation Investment Generating Economic Recovery (TIGER), Better Utilizing Investments to Leverage Development (BUILD), Urbanized Area Formula Funding Program, and State of Good Repair (*Casale and Mahoney, 2018*). The survey conducted by the NASEM reports that 61% of the transit agencies use federal or state grants in procuring battery-electric vehicles (*NASEM, 2018*). Some state and regional authorities have also initiated incentive programs, such as the California's Zero-Emission Truck and Bus (Heavy-Duty Vehicle) Voucher Incentive Project (HVIP) and Chicago's Drive Clean program.

In addition to the funding support for fleet procurement, some other types of funding programs also help with the transition to electrified fleets, such as leasing programs and utility support (*Miller, et al., 2018*). FTA recently added a new program to support

leasing arrangements in the Fixing America's Surface Transportation (FAST) Act (*FTA, 2018*). Agencies can now separately purchase zero-emission vehicle components (e.g. batteries) through a capital lease program. Some utility companies have already invested in installing charging infrastructure to partner with transit agencies, and some have developed appropriate utility rate structures to help agencies minimize utility costs.

2.4.2 Charging Facilities

Battery SOC can be sustained through charging. The three types of charging facilities commonly used include overnight plug-in depot charging and two fast charging options, overhead conductive and wireless inductive. Table 1 summarizes the key characteristics of each charger type. Note that this table only shows the common practice, and does not represent the entire market. For example, an agency can install overhead conductive charging at a depot, allowing buses to be dispatched again after a short recharging time. Battery capacity fades as battery ages, and the degradation is attributable to the applied charging power, depth of discharge, and initial SOC when charging is applied (*Kunith, et al., 2013*). Avoiding deep discharge is the most common way to keep battery health and decelerate the degradation. The minimum battery SOC that has been generally used ranges from 15% to 30% (*Bi, et al., 2018; Xylia, et al., 2017; Ke, et al., 2016; Kunith, et al., 2016*).

Table 1 – Charging Options

	Depot Plug-In	**Overhead Conductive**	**Wireless Inductive**
Locations	Depot	On-route, transit centers	On-route, transit centers
Space	Require large space when equipping one charger per bus	Require land use permission	Require land use permission

	Depot Plug-In	Overhead Conductive	Wireless Inductive
Infrastructure Cost	Low	High	High
Charge Power	40-120kW	175-500kW	50-500kW
Recharge Duration	1-8 hours	5-20 minutes[1]	5-20 minutes[1]
Battery Type	Large battery pack with high range	Small battery pack with short range	Medium battery pack with medium range
Fuel Efficiency	Lower compared with the other two options	High	High
Utility Rate	Low off-peak electricity rate when charged overnight	Peak demand may significantly increase cost	Peak demand may significantly increase cost
Operating	Additional depot pull-in/pull-out trips for long tours	Supports 24-hour revenue service if coordinated properly	Supports 24-hour revenue service if coordinated properly
Concerns	Range limit	Miss charging due to delays or emergencies	Infeasible to some roadways design

[1]Averaged duration per charge to maintain bus operations, batteries are not necessarily fully charged.

Plug-in chargers require staffing to plug/un-plug the vehicle with the charger, whereas drivers do not need to get out of the bus when using on-route charging options. Agencies choose one or several charging facilities based on their available grid, service demands, and preferences. According to the survey results from the NASEM, all 18 transit agencies tht responded use the depot plug-in charging option, and half of them also use the on-route fast charging options (*NASEM, 2018*). Some agencies indicate that they will install fast charging facilities once they decide to scale up the battery-electric fleet because of their limited depot space. For fast charging, delivering high currents requires a dedicated high-voltage power supply line, which may not be available in some local grid systems and can thus significantly increase infrastructure cost. Some agencies also report that they

prefer automated connections to the manual plug-in to minimize staffing and safety risks, whereas some agencies do not consider this an issue, compared with refueling CNG buses.

2.4.3 Scheduling and Operating

When integrating battery-electric buses into the existing fleets, agencies may need to adjust their schedules for recharging events. The survey conducted by NASEM (*2018*) reports that only 60% agencies adjust their schedules. Among them, 40% agencies adjust their layover time, and 20% re-design their tours.

Antelope Valley Transit Authority uses wireless inductive charging during layovers and depot charging overnight. King County Metro has one on-route conductive charger and one depot plug-in charger. On average, it takes around 8 minutes to recharge the bus on-route to maintain revenue operations, which is within the 15-minute layover time at the charging station. For further expansion, they plan to add more chargers to the existing charging station and build more charging stations. Chicago Transit Authority dispatches their battery-electric vehicles twice a day for morning and afternoon services, and uses depot plug-in charging during mid-day and overnight. The City of Seneca uses both on-route conductive and depot plug-in chargers. They report that the 10-minute layover time is already enough to recharge the bus in flight and maintain their existing schedule. The Central Contra Costa Transit Authority uses both depot plug-in charging and on-route wireless inductive charging during layovers (*Eudy and Jeffers, 2018a*).

2.4.4 Electricity Rate Structure

The cost of refueling diesel or CNG vehicles depends mainly on usage; however, the utility cost of recharging battery-electric vehicles has two components: usage charge and demand charge. Similar to diesel and CNG, the usage charge of battery-electric vehicles depends on the amount of electricity used. The demand charge relates to the maximum amount of electricity delivered within a certain time period, typically 15-minutes (these costs represent the costs associated with maintaining utility infrastructure capacity required to deliver electricity during periods of peak consumption). A study conducted by Gallo, et al. (*2014*) finds that demand charging costs may offset the energy efficiency benefits of battery-electric vehicles and proposes that spreading the charge activity over more buses and longer time periods through optimized charging schedules can regain the advantages. King County Metro reports that the demand charge portion of the utility bill ranges from 34% to 54% during their 13-month evaluation period (*Eudy and Jeffers, 2018c*). The survey conducted by the NASEM (*2018*) reports that over 60% of the agencies would like to have technical support associated with determining utility rate structures when adopting electrified fleets.

2.5 Costs of Fleet Electrification

The NASEM survey reports that nearly 90% of the transit agencies that are operating battery-electric buses state that they need technical support to understand life-cycle costs so that they can make proper adjustments to service and/or make reasonable future purchase decisions (*NASEM, 2018*). Therefore, this study conducts a comprehensive literature review on the costs of transit fleet electrification. The sources include current

practices of transit agencies in the U.S., and life-cycle technologies. The review of current practices relies heavily on two reports, which are based on two recent surveys targeted to experienced U.S. transit agencies. The first report is conducted by the University of Massachusetts Amherst (UMass) research team, which summarizes responses from 13 transit agencies, four universities, and five other organizations (*Christofa, et al., 2017*). The second report was released by the NASEM, which summarizes the responses from 21 transit agencies and describes the deployments of five agencies in detail (*NASEM, 2018*). Cost components, including vehicle procurement, operation, maintenance, and infrastructure, are discussed in detail.

2.5.1 Vehicle Procurement Cost

Table 2 provides an inventory of vehicle procurement costs from the literature (when information is not available or not applicable, the cell is left blank). For comparative purposes, if the study includes counterparts of other fuel technologies, those costs are also listed. One caveat is that cost values are not converted to the same calendar year values (i.e., they are not inflation-adjusted).

Table 2 – Vehicle Procurement Cost

Cost	Fuel Technology	Battery Capacity (kWh)	Model Year	Transit Agency	Source
$537,000-900,000	BEV	72-660	2014-2016	Responding agencies	Christofa, et al., 2017
$579,000-$1,200,000	BEV	72-325	2009-2016	Responding agencies	NASEM, 2018
$797,882	BEV	105	2015	King County	NASEM, 2018; Eudy and Jeffers, 2018c
$584,591	HEV	11.6	2015		
$497,103	Diesel		2015		
$950,000	BEV	74-105	2014	City of Seneca	NASEM, 2018

Cost	Fuel Technology	Battery Capacity (kWh)	Model Year	Transit Agency	Source
$579,000	BEV	305	2013	IndyGo	NASEM, 2018
$1,053,689	BEV	100	2016	County Connection	Eudy and Jeffers, 2018a
$459,935	Diesel		2014		
$789,000-823,000	BEV	72	NA	Foothill	NASEM, 2018
$904,490	BEV	88	2014	Foothill	Eudy and Jeffers, 2018b
$879,845	BEV	106	2016		
$575,000	CNG		2014		
$825,000	BEV			SEPTA	DVRPC, 2015
$567,678	HEV		2014		
$450,000-750,000	Diesel			New York City Transit	Barnitt , J., 2016
$750,000-1,050,000[1]	BEV				
$790,000	BEV			Hong Kong New World First Bus (NWFB)	Li, et al., 2018a
$342,366	CNG				
$531,605	Hybrid				
$321,143	Diesel				
$600,000	BEV	333.6			Lajunen and Lipman, 2016
$750,000	BEV	62.6			
$330,000	CNG				
$420,000	Hybrid				
$300,000	Diesel				
$686,000-750,000	BEV				Miller, et al., 2018
$450,000-620,000	CNG				
$500,000	Diesel				
$900,000	BEV				Ercan, et al., 2015
$350,000	CNG				
$510,000	Hybrid				
$330,000	Diesel				
$800,000	BEV	88			Tong, et al., 2017
$800,000	BEV	324			
$525,000	CNG				
$758,000	HEV	5			
$485,000	Diesel				
$383,000	CNG				Durango-Cohen and McKenzie, 2018
$460,000	Hybrid				
$374,000	Diesel				

[1] converted based on "electric buses cost about $300k more than diesel buses"

The costs and battery capacities in the table above exhibit encompass large ranges, sue to the fact that a wide variety of options are currently available and have changed over time. Unit battery cost is assumed to range from $561-$898/kWh (€500-800/kWh) depending on high-energy or high-power battery type (*Lajunen, 2018*). Lindgren (*2015*) assumes $422/kWh (4000 SEK/kWh) in the simulation analysis of electrified fleet. Jeong, et al. (*2019*) assume $800/kWh when evaluating the economic impact of battery capacity. Chen, et al. (*2018*) conservatively assume $570/kWh, based on the range of $220-570/kWh from BYD models. Gao, et al. (*2019*) review that the battery production cost is $300-500/kWh.

Larger battery capacity enables a longer range, but also results in an increase in battery cost and energy use because of the higher vehicle curb mass. Table 3 shows the unit battery weight values from several previous studies.

Table 3 – Unit Battery Weight

Battery Weight (kg/kWh)	Source
4.1-8.9[1]	Ercan, et al., 2015
7.7	Bi, et al., 2015
10.6-12.9[2]	Zhou, et al., 2016
8.3[1]	Yu, et al., 2016
6.7	Gao, et al., 2017
5.9[1]	Chen, et al., 2018
10	Jeong, et al., 2019
10[1]	Gao, et al., 2019

[1] Adjusted for energy density, evaluated as MJ/kg, Wh/kg, or kWh/kg

[2] Calculated based on three battery-electric models

When projecting procurement cost in future years, some studies assume a decreasing trend with technology development. For example, Lajunen and Lipman assume the purchase cost decreased by 1% for hybrid-electric vehicles, 2% for electric vehicles, and a later study focusing on comparing different charging methods assumes a discount rate of 3% in all calculations (*Lajunen and Lipman, 2016; Lajunen, 2018*). Christofa, et al. (*2017*) state that annual increase rate of hybrid-electric buses is 2.35%. They also project that the capital cost of battery-electric buses will first decrease as technology matures, and then increase over time to return to 2016 values in 2037.

2.5.2 Operating Cost

Operating cost consists of energy cost and employee wages. When adopting electrified fleets, additional cost will be spent in training bus operators to recharge the vehicle. Although on-route charging is automatic, bus operators still need to learn to dock the bus and they need to coordinate with other operators in case of a missed charge due to delay. Additional staffing is needed for depot plug-in charging, especially when scaling up electrified fleets.

Evaluating energy cost is more complicated for electric vehicle fleets because cost depends on both energy efficiency and the utility rate structure. Table 4 lists the fuel efficiency performance from previous studies, evaluated as miles per diesel gallon equivalent (MPDGE). Battery-electric vehicles show significant improvement of fuel efficiency performance over their diesel and CNG counterparts. The large variation occurs because of vehicle specifications, the ambient temperature, as well as operating conditions.

Therefore, a solid evaluation of the actual energy use is necessary when making recharging schedules to ensure revenue operations.

Table 4 – Fuel Efficiency Performance Comparison

MPDGE	Fuel Technology	Battery Capacity (kWh)	Transit Agency	Source
12.1-27.32	BEV		All responded agencies	Christofa, et al., 2017
2.7-5.4	Diesel			
13.3-17.6 Average: 15.9	BEV	105	King County	Eudy and Jeffers, 2018c
6.3	HEV	11.6		
5.3	Diesel			
17.32	BEV	88	Foothill	Eudy and Jeffers, 2018b
16.98	BEV	106		
4.23-4.4	CNG			
13.3	BEV	100	County Connection	Eudy and Jeffers, 2018a
5.1	Diesel			
20.5	BEV		Altoona Bus Testing	NASEM, 2018
4.8	CNG			
4.8	Diesel			
5.84	HEV			
46.8	BEV	90	City of Aachen, Germany	Rogge, et al., 2018
26 [1]	BEV	380	City of Aachen, Germany	Rogge, et al., 2018
15.59[1]	BEV	60	Stockholm, Sweden	Xylia, et al., 2017
14.52	BEV		MARTA	MARTA, 2016
18.53	BEV		MARTA	MARTA, 2016
22.1	BEV	88		Tong, et al., 2017
18.9	BEV	324		
4.3	CNG			
5.76	HEV	5		
4.8	Diesel			

[1]Simulated or adjusted from other studies

Table 5 shows the utility rate of several U.S. transit agencies. As mentioned in Section 2.4.4, electricity utility rate structures vary significantly, impacting the actual energy cost. Utility cost depends on not only utility usage, but also demand charge.

Demand charges rates from $0.00/kW-$23.65/kW (*Gallo, et al., 2014*). However, CNG and diesel cost rates are more stable.

Table 5 – Utility Rate of U.S. Transit Agencies with Electrified Sub-Fleets

Cost Rate ($/kWh)	Fuel Technology	Transit Agency	Source
0.07-0.30	BEV	All responded agencies	Christofa, et al., 2017
0.2	BEV	King County	Eudy and Jeffers, 2018c
0.04	Diesel		
0.90-1.5[1]	BEV	City of Seneca	NASEM, 2018
0.19-0.2	BEV	Foothill	Eudy and Jeffers, 2018b; Eudy and Jeffers 2019
$0.03-0.04	CNG		
0.22	BEV	County Connection	Eudy and Jeffers, 2018a
0.05	Diesel		
0.055	BEV		Tong, et al., 2017
0.06	Diesel		
0.04	CNG		

[1] depends on utility rate structure

Table 6 shows the operating energy cost. In some agencies, the high electricity cost offsets the fuel-saving benefits of battery-electric vehicles. This implies the need for a partnership between transit agencies and utility companies to ensure that appropriate utility rates will be available. Also, to reduce the demand charge element of electricity cost, charging location selection and recharging scheduling should be planned collectively, especially when scaling up the system.

Table 6 – Operating Energy Cost of Agencies with Electrified Sub-Fleets

Cost Rate ($/mile)	Fuel Technology	Transit Agency	Source
0.15-0.89 average 0.36	BEV	All responded agencies	NASEM, 2018
0.18-0.72	BEV		Christofa, et al., 2017

Cost Rate ($/mile)	Fuel Technology	Transit Agency	Source
0.44-0.90	Diesel	All responded agencies	
0.82	BEV	King County	Eudy and Jeffers, 2018c
0.57	HEV		
0.77	Diesel		
0.41-0.46	BEV	Foothill	Eudy and Jeffers, 2018b; Eudy and Jeffers 2019
0.51-0.66	CNG		
0.74	HEV	SEPTA	DVRPC, 2015
0.27	BEV		
0.4	Diesel	County Connection	Eudy and Jeffers, 2018a
0.73	BEV		

2.5.3 Maintenance Cost

Table 7 summarizes vehicle maintenance cost across a variety of studies. Battery-electric vehicles exhibit lower maintenance costs compared with other fuel technologies across all of the studies. This is not surprising given that battery-electric buses have fewer moving parts than other fuel technologies. Although some agencies have concerns that battery performance may deteriorate over time, most batteries come with a warranty, ranging from 3 to 12 years. Some studies also indicate that battery-electric vehicles have a longer life than the warranties imply, e.g. 12 years (*BYD Motors, Inc. 2015*).

Table 7 – Vehicle Maintenance Cost of Agencies with Electrified Sub-Fleets

Cost Rate ($/mile)			Fuel Technology	Transit Agency	Source
Min	Max	Average			
0.16	1.00	0.72	BEV	All responded agencies	Christofa, et al., 2017
0.22	3.00	1.34	Diesel		
0.22	0.33	0.26	BEV	King County	Eudy and Jeffers, 2018c
0.24	0.4	0.32	HEV		
0.38	0.51	0.46	Diesel		
0.31	0.44		BEV	Foothill	Eudy and Jeffers, 2018b; Eudy and Jeffers 2019
0.23	0.26		CNG		

Cost Rate ($/mile)			Fuel Technology	Transit Agency	Source
Min	Max	Average			
		1.54	BEV	SEPTA	DVRPC, 2015
		2.2	HEV		
0.18	1.47	0.64	BEV	All responded agencies	NASEM, 2018
0.31	0.48	0.39	BEV	County Connection	Eudy and Jeffers, 2018a
0.33	0.62	0.44	Diesel		
		0.6	BEV		Tong, et al., 2017
		0.85	CNG		
		0.74	HEV		
		0.85	Diesel		

2.5.4 Charging Infrastructure Cost

Table 8 summarized charging station cost for a variety of fleets, evaluated as capital and installation cost per charger. An on-route fast charging station costs around 10 times more than a depot plug-in charger. The feasibility and cost of chargers depend on physical space, availability of grid power, property ownership, ease of installation, etc. In addition, chargers installed at the same station can share a transformer, which can reduces the infrastructure cost (*Kunith, et al., 2017*); however, it is important to assess total transformer capacity well in advance of making fleet purchase decisions.

Table 8 – Charging Station Cost of Agencies with Electrified Sub-Fleets

Cost Rate	Type	Transit Agency	Source
$50,000	Depot plug-in	Foothill Transit	Eudy and Jeffers, 2017
$60,000	Depot plug-in	King County	NASEM, 2018
$68,000	Depot plug-in	City of Seneca	NASEM, 2018
$15,000	Depot plug-in	IndyGo	NASEM, 2018
$67,050	Depot plug-in	All responded agencies	NASEM, 2018
$55,000	Depot plug-in		Tong, et al., 2017
$841,510	Overhead conductive	King County	NASEM, 2018
$825,000	Overhead conductive	City of Seneca	NASEM, 2018
$700,000	Overhead conductive	Foothill	NASEM, 2018

Cost Rate	Type	Transit Agency	Source
$698,447	On-route charger[1]	All responded agencies	NASEM, 2018
$1,000,000	On-route charger[1]	SEPTA	DVRPC, 2015

[1] Overhead conductive and wireless inductive are not differentiated.

2.5 Literature Review Summary

In this chapter, we first reviewed previous studies that employed transit fleet replacement models, addressing the different sub-areas used as constraints or objective functions in these different studies. The sub-areas include system monetary cost, environmental performance, health impacts, vehicle routing and scheduling, and infrastructure location selection. These sub-areas interact with each other, implying that focusing on one sub-area may cause a penalty in another. However, to the best of our knowledge, no previous studies explicitly take all of these the sub-areas into account. This is consistent with the argument "*The BEB industry appears to be lacking in standardized technical support and software tools to aid agencies in making procurement decisions and managing BEB fleets. The majority of transit agencies responded that these tools would be beneficial when making decisions regarding range predictions, utility rate analysis, and life cycle cost analyses and adjustments*", from the most report from the NASEM (*2018*). For example, when optimizing fleet procurement and salvage, buses are replaced on a one-to-one basis, with the new bus serves the same route as the salvaged bus. However, this is not necessarily energy-efficient, because fuel efficiency performance varies among different vehicle fuel technologies and among different routes. The one-to-one

replacement strategy may even be infeasible when converting to electrified fleets due to potential range and performance limitations.

Then we review the previous studies about vehicle energy consumption and emissions in fleet optimization models. Some studies simplify this process by applying generalized distance-based energy rates or converting from conventional fuels. However, the approach of using kinematic characteristics and roadway topology to model energy use seems to be a viable option that can achieve reasonable accuracy. We also point out the necessity of life-cycle analysis, i.e. including both upstream and on-road operations.

Then we introduce tools used in this study. We use Autonomie® and MOVES-Matrix for energy and emission modeling, described in Chapter 4. Also, we use the commercial solver CPLEX for solving the proposed optimization models in Chapter 5-Chapter 7.

New topics and problems raised when adopting battery-electric transit fleets, focusing on the common practice in the U.S. are also addressed in the literature review. We briefly go through the grants and incentive programs from federal, state, and regional, introduce the three most common charging facilities, describe the scheduling adjustment practice in several agencies, and point out the impact of utility rate structure.

Finally, we review the fleet electrification costs, including vehicle procurement, operation, maintenance, and infrastructure. These cost values will be the basis of the parameter inputs in the optimization chapters. Table 9 lists the cost values used in the study.

Table 9 – Cost Values Used in the Study

Bus cost		
Bus type	Purchase	Maintenance
Diesel	NA[1]	$0.3/mile
CNG	$400,000	$0.35/mile
Hybrid-electric	NA[1]	$0.4/mile
Battery-electric (100kWh)	$700,000	$0.30/mile
Battery-electric (150kWh)	$725,000	$0.31/mile
Battery-electric (200kWh)	$750,000	$0.32/mile
Battery-electric (300kWh)	$800,000	$0.33/mile
Battery-electric (400kWh)	$850,000	$0.34/mile
Depot plug-in charger cost		
Charger power	Capital	Maintenance
80kW	$50,000	$150/year
On-route fast charging station cost		
Station location	Capital	Maintenance
Within city	$600,000	$1,000/year
Outside city	$500,000	$1,000/year
On-route fast charger cost		
Charger power	Capital	Maintenance
200kW	$20,000	$200/year
300kW	$50,000	$300/year
Energy cost		
Diesel	$2.3/DGE	
CNG	$1.0/DGE	
Demand Charge		
Demand charge rate	$10/kW per month	
Demand Interval	15 minutes	

[1]Not used

CHAPTER 3. DATA INPUTS AND PRE-PROCESSING METHODOLOGY

This chapter describes the data inputs, pre-processing methods, and results. Section 3.1 describes the Metropolitan Atlanta Rapid Transit Authority (MARTA) local transit system used for model implementation throughout the study. Section 3.2 describes the data used in the study. Section 3.3 describes the methodology for developing routing paths for deadheading operations. Routing paths are key inputs when assessing the deadheading energy use, operator cost, and vehicle maintenance cost. Section 3.4 describes the methodology for processing GPS traces. The goal of this process is to generate micro-trip features to represent the roadways traversed and the on-road operating characteristics. The features generated will be used for developing energy use prediction models. Section 3.5 describes the methodology of processing transit feeds data, used to assess the fleet-wide energy use. Section 3.6 provides a summary of this chapter.

3.1 Local Transit Service

The local transit system selected for case study is the Metropolitan Atlanta Rapid Transit Authority (MARTA), the major local urban transit services in Atlanta, Georgia, U.S. Currently, MARTA provides transit bus service to three counties, Fulton, DeKalb, and Clayton, and offers free transfer with its rail service. Most bus routes are designed to feed rail routes, by designing multiple connection points per route with rail stations. The MARTA fleet consists of 455 CNG and 176 diesel vehicles, among which 422 CNG and 125 diesel vehicles are active (*NTD, 2017*). Among the 1,178 transit agencies that provide

fixed-route service, the average number of total fleet vehicles is 61 (*NTD,2017*). Figure 4 shows the model year distribution of the fleet.

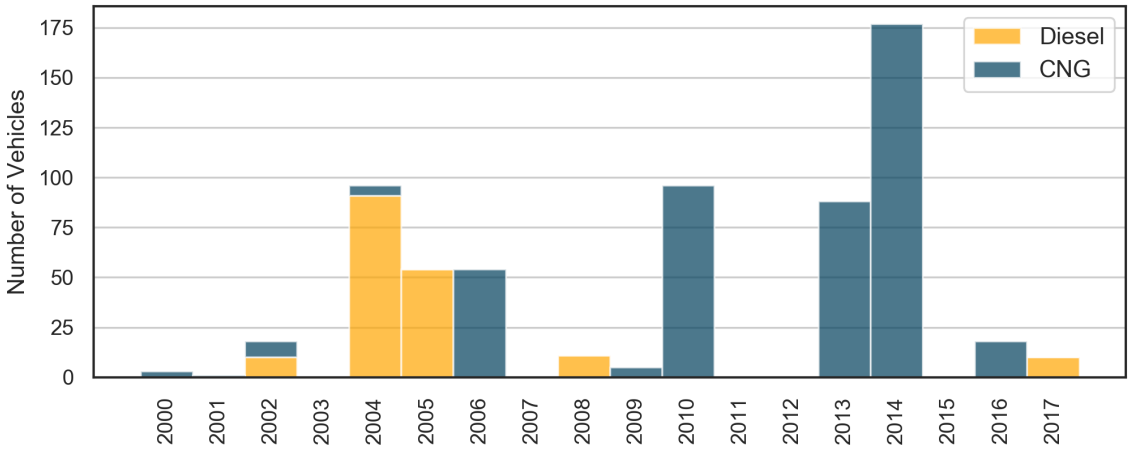

Figure 4 – MARTA Fleet Composition

MARTA operates 110 regular bus routes, connecting 9,188 bus stops (*MARTA, 2018*). Certain commuter routes are offered only during peak service hours, while some other routes are operated for as many as 21 hours per day. Bus stops are placed with a range of 800 to 1,200 feet when possible, typically representing a spacing of no less than two city blocks (*MARTA, 2019*). Revenue routes start and end at 137 unique bus stops, and 55 of them are located within metro rail stations, providing a transfer opportunity to MARTA rail service. In 2017, buses operate 26,238,748 revenue miles and 3,570,589 deadheading miles. Deadhead covers 12% of the total mileage because the starting/ending stops of some transit routes are far away from depots, and interlining events from one route to another occur frequently. The fleet operates 571 tours on weekdays, 342 tours on Saturdays, and 336 on Sundays (*MARTA, 2018*). Figure 5 shows the spatial locations of revenue routes, starting/ending stop, and the three depots that house these vehicles.

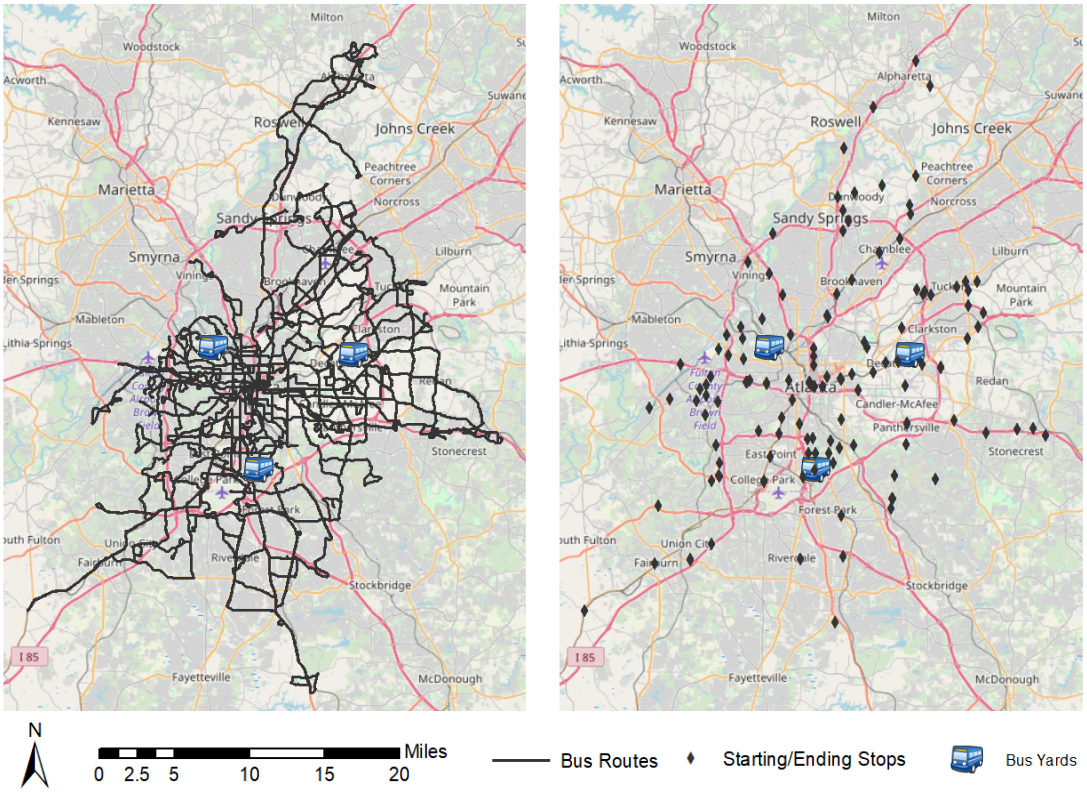

Figure 5 – Spatial Coverage of Local Transit Service

3.2 Data Inputs

The three main data inputs in this framework are transit operations data, taken from the General Transit Feed Specification (GTFS) data; vehicle GPS traces, which can be collected from any bus with a low-cost electronic device or simulated; and roadway GIS files, which are readily available from regional transportation planning agencies. These three data sources can be readily obtained for any major metropolitan area, making the modeling framework readily transferrable to other regions. Each data source is described in the sections that follow.

3.2.1 Transit Operations Data

3.2.1.1 Transit Routes and Scheduling

Transit routes and scheduling data are obtained in the format of the General Transit Feed Specification (GTFS). GTFS is "a data specification that allows public transit agencies to publish their transit data in a format that can be consumed by a wide variety of software applications" (*GTFS website*). GTFS data published in November 2018 are used in this study (*MARTA, 2018*). The extracted information includes: 1) geographic locations of transit stops, 2) shape points of transit routes, 3) time arrival at stops per revenue route, and 4) tour design.

3.2.1.2 Ridership

Ridership data are important inputs in assessing the fuel use of bus operations. Increased vehicle weight due to higher ridership, especially at peak periods, corresponds to higher energy use. This may require more frequent refueling and recharging activities. MARTA collects boarding and alighting counts at the stop level per revenue trip using Automated Passenger Counters. Rider loadings per two consecutive bus stops are then calculated from MARTA's 2018 data, shown in Figure 6. The daily average loading per bus is 8.8 and 6.8 per vehicle during weekday and weekend operations. Average loadings during morning and evening peak can be as high as 9.7 and 9.8 per vehicle, respectively. Loadings above 20 persons per bus only constitute 3.8% of trips and stops, and loadings above 40 persons per bus are less than 0.1%.

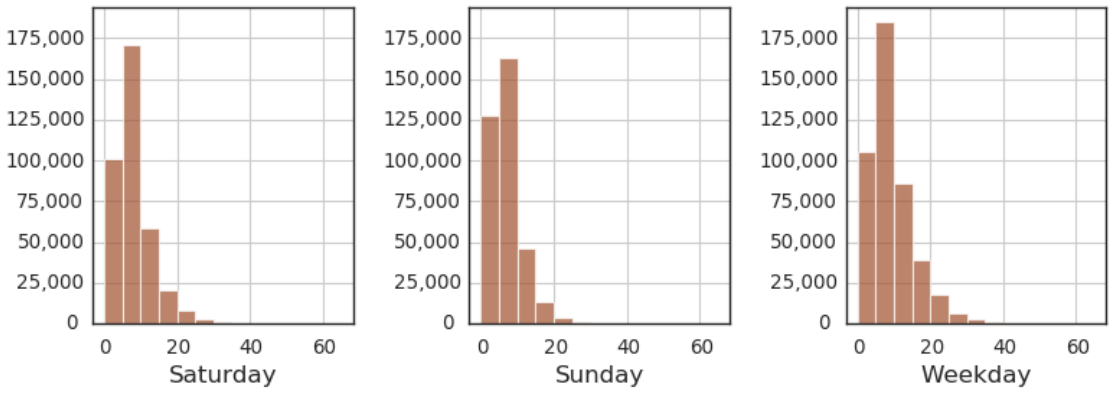

Figure 6 – Histogram of Daily Loadings

3.2.2 Vehicle GPS Data

MARTA does not currently collect their second-by-second vehicle location data for the entire fixed route system. To develop on-road operating characteristics for this study, the research employs second-by-second transit operations data that were collected from 13 buses over a period of 381 days (June 28, 2004 to Oct 24, 2005) using the Georgia Tech Trip Data Collector (*Ogle, et al., 2006*). The data include second-by-second geographic location (latitude and longitude) and vehicle speed. In total, 440 hours of GPS traces are used, and the total distance traveled is 9,270 miles. Figure 7 shows the spatial coverage of the collected GPS traces.

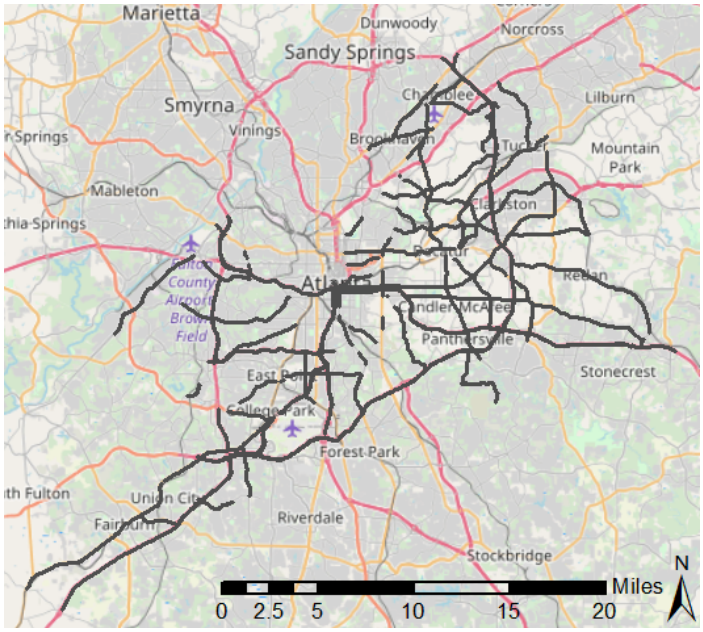

Figure 7 – Spatial Coverage of GPS Traces

3.2.3 Roadway Data

Roadway GIS files in metro Atlanta were obtained from the Atlanta Regional Commission, the metropolitan transportation planning organization (*ARC Website*). The roadway network was originally developed for travel demand modeling, consisting of more than 200,000 roadway links connecting transportation nodes where vehicles enter and exit the links. Each link has a starting node and ending node, indicating its direction. Links also carry a variety of parameters, including information about facility type, free flow speed, and speed limit. Nodes at intersections also carry traffic signal information. In addition, Digital Elevation Model (DEM), an open-source elevation database, (*USGS, 2016*) is used to estimate road grade (*Liu, et al., 2019*).

3.3 Deadhead Routing

Deadheading is an empty bus operation when a bus is moving between a depot and revenue route (or between revenue routes) and is purposefully not serving passengers. Because deadheading consumes energy and provides no passenger revenue, transit agencies strive to reduce deadheading operations. Depot pull-out is the drive from the depot to the first revenue stop, and depot pull-in is the drive from the last revenue stop to the depot. The other deadheading type is interlining between two bus routes, i.e. traveling from the ending stop of one revenue route to the starting stop of another. Deadheading is a non-trivial portion of transit operations, especially for large transit agencies with multiple depots and revenue routes. The start and end points of revenue routes do not necessarily occur at bus depots. In this study, deadheading paths are obtained by implementing a shortest-path routing module.

3.3.1 Shortest-path Routing Module

Shortest-path routing is conducted by using the Transit Simulator, developed by Georgia Tech (*Li, et al., 2018b*). The roadway network from ARC, consisting of 200,000 links, is used for launching the routing module. In fact, the tool can be used to find the shortest network path of any origin-destination pair. The speed and travel time of each link can come from any source, including monitored data or the ARC travel demand model for congested speed. The module generates the paths of each origin-destination pair with the minimum travel time. The background routing graph is established by using roadway links as directed edges, and travel time as weight. Main steps of the routing module are:

1) Find the closest node of the origin location as the origin node;

2) Find the closest node of the destination location as the destination node;
3) Use Dijkstra's algorithm to find the routing path between the origin and destination nodes;
4) Output the shortest-path, consisting of a directed list of roadway links.

3.3.2 Deadheading Operations

Three sets of deadheading routing paths are generated: 1) depot pull-in paths, generated by using the last bus stop of a revenue route as origin, and bus depot as destination; 2) depot pull-out paths, generated by using the bus depot as origin, and the first bus stop of a revenue route as destination; and 3) interlining paths, generated by using the last bus stop of one transit route as origin, and the first bus stop of the next transit route as destination. The paths of existing deadheading operations from MARTA are generated first, and then potential deadheading alternatives are generated.

3.3.2.1 Existing Deadheading Operations

Table 10 summarizes the origins/destinations and frequencies of the MARTA deadheading operations. More frequent pull-in/pull-out activities occur on weekdays because some buses are dispatched specifically for peak hour service. The number of ending stops for depot pull-in is different from the number of starting stops for depot pull-out because of the interlining activities during a tour. That is, a bus is pulled out to one revenue route, and is finally pulled in from a different revenue route. Interlining is categorized into two types, based on whether or not driving is involved.

Table 10 – Current Deadheading Practice

Deadhead Type	Origins (Count)	Destinations (Count)	Daily Frequency		
			Weekday	Saturday	Sunday
Depot pull-out	Depots (3)	Starting stops (118)	571	342	336
Depot pull-in	Ending stops (110)	Depots (3)	571	342	336
Non-driving interlining	Ending stops (117)	Starting stops (117)	8,744	7,252	7,215
Driving interlining	Ending stops (21)	Starting stops (23)	91	2	2

Table 11 shows the fleet-wide daily pull-in/pull-out distance and travel time. The daily amount on weekends are around 60% of a weekday in terms of both distance and time.

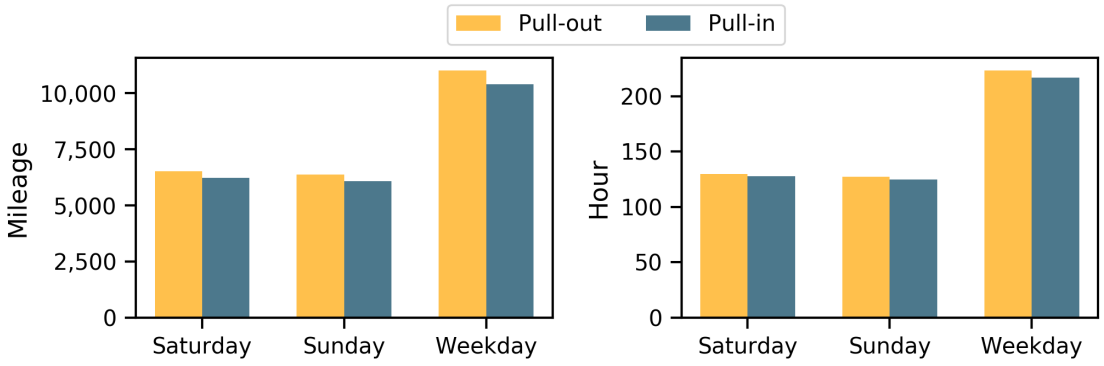

Figure 8 – Daily Pull-in/Pull-out Mileage

Deadheading paths of buses per depot are shown in the map below. In total, 67% and 33% of pulling in/pull-out operations are on highway and local roads, respectively.

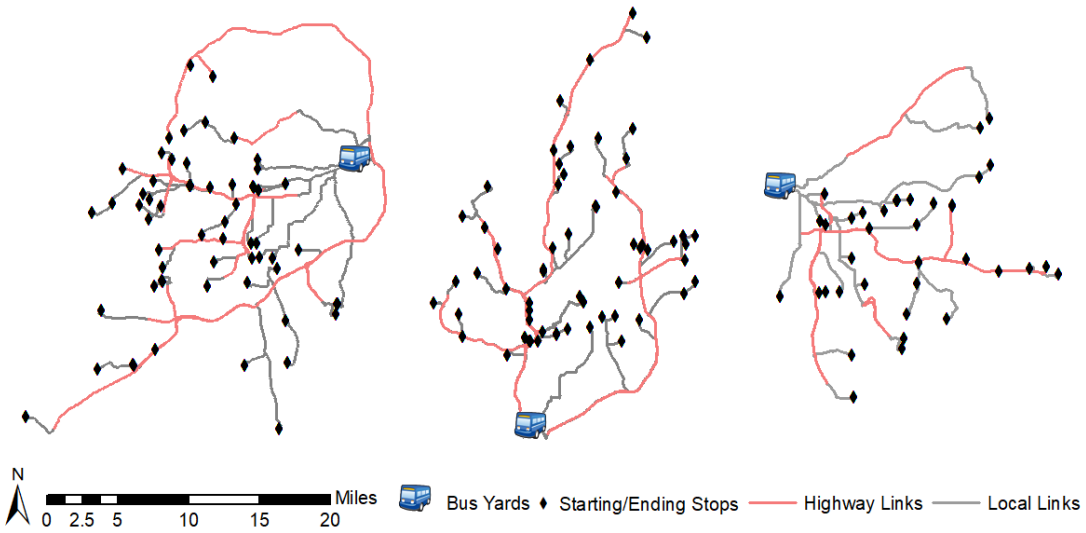

Figure 9 – Depot Pull-in/Pull-out Paths

3.3.2.2 Potential Deadheading Alternatives

Reducing deadheading can be an effective strategy to reduce transit vehicle energy use and operating costs (*Li, et al., 2016*). Therefore, this study evaluates the benefits of reducing deadhead through re-assigning buses to depots in Section 5.3 and re-coordinating transit trips through revenue trip chaining (tour design) in Section 5.4. Paths of potential deadheading alternatives are generated among all the stop-depot, depot-stop, and stop-stop pairs. Table 11 summarizes all the deadheading alternatives.

Table 11 – Deadheading Alternatives

Deadhead Type	Origins (Count)	Destinations (Count)	Number of Pairs	Average Mileage
Depot pull-out	Depots (3)	Starting stops (137)	411	13.4
Depot pull-in	Ending stops (137)	Depots(3)	411	13.6
Non-driving interlining	Ending stops (137)	Starting stops (137)	137	0
Driving interlining	Ending stops (137)	Starting stops (137)	18,632	15.8

Figure 10 shows the distribution of deadheading distance. The driving distance of depot pull-in/pull-out mileage varies greatly, indicating the importance of optimizing bus-to-depot assignment to reduce deadheading cost. More than 8.5% of the interlining alternatives are less than five miles and more than 2.4% of the interlining alternatives are less than two miles.

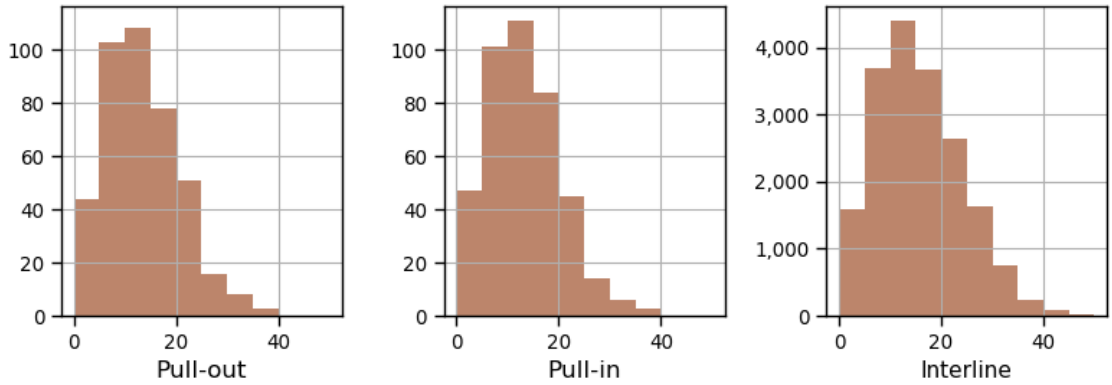

Figure 10 – Distance Distribution (Miles) of All Deadheading Alternatives

3.4 GPS Traces Pre-processing

3.4.1 Workflow

Figure 11 shows the flowchart of pre-processing raw GPS traces to generate two types of outputs, operating cycles and operation-related features. Operating cycles include second-by-second on-road operating speeds with grade appended, created at the level of micro-trips. In this study, micro-trips are defined as operations between two consecutive transit stops. Operating cycles are used as simulation inputs to generate vehicle energy use per cycle. One caveat is that idling is excluded from the modeling work because engine on/off data were not collected. Meanwhile, eight operation-related features are generated per micro-trip, representing the roadway and operating features. Feature engineering is

described in detail in Section 3.4.2. These features are used as modeling inputs to predict energy use.

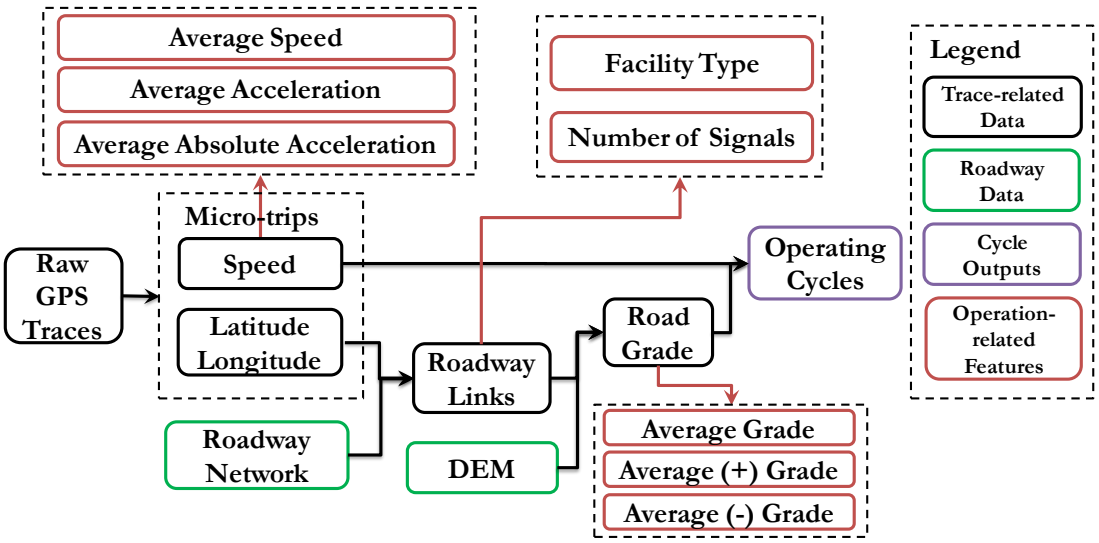

Figure 11 – Flowchart of GPS Data Pre-processing

3.4.2 Feature Engineering

3.4.2.1 Facility type

When operating on local roads, buses have more frequent stop-and-go activities whereas on restricted highways, buses mostly cruise. Therefore, facility type is used to categorize operations into restricted highways and local roads. We first match each GPS point with its roadway link, and then append the facility type information to each point. Then each micro-trip is labeled with the majority of the facility type of its GPS points. In total, we identified 17,206 micro-trips on local roads, covering 651 miles and 389 hours, and 638 micro-trips on restricted highways, covering 2,619 miles and 51 hours.

3.4.2.2 Number of Traffic Signals

Number of traffic signals is used to reflect stop-and-go operations. After matching the GPS points of a micro-trip with roadway links, the number of signals during this micro-trip can be obtained by counting the links with signals. Figure 12 shows the distribution of the number of signals per local micro- trip.

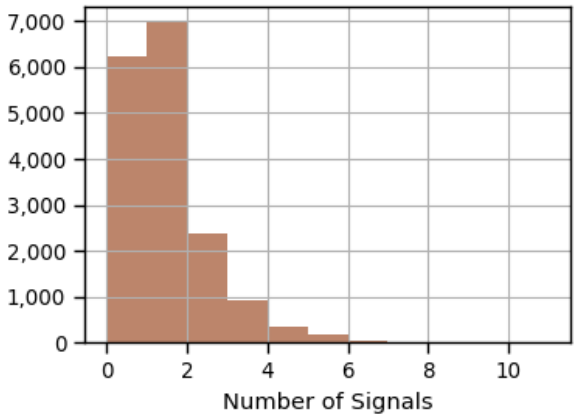

Figure 12 – Distribution of Number of Signals: Micro-trips from GPS Traces

3.4.2.3 Average Speed

Speed is a key factor impacting energy consumption because speed relates to the loading demand of the vehicle power system. Per micro-trip, the average speed feature is calculated by dividing the distance (mile) with the duration (hour). Figure 13 shows the average speed distribution of local and highway operations.

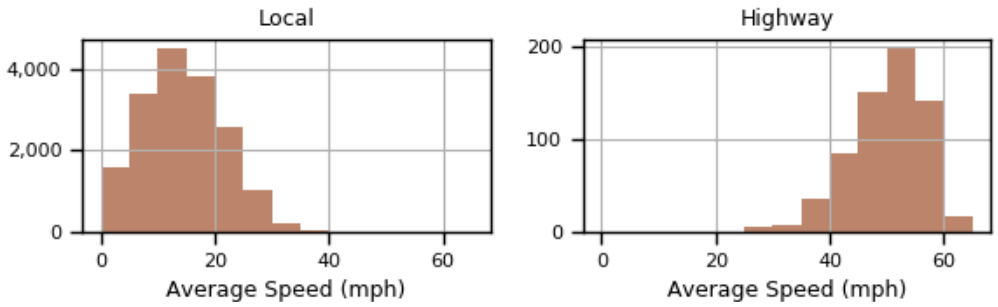

Figure 13 – Distribution of Average Speed: Micro-trips from GPS Traces

3.4.2.4 Average Grade

Road grade is another factor that significantly impacts energy consumption. Grade (rad) per GPS point is generated by using the method developed by Liu, et al. (*2018*). Then the average grade feature (Avg_{Grade}) is generated by using speed as weight, denoted in equation (1), where mph_i represents speed at timestamp i, $grade_i$ represents grade value at timestamp ti, and Dur represents the micro-trip duration. Two other grade-related features, average positive grade (Avg_{Grade_pos}) and average negative grade (Avg_{Grade_neg}) are generated using equation (2)-(3). The reason for creating these two features is to capture the ups and downs of roadway curvature. For example, $Avg_{Grade} = 0$ when the roadway is entirely flat, or ups and downs offset each other; however, energy use can be different between these two cases.

$$Avg_{Grade} = \frac{\sum_{ti=1}^{ti=Dur} mph_{ti} grade_{ti}}{\sum_{ti=1}^{ti=Dur} mph_{ti}} \quad (1)$$

$$Avg_{Grade\_pos} = \frac{\sum_{\forall grade_i>0, 1\le ti\le Dur} mph_{ti} grade_{ti}}{\sum_{ti=1}^{ti=Dur} mph_{ti}} \quad (2)$$

$$Avg_{Grade\_neg} = \frac{\sum_{\forall grade_i<0, 1\le ti\le Dur} mph_{ti} grade_{ti}}{\sum_{ti=1}^{ti=Dur} mph_{ti}} \quad (3)$$

Figure 14 shows the distributions of the three grade features. Grade on restricted highways are smoother than local roads.

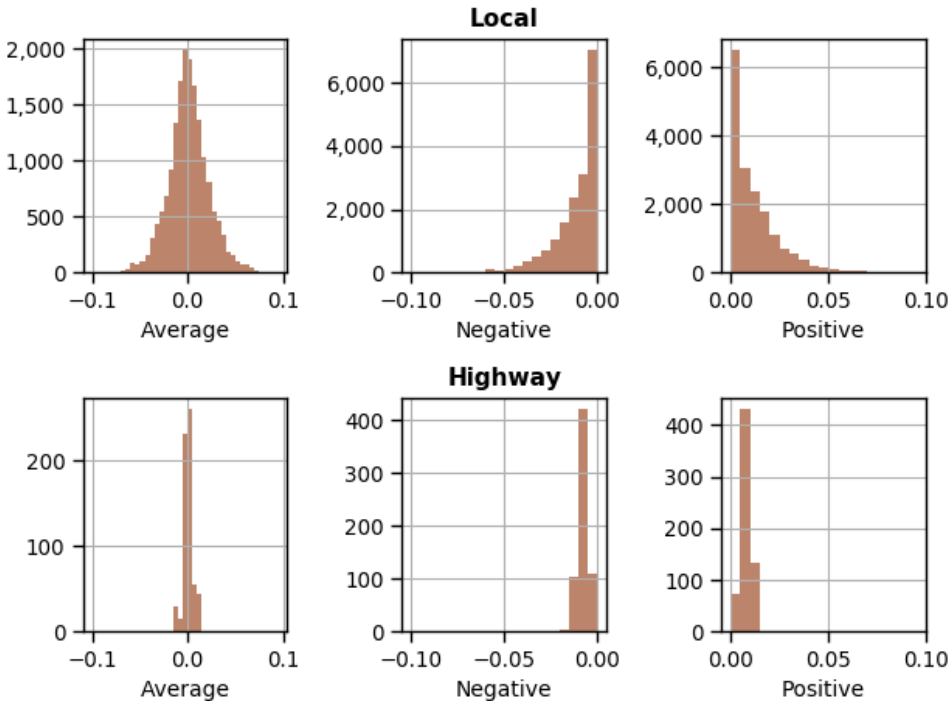

Figure 14 – Distribution of Grade Features: Micro-trips from GPS Traces

3.4.2.5 Average Acceleration

Acceleration and braking activities greatly impact energy use. Two features are created to capture acceleration activities, i.e. average acceleration and average absolute acceleration. The distributions of these two features are shown Figure 15. We see smoother accelerating behavior on highways. This is because most of the highway operations occur during depot pull-in/pull-out activities at off-peak hours. However, on local roads, there are frequent stop-and-go activities due to stop signs, traffic signals, traffic congestion, and transit stop design.

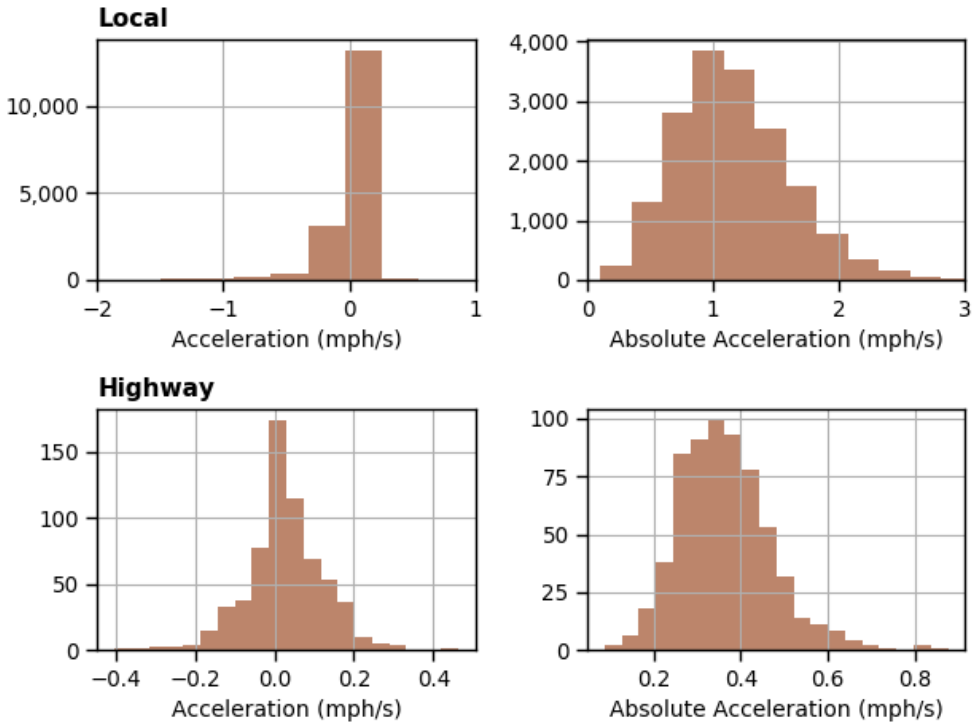

Figure 15 – Distribution of Average Acceleration: Micro-trips from GPS Traces

3.5 GTFS Data Pre-processing

3.5.1 Workflow

To be consistent with the terms used in Section 3.4, the operations between each two consecutive stops of a revenue trip are defined as a micro-trip. Unlike GPS traces whose second-by-second locations and speed are recorded, locations and timings from GTFS data are limited to the stop level and cannot directly represent the operating trajectories. To solve this problem, shortest-path routing module is implemented to identify the routing paths (a set of roadway links) per micro-trip, in a way similar to the deadheading routing in Section 3.3.

3.5.2 Feature Engineering

3.5.2.1 Average speed

Average speed is calculated as the total distance of the micro-trip (mile) divided by the total duration of the micro-trip (hour). Because micro-trip distance is not readily available in the MARTA GTFS data, distance is estimated in three steps:

1) Extract the shape points (shapes.txt) based on geographic locations of the two consecutive stops from (stop.txt);
2) Connect consecutive shape points and calculate the distance;
3) Aggregate the distance to obtain the micro-trip distance.

Figure 16 shows the distance distribution of the micro-trips. The micro-trips with distance longer than 1 mile are not shown here. These long micro-trips only cover 0.6% of the trips and operate on highways. The micro-trip duration is calculated using the departure time from a stop and the arrival time at the next stop.

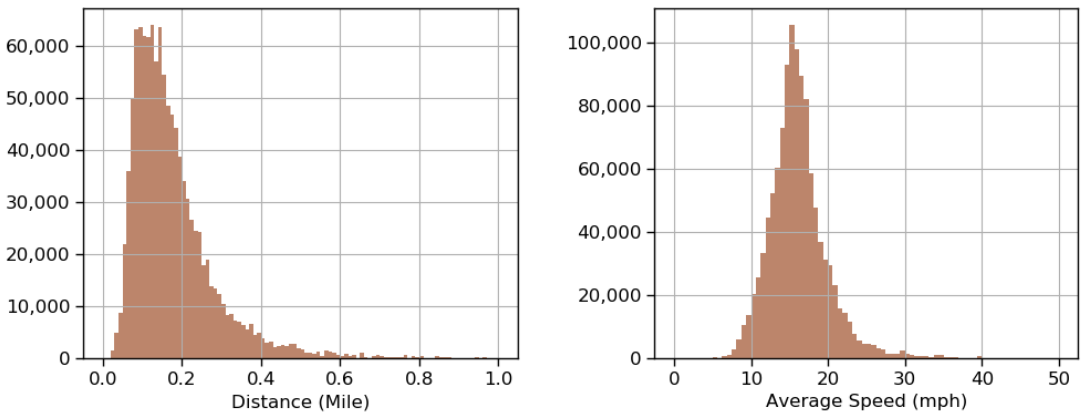

Figure 16 – Distribution of Distance and Average Speed: Micro-trips from GTFS Data

3.5.2.2 Average Grade

Grade points are created every 50 feet along the roadway links by using the method developed by Liu, et al. (*2019*). Then the three grade features are generated by averaging the values of the grade points among all links, denoted in equation (4)-(6). $Links$ represents the set of links and li is the link identifier. The number of grade points from Link li is Num_{li}, and pi is the grade point identifier. The grade value of the grade point pi from link li is denoted as $grade_{li,pi}$.

$$Avg_{Grade} = \frac{\sum_{\forall li \in Links} \sum_{pi=1}^{pi=Num_{li}} grade_{li,pi}}{\sum_{\forall li \in Links} Num_{li}} \quad (4)$$

$$Avg_{Grade\_pos} = \frac{\sum_{\forall li \in Links} \sum_{\forall grade_{li,pi}>0, pi \in \{1,\ldots,Num_{li}\}} grade_{li,pi}}{\sum_{\forall li \in Links} Num_{li}} \quad (5)$$

$$Avg_{Grade\_neg} = \frac{\sum_{\forall li \in Links} \sum_{\forall grade_{li,pi}<0, pi \in \{1,\ldots,Num_{li}\}} grade_{li,pi}}{\sum_{\forall li \in Links} Num_{li}} \quad (6)$$

Figure 17 shows the distribution of grade features. The proportion of micro-trips with average grade within (-0.01, +0.01) radian is 46.3%.

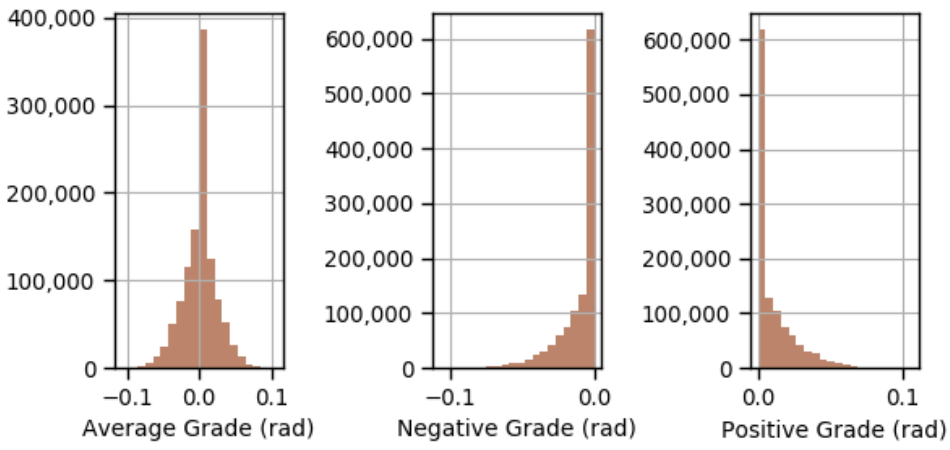

Figure 17 – Distributions of Grade Features: Micro-trips from GTFS Data

3.5.2.3 Other Features

Routing paths of each micro-trip is represented as a set of roadway links. Facility type is identified by using the majority facility type of the roadway links. Highway micro-trips only cover 0.4% of the total revenue mileage. The number of signals is obtained by counting the number of roadway nodes with signals. Figure 18 shows the distribution of the number of signals per micro-trip. As for the acceleration features, we use the average values from GPS traces because no speed trajectories are available from the GTFS data.

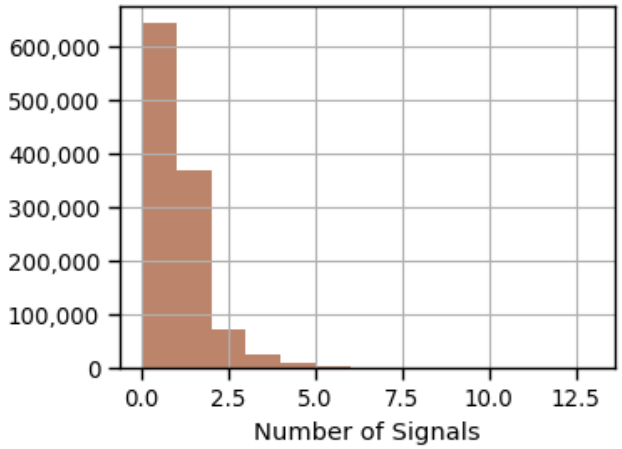

Figure 18 - Distribution of Number of Signals: Micro-trips from GTFS Data

3.6 Summary

In this chapter, we describe local transit agency for model application, the main data inputs, and pre-processing methods. Most of the data sources are open to public or easy to collect. Deadheading paths are generated using the shortest-path algorithm described in this chapter. These paths will be used for the energy evaluation in Chapter 4 and optimization models in Chapter 5 through Chapter 7. In real-world practice,

deadheading paths of the existing transit network may be readily available in some agencies; however, deadheading paths will still need to be generated when evaluating potential deadheading alternatives, like interlining from one route to another new route, and pulling buses to a new depot. The pre-processing steps of GPS traces and GTFS data to generate micro-trip features are described in detail. The features consist of number of signals, facility type, average speed, acceleration and grade, which will impact the vehicle energy use. The methods can be easily applied to other transit agencies.

CHAPTER 4. ENERGY SIMULATION AND MODELING APPLICATIONS

This chapter describes the methodology of energy simulation and modeling applications that will be used in the overall optimization frameworks. The goal of this process is to estimate vehicle energy use under a variety of different environmental and on-road operating conditions. Section 4.1 introduces the energy simulation and modeling methodologies. Section 4.2 describes the process of energy simulation. Section 4.3 describes the models constructed from the simulations for predicting micro-trip energy use. Section 4.4 applies these energy models to MARTA transit agency operations to estimate the fleet-wide energy use. Section 4.5 summarizes the energy simulation and modeling results.

4.1 Energy Simulation and Modeling Workflow

Figure 19 shows the flowchart of model development and application. Energy use is simulated using Autonomie® and MOVES-Matrix based on the real-world second-by-second operating cycles. The methods for pre-processing GPS traces were described earlier (Section 3.4). Roadway network development and processing of DEM data to obtain road grade are required for the model, but omitted from this workflow diagram. Several sets of parameters are required to represent vehicle fleet specifications. Then, machine learning models are used to predict the energy rate at the micro-trip level based upon vehicle-related and operations-related features. The model with the best performance is selected as the final model to predict the energy use of micro-trips from the real-world

GTFS data. Methods for pre-processing GTFS data were described earlier (Section 3.5). Finally, micro-trips can be aggregated for any route or tour to estimate emissions from a vehicle, and all micro-trips can be aggregated to estimate fleet-wide energy use.

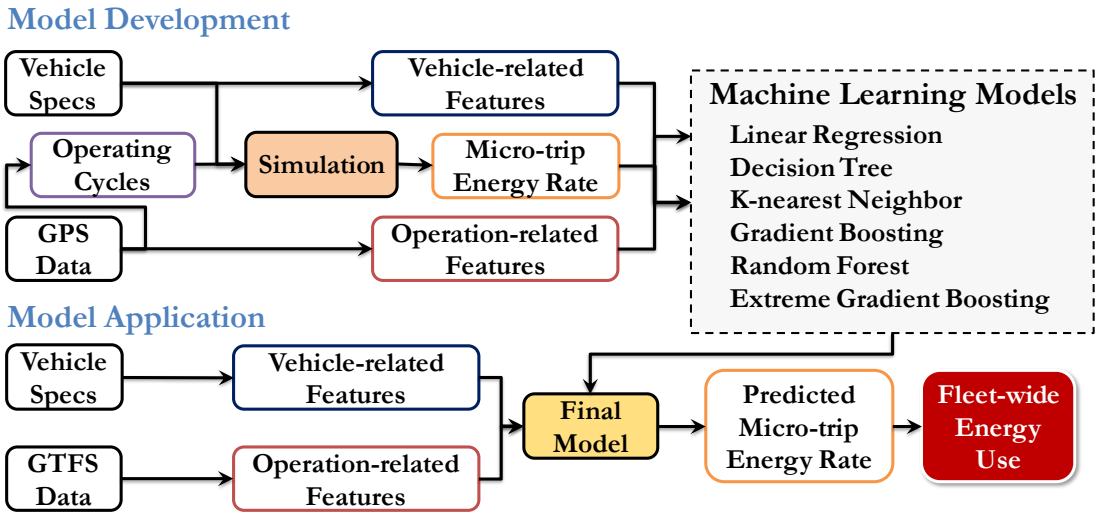

Figure 19 – Energy Use Model Development and Application

4.2 Energy Simulation

4.2.1 Energy Simulation Workflow

Figure 20 shows the flowchart for energy simulation. Two energy modeling tools are used, Autonomie® and MOVES-Matrix. The reason for using two tools is that neither of them can directly model all of the scenarios needed in this study; however, linking the two of them provides a feasible alternative. Both models simulate the energy use based on the input operating cycles and vehicle characteristics. Three vehicle fuel technologies (diesel, hybrid-electric, and battery-electric) are simulated in Autonomie®, and two (diesel and CNG) are simulated in MOVES-Matrix. The two tools are linked via the conversion

factor in the base model, and finally the energy rate per micro-trip of all vehicle technologies are generated.

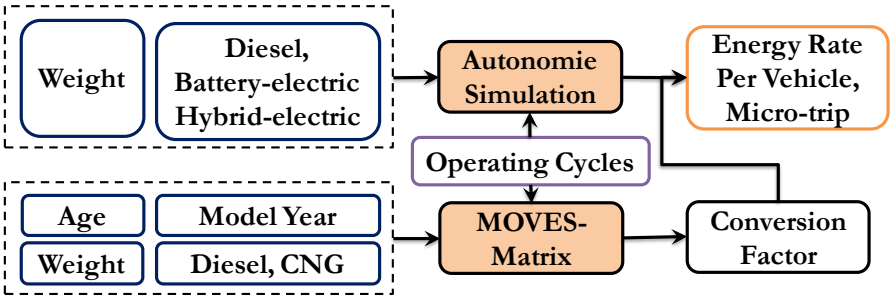

Figure 20 – Flowchart of Micro-trip Energy Simulation

MOVES-Matrix has the capability of modeling the on-road energy use of diesel and CNG buses with different environmental conditions, year, and vehicle model year. But, MOVES cannot directly model the energy consumption of hybrid-electric or battery-electric buses. While MOVES-Matrix allows the incorporation of vehicle weight and passenger load in energy use and emissions calculations, by properly calculating scaled tractive power (*Xu, et al., 2015*), the increased vehicle weight at moderate ridership levels is generally not large enough to shift activities into STP modeling bins with a higher energy rate. That is, even though fuel efficiency does differ significantly between a fully-loaded bus at peak periods and a deadheading empty bus, the binned energy and emission rates used in MOVES are not sensitive enough to fully account for the impacts of ridership.

On the other hand, Autonomie® has the capability of modeling hybrid electric, battery-electric, and diesel vehicles, with base models embedded. Users also have the flexibility of customize the base models with specific characteristics. Autonomie® has been widely used to evaluate the impact of different vehicle components on fuel efficiency performance, especially vehicle weight (*Pagerit et al., 2006*). However, the current version

does not have a CNG base model. Autonomie® provides the alternative of designing a vehicle from scratch, but the design would not be accurate without detailed calibration and model component verification. One key input is the engine map, which varies across makes, models, and model years and is not practical for implementing in this research effort. Moreover, vehicle model year and future year scenarios also require customized inputs that are not available in this study.

The two tools are linked via a base diesel vehicle, which can be simulated in both tools. Conversion factors for these two tools are calculated relative to the base vehicle, and then applied to estimate the energy use for all scenarios. Details of the conversion process are discussed in Section 4.2.4.

4.2.2 Autonomie® Simulations

Table 12 shows the parameters of the four vehicle models, specified based on current vehicle market and previous studies. Five ridership levels are simulated, representing empty, 25%, half-full, full, and overloaded. The average weight of a passenger is set as 150 lbs. referring to the standards from Federal Transit Administration (*FTA, 2016*).

Table 12 – Simulation Parameters

Vehicle Type	Diesel	Hybrid	EV	CNG[1]
Frontal area (m^2)	8.5	8.5	8.5	8.5
Aerodynamic drag (CdA in m^2)	0.79	0.79	0.79	0.79
Coefficient of tire rolling resistance	0.0098	0.0098	0.0098	0.0098
Tare weight (kg)	11,793	12,927	13,835	12,927
Ridership	5 levels: 0, 10, 20, 40, 60			
Battery capacity (kWh)	NA	5	200	NA
Max motor power (kW)	NA	120	190	NA
Max engine power (kW)	209	191	NA	209

[1]CNG bus is not directly simulated, but converted from diesel shown in Section 4.2.4

Batch runs are launched for each set of micro-trips and vehicle specification. In total, all the micro-trips (17,206 on local roads and 638 on restricted highways) are simulated at each ridership level with each vehicle fuel technology. Figure 21 shows the energy rates of each micro-trip, evaluated as MJ/mile, when vehicles run empty. The extreme cases with high fuel use are because of aggressive acceleration or climbing high hills. Energy rates are high on local roads due to the frequent stop-and-go operations, especially for conventional diesel and CNG vehicles. The effect of regenerative braking on hybrid-electric and battery-electric vehicles, yields significantly lower energy use rates for these vehicles on local roads. In some micro-trips, energy rate values are negative, which mostly occur when vehicles brake and go downhill.

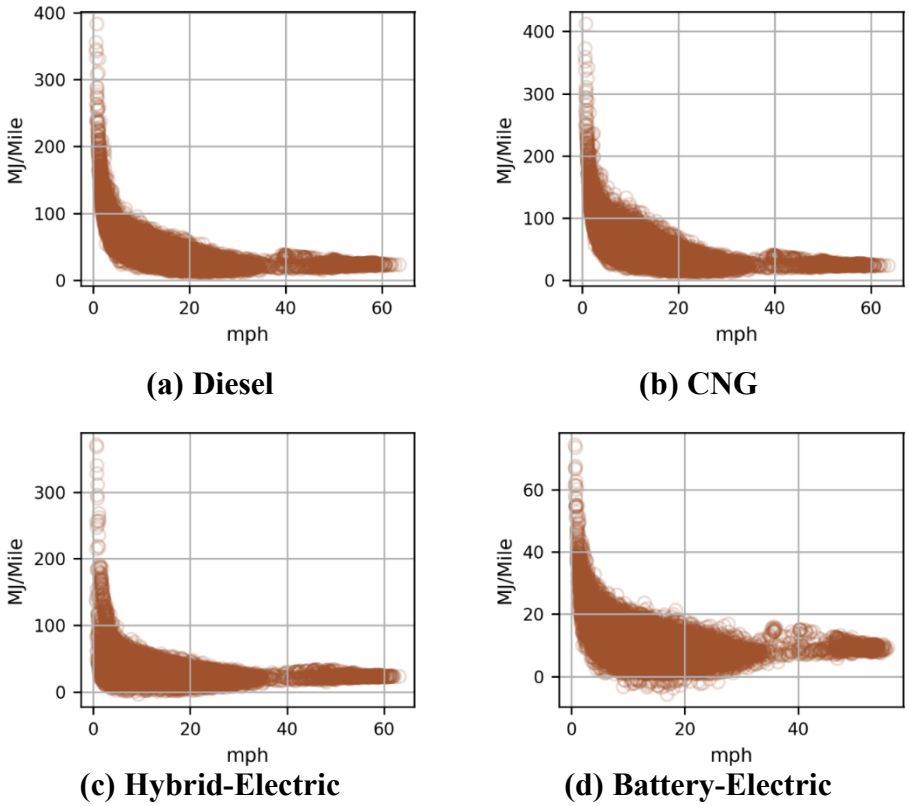

Figure 21 – Energy Rate vs. Average Speed per Micro-trip

The impact of vehicle weight on energy rate is explored by categorizing vehicle weight into five ridership levels, shown in Figure 22. As expected, energy rates increase greatly with ridership for both CNG and diesel vehicles; whereas we see a smaller increase for battery-electric vehicles. On average, for battery-electric vehicles, fuel rate increases by 0.33MJ/mile per 1,000 metric tonnes of weight increase.

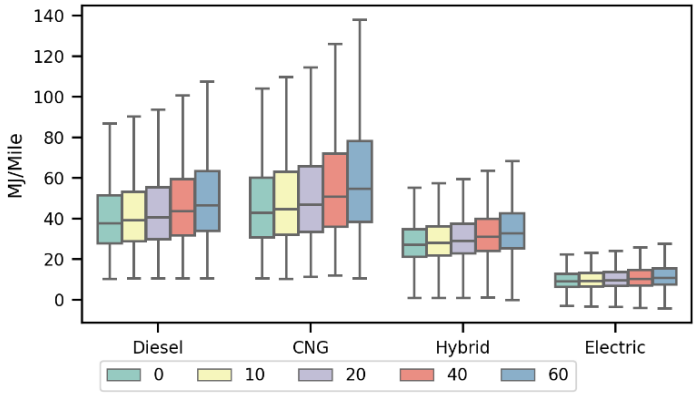

Figure 22 – Impact of Ridership on Energy Rates

4.2.3 MOVES-Matrix Modeling

4.2.3.1 Scenario Set-up

MOVES-Matrix is launched to obtain the energy rates for diesel and CNG transit buses. The meteorology selected for the case studies is the default summer morning peak hour in Atlanta, with a temperature of 70F, and humidity of 85%. The energy use and emission rates cover calendar year ranging from 2019 to 2039, and vehicle ages range from 0 to 30 years. For each second of operation, STP operating mode bin is calculated based on vehicle weight, speed, acceleration, and grade (*Guensler, et al., 2017*). After that, the corresponding emission rate of each set of fuel type, calendar year, and vehicle age is appended to that second based on the STP bin.

4.2.3.2 STP Operating Mode Bin Distribution

STP bin is calculated for each second per micro-trip. STP bin distributions among all micro-trips are shown in Figure 23. Cruising/acceleration is the dominant mode for highway operations because most highway operations occur when buses deadhead at off-peak periods. In contrast, braking and idling are modes are more frequent in local operations. In Appendix B, equation (187) denotes the calculation of STP value, and Table 40 lists the description and definition of each operating mode bin in MOVES.

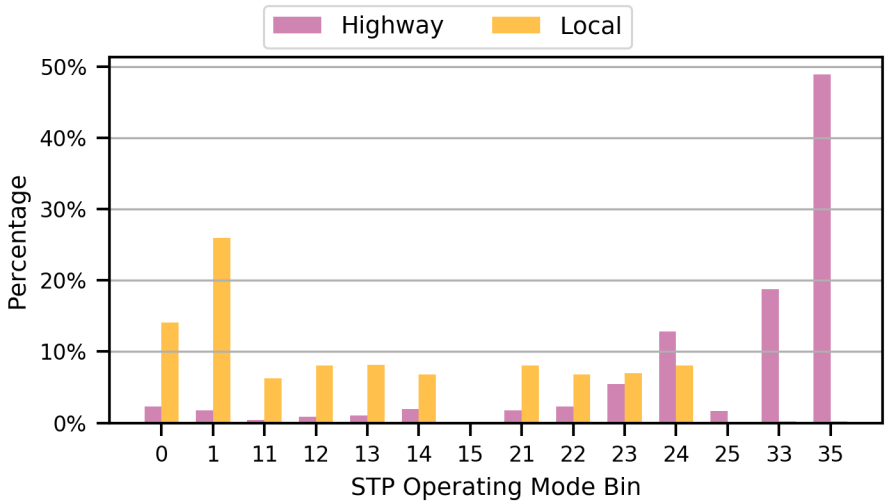

Figure 23 – MOVES STP Bin Distribution

4.2.4 Conversion Ratio

Conversion ratio is used to model energy rates in scenarios that cannot be directly simulated in Autonomie®, but can be modeled in MOVES-Matrix. These scenarios include: 1) CNG buses, and 2) diesel and hybrid-electric buses with model year earlier than 2019, i.e. vehicle age older than zero years. These scenarios are defined as "new bus scenarios." The establishment of the conversion ratio is based upon the assumption that for one micro-trip, the ratio of energy rates between two bus types modeled in MOVES-

Matrix should hold when modeled in Autonomie®. Therefore, a conversion ratio is generated per micro-trip between the new bus scenario and the base scenario. In this study, the base scenario is selected as diesel buses, with empty weight, model year 2019, and calendar year 2019. The energy use of the base scenario can be quantified in both Autonomie® and MOVES-Matrix. The conversion ratio is applied in two steps:

1) Calculate the conversion ratio in MOVES-Matrix, denoted in equation (7). Conversion ratio for micro-trip mi is calculated as energy use of the new scenario ($EM_{mi}^{f_{New}}$) divided by the energy use of the base scenario ($EM_{mi}^{f_{Base}}$). For micro-trip mi, its energy use is calculated by aggregating the energy use of each second. BIN_{mi} denotes the set of STP bins in trip mi. $Dur_{mi,si}$ denotes the total duration with operating mode bin si in trip mi, and $ER_{si}^{f_{New}}$ ($ER_{si}^{f_{Base}}$) denotes the MOVES energy rate of the new (base) scenario.
2) Apply the conversion ratio to obtain the estimated energy use ($EA_{mi}^{f_{New}}$) of micro-trip mi, denoted in equation (8). $EA_{mi}^{f_{Base}}$ denotes the energy use of the base scenario, obtained from Autonomie®.

$$Ratio_{mi}^{f_{New}} = \frac{EM_{mi}^{f_{New}}}{EM_{mi}^{f_{Base}}} = \frac{\sum_{\forall si \in BIN_{mi}} Dur_{mi,si} ER_{si}^{f_{New}}}{\sum_{\forall si \in BIN_{mi}} Dur_{mi,si} ER_{si}^{f_{Base}}} \quad (7)$$

$$EA_{mi}^{f_{New}} = Ratio_{mi}^{f_{New}} EA_{mi}^{f_{Base}} \quad (8)$$

Figure 24 shows the conversion ratio distribution of CNG vehicles. On average, the ratio is 1.15, indicating 15% higher energy use at the vehicle for CNG buses compared with its diesel counterpart, which is consistent with the previous eco-driving for transit study (*Xu, et al., 2016*),

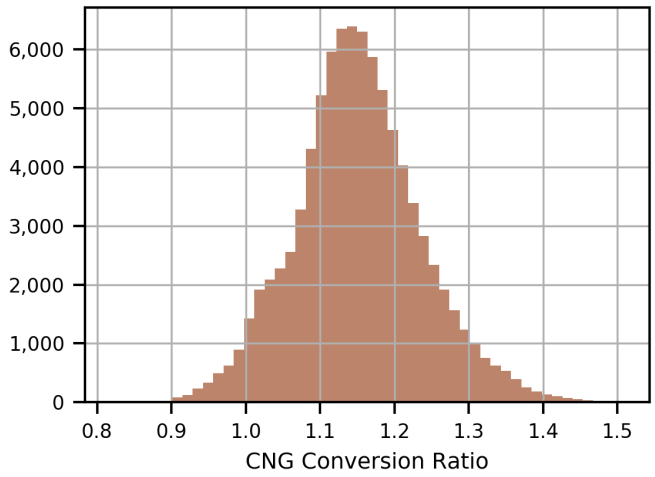

Figure 24 – Histogram of Micro-trip Conversion Ratios for CNG Vehicles

4.3 Energy Prediction Models

The energy rate at the micro-trip level is used as the dependent variable in the prediction model, evaluated as MJ per mile. Prediction features include: 1) operation-related characteristics: trip duration, facility type, number of signals, average speed, road grade, acceleration, and 2) vehicle-specific characteristics: age and ridership level. Age categories are defined as 0-2 (MY 2017-2019), 3-5 (MY 2014-2016), 6-17 (MY 2002-2013), and >17 (MY before 2002), because fuel efficiency per vehicle fuel technology does not differ significantly within each age category. Data are randomly split into 80% training and 20% testing. A training model is developed for each fuel technology and facility type. Common machine learning algorithms are implemented, including linear regression, decision tree, K-nearest neighbor (KNN), gradient boosting, random forest, and extreme gradient boosting (XGBoost) methods. Five-fold cross-validation is used to tune the hyperparameters in each model. The evaluation metric is designed as a combination of R^2 and mean absolute percentage error (MAPE). The option of log-transforming the

dependent variable is also tested. The training and tuning process is implemented using the grid search features in the Python scikit-learn package.

Figure 25 shows the model performance without log-transformation. The simplest algorithm, linear regression, shows the worst performance compared with the other algorithms, especially for highway operations. KNN algorithm shows overfitting with the training dataset, especially in the battery-electric bus model. The performance of the decision tree algorithm is better than linear regression and KNN; however, the MAPE for highway operations is higher than 20% across all vehicle types. The three ensemble algorithms, i.e. random forest, gradient boosting, and XGBoost all show consistently good performance in terms of the R^2 metric. However, XGBoost shows better performance in terms of MAPE than gradient boosting and random forest. Therefore, XGBoost is selected as the final model.

The XGBoost MAPE for battery-electric vehicles is higher than the other types for two main reasons: 1) the fuel rate values are small, and a slight change in absolute value will cause a high percentage change; and 2) the use of regenerative braking adds complexity to the energy estimation. For future studies, the model can take into control-related variables, such as battery state of charge and rule-based control strategies to obtain better results.

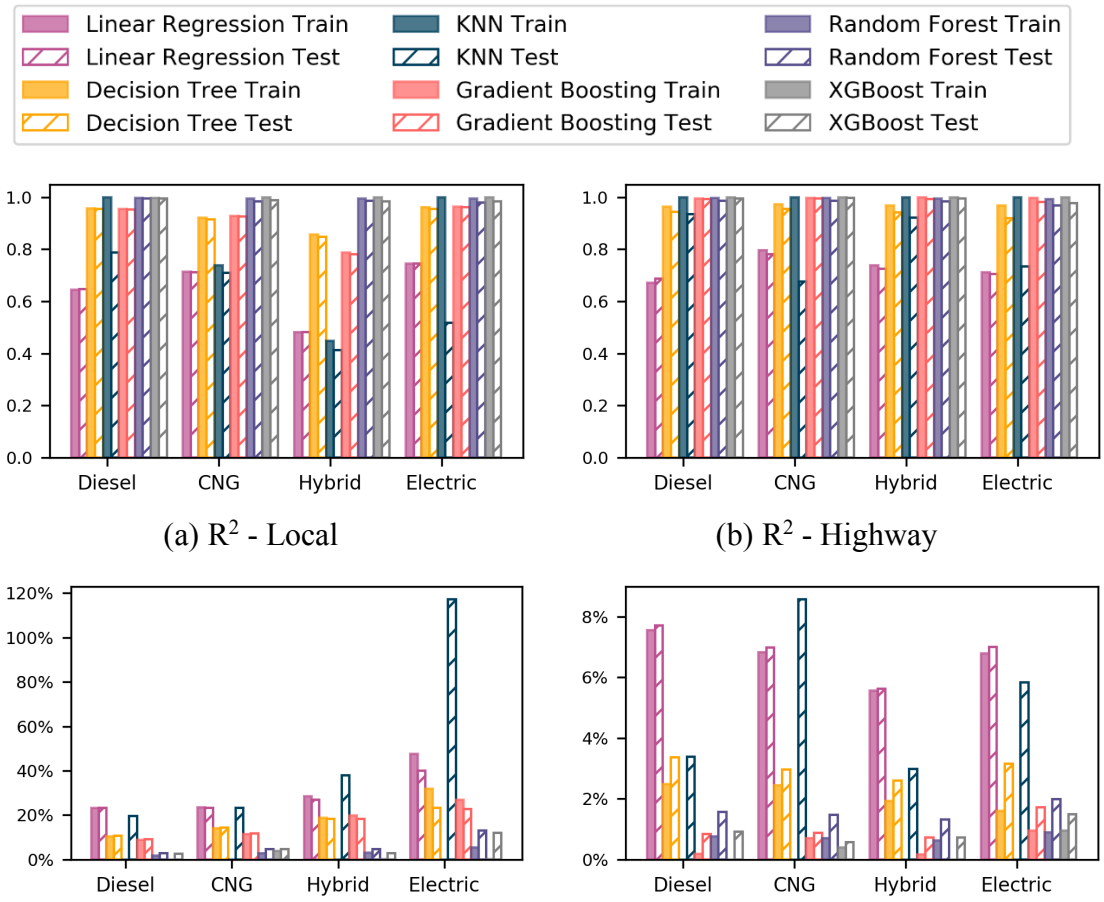

Figure 25 – Machine Learning Model Performance

Comparing the results between whether or not log-transforming the data, the difference is trivial for XGBoost algorithm in terms of R^2, i.e. 0.002 on average for both training and testing sets. When it comes to MAPE, log-transformation achieves better results in most models, especially for CNG vehicles on local roads, shown in Figure 26. Therefore, log-transformation is conducted for all modeling scenarios, except the diesel-local and hybrid-local scenarios. In summary, the average R^2 across eight prediction models is 0.9998 for training and 0.991 for testing. The MAPE achieves an average of 0.3% for training and 2.7% for testing. Although RMSE is not used as an evaluation metric during the model training process, it still gives insights of the model performance. The

RMSE is 1.0 MJ/mile for training, and 1.2 MJ/mile for testing, still indicating good performance.

It is not surprising tha the R^2 values are extremely high for two main reasons. The first reason is that the training set includs over 71,000 micro-trips per vehicle type, large enough to cover a wide range of roadway and operating conditions. The second reason is that the energy use prediction models are fitted to the outputs of a simulation model. In other words, we are essentially identifying the internal model equations and variable relationships that are explicitly embeeded into the simulation modeling tools. The developed energy prediction models are a simplified version of the simulation tools, but have the advantages of achieving early the same results as well as being easy to plug in to the optimization models introduced in the following chapters. One caveat is that the accuracy of these developed models are limited to the accuracy of the simulation tools.

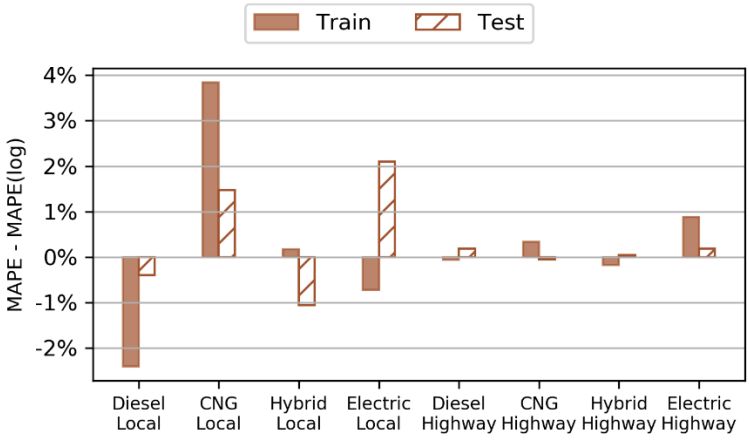

Figure 26 – MAPE Performance Comparison between No-transformation and Log-transformation: XGBoost Algorithm

Figure 27 shows two examples of local revenue service trips, and both of them include 16 micro-trips. The difference of micro-trip energy use between XGBoost-

predicted and Autonomie® simulated ranges from -0.32MJ to 0.30MJ in the hybrid-electric example, and -0.90MJ to 0.91MJ in the battery-electric example. The trip-level energy difference is 0.32% and 0.63% in the hybrid-electric and battery-electric example, respectively. This implies good overall performance.

In fact, XGBoost is generally used for supervised learning problems, and is based on gradient boosting decision tree algorithm (*XGBoost Website*). This is an ensemble technique, in which multiple trees are used together to enhance the predictive performance. Simple models are trained first, and then new models are added sequentially to correct the errors made by existing models until no further improvements can be made. XGBoost has the advantages of fast prediction speed and accurate model performance.

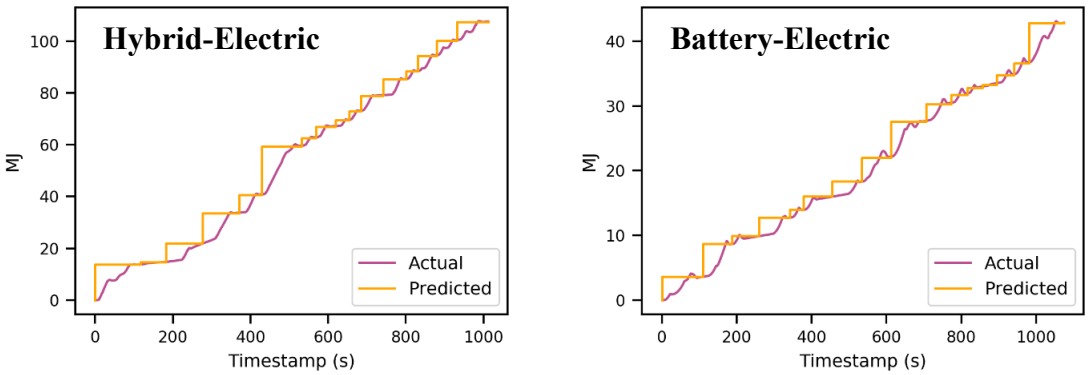

Figure 27 – Cumulative Energy Use: Predicted vs. Actual

Figure 28 shows the results of comparing predicted and actual energy rates of all micro-trips. Overall, the final models achieve good predicting results. As previously mentioned, several micro-trips in the testing sets for battery-electric models show some discrepancies between the predicted and actual values, but overall the simplified modeling approach provides a reasonable fit to complex modeling with Autonomie®. This

performance is not surprising because we are essentially using machine learning to predict the embedded models in the simulation tool.

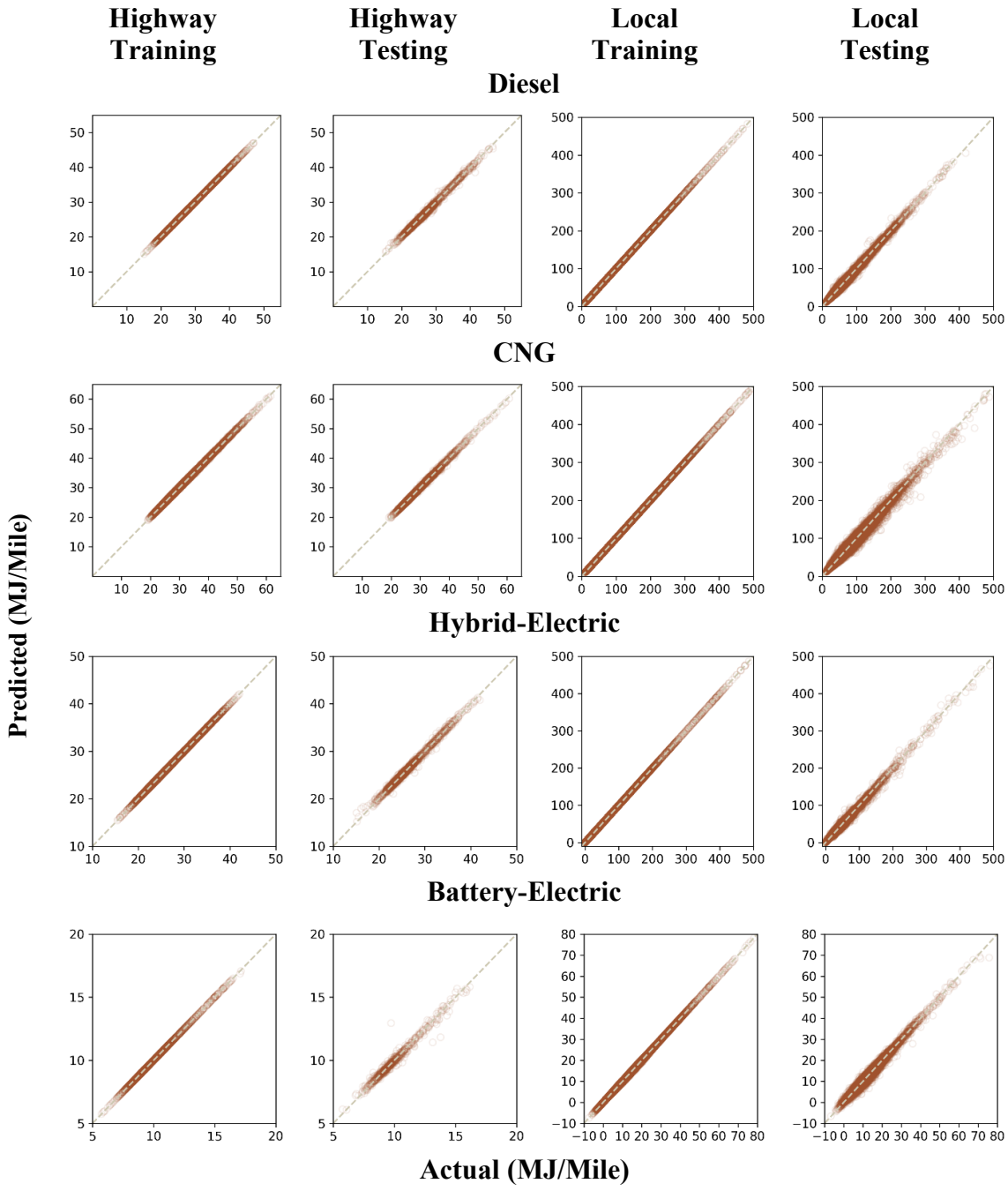

Figure 28 – Predicted vs. Actual per Micro-trip

4.4 Energy Model Applications

Energy use for revenue and deadheading operations are estimated individually first. Then the fleet-wide energy use is estimated per vehicle fuel technology. The energy use is used as inputs in the optimization models in the following chapters.

4.4.1 Revenue Service Energy Use

Using the final energy prediction model, revenue energy use is predicted at the micro-trip level and then aggregated to obtain trip-level and tour-level energy use. Operation-related features are generated by using MARTA GTFS data, described in Section 3.5.2. Ridership is appended to the GTFS data, categorized into five levels. Equation (9) denotes the energy use of revenue trip m if served with a type f vehicle. Revenue trip m consists of a set of micro-trips, we use mi as micro-trip identifier (stop sequence) and R_m as the set of micro-trips in trip m. Per micro-trip mi, its energy use (E_{mi}^f) is generated by multiplying the micro-trip distance (D_{mi}) with the energy rate (ER_{mi}^f), predicted by using the final model described in Section 4.3. We use the unit kWh for trip energy use throughout the study.

$$E_m^f = \sum_{\forall mi \in R_m} \varepsilon_{MJ2kWh} D_{mi} ER_{mi}^f \tag{9}$$

Figure 29 shows a revenue trip example, consisting of 45 micro-trips. We see significant energy-savings from the battery-electric vehicle at the micro-trip 5, 13, and 28.

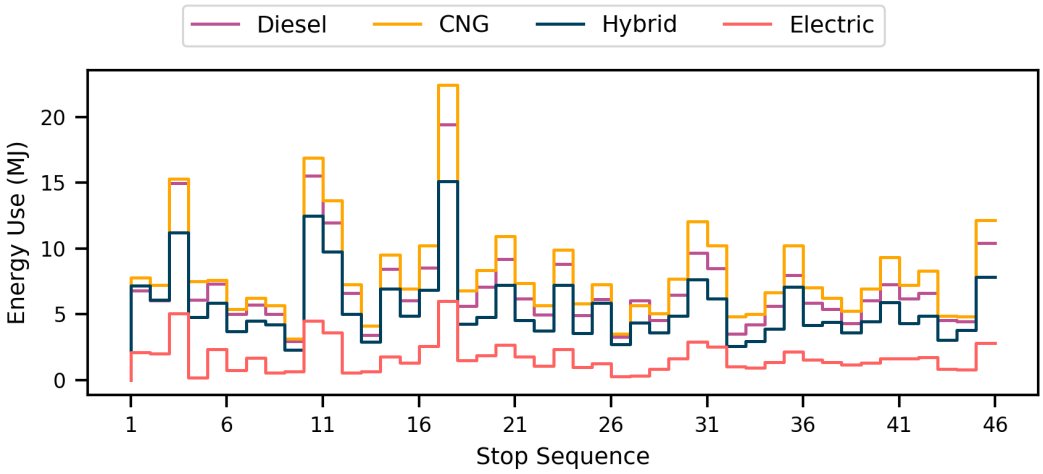

Figure 29 – Example of Revenue Trip Energy Use

Fuel efficiency performance varies greatly due to the variability of traffic due to the variabilities of operation-related and vehicle-specific characteristics. Figure 30 shows the relationship between average speed (mph) and fuel efficiency, evaluated as miles per diesel gallon equivalent. At the same average speed, fuel efficiency performance of battery-electric vehicles varies to a greater extent than the other three vehicle types. This is because the impact of regenerative braking is dependent on real-world operations. For example, the frequency of braking events is closely related to the number of traffic signals and road grades.

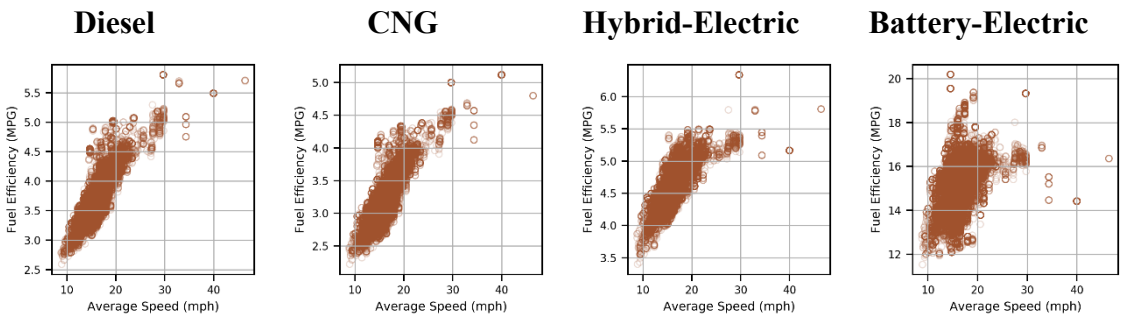

Figure 30 – Fuel Efficiency vs. Average Speed: Revenue Micro-trips

Figure 31 shows fuel efficiency performance difference of CNG, hybrid-electric, and battery-electric vehicles per revenue micro-trip, compared with diesel vehicles. There is a clear trend that as the average speed increases, the fuel efficiency difference (the absolute percentage values) becomes smaller. Fuel efficiency of CNG vehicles decreases by 7% to 21% per micro-trip with an average of 14%. The difference of fuel efficiency performance between hybrid-electric and diesel vehicles ranges from -6% to 40%, with an average of 23%. Battery-electric vehicles increase the fuel efficiency by up to 407% with an average of 302%. The range is much larger than the other fuel types because of the interactions with regenerative braking. The results imply the importance of assigning buses to the revenue trips that can achieve the most energy-saving benefits.

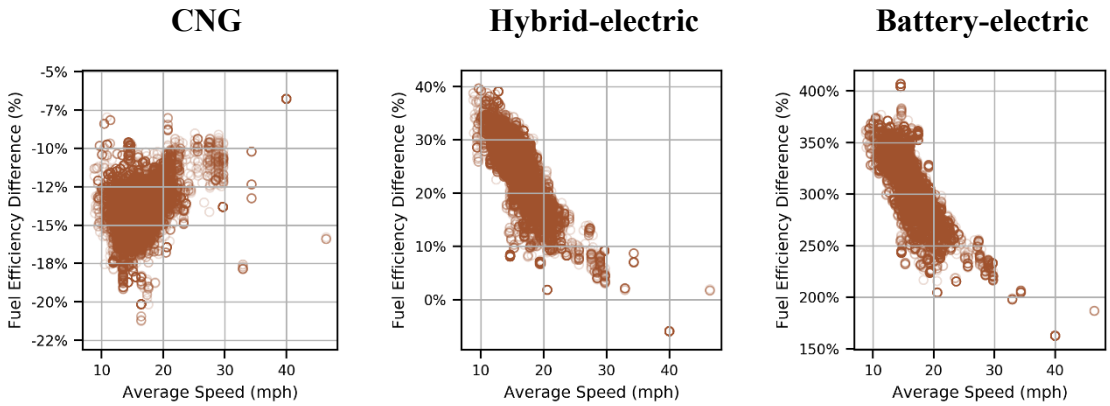

Figure 31 – Fuel Efficiency Difference of CNG, Hybrid-electric, and Battery-electric, Compared with Diesel: Revenue Micro-trips

Figure 32 shows the energy use per vehicle weight and revenue micro-trip, evaluated as DGE. Weight is categorized into five ridership levels. As mentioned in Section 3.2.1.2, the average loading in MARTA is around 10. This is why the current fuel use is close to the ridership level of 10.

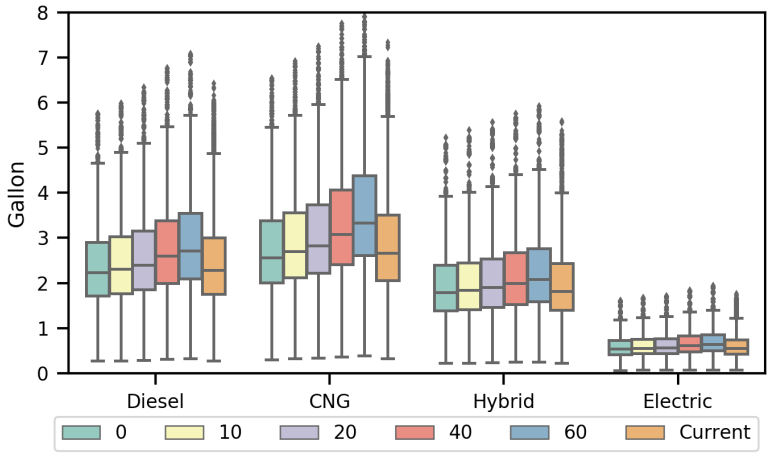

Figure 32 – Revenue Trip Fuel Use vs. Ridership Level

Revenue micro-trips are aggregated to evaluate the fleet-wide energy use from revenue operations, if the entire fleet is served by one vehicle fuel technology. Figure 33 shows energy use per day with daily operating distance of 76,000 miles (Saturday), 74,000 miles (Sunday), and 98,000 miles (weekday). Looking at the revenue operations alone, significant energy-savings can be achieved through fleet electrification. If converting the entire fleet from diesel to hybrid-electric vehicles, the fleet-wide energy use of revenue operations on a weekday can be reduced by 4,300 DGE; if converting to battery-electric vehicles, energy use can be reduced by 17,000 DGE. In other words, fuel cost can be reduced by $9,900 on a weekday if converting to hybrid-electric vehicles, and can be reduced by $39,100 if converting to battery-electric vehicles.

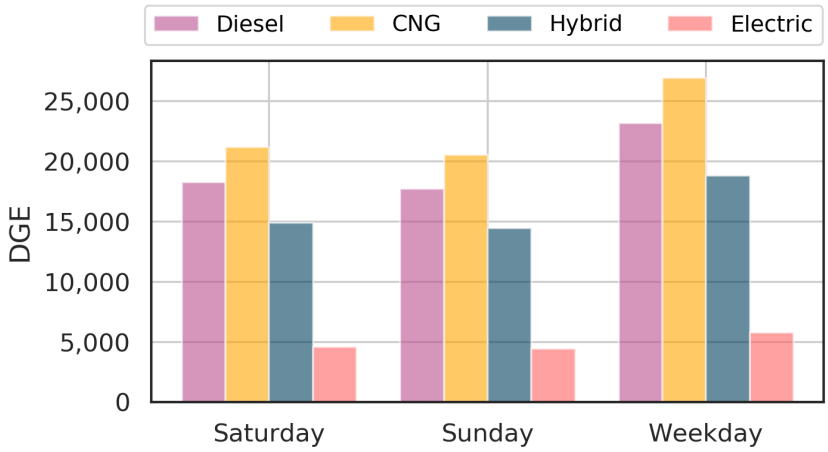

Figure 33 – Fleet-wide Revenue Energy Use by Fuel Type, Service Day

4.4.2 Deadheading Energy Use

Using the final energy prediction model, deadheading energy is predicted per roadway link and vehicle fuel technology, and then aggregated to obtain deadhead trip-level energy use. Ridership is set as zero because buses run empty during deadheading. Equation (10) denotes the energy use for a deadheading trip, which is calculated in a way similar to a revenue trip. DD_m denotes the set of deadheading micro-trip indices in trip mi.

$$E_m^f = \sum_{\forall mi \in DD_m} \varepsilon_{MJ2kWh} D_{mi} ER_{mi}^f \tag{10}$$

Figure 34 shows the relationship between average speed and fuel efficiency per micro-trip, evaluated as miles per DGE. Fuel efficiency decreases as average speed increases, which is the opposite direction compared to revenue service. The bottom line here is that vehicles tend to operate under very different conditions during deadheading

than during revenue operations, and are closer to the "sweet spot" on the morot/engine efficiency map (fuel efficiency decreases as the speed deviates from these conditions).

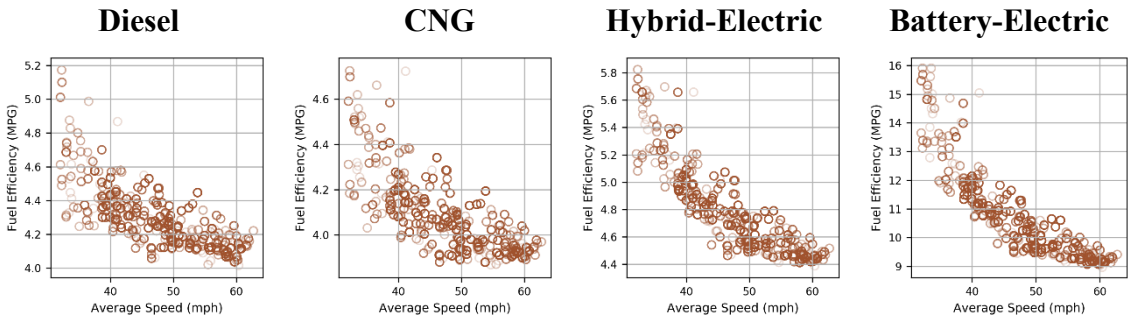

Figure 34 – Fuel Efficiency vs. Average Speed: Deadheading Micro-trips

Figure 35 shows fuel efficiency performance difference of CNG, hybrid-electric, and battery-electric vehicles per micro-trip, compared with diesel buses. CNG vehicles decrease fuel efficiency by -9% to 0.1% with an average of 5%. The difference of fuel efficiency performance between hybrid-electric and diesel vehicles ranges from 7% to 23%, with an average of 11%. Battery-electric vehicles increase the fuel efficiency by up to 254% with an average of 146%.

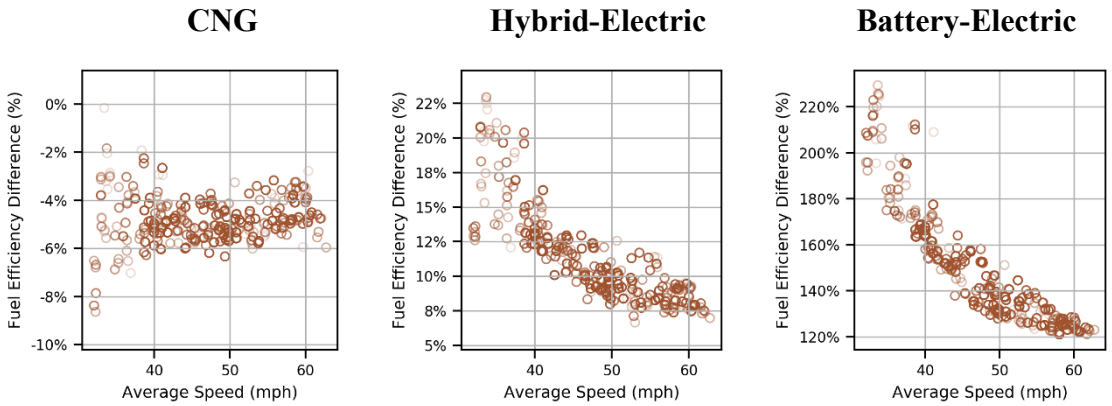

Figure 35 – Fuel Efficiency Difference of CNG, Hybrid-electric, and Battery-electric Vehicles, Compared with Diesel: Deadheading Micro-trips

Deadheading micro-trips are aggregated to evaluate the energy use of different vehicle fuel technologies. Figure 36 shows the daily energy use from each depot. Converting the entire fleet from diesel buses to battery-electric buses can significantly reduce the energy use, especially from the Hamilton depot. The energy-savings from hybrid-electric buses compared with diesel is relatively small.

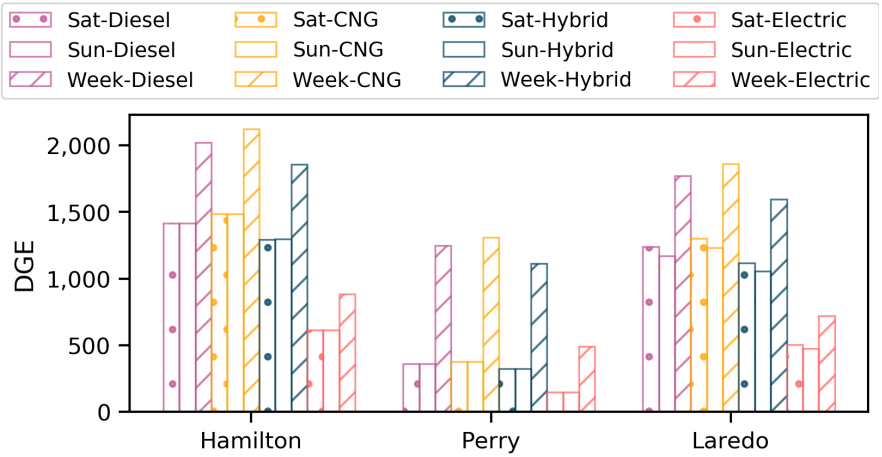

Figure 36 – Fleet-wide Energy Use from Depot Pull-in/Pull-out Operations, by Fuel Type, Service Day, Depot

4.4.3 Fleet-wide Energy Use

Figure 37 shows the annual fleet-wide energy use by vehicle fuel technology and operation types (revenue and deadheading operations). Although it is not realistic to convert the entire fleet from diesel to alternative fuel buses, these values still showcase the impact of the fleet conversion. Annual energy use will be increased by 1,370 gallons if converting to CNG vehicles, whereas energy use will be reduced by 1,700,000 and 6,900,000 gallons if converting to hybrid-electric and battery-electric vehicles, respectively. That is, annual fuel cost will be reduced by 3.9 and 15.9 millions of USD if converting to hybrid-electric and battery-electric vehicles, respectively. In particular, more

energy-savings can be achieved from revenue service than deadheading operations if switching to hybrid-electric and battery-electric buses. The difference of energy use reduction rates among different service days is trivial.

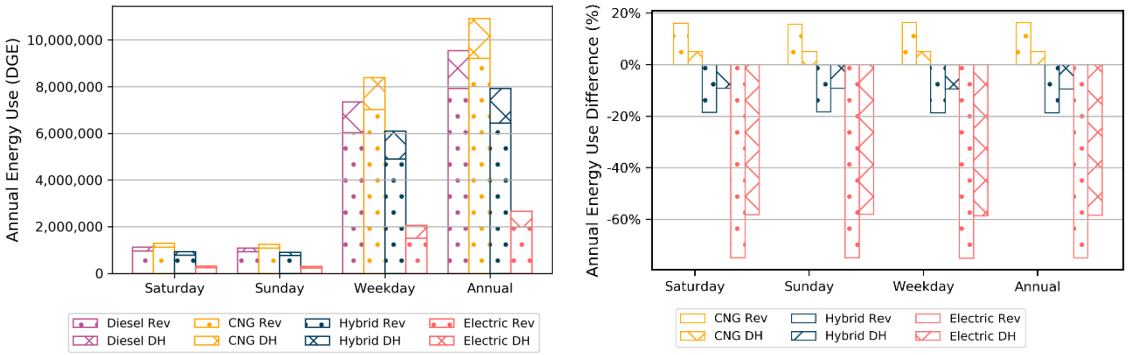

(a) Absolute Values **(b) Percentage Difference Compared with Diesel**

Figure 37 – Annual Fleet-wide Energy Use by Fuel Type, Operating Type

4.5 Summary

This chapter describes the methodology of energy simulation and modeling. Four types of vehicle fuel technologies are simulated, including diesel, CNG, hybrid-electric, and battery-electric. Per fuel and facility type, energy prediction models are developed to predict vehicle energy rate at the micro-trip level. The developed energy prediction models are a simplified version of the simulation tools, but have the advantages of achieving early the same results as well as being easy to be applied to the entire fleet. These models use machine learning algorithms by taking in operation-related and vehicle-specific features. The XGBoost algorithm is selected as the final model, which achieves the best performance with the average value of R^2 close to 1 and MAPE less than 3%, meaning that the algorithms closely replicate Autonomie® outputs. We apply the final model to predict the

energy use of both revenue service and deadheading operations per vehicle fuel technology. These values will be used for the fleet operation optimization in the following chapters.

CHAPTER 5. OPERATION OPTIMIZATION OF EXISTING MIXED FUEL FLEETS

5.1 Overview

The goal of this set of optimization models is to minimize current fleet operating costs through optimized depot, trip, and route assignment. Table 13 shows the overview of the four proposed models. Each model optimizes operations through minimizing three individual cost metrics, i.e. life-cycle CO_2 emissions, operating monetary cost, and on-road energy use. Section 5.2 describes the baseline scenarios, in which buses are randomly dispatched to serve pre-determined tours. Two baseline fleet compositions are designed. Section 5.3 describes the first model, deadheading minimization model, which is to reduce depot pull-in/pull-out cost by re-assigning buses to depots in a multi-depot network. Section 5.4 describes the second model, bus-to-tour assignment model, which is to reduce tour cost through re-assigning buses to depot-based tours (combinations of routes) accounting for the fact that fuel efficiency differs across transit routes. Section 5.5 describes the third model, tour design model, which is to reduce tour cost through re-chaining trips to transit tours. Section 5.6 describes the fourth model, a combined model, which is combines the deadheading minimization model with the bus-to-tour or the tour design model. In each model, optimization equations are formulated, and applied to the local MARTA transit network. Results are compared with the baseline scenarios to showcase the effectiveness of the proposed models. Finally, Section 5.7 summarizes findings and limitations of the proposed models.

Table 13 – Model Overview: Existing Fleet Operation Optimization

No.	Model	Chaining of Depot to Revenue Trips	Chaining of Revenue Trips	Vehicle Type of Tours
0	Baseline	Fixed	Fixed	Random[1]
1	Deadheading Minimization	Decisions	Fixed	Random[1]
2	Bus-to-Tour Assignment	Fixed	Fixed	Decisions
3	Tour Design	Fixed	Decisions	Decisions
4	Deadheading Minimization and Bus-to-Tour Assignment	Decisions	Fixed	Decisions
	Deadheading Minimization and Tour Design	Decisions	Decisions	Decisions

[1]Each vehicle in the fleet has equal probability of being dispatched to serve a tour

Table 14 shows the notations of the decision variables used in the model formulations covered in this chapter. We use f, y, b, and $l_{i,j}$ as vehicle type, depot, tour, and trip identifier. $W_{b,y}$, W_b^f, and $W_{l_{i,j}}^f$ to denote the tour-depot, bus-to-tour, and trip-chaining (tour design) decisions. $W_{y,b}^f$ and $W_{l_{i,j}}^f$ denote the decision variables in the combined model. Indices and subscripts of these variables will be described in detail in the model formulation sections.

Table 14 – Decision Variables: Operation Optimization of Existing Mixed Fuel Fleets

Notation		Meaning
$W_{b,y}$	$\forall\, b \in B, y \in Y$	Tour-to-depot variable Binary variable 1 if the vehicle that serves tour b is housed in depot y
W_b^f	$\forall\, b \in B, f \in F_1$	Bus-to-tour variable Binary variable 1 if a type f vehicle is used to serve tour b

$W_{l_{i,j}}^{f}$	$\forall b \in B, f \in F_1,$ $l_{i,j} \in \bigcup_{1 \le ai \le 4} A_{ai,s,y}$	Trip-chaining decision variable for the trip-vehicle combination Binary variable 1 if trip $l_{i,j}$ is served by a type f vehicle.
$W_{y,b}^{f}$	$\forall\, b \in B, f \in F_1, y \in Y$	Trip-chaining decision variable for the vehicle-depot combination Binary Variable 1 if on service day s, the tour b is served by a type f vehicle housed in depot y

5.2 Baseline Scenario

Two sets of fleet compositions are designed as baseline scenarios. The first scenario uses the current MARTA fleet composition, described in Section 3.1. The fleet consists of CNG and diesel buses. Baseline scenario uses tours are formulated consisting of revenue trips, depot pull-in/pull-out trips, and interlining trips. Because hybrid-electric buses have been widely adopted across the country, a second scenario with hybrid-electric buses is created. Figure 38 shows the number of vehicles per type (f), categorized by vehicle age group and fuel technology. Each scenario has four types of vehicles. The current practice in MARTA is to randomly assign buses to tours, as long as ridership demand is satisfied. Therefore, fleet composition distribution is used to evaluate the fleet-wide cost. We use F_1 to denote the vehicle types in the fleet, and χ^f to denote the number of type f vehicles in the fleet.

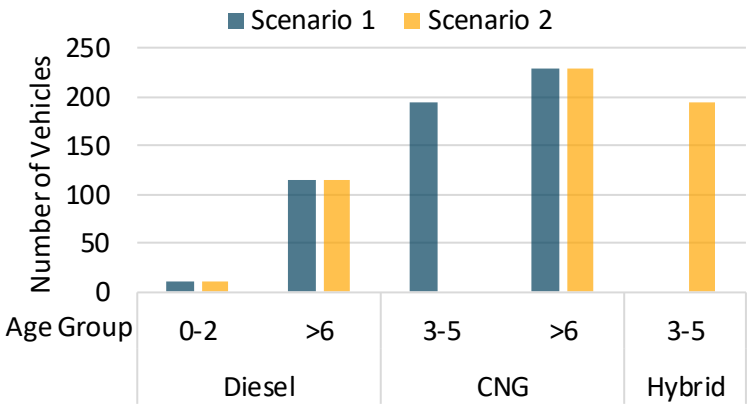

Figure 38 – Fleet Composition of Baseline Scenario

Equation (11)-(18) denote the formulation of cost metrics. Equation (11) denotes the fleet-wide cost (C_ρ), evaluated with metric ρ, which is calculated by aggregating the cost of all individual trips based on the weight of number of vehicles per type. $C_{m,\rho}^f$ denotes the cost of trip m, evaluated with metric ρ, if a type f vehicle. L_b^D, L_b^I, and L_b^R denote the sets of depot pull-in/pull-out, interlining, and revenue trips. Because daily operations differ between weekdays and weekends, we use s to differentiate service day types, and use $Freq_s$ to represent the frequency, i.e. the number of days in a year. Equation (12) denotes the first cost metric, life-cycle CO_2 emissions (C_δ). It is calculated by multiplying the energy use for each trip (E_m^f) by the life-cycle CO_2 emission rate (δ^f). Life-cycle CO_2 emissions consists of on-road and upstream emissions. On-road CO_2 emission rates are calculated based on carbon content and oxidation fraction of each fuel type, as denoted in equation (13). Upstream CO_2 emission rates are extracted based on the GREET model, denoted in equation (14). The second cost metric is operating monetary cost (C_{op}), denoted in equation (15). Operating cost of trip m consists of fuel cost ($C_{m,\alpha}^f$) and maintenance cost ($C_{m,\beta}^f$). Fuel cost is calculated based on energy use (E_m^f) and fuel cost rate (α^f),

denoted in equation (16). Maintenance cost is calculated based on distance (D_m^f) and maintenance cost rate (β^f), denoted in equation (17). The third cost metric is energy use (C_e), evaluated as diesel gallon equivalent (DGE), denoted in equation (18).

$$C_{\rho\in\{\delta,op,e\}} = \sum_{\forall s\in S}\sum_{\forall b\in B_s}\sum_{\forall f\in F_1}\sum_{\forall m\in L_b^D\cup L_b^I\cup L_b^R}\{Freq_s C_{m,\rho}^f\,(\frac{\chi^f}{\sum_{f\in F_1}\chi^f})\} \tag{11}$$

$$C_{m,\delta}^f = E_m^f\delta^f = E_m^f(\delta_{Upstream}^f + \delta_{Onroad}^f) \qquad \forall f\in F_1, m\in\{L_b^D, L_b^I, L_b^R\} \tag{12}$$

$$\delta_{Onroad}^f = (44/12)\varepsilon_{kWh2MJ}\delta_{\mathrm{CC}}^f\,\delta_{\mathrm{OF}}^f \qquad \forall f\in F_1 \tag{13}$$

$$\delta_{Upstream}^f = \varepsilon_{kWh2MJ}\delta_{\mathrm{FP}}^f \qquad \forall f\in F_1 \tag{14}$$

$$C_{m,op}^f = C_{m,\alpha}^f + C_{m,\beta}^f \qquad \forall f\in F_1, m\in\{L_b^D, L_b^I, L_b^R\} \tag{15}$$

$$C_{m,\alpha}^f = E_m^f\varepsilon_{kWh2Gal}\alpha^f \qquad \forall f\in F_1, m\in\{L_b^D, L_b^I, L_b^R\} \tag{16}$$

$$C_{m,\beta}^f = D_m^f\beta^f \qquad \forall f\in F_1, m\in\{L_b^D, L_b^I, L_b^R\} \tag{17}$$

$$C_{m,e}^f = E_m^f\varepsilon_{kWh2Gal} \qquad \forall f\in F_1, m\in\{L_b^D, L_b^I, L_b^R\} \tag{18}$$

Table 15 shows the parameter values. These settings are extracted based on previous studies, discussed in Section 2.5. CO_2 upstream emission rates (δ_{FP}^f) are shown in Appendix C, Table 41. [Note that we use the North America default mix, which ignores the regional difference. The results and trends may be different when using the local mix.]

Table 15 – Parameter Settings: Baseline Scenario

Item	Notation	Value
Frequency	$Freq_s$	Weekday: 260, Saturday: 52.5, Sunday: 52.5
Depot Capacity	χ_y	All 300
Vehicle Maintenance ($/mile)	α^f	Diesel: 0.3, CNG: 0.35, Hybrid-Electric: 0.4
Energy Cost ($/DGE)	β^f	Diesel: 2.3, CNG: 1.0
Depot Capacity by Fuel Type	χ_y^f	All 300
Carbon Content (kg/MJ)[1]	δ_{CC}^f	Diesel: 0.0201904, CNG: 0.0161
Oxidation Fraction (kg/MJ) [1]	δ_{OF}^f	Diesel: 1, CNG: 1
Conversion factor from kWh to MJ	ε_{kWh2MJ}	3.6
Conversion factor from kWh to DGE	$\varepsilon_{kWh2Gal}$	0.026556

[1]US EPA

[2]Lower heating value: 1DGE=128,488btu

Table 16 shows the results of the baseline Scenarios 1 and 2. Values of the three cost metrics are specifically pointed out here. These values will be used to for evaluating the cost reductions from each proposed optimization model.

Table 16 – Annual Summary of Baseline Scenarios

		C_ρ	Saturday	Sunday	Weekday	Total
	Number of Tours (1,000)		18.0	17.6	148.5	184.1
	Total Duration (1,000's of Hours)		297	290	1,881	2,468
	Total Distance (1,000's of Miles)		3,977	3,883	25,565	33,425
Scenario 1	Fuel Use (1,000's of DGE)	C_e	1,193	1,155	7,740	10,088
	CO_2 Emissions (Metric Tonnes)	C_δ	15,963	15,464	103,619	135,046
	Fuel Cost (Millions of USD)		1.5	1.5	9.8	12.8
	Maintenance Cost (Millions of USD)		1.3	1.3	8.7	11.3

	Operating Monetary Cost (Millions of USD)	C_{op}	2.9	2.8	18.5	24.1
Scenario 2	Fuel Use (1,000's of DGE)	C_e	1,071	1,038	6,952	9,061
	CO_2 Emissions (Metric Tonnes)	C_δ	15,711	15,241	102,016	132,968
	Fuel Cost (Millions of USD)		1.8	1.7	11.6	15.2
	Maintenance Cost (Millions of USD)		1.4	1.4	9.1	11.9
	Operating Monetary Cost (Millions of USD)	C_{op}	3.2	3.1	20.7	27.1

5.3 Deadheading Minimization Model

In a multi-depot transit network, the depot selection within a tour is commonly decided based on the spatial locations of their revenue trips. That is, the depot closest to the starting/ending stops of the set of revenue trips is selected. It is necessary to pay attention to depot location selection because deadheading percentage from depot pull-in/pull-out is not trivial, e.g. 12% of the total mileage in MARTA. However, deadheading cost may not be minimized in terms of energy use, emissions, and monetary cost if deadheading distance alone is considered in the decision-making process. This is because minimum distance cannot be directly translated to minimum energy use. Fuel efficiency performance varies significantly with different vehicle types and operating characteristics. The goal of the deadheading minimization model is to reduce depot pull-in/pull-out cost by re-assigning buses to depots in a multi-depot network. The model outputs the decisions of tour-to-depot assignment.

5.3.1 Model Formulation

Equation (19) denotes the objective function. Compared with the cost equation (11) in the baseline scenario, the deadheading cost component differs by incorporating the

binary decision variable $W_{b,y}$. $W_{b,y}$ equals 1 if the vehicle serves b is housed in depot y, and we use the set $L_{b,y}^{D}$ to denote its depot pull-in/pull-out trips. Equation (20) denotes the constraint of the one-one relationship between a tour and depot.

$$\min_{W_{b,y}} C_{\rho\in\{\delta,op,e\}} = \sum_{\forall s\in S}\sum_{\forall b\in B_s}\sum_{\forall f\in F_1} Freq_s\left(\frac{\chi^f}{\sum_{f\in F_1}\chi^f}\right)\left(\sum_{\forall m\in L_b^I\cup L_b^R} C_{m,\rho}^f + \sum_{\forall y\in Y}\sum_{\forall m\in L_{b,y}^D} W_{b,y}C_{m,\rho}^f\right) \tag{19}$$

$$\sum_{\forall y\in Y} W_{b,y} = 1 \qquad \forall s\in S, b\in B_s \tag{20}$$

5.3.2 Implementation

The proposed model is programmed in Python environment and solved using the commercial solver CPLEX 12.8. All numerical experiments are run on a desktop with 32 GB of RAM and 3.40 GHz of CPU under a Windows 10 environment. The same environment is used for all the implementations throughout this study. The assumptions are listed below:

1) Vehicles that serve a tour can be housed in any depot candidate
2) Each vehicle has the same probability of serving a tour, i.e. the frequency of tours served by each vehicle type is based on the number of vehicles that type
3) Deadhead routing is obtained via minimum traveling duration
4) Each tour can be served by all vehicle types
5) Ridership is zero when deadheading
6) Ridership is categorized to five levels, i.e. 0, 10, 20, 40, and 60

7) Time horizon is 365 days

8) Holiday special operations are excluded

Table 17 shows the results of depot assignment for each tour. Using this model, about 11% of tours are re-located to a different depot across all scenarios. The depot assignment decisions are the same when using CO_2 emissions and energy use as cost metrics. This is not surprising as energy use correlates well to CO2 emissions for diesel and CNG.

Table 17 – Depot Re-assignment

Scenario	Cost Metric	Number of Tours		Relocation Percentage
		Relocate=True	Relocate=False	
1	CO_2 Emissions	20,218	163,838	10.98%
	Operating Cost	19,333	164,723	10.50%
	Energy Use	20,218	163,838	10.98%
2	CO_2 Emissions	20,218	163,838	10.98%
	Operating Cost	19,698	164,358	10.70%
	Energy Use	20,218	163,838	10.98%

Table 18 shows the reductions in each of the three metrics after depot relocation, compared with baseline scenarios. Reduction values are highlighted if they are used as the objective cost metric. Optimizing depot assignment can reduce CO_2 emissions by up to 572-601 metric tonnes (0.5%), operating cost by $110,000 - $130,000 (0.5%), and energy use by 41,000 - 43,000 DGE (0.5%) compared with baselines. When using different cost metrics in the objective function, the difference of the reductions achieved is trivial. Note that whether driver labor (hours of operation) is explicitly addressed in this equation.

Table 18 – Reductions Compared with Baselines: Deadheading Minimization Model

		CO_2 Emissions	Monetary Cost	Energy Use
Scenario 1	Duration (1,000 Hours)	-3.70	-3.75	-3.70
	Distance (1,000 Miles)	-167.41	-167.91	-167.41
	Energy Use (1,000 DGE)	-42.58	-42.49	**-42.58**
	CO_2 Emissions (Metric Tonnes)	**-572.42**	-571.25	-572.42
	Energy Cost (Million USD)	-0.05	-0.05	-0.05
	Maintenance Cost (Million USD)	-0.06	-0.06	-0.06
	Monetary Cost (Million USD)	-0.11	**-0.11**	-0.11
Scenario 2	Duration (1,000 Hours)	-3.70	-3.72	-3.70
	Distance (1,000 Miles)	-167.41	-167.66	-167.41
	Energy Use (1,000 DGE)	-40.55	-40.52	**-40.55**
	CO_2 Emissions (Metric Tonnes)	**-600.81**	-600.36	-600.81
	Energy Cost (Million USD)	-0.07	-0.07	-0.07
	Maintenance Cost (Million USD)	-0.06	-0.06	-0.06
	Monetary Cost (Million USD)	-0.13	**-0.13**	-0.13

5.4 Bus-to-Tour Assignment Model

Some agencies randomly assign vehicles to tours as long as it satisfies the ridership demand, without considering the differences of fuel efficiency performance among different vehicle fuel technologies. Intuitively, it is beneficial to assign vehicles to their cost-minimum tours. The goal of this model is to minimize cost through re-assigning buses to depot-based tours (combinations of routes) accounting for the fact that fuel efficiency differs across transit routes.

5.4.1 Model Formulation

The decision variable in this model is binary variable W_b^f, which equals 1 if a type f vehicle is selected for tour b. Equation (21) shows the objective of this optimization model, minimizing fleet-wide cost, evaluated with metric ρ. The three cost metrics are

optimized separately. Constraints are denoted in equation (22)-(27). Equation (22) denotes the constraint that one vehicle type is selected for a tour. F_b is the set of vehicle types that can serve tour b, this addresses the limitation that some tours cannot be served by some vehicle types based upon ridership demand, roadway characteristics, or some other reason. If allowing a vehicle to run multiple tours during the same day, i.e. pull in/pull-out depot multiple times, then timing is incorporated to the model. Time is discretized to slots with equal intervals, shown in Figure 39. In this example, the vehicle is pulled out in slot t_3, and then pulled in slot t_6. Therefore, this tour's time slots T_b is represented by $t_k \in \{t_3, t_4, t_5, t_6\}$. The discretization of the time slots and timing constraints ensure that buses cannot be modeled as departing a station before they arrive at that station.

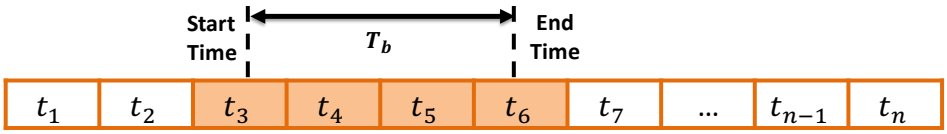

Figure 39 – Discretize Time to Slots

Equation (23) denotes the number of type f vehicles from depot y that are in use, at time slot t_k on service day type s. For each tour b, its in-service time slots starts from depot pull-out (t_{TO_b}) and ends with depot pull-in (t_{TI_b}). Equation (24) denotes the vehicle availability, i.e. at each time slot t_k of service day type s, the supply of type f vehicles at depot y (w_y^f), is enough for the demand (w_{y,s,t_k}^f). Equation (25)-(27) denote the relationship between vehicle supply and capacity. Equation (25) denotes the constraint that the vehicle supply of type f from depot y (w_y^f) does not exceed its availability (χ_y^f). If the depot y does not have facilities to house vehicles of type f, then χ_y^f is zero. Equation (26) denotes the constraint that the number of vehicles at depot y cannot exceed its capacity

(χ_y). Equation (27) denotes the constraint that the number of vehicles of type f cannot exceed the availability (χ^f), i.e. the number of vehicles in the fleet.

$$\min_{W_b^f} C_{\rho\in\{\delta,op,e\}} = \sum_{\forall s\in S}\sum_{\forall b\in B_s}\sum_{\forall f\in F_b}\sum_{\forall m\in L_b^D\cup L_b^I\cup L_b^R} Freq_s W_b^f C_{m,\rho}^f \tag{21}$$

$$\sum_{f\in F_b} W_b^f = 1 \qquad \forall s\in S, b\in B_s \tag{22}$$

$$w_{y,s,t_k}^f = \sum_{\forall b\in B_{s,y}, t_k\in T_b} W_b^f \qquad \forall s\in S, y\in Y, f\in F, t_k\in T, \; T_b=\{t_{TO_b}, t_{TO_b+1}, \dots, t_{TI_b}\} \tag{23}$$

$$\max_{\forall s\in S, t_k\in T} w_{y,s,t_k}^f \le w_y^f \qquad \forall y\in Y, f\in F \tag{24}$$

$$w_y^f \le \chi_y^f \qquad \forall y\in Y, f\in F \tag{25}$$

$$\sum_{f\in F} w_y^f \le \chi_y \qquad \forall y\in Y \tag{26}$$

$$\sum_{y\in Y} w_y^f \le \chi^f \qquad \forall f\in F \tag{27}$$

5.4.2 Implementation

Assumptions (3) through 8) from Section 5.3.2 still apply to this model. The time slots are set to 30 minutes, and a vehicle can cannot be pulled out until the next time slot. Table 19 shows the cost reductions of the bus-to-tour assignment model, compared with the baseline scenarios. Because the original tour design (i.e. chaining of revenue and deadheading trips) is retained, the duration and mileage remain the same. The metric used

in each objective function is highlighted in the table columns. If lifecycle CO_2 emissions is used as the objective metric, bus-to-tour assignment could reduce CO_2 by 3.98% (5,372 metric tonnes) and 6.53% (8,678 metric tonnes) in Scenario 1 and 2, respectively. If operating cost is used as the objective metric, bus-to-tour assignment could reduce costs by 8.19% ($1.98 million USD) and 8.71% ($2.36 million USD) in Scenario 1 and 2, respectively. If energy is used as the objective metric, bus-to-tour assignment could reduce energy use by 2.53% (256,000 DGE) and 9.00% (815,000 DGE) in Scenario 1 and 2, respectively. However, reducing energy use may increase the fleet-wide CO_2 emissions because diesel vehicles have better fuel efficiency performance (evaluated as MPDGE) than their CNG counterparts; however, diesel vehicles have higher life-cycle CO_2 emissions per gallons of energy used. In Scenario 1, the difference between using CO_2 emissions and operating cost is trivial; however, the gap is bigger in Scenario 2. This is because of the bigger difference in cost introduced by the hybrid-electric vehicles.

Table 19 – Reduction Percentages Compared with Baselines: Bus-to-Tour Assignment Model

		CO_2 Emissions	Monetary Cost	Energy Use
Scenario 1	Duration	0.00%	0.00%	0.00%
	Distance	0.00%	0.00%	0.00%
	Energy Use	2.19%	2.21%	**-2.53%**
	CO_2 Emissions	**-3.98%**	-3.97%	1.63%
	Energy Cost	-18.19%	-18.22%	11.24%
	Maintenance Cost	3.15%	3.16%	-2.11%
	Monetary Cost	-8.18%	**-8.19%**	4.98%
Scenario 2	Duration	0.00%	0.00%	0.00%
	Distance	0.00%	0.00%	0.00%
	Energy Use	-4.07%	3.24%	**-9.00%**
	CO_2 Emissions	**-6.53%**	-4.05%	-1.33%
	Energy Cost	-10.82%	-16.80%	12.08%
	Maintenance Cost	4.62%	1.58%	0.90%
	Monetary Cost	-4.02%	**-8.71%**	7.17%

Figure 40 shows the results by fuel type. As expected, in minimizing energy use, more diesel and hybrid-electric vehicles are dispatched than CNG vehicles. The trend is the opposite when minimizing CO_2 emissions. When minimizing operating cost, the percentage of hybrid-electric vehicles in Scenario 2 is smaller. Even though hybrid-electric vehicles have better fuel efficiency and thus lower fuel cost, the cost-saving benefits are offset by the high maintenance cost (high purchase costs would further exacerbate this difference if included). Therefore, operation plans should be designed based on the fleet-specific compositions and agency preferences.

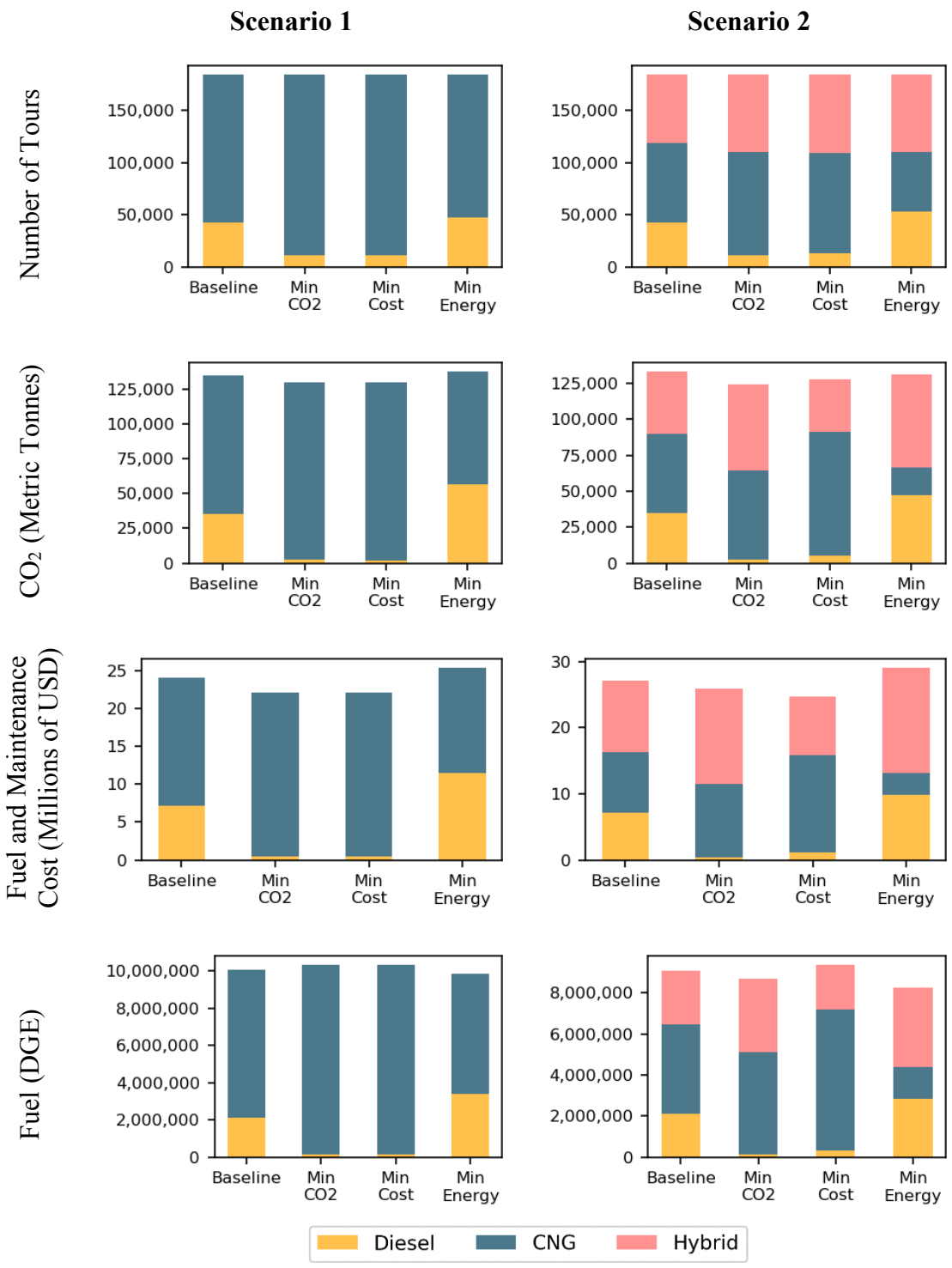

Figure 40 - Results of the Bus-to-Tour Assignment Model by Fuel Type

5.5 Tour Design Model

The bus-to-tour assignment optimization model is built at the level of tours. The set of revenue trips are pre-chained for a tour, and then the decisions are made to determine the vehicle fuel technology and depot location of a tour. The rationale is to assign vehicles to an energy-efficient tour within fleet and depot availability. However, identification of individual energy-efficient tours does not enure that the revenue trips within this tour are energy-efficient. In fact, bus interlining between different revenue routes occurs frequently in large transit agencies, to maximize the utilization of buses. Hence, interlining between routes on tours must be explicitly addressed in optimization.

Figure 41 shows a simplified example of tour differences. Tour 1 and Tour 2 each include four revenue trips, three interlining trips, and two depot pull-in/pull-out trips. They are served by vehicle fuel technology A and B, respectively. However, vehicle A is more energy-efficient on Route 3 than Route 2, and vehicle B is more energy-efficient on Route 2 than Route 4. The gap can be large enough to offset the additional energy use for vehicle A to interline from Route 1 to Route 3. In this case, the overall energy use is reduced via re-chaining revenue trips.

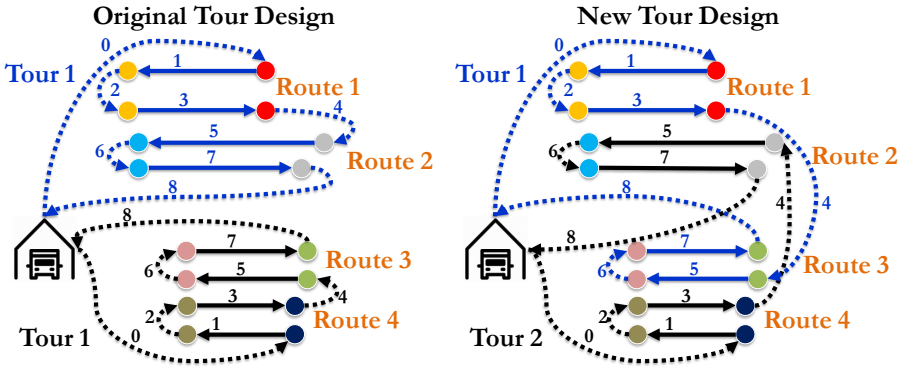

Figure 41 – Tour Design Example

This goal of this model is to minimize each cost metric through tour design in an existing multi-depot transit fleet. The optimization is conducted at the trip level, and decisions are made to chain trips sequentially to a tour, along with which vehicle technology will be assigned. One thing to mention is that in this model, tour-to-depot assignment is not changed; that is, the vehicle that serves a revenue trip is still housed in the same pre-determined depot.

5.5.1 Tour Setup

We use $\bigcup_{1\leq ai\leq 4} A_{ai,s,y}$ to represent all the operating trips on service day type s from depot y, where ai represents the type of trip, and the four types are: 1) $A_{1,s,y}$ denotes the set of revenue trips, served by vehicles from depot y; 2) $A_{2,s,y}$ and $A_{3,s,y}$ denote the set of depot pull-in/pull-out trips from depot y; and 3) $A_{4,s,y}$ denotes the interlining trips served by vehicles from depot y, i.e. operating from the last stop of one revenue trip to the first stop of the next revenue trip. $A_{1,s,y}, A_{2,s,y}, A_{3,s,y}$ can be established based on pre-determine revenue trips and the tour-depot assignment. The interlining trips extracted from GTFS scheduling data are decided by the agencies. In fact, it is a potential interlining opportunity if the duration from the end of one revenue trip to the start of another is enough for the vehicle to travel between these two stops. Therefore, a thorough analysis should be conducted to generate all the interlining trip candidates.

If all interlining candidates are incorporated, the computational efforts is the square of number of trips. To solve the complex formulation, this study uses the time-space-based network proposed by Kliewer, et al. (*2016*), to reduce the computational efforts to the number of trips multiplied by the number of bus starting/ending stops. In this model, a trip

is represented as $l_{i,j}$ two time-space nodes, i.e. carrying the information of location and timestamp. Trips are aggregated in three stages, as defined by Kliewer, et al. (*2016*). At the first stage, called first match, two revenue trips are connected as long as the there is enough time to travel from the ending stop of one trip to the starting stop of another trip. At the second and third stages, the number of connections is reduced through determining "latest-first matches" and eliminating connections with "no latest first matches". Figure 42 shows a time-space-based network example, including seven revenue trips (e.g. $l_{a1,b1}, l_{a2,b2}$) that end with station M, and seven revenue trips (e.g. $l_{c1,d1}, l_{c2,d2}$) that start with station N. These revenue trips are connected with three interlining trips ($l_{b2,c1}, l_{b4,c3}, l_{b7,c5}$). Twelve "waiting/connecting" trips (e.g. $l_{b1,b2}, l_{c1,c2}$) are created to ensure the connectivity of the network.

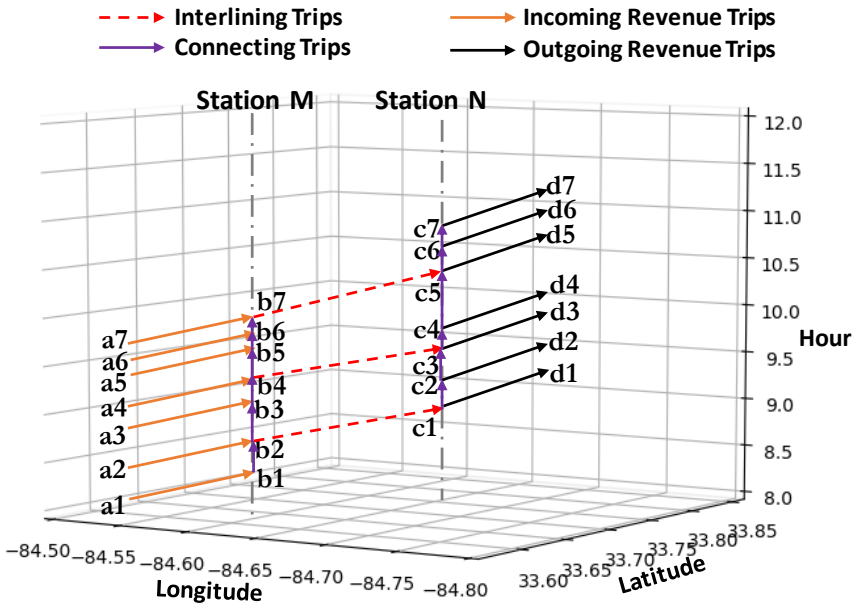

Figure 42 – Time-Space Network Example

For comparison, Figure 43 shows the interlining trips if using the connection-based network. In this example, the revenue trip $l_{a1,b1}$ and $l_{a2,b2}$ can each be matched with seven revenue trips (e.g. $l_{c1,d1}, l_{c2,d2}$). In addition, revenue trip $l_{a3,b3}$ and $l_{a4,b4}$ can each be matched with five revenue trips, and revenue trip $l_{a5,b5}, l_{a6,b6}, l_{a7,b7}$ can each be matched with three revenue trips. The time-space-based network constraints significantly reduce the number of possible trips.

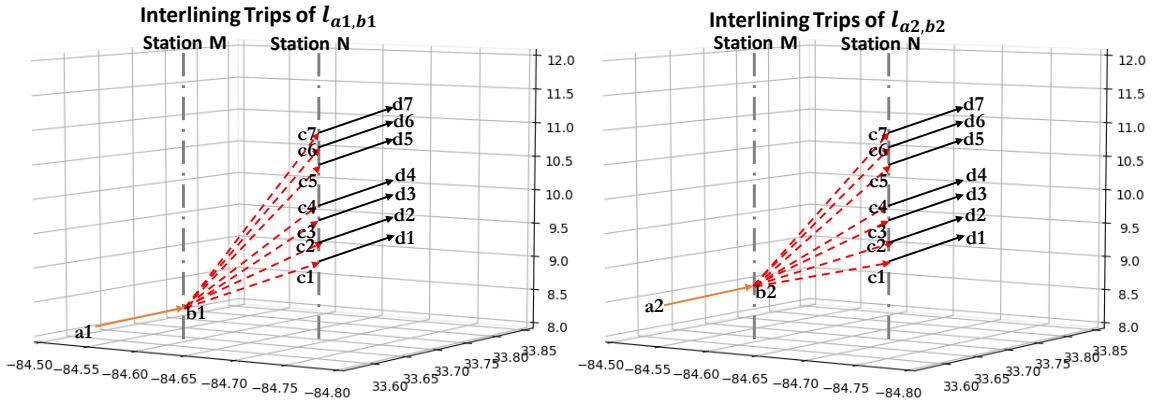

Figure 43 – Connection-based Network

5.5.2 Model Formulation

The objective of this optimization model is to minimize the total cost, shown in equation (28). The binary decision variable is $W_{l_{i,j}}^{f}$, which equals 1 if trip $l_{i,j}$ is served by a type f vehicle. Equation (29) denotes the constraint that each revenue trip is fulfilled by one type of vehicle. Equation (30) denotes the conservation of trip flow, i.e. for node i, the sum of the in-flows equal the sum of the out-flows. Equation (23) is updated with equation

(31) to denote the number of in-use vehicles. The supply-demand and depot capacity constraints, equation (24)-(27) are also used in this scenario.

$$\min_{W^f_{l_{i,j}}} C_{\rho\in\{\delta,op,e\}} = \sum_{\forall s\in S}\sum_{\forall y\in Y}\sum_{\forall l_{i,j}\in \cup_{1\le ai\le 4} A_{ai,s,y}}\sum_{\forall f\in F_{l_{i,j}}} \{Freq_s W^f_{l_{i,j}} C^f_{l_{i,j},\rho}\} \tag{28}$$

$$\sum_{\forall f\in F_{l_{i,j}}} W^f_{l_{i,j}} = 1 \qquad \forall s\in S, y\in Y, l_{i,j}\in A_{1,s,y} \tag{29}$$

$$\sum_{\forall l_{i,j}\in l_{i,\cdot}} W^f_{l_{i,j}} = \sum_{\forall l_{i,j}\in l_{\cdot,i}} W^f_{l_{i,j}} \qquad \forall s\in S, y\in Y, \; l_{i,j}\in \bigcup_{1\le ai\le 4} A_{ai,s,y} \tag{30}$$

$$w^f_{y,s,t_k} = \sum_{\forall l_{i,j}\in\cup_{1\le ai\le 4} A_{ai,s,y}, t_k\in T_{l_{i,j}}} W^f_{l_{i,j}} \qquad \forall s\in S, y\in Y, f\in F_1, t_k\in T \tag{31}$$

5.5.3 Implementation

All of the previous assumptions in the bus-to-tour assignment model also apply to this model. The additional assumptions related to interlining trips are listed below:

1) Maximum duration of interlining between two revenue trips is 30 minutes;
2) Minimum duration of interlining between two revenue trips without driving involved is 0 minutes;
3) Minimum duration of interlining between two revenue trips with driving involved is 2 minutes;
4) Routing between interlining trips is obtained via minimum traveling duration.

Table 20 shows the results of tour design model, compared with the baseline scenarios. Significant reductions across all metrics are achieved through tour design. In particular, the reductions of CO_2 emissions and energy use are almost twice as large as the reductions achieved from the bus-to-tour assignment model, in Scenario 1. One caveat is that operating cost is still only defined as energy cost and maintenance cost. Even though operating cost is reduced by over 11% in both scenarios compared with baseline, the operating duration is increased by 5% and 8% and will thus increase operator cost (labor hours). Operator cost needs to be explicitly incorporated into the cost objective function in future models.

Table 20 – Reduction Percentages Compared with Baselines: Tour Design Model

		CO_2 Emissions	Monetary Cost	Energy Use
Scenario 1	Duration	7.52%	4.71%	7.63%
	Distance	-2.52%	-2.55%	-2.49%
	Energy Use	-0.08%	-0.07%	**-5.59%**
	CO_2 Emissions	**-6.50%**	-6.50%	0.30%
	Energy Cost	-21.31%	-21.30%	13.87%
	Maintenance Cost	0.77%	0.74%	-5.46%
	Monetary Cost	-10.95%	**-10.96%**	4.80%
Scenario 2	Duration	9.91%	4.57%	6.94%
	Distance	-2.51%	-2.35%	-2.37%
	Energy Use	-8.58%	4.45%	**-13.97%**
	CO_2 Emissions	**-9.50%**	-5.76%	-4.21%
	Energy Cost	-11.11%	-23.61%	12.86%
	Maintenance Cost	3.16%	-1.56%	0.01%
	Monetary Cost	-4.83%	**-13.91%**	7.21%

5.6 Combined Model

The combined model is to combine the deadheading minimization model with bus-to-tour assignment or tour design model. That is, to build up on the models in Section 5.4 and 5.5 by incorporating the flexibility of relocating revenue trips to other available depot candidates, as proposed in Section 5.3.

5.6.1 Model Formulation

5.6.1.1 Deadheading Minimization and Bus-to-Tour Assignment

The model is formulated in a similar fashion as in Section 6.4.1. The binary decision variable is $W_{y,b}^{f}$, which equals 1 if on service day s, the tour b is served by a type f vehicle housed in depot y. The objective function is updated with equation (32), with deadheading trips represented as $L_{b,y}^{D}$, to incorporate the option of different depots. Equation (33) denotes the constraint that one tour is served by vehicle with one fuel technology from one depot. The vehicle demand, quantified in equation (23) is replaced with equation (34), which updates the set of tours from $B_{s,y}$ to B_s. The constraints in equation (24)-(27) still apply to this strategy.

$$\min_{W_{y,b}^{f}} C_{\rho\in\{\delta,op,e\}} = \sum_{\forall s\in S}\sum_{\forall b\in B_s}\sum_{\forall f\in F_b}\sum_{\forall y\in Y}\sum_{\forall m\in L_{b,y}^{D}\cup L_b^{I}\cup L_b^{R}} Freq_s W_{b,y}^{f} C_{m,\rho}^{f} \tag{32}$$

$$\sum_{\forall y\in Y}\sum_{f\in F_b} W_{b,y}^{f} = 1 \qquad \forall s\in S, b\in B_s \tag{33}$$

$$w_{y,s,t_k}^{f} = \sum_{\forall b \in B_s, t_k \in T_b} W_{b,y}^{f} \qquad \begin{matrix} \forall s \in S, y \in Y, f \in F, t_k \in T \\ T_b = \{t_{TO_b}, t_{TO_b+1}, \dots, t_{TI_b}\} \end{matrix} \qquad (34)$$

5.6.1.2 Deadheading Minimization and Tour Design

This model builds up the tour design model by providing the flexibility of relocating the trips to another depot. The formulation of model is the same as the tour design model in Section 6.5.2, with the only difference in terms of the deadheading pull-in/pull-out trips, $A_{2,s,y}$ and $A_{3,s,y}$. Each revenue trip is not constrained to a pre-determined depot, but can be linked with all the other depot candidates. Therefore, the sizes of $A_{2,s,y}$ and $A_{3,s,y}$ are the same as the $\bigcup_{y \in Y} A_{2,s,y}$ and $\bigcup_{y \in Y} A_{3,s,y}$ in the tour design model.

5.6.2 Implementation

5.6.2.1 Deadheading Minimization and Bus-to-Tour Assignment

All the assumptions in 5.4.2 apply to this model. The one additional assumption is that vehicles that serve a tour can be housed in any depot candidate. Table 21 shows the results of the combined model, compared with the baseline scenarios. Because this model is built upon the bus-to-tour assignment model, greater reductions of CO_2 emissions, operating cost, and energy use are achieved. Overall, the objective value of each metric is further reduced by an absolute value of 0.5%. This demonstrates the importance of taking account of depot pull-in/pull-out activities when designing tours.

Table 21 – Reductions Percentages Compared with Baselines: Deadheading Minimization and Bus-to-Tour Assignment Model

		CO_2 Emissions	Monetary Cost	Energy Use
Scenario 1	Duration	-0.15%	-0.15%	-0.15%
	Distance	-0.49%	-0.49%	-0.50%
	Energy Use	1.77%	1.80%	**-2.96%**
	CO_2 Emissions	**-4.39%**	-4.38%	1.20%
	Energy Cost	-18.59%	-18.63%	10.79%
	Maintenance Cost	2.66%	2.67%	-2.61%
	Monetary Cost	-8.62%	**-8.64%**	4.51%
Scenario 2	Duration	-0.15%	-0.15%	-0.15%
	Distance	-0.49%	-0.49%	-0.50%
	Energy Use	-4.54%	2.88%	**-9.47%**
	CO_2 Emissions	**-6.96%**	-4.45%	-1.82%
	Energy Cost	-11.19%	-17.27%	11.56%
	Maintenance Cost	4.14%	1.09%	0.49%
	Monetary Cost	-4.45%	**-9.20%**	6.69%

5.6.2.2 Deadheading Minimization and Tour Design

All the assumptions in 5.5.2 apply to this model, and one additional assumption is that vehicles that serve a tour can be housed in all depot candidates. Table 22 shows the results of the enhanced tour design model, compared with the baseline scenarios. Similar to the results in 5.6.2.1, the objective value of each metric is further reduced by an absolute value of 0.4%.

Table 22 – Reduction Percentages Compared with Baselines: Deadheading Minimization and Tour Design Model

		CO_2 Emissions	Monetary Cost	Energy Use
Scenario 1	Duration	8.76%	3.12%	4.90%
	Distance	-3.04%	-3.06%	-3.01%
	Energy Use	-0.50%	-0.49%	**-6.00%**
	CO_2 Emissions	**-6.89%**	-6.88%	-0.09%
	Energy Cost	-21.64%	-21.63%	13.55%
	Maintenance Cost	0.23%	0.21%	-6.00%
	Monetary Cost	-11.38%	**-11.39%**	4.38%

		CO_2 Emissions	Monetary Cost	Energy Use
Scenario 2	Duration	10.34%	2.98%	6.79%
	Distance	-3.04%	-2.87%	-2.86%
	Energy Use	-9.02%	4.04%	**-14.33%**
	CO_2 Emissions	**-9.92%**	-6.14%	-4.61%
	Energy Cost	-11.48%	-23.94%	12.38%
	Maintenance Cost	2.60%	-2.10%	-0.48%
	Monetary Cost	-5.29%	**-14.34%**	6.72%

5.7 Summary

In this chapter, four models are developed, with the goal of minimizing operating costs for transit agencies with multiple depots and mixed fuel fleets. The formulation of each proposed model is described in detail. The implementation results show that through operation optimization, fleet-wide life-cycle CO_2 emissions can be reduced by 10%, operating cost by 12%, and energy use by 11%.

The main contributions of the proposed models: 1) deadheading minimizing model, 2) bus-to-tour assignment model, 3) tour design model, and 4) combined model are:

1) Vehicle energy use at the micro-trip level are more accurately evaluated in this work compared to previous literature work by incorporating vehicle specifications, onroad operating conditions, and roadway characteristics with an energy use model.
2) The fleet-wide energy use is assessed more thoroughly than in previous studies by including revenue service, depot pull-in/pull-out, and interlining trips.
3) The models can optimize various operations and specific operational elements, including depot selection, bus-to-tour assignment, and tour design.

4) Three cost metrics are proposed, and thus decision-makers can compare the trade-offs across these different objectives.
5) The proposed models can be readily applied by local transit agencies using data that are already available or can be easily obtained, and these models can be customized with fleet-specific characteristics.

The limitations of the models developed and applied in this chapter can be addressed in future work, include:

1) Operating monetary cost only consists of vehicle maintenance and fuel. Labor costs are not included in the optimization function, and in the tour design model, the operator cost is increased due to increased operating time. Capital costs are also ignored in this chapter because the models assume we are dealing with an existing fleet.
2) The tour design model does not include any duration or mileage limits per tour. This can be a challenge to vehicles with range limits, like battery-electric vehicles, and for drivers who may be limited to specific operating hours.

CHAPTER 6. OPTIMIZATION OF FLEET ELECTRIFICATION

6.1 Overview

The suite of models developed in this chapter are designed to optimize transit fleet operations while introducing electric vehicle sub-fleets to the existing fleet. The three models developed for this chapter include the electrification cost model, operation optimization model for depot-charged electric vehicle sub-fleets, and a budget-constrained sub-fleet electrification optimization model. These models allow modelers to assess tradeoffs between electric vehicle charger types, number of vehicles per charger type, electric bus-to-tour assignment, non-electric bus to tour assignment, number of depot chargers, depot charging schedule, number of on-route fast chargers, and on-route charging schedule (Table 23). Section 6.2 describes the electrification cost model, which is designed to minimize the total cost of electrification (vehicle capital, charging facility, utility, and driver costs) when electrifying a set of tours. Two sub-models are formulated, one with depot charging only, and the other with both depot charging and on-route fast charging. The optimized decisions include vehicle procurement, charging facility procurement and placement, and charging schedules. Section 6.3 describes the operation optimization model for depot-charged electric vehicle sub-fleets. With electric vehicle sub-fleets and charging facilities already in place, this model minimizes operating costs in a mixed fleet by optimizing bus-to-tour assignment and charging schedules. The same three cost metrics (life-cycle CO_2 emissions, operating monetary cost, and on-road energy use), presented in Chapter 5 are used in the objective function. Section 6.4 introduces the budget-constrained sub-fleet electrification optimization model. The goal of this model is to maximize the

benefits of reducing life-cycle CO_2 emissions through the adoption of electric vehicle fleets, while satisfying a prescribed budget constraint. In each model, optimization equations are formulated and applied to the local transit network. Finally, Section 6.5 summarizes the findings and limitations of the proposed models.

Table 23 – Model Overview: Fleet Electrification

	Model 1 Electrification Cost		**Model 2 Operation Optimization**	**Model 3 Budget-Constrained Sub-fleet Electrification**	
Charging Option	Depot	Depot and On-route	Depot	Depot	Depot and On-route
Number of Vehicles per Type	Decisions	Decisions	Fixed	Decisions	Decisions
Electric Bus-to-Tour Assignment	Decisions	Decisions	Decisions	Decisions	Decisions
Non-electric Bus-to-Tour Assignment	NA	NA	Decisions	NA	NA
Number of Depot Chargers	Decisions	Decisions	Fixed	Decisions	Decisions
Depot Charging Schedule	Decisions	Decisions	Decisions	Decisions	Decisions
Number of On-route Chargers	NA	Decisions	NA	NA	Decisions
On-route Charging Schedule	NA	Decisions	NA	NA	Decisions

Table 24 shows the notations of the decision variables used in this chapter. F_1 denotes the set of vehicle types of existing fleets, and F_2 denotes the set of vehicle types (battery capacities) for the electric vehicles. For simplicity, we use type (notation f) to represent either fuel and age category of non-electric fleets, or battery capacity of electric

vehicle fleets. In addition to the bus-to-tour assignment decision variable (W_b^f) as described in Chapter 5, we introduce charging facility variables for depots (N_y) and for on-route charging (N_p, $N_{p,q}$). Charging event variables ($X_{b,m,q,o}^f$, $V_{b,m,q,o}^f$) are used to constrain battery energy levels and charger availability. Indices and subscripts for these variables are described in detail in the model formulation sections.

Table 24 – Decision Variables: Fleet Electrification

Notation		Meaning
N_p	$\forall\, p \in P$	On-route charging station variable Binary variable 1 if on-route charging station is built at stop p
$N_{p,q}$	$\forall\, p \in P, q \in Q_p$	Number of on-route chargers variable Integer variable Number of on-route type q chargers at stop y
N_y	$\forall y \in Y$	Number of depot chargers variable Integer variable Number of depot chargers at depot y
$V_{b,m,q,o}^f$	$\forall\, b \in B, f \in F_2,$ $m \in \{1, \dots, m_b\},$ $o \in \{1,2\}, q \in Q_{P_{b,m,o}}$	On-route charging event occurrence variable Binary variable 1 if charging event occurs when charged with type q charger, using charging option o, after finishing revenue trip m in tour b
W_b^f	$\forall\, b \in B, f \in F_1 \cup F_2$	Bus-to-tour variable Binary variable 1 if tour b is served by a type f vehicle
$X_{b,m,q,o}^f$	$\forall\, b \in B, f \in F_2,$ $m \in \{1, \dots, m_b\}$ $o \in \{1,2\}, q \in Q_{P_{b,m,o}}$	On-route charging duration variable Continuous variable Charging duration when charged with type q charger, using charging option o, after finishing revenue trip m in tour b

6.2 Electrification Cost Model

The electrification cost model is designed to identify the type of vehicle (battery capacity) needed for each tour, where to place the chargers, and when to charge the vehicles

once the decision has been made to electrify a set of tours. Two models are designed: one only allows vehicles to be charged at a depot, and the other allows for both depot charging and on-route fast charging. In the depot-charging-only model, the cost components include vehicle procurement, depot charger procurement and installation, electricity costs, vehicle maintenance, and driver costs. Utility costs include both the standard electricity use rate as well as the peak demand charge cost. Depot chargers are shared and available to all electric vehicles, as long as there is no time conflict (i.e., the charger station cannot already be occupied). In the depot and on-route charging model, the costs of building on-route charging stations and chargers are included. On-route chargers are shared and available to all vehicles that dwell at the stations as long as there is no time conflict for the connection.

6.2.1 Model Formulation – Depot Charging Only

Battery-electric buses with only depot-charging assume that a bus with full battery pulls out of the depot to serve a tour, and that bus is charged immediately after pulling into the depot at the end of the tour. The bus stays in the depot until fully charged (using a plug-in charger), and then becomes available to be pulled out to serve another tour. If the energy demand of a tour is higher than the battery capacity, the original tour is split into several sub-tours. Similar to a tour, a sub-tour includes pull-in/pull-out and revenue operations. The number of sub-tours may differ when served by different battery capacities. This is because a larger battery capacity has a longer range, and thus may result in fewer sub-tours. I_b^f denotes the set of sub-tour indices in tour b if served by vehicle with battery capacity f. If the battery capacity is large enough to serve the entire tour b, I_b^f only includes one sub-tour, i.e. $I_b^f = \{1\}$, and thus the trips in sub-tour $(b, 1)$ are the same as in

tour b. For each sub-tour, buses are designed to operate to their maximum available range. For the purposes of the case studies, time is discretized into equal duration time slots, i.e. $T = \{\cup\, t_k\}$, where t_k is one time slot. 5-minute time slots are employed (although a user could specify any desired binning duration). If a bus is charged at that slot t_k, the charger is not available until the next slot t_{k+1}.

The two decision variables are used: binary variable W_b^f, which equals 1 if the bus with battery capacity f is assigned to tour b, and an integer variableN_y, which represents the number of chargers built at depot y. F_2 is the set of all battery capacities. Equation (35) denotes the objective function, minimizing the tour electrification cost, consisting of six components. Equation (36) denotes the battery-electric bus investment (C_θ). Cost per vehicle battery capacity f is calculated by multiplying the number of vehicles (w^f) by the vehicle cost rate (θ^f). Equation (37) denotes the charger cost (C_μ), including investment (with installation) and its ongoing maintenance cost. For each depot y, charger cost is calculated by multiplying the number of chargers (N_y) by the sum of investment cost rate ($\mu 1_y$) and maintenance cost rate ($\mu 2_y$). Equation (38) denotes the utility cost from demand charge (C_φ), calculated by multiplying peak power (U_{Peak}) by demand charge cost rate (φ). Equation (39) denotes the utility cost from electricity usage on service day type s ($C_{\alpha,s}$). Electricity use per sub-tour (b, i), is calculated by multiplying the amount of energy use ($E_{b,i}^f$) by the electricity cost rate at that time slot ($\pi_{TC_{b,i}}$). Equation (40) denotes the vehicle maintenance cost on service day type s ($C_{\beta,s}$). Maintenance cost per sub-tour (b, i) is calculated by multiplying the distance traveled of the sub-tour ($D_{b,i}^f$) by the vehicle maintenance cost rate (β^f). Equation (41) denotes the driver cost on service day type s

($C_{\gamma,s}$). Operator cost per sub-tour (b,i) is calculated by multiplying the operating duration of the sub-tour ($T_{b,i}^{f}$) by the labor salary rate (γ^{f}).

$$\min_{W_b^f, N_y} C_\theta + C_\mu + C_\varphi + \sum_{\forall s \in S} Freq_s \left(C_{\alpha,s} + C_{\beta,s} + C_{\gamma,s}\right) \tag{35}$$

$$C_\theta = \sum_{\forall f \in F_2} w^f \, \theta^f \tag{36}$$

$$C_\mu = \sum_{\forall y \in Y} N_y \left(\mu 1_y + \mu 2_y\right) \tag{37}$$

$$C_\varphi = U_{Peak} * \varphi \tag{38}$$

$$C_{\alpha,s} = \sum_{\forall b \in B_s} \sum_{\forall f \in F_2} \sum_{\forall i \in I_b^f} W_b^f \, E_{b,i}^f \pi_{TC_{b,i}} \tag{39}$$

$$C_{\beta,s} = \sum_{\forall b \in B_s} \sum_{\forall f \in F_2} \sum_{\forall i \in I_b^f} W_b^f \, D_{b,i}^f \beta^f \tag{40}$$

$$C_{\gamma,s} = \sum_{\forall b \in B_s} \sum_{\forall f \in F_2} \sum_{\forall i \in I_b^f} W_b^f \, T_{b,i}^f \gamma^f \tag{41}$$

Equation (42) through (49) are constraints relative to vehicle availability. Equation (42) denotes the constraint that each tour is served by one type of vehicle. In equation (43), $T_{b,i}^{f}$ denotes the set of in-use time slots if sub-tour (b,i) is served with a type f vehicle, i.e. from the time slot of depot pull-out ($t_{TO_{b,i}^f}$) to the time slot when fully charged at depot ($t_{TI_{b,i}^f + TD_{b,i}^f}$). $TO_{b,i}^{f}$, $TI_{b,i}^{f}$ denote the timestamps of departure time of depot pull-out and

arrival time of depot pull-in, and $TD_{b,i}^{f}$ denotes the duration of depot charging. In equation (44), w_{y,s,t_k}^{f} denotes the number of type f vehicles from depot y that are in use at time slot t_k on service day type s, calculated by counting the number of type f vehicles whose in-use time slot set ($T_{b,i}^{f}$) includes slot t_k. Equation (45) denotes the vehicle availability constraint (i.e., at each time slot t_k, the supply of type f vehicles from depot y (w_y^f) is sufficient to meet the demand (w_{y,s,t_k}^{f})). Equation (46) denotes the constraint of the availability of vehicles for each depot, i.e. at each time slot, the total number of available vehicles of all types ($\sum_{\forall f \in F_2} w_y^f$) should exceed the number of total in-use vehicles and spares. The spares are not required to be of the same type of the in-use vehicles (most agencies use diesel vehicles as spares). The vehicle spare ratio ($\eta 1$) is introduced here, because most agencies have vehicles in spare to serve breakdowns, emergencies, and special events. In equation (47), w^f denotes the fleet-wide demand for type f vehicles. In equation (48), w_y denotes the demand of vehicles at depot y, which should not exceed the depot capacity (χ_y) as denoted in equation (49).

$$\sum_{f \in F_2} W_b^f = 1 \qquad \forall b \in B \qquad (42)$$

$$T_{b,i}^{f} = \{t_{TO_{b,i}^{f}}, t_{TO_{b,i}^{f}+1}, \dots, t_{TI_{b,i}^{f}+TD_{b,i}^{f}}\} \qquad \forall b \in B, f \in F_2, i \in I_b^f \qquad (43)$$

$$w_{y,s,t_k}^{f} = \sum_{\forall b \in B_{s,y}, i \in I_b^f, t_k \in T_{b,i}^{f}} W_b^f \qquad \forall s \in S, y \in Y, f \in F_2, t_k \in T \qquad (44)$$

$$\max_{\forall s \in S, t_k \in T} w^f_{y,s,t_k} \leq w^f_y \qquad \forall\, y \in Y, f \in F_2 \qquad (45)$$

$$\max_{\forall s \in S, t_k \in T} (1+\eta 1) \sum_{\forall f \in F_2} w^f_{y,s,t_k} \leq \sum_{\forall f \in F_2} w^f_y \qquad \forall y \in Y \qquad (46)$$

$$w^f = \sum_{\forall y \in Y} w^f_y \qquad \forall f \in F_2 \qquad (47)$$

$$w_y = \sum_{\forall f \in F_2} w^f_y \qquad \forall y \in Y \qquad (48)$$

$$w_y \leq \chi_y \qquad \forall y \in Y \qquad (49)$$

Equations (50) through (53) are constraints related to depot chargers. In equation (50), $TC^f_{b,i}$ denotes the set of depot charging time slots for sub tour (b,i) if served with a type f vehicle, i.e. from the time slot of depot pull-in ($t_{TI_{b,i}}$), to the time slot when depot charging is complete ($t_{TI_{b,i}+TD^f_{b,i}}$). In equation (51), n^f_{y,s,t_k} denotes the number of type f vehicles that are charged at depot y in time slot t_k on service day type s, calculated by counting the number of type f vehicles whose depot charging time slot ($TC^f_{b,i}$) includes time slot t_k. Equation (52) denotes the charger availability constraint, i.e. in each time slot t_k, ensuring that the supply (N_y) is sufficient to meet the charging demand. The spare ratio of depot chargers at each depot is represented by $\eta 2$ (we assume that these spares can be used if necessary, and the number of spares can be set to zero by the user). Equation (53) denotes the constraint that the number of chargers at each depot (N_y) cannot exceed its

capacity (χ_y^{Depot}). In equation (54), U_{Peak} denotes the peak charging power, which is the maximum charging power across all time slots and days.

$$TC_{b,i}^f = \{t_{TI_{b,i}}, t_{TI_{b,i}+1}, \dots, t_{TI_{b,i}+TD_{b,i}^f}\} \qquad \forall b \in B, f \in F_2, i \in I_b^f \qquad (50)$$

$$n_{y,s,t_k}^f = \sum_{\forall b \in B_{s,y}, t_k \in TC_{b,i}^f} W_{b,i}^f \qquad \forall s \in S, y \in Y, f \in F_2, t_k \in T, i \in I_b^f \qquad (51)$$

$$\max_{\forall s \in S, t_k \in T} (1 + \eta 2) \sum_{f \in F_2} n_{y,s,t_k}^f \leq N_y \qquad \forall y \in Y \qquad (52)$$

$$N_y \leq \chi_y^{Depot} \qquad \forall y \in Y \qquad (53)$$

$$U_{Peak} = \max_{\forall s \in S, t_k \in T} \sum_{y \in Y} n_{y,s,t_k}^f U_{Depot} \qquad (54)$$

6.2.2 Model Formulation - Depot and On-Route Charging

Battery-electric buses that can use both depot and on-route charging make the modeling a bit more complex. A bus with fully battery is pulled out of the depot to serve a tour, charged when dwelling at starting/ending stops during interlining, and also charged right after pulling in to a depot. The bus stays in the depot to be fully charged, and is then ready to be pulled out to serve another tour. The original tour design is maintained, because batteries can sustain their energy levels through on-route charging. All variables in Table 24 are used in this model. Because non-electric vehicle fleets are not considered, we set $f \in F_2$ for the bus-to-tour assignment variable W_b^f. The two variables of battery capacity

choice (W_b^f) and number of chargers at depot (N_y) in the depot-charging-only model still apply to this model. In addition, $X_{b,m,q,o}^f$, which represents the charging duration when charged with type q charger using charging option o after finishing revenue trip m in tour b, and $V_{b,m,q,o}^f$, which equals 1 if the charger event occurs (the corresponding $X_{b,m,q,o}^f$ is above zero), are used to denote on-route charging events. For the trip m in tour b, it has two charging options: o=1 if charged at the ending stop of revenue trip m, o=2 if charged at the starting stop of revenue trip $m+1$. If using option 1, the charging stop is $P_{b,m,1}$ and its available chargers are $q \in Q_{P_{b,m,1}}$; using option 2, the charging stop is $P_{b,m,2}$ and its available chargers are $q \in Q_{P_{b,m,2}}$. That is, charger location can be uniquely identified with the information of tour (b), trip sequence (m), and charging option (o). Variable N_p and $N_{p,q}$ are used to represent the existence of on-route charging station and the number of chargers. Assumptions related to bus operations as well as charging activities are listed below:

1) Both depot-charging and on-route fast-charging are available to all the buses
2) Fast on-route charging facilities are installed at starting/ending stops of each revenue route, and plug-in chargers are installed at depots
3) Buses with the same battery capacity are assumed to stay in the depot for the same amount of time to be fully charged
4) When interlining from trip m to trip $m+1$, a bus can be charged only once (i.e., either at the ending stop of trip m, or at the starting stop of trip $m+1$)
5) On-route charging is feasible when available layover duration is greater than or equal to five minutes (i.e., interlining duration excluding driving duration)

6) Time is discretized into time slots with equal durations, i.e. $T = \{\bigcup t_k\}$, where t_k is a time slot. For the purposes of the modeling conducted in the case studies, time duration bins are set to 5 minutes, but the user can specify these time periods. If a bus is charged at that time slot, the charger is not available until the next slot

Equation (55) shows the objective function, minimizing fleet electrification cost. C_θ, C_μ, and C_φ denotes the bus investment, depot charger, and demand charge cost, formulated in the same way as the depot charging model in equation (36)-(38). Equation (56) denotes the on-route charging station cost (C_τ), including capital investment (with installment) and maintenance costs. Equation (57) denotes the on-route charger cost (C_ϵ), including capital investment (with installment) and maintenance costs. Equation (58) denotes the daily electricity usage cost on service day type s ($C_{\alpha,s}$), including both depot and on-route charging, calculated by multiplying energy use by the utility rates. Utility rates are dependent on the time slot of charging events. Equation (59) denotes the vehicle maintenance cost ($C_{\beta,s}$), calculated by multiplying the distance traveled (D_b^f) by the maintenance cost rate (β^f). Equation (60) denotes the operator cost ($C_{\gamma,s}$), calculate by multiplying the operating duration (T_b^f) by the operator labor salary rate (γ^f). Equation (61) denotes the on-route charging penalty on service day type s ($C_{\sigma,s}$), calculated by multiplying the number of on-route charging events (v_s) by the penalty rate (σ_s). Charging penalty is used because agencies prefer concentrated charging with fewer charging events involved because it is easier to manage. Also, too many charging events may increase the

maintenance cost of chargers and batteries, which can also be incorporated in the penalty component if desired.

$$\min_{\substack{W_b^f, N_y, V_{b,m,q,o}^f, \\ X_{b,m,q,o}^f, N_p, N_{p,q}}} C_\theta + C_\mu + C_\varphi + C_\tau + C_\epsilon + \sum_{\forall s \in S} Freq_s \left(C_{\alpha,s} + C_{\beta,s} + C_{\gamma,s} + C_{\sigma,s}\right) \tag{55}$$

$$C_\tau = \sum_{\forall p \in P} N_p(\tau 1_p + \tau 2_p) \tag{56}$$

$$C_\epsilon = \sum_{\forall p \in P} \sum_{\forall q \in Q_p} N_{p,q}(\epsilon 1_q + \epsilon 2_q) \tag{57}$$

$$C_{\alpha,s} = \sum_{\forall b \in B_s} \left(E_b \pi_{TC_b} + \left(\sum_{\forall f \in F_2} \sum_{m=1}^{m_b - 1} \sum_{o \in \{1,2\}} \sum_{\forall q \in Q_{p_{b,m,o}}} X_{b,m,o,q}^f U_q \, \pi_{T_{b,m,o}} \right) \right) \tag{58}$$

$$C_{\beta,s} = \sum_{\forall b \in B_s} \sum_{\forall f \in F_2} W_b^f D_b^f \, \beta^f \tag{59}$$

$$C_{\gamma,s} = \sum_{\forall b \in B_s} \sum_{\forall f \in F_2} W_b^f T_b^f \, \gamma^f \tag{60}$$

$$C_{\sigma,s} = v_s \sigma_s \tag{61}$$

The constraints related to depot charging events and vehicle availability (equation (42)-(53)) in the depot charging model also apply to this model. However, equations (43) through (44) are updated with equation (62) through (63), and equation (50) through (51) are updated with equations (64) through (65) by replacing sub-tours with tours to maintain the original tour design.

$$T_b^f = \{t_{TO_b}, t_{TO_b+1}, \dots, t_{TI_b+TD_b^f}\} \qquad \forall b \in B, f \in F_2 \qquad (62)$$

$$w_{y,s,t_k}^f = \sum_{\forall b \in B_{s,y}, t_k \in T_b^f} W_b^f \qquad \forall s \in S, y \in Y, f \in F_2, t_k \in T \qquad (63)$$

$$TC_b^f = \{t_{TI_b}, t_{TI_b+1}, \dots, t_{TI_b+TD_b^f}\} \qquad \forall b \in B, f \in F_2 \qquad (64)$$

$$n_{y,s,t_k}^f = \sum_{\forall b \in B_{s,y}, t_k \in TC_b^f} W_b^f \qquad \forall s \in S, y \in Y, f \in F_2, t_k \in T \qquad (65)$$

Constraints related to energy flows, on-route charging events and facilities, and peak charging events are formulated and described below. Equation (66) through (72) denote the energy flow formulation. In equation (66), $Batt_b$ denotes the initial energy level for tour b, where vehicles are assumed at full charge before depot pull-out. In equation (67), $EC1_{b,m}$ denotes the energy use of trip m from tour b: if $m = 0$, it represents the energy use of depot pull-out; if $m \in \{1,2, \dots, m_b\}$, it represents the energy use of a revenue trip; if $m = m_b + 1$, it represents the energy use of depot pull-in. In equation (68), $EC2_{b,m}$ denotes the energy use of interlining from trip m to $m + 1$. In equation (69), $E_{b,0}$ denotes the energy level after pulling out of depot, before starting its first revenue trip. In equation (70), $E_{b,m}$ denotes the energy level after finishing revenue trip m, before starting the trip $m + 1$. The summation portion of the equation denotes the energy amount charged at either the ending stop of trip m, or the next starting stop $m + 1$. For simplification, we assume the energy charged equals the charging duration ($X_{b,m,o,q}$) multiplied by the charger

power (U_q). In equation (71), E_{b,m_b+1} denotes the energy level after pulling into depot. In equation (72), E_b denotes the energy amount to be charged at depot.

$$Batt_b = \sum_{f \in F_2} W_b^f \, Batt^f \qquad \forall b \in B \tag{66}$$

$$EC1_{b,m} = \sum_{f \in F_2} W_b^f \, EC1_b^f \qquad \forall m \in \{0,1,2,\dots,m_b+1\}, \; b \in B \tag{67}$$

$$EC2_{b,m} = \sum_{f \in F_2} W_b^f \, EC2_b^f \qquad \forall m \in \{1,2,\dots,m_b\}, \; b \in B \tag{68}$$

$$E_{b,0} = Batt_b - EC1_{b,0} \qquad \forall b \in B \tag{69}$$

$$E_{b,m} = E_{b,m-1} - EC1_{b,m} - EC2_{b,m} + \sum_{\forall o \in \{1,2\}} \sum_{\forall q \in Q_p, p = P_{m,o}} X_{b,m,o,q} U_q \qquad \forall m \in \{1,2,\dots,m_b\}, \; b \in B \tag{70}$$

$$E_{b,m_b+1} = E_{b,m_b} - EC1_{b,m_b+1} \qquad \forall b \in B \tag{71}$$

$$E_b = Batt_b - E_{b,m_b+1} \qquad \forall b \in B \tag{72}$$

Equations (73) through (78) denote the constraints related to energy flows. Equation (73) denotes the constraint that after finishing the trip m, the energy level is constrained to remain above the minimum SOC limit. Equation (74) denotes the constraint that if charging before interlining to the next trip, the energy level cannot exceed the maximum SOC limit. Equation (75) denotes the constraint that after interlining from revenue trip m to $m+1$, the remaining energy level still satisfies the minimum SOC limit. Equation (76) denotes the constraint that if charging after interlining to the next trip, the

energy level cannot exceed the maximum SOC limit. Equation (77) denotes the constraint that no more than one charging event occurs after each revenue trip. Equation (78) denotes the constraint that after depot pull-in, the energy level is still above the minimum SOC limit.

$$E_{b,m-1} - EC1_{b,m} \geq Batt_b SOC_{min} \qquad \forall m \in \{1,2,\dots,m_b - 1\}, b \in B \qquad (73)$$

$$E_{b,m-1} - EC1_{b,m} + \sum_{\forall q \in Q_p, p = P_{m,1}} X_{b,m,1,q} U_q \leq Batt_b SOC_{max} \qquad \forall m \in \{1,2,\dots,m_b - 1\}, b \in B \qquad (74)$$

$$E_{b,m-1} - EC1_{b,m} + \left(\sum_{\forall q \in Q_p, p = P_{m,1}} X_{b,m,1,q} U_q \right) - EC2_{b,m} \geq Batt_b SOC_{min} \qquad \forall m \in \{1,2,\dots,m_b - 1\}, b \in B \qquad (75)$$

$$E_{b,m} \leq Batt_b SOC_{max} \qquad \forall m \in \{1,2,\dots,m_b - 1\}, b \in B \qquad (76)$$

$$\sum_{\forall o \in \{1,2\}} \sum_{\forall q \in Q_p, p = P_{m,o}} V_{b,m,o,q} \leq 1 \qquad \forall m \in \{1,2,\dots,m_b - 1\}, b \in B \qquad (77)$$

$$E_{b,m_b+1} \geq Batt_b SOC_{min} \qquad \forall b \in B \qquad (78)$$

Equations (79) through (89) denote the constraints related to charging events. Equation (79) denotes the constraint that the charging duration cannot exceed the available time. The maximum charging duration is calculated as the duration from the end of trip m ($TE_{b,m}$) to the start of the trip $m+1$ ($TS_{b,m+1}$), excluding the driving time ($TI_{b,m,m+1}$). Equation (80) uses big $\boldsymbol{M}$ to denote the relationship between charging event and charging duration, i.e. $V_{b,i,o,q}$ equals 1 if the vehicle is charged after trip m.

$$\begin{cases} \sum_{\forall o\in\{1,2\}} \sum_{\forall q\in Q_p, p=P_{b,m,o}} X_{b,m,o,q} \le TS_{b,m+1} - TE_{b,m} - TI_{b,m,m+1} & (79) \\ \sum_{\forall o\in\{1,2\}} \sum_{\forall q\in Q_p, p=P_{b,m,o}} X_{b,m,o,q} \le \boldsymbol{M} \sum_{\forall o\in\{1,2\}} \sum_{\forall q\in Q_p, p=P_{b,m,o}} V_{b,m,o,q} & (80) \end{cases}$$
$$\forall m \in \{1,2,\dots,m_b - 1\}, b \in B$$

Equation (81) through (87) denote the constraints related to on-route charging facilities. In equation (81), n_{p,q,s,t_k} denotes the charger demand of type q installed at station p at time slot t_k on service day type s, calculated by counting the number of charging events whose charging time slot set ($T_{b,m,o}$) includes slot t_k. Equations (82) and (83) denote the charging slot set if charged before interlining (option 1) and after interlining (option 2), respectively. Equation (84) denotes the constraint that the demand of type q charger at station p at time slot t_k on service day type s (n_{p,q,s,t_k}) cannot exceed the number of total chargers of that type at that station($N_{p,q}$). Equation (85) denotes the constraint that the charger demand of type q at station p cannot exceed its charger capacity ($\chi_{p,q}^{OnRoute}$), which is dependent on the real-world environment, e.g. the available lot area and grid power limits. Equation (86) denotes the constraint of the relationship between charging station and charger, i.e. a charging station must exist if there is a charger. Equation (87) denotes the constraint of the relationship between chargers and charging events, i.e. a charger must exist if it is used for charging. In equation (88), U_{Peak} denotes the peak charging power, which is the maximum charging power of the sum of both depot and on-route charging, across all time slots and days. Equation (89) quantifies the daily number of on-route charging events on service day type s.

$$n_{p,q,s,t_k} = \sum_{\forall p=P_{b,m,o}, b\in B_s, t_k \in T_{b,m,o}} V_{b,m,o,q} \qquad \forall p \in P, q \in Q_p, \; s \in S, t_k \in T \tag{81}$$

$$T_{b,m,1} = \{t_{TE_{b,m}}, t_{TE_{b,m}+1}, \dots, t_{TS_{b,m+1}-TI_{b,m,m+1}}\} \qquad \forall m \in \{1,2,\dots,m_b\}, \; b \in B \tag{82}$$

$$T_{b,m,2} = \{t_{TE_{b,m}+TI_{b,m,m+1}}, t_{TE_{b,m}+TI_{b,m,m+1}+1}, \dots, t_{TS_{b,m+1}}\} \qquad \forall m \in \{1,2,\dots,m_b\}, \; b \in B \tag{83}$$

$$\max_{\forall s\in S, t_k \in T} n_{p,q,s,t_k} \le N_{p,q} \qquad \forall p \in P, q \in Q_p \tag{84}$$

$$N_{p,q} \le \chi_{p,q}^{OnRoute} \qquad \forall\, p \in P, q \in Q_p \tag{85}$$

$$\sum_{q\in Q_p} N_{p,q} \le \boldsymbol{M} N_p \qquad \forall\, p \in P \tag{86}$$

$$\sum_{\forall q\in Q_p, p=P_{b,m,o}} V_{b,m,o,q} \le \boldsymbol{M} N_{p,q} \qquad \forall\, p \in P, q \in Q_p \tag{87}$$

$$U_{Peak} = \max_{\forall s\in S, t_k \in T} \left(\sum_{y\in Y} n_{y,s,t_k}^{f} U_{Depot} + \sum_{\forall b\in B_s, t_k \in T_{b,m,o}} \sum_{\forall p=P_{b,m,o}, q\in Q_p} V_{b,m,o,q} U_q \right) \tag{88}$$

$$v_s = \sum_{\forall b\in B_s} \sum_{m=1}^{m_b-1} \sum_{\forall o\in\{1,2\}} \sum_{\forall q\in Q_p, p=P_{b,m,o}} V_{b,m,o,q} \qquad \forall s \in S \tag{89}$$

6.2.3 Additional Constraints

In the practical world, some agencies may have additional constraints or adjustments for fleet electrification that are not covered in the two proposed basic cost models. Some additional constraints and adjustments are discussed below.

6.2.3.1 Schedule Adjustment

As mentioned in Section 2.4.3, two-thirds of the transit agencies who adopt battery-electric vehicles adjust their schedules after procuring the vehicles. Adjusting schedules is a complex process, especially for large transit networks. However, sometimes, it may be more cost-effective or even necessary to adjust schedules to accommodate fleet electrification. In our proposed cost model, current tours are integrated from the GTFS data feed for the transit agency and then these tours are retained in the analytical models. Hence, on-route charging is limited to interlining between revenue trips. Agencies can use a hypothetical GTFS file, to experiment with proposed changes to schedules. However, agencies may find it much more beneficial to be able to assess the impacts of more complex charging decisions directly within the optimization modeling tools. For example, it may be more beneficial to charge vehicles before the first revenue trip or after the last revenue trip, especially when the starting and ending stop of the tour is far away from the depot. Charging before and after the tour can avoid the high electricity rate at peak periods, which can further reduce the electricity cost, but may come with additional battery costs (to ensure that sufficient charge is available for the routes). Adding pre/post-revenue on-route charging opportunities could be an easy way to resolve the range issue and an effective approach to maintain vehicle energy level and reduce operating costs. One caveat is this may require shift changes for transit operators, with an earlier starting time and a later ending time to maintain revenue trip schedules.

To support the assessment of more complex charging schedules, we use TR_1 and TR_2 to represent the maximum on-route charging duration of the pre-revenue and post-revenue trips. In the depot and the depot plus on-route charging models, starting time of a

tour b is updated to $TO_b - TR_1$, which shifts the original pull-out timestamp earlier by TR_1, and ending time is updated to $TI_b + TR_2 + TD_b^f$, which shifts the original pull-in timestamp later by TR_2 and the vehicle is use until finishing the depot charging. The set of in-use time slots (T_b^f) denoted in equation (62) is updated with equation (90). The set of depot-charging time slots (TC_b^f) denoted in equation (64) is updated with equation (91).

$$T_b^f = \{t_{TO_b - TR_1}, t_{TO_b - TR_1 + 1}, \dots, t_{TI_b + TR_2 + TD_b^f}\} \qquad \forall b \in B, f \in F_2 \qquad (90)$$

$$TC_b^f = \{t_{TI_b + TR_2}, t_{TI_b + TR_2 + 1}, \dots, t_{TI_b + TR_2 + TD_b^f}\} \qquad \forall b \in B, f \in F_2 \qquad (91)$$

Continuous variables, $X_{b,0,2,q}$ and $X_{b,m_b,1,q}$ are added to denote the duration of pre-revenue and post-revenue charging events in tour b if using type q charger. Binary variables, $V_{b,0,2,q}$ and $V_{b,m_b,1,q}$ are added accordingly to represent whether or not the charging event occurs. Equation (92) and (93) denote the constraints that charging durations cannot exceed prescribed time limits. Equation (69) is updated with equation (94), which adds the charging event at the first revenue stop in the tour. Then equation (95) is added to ensure that the SOC level is satisfied if the vehicle is charged before serving its first revenue trip. All charging-rated constraints in equations (74) through (77), and (79) through (80) are updated to $\forall i \in \{1,2, \dots, m_b\}$ to incorporate post-revenue charging events. Correspondingly, the electricity cost in equation (58) is updated with equation (96), which adds the pre-revenue and post-revenue charging events. Finally, equation (89) is updated with equation (97) to incorporate the pre/post-charging events.

$$\sum_{\forall q \in Q_p, p = P_{0,2}} X_{b,0,2,q} \leq TR_1 \qquad \forall b \in B \quad (92)$$

$$\sum_{\forall q \in Q_p, p = P_{0,2}} X_{b,m_b,1,q} \leq TR_2 \qquad \forall b \in B \quad (93)$$

$$E_{b,0} = Batt_b - EC1_{b,0} + \sum_{\forall q \in Q_p, p = P_{0,2}} X_{b,0,2,q} U_q \qquad \forall b \in B \quad (94)$$

$$E_{b,0} \leq Batt_b SOC_{max} \qquad \forall b \in B \quad (95)$$

$$C_{\alpha,s} = \sum_{\forall b \in B_s} \left(E_b \pi_{TC_b} + \left(\sum_{\forall f \in F_2} \sum_{m=0}^{m=m_b} \sum_{o \in \{1,2\}} \sum_{\forall q \in Q_{p_{b,m,o}}} X^f_{b,m,o,q} U_q \, \pi_{T_{b,m,o}} \right) \right) \qquad \forall s \in S \quad (96)$$

$$v_s = \sum_{\forall b \in B_s} \sum_{m=0}^{m=m_b} \sum_{\forall o \in \{1,2\}} \sum_{\forall q \in Q_p, p = P_{b,m,o}} V_{b,m,o,q} \qquad \forall s \in S \quad (97)$$

6.2.3.2 Demand Charge Cost

If the time slot t_k is smaller than the time interval used for peak demand pricing calculations used by the utility, then peak power demand is calculated not from one time slot, but the aggregated average of multiple time slots. For example, if the demand interval is ϖt_k, where ϖ is a positive integer, then the set of the time slots in a demand interval (TU_k) can be denoted in equation (98). The peak demand equations in the two cost models,

shown in equation (54) and (88), are updated with equation (99) and (100), respectively to calculate the peak demand power by averaging the aggregated power per demand interval.

$$TU_k = \{t_k, t_{k+1}, \dots, t_{k+\varpi-1}\} \quad \forall t_k \in T \tag{98}$$

$$U_{Peak} = \max_{\forall s \in S, t_k \in T} \left(\frac{1}{\varpi} \sum_{y \in Y} \sum_{t_k \in TU_k} n^f_{y,s,t_k} U_{Depot} \right) \tag{99}$$

$$\begin{aligned} U_{Peak} = \max_{\forall s \in S, t_k \in T} \Bigg(& \frac{1}{\varpi} \left(\sum_{y \in Y} \sum_{t_k \in TU_k} n^f_{y,s,t_k} U_{Depot} \right) \\ & + \left(\sum_{\forall b \in B_s, TU_k \cap T_{b,m,o} \neq \emptyset} \; \sum_{\forall p = P_{b,m,o}, q \in Q_p} V_{b,m,o,q} U_q \right) \Bigg) \end{aligned} \tag{100}$$

6.2.3.3 On-Route Charging Power Limit

The grid load limits for depot charging and on-route charging are denoted in equation (53) and (85), respectively. The load limit is represented as the maximum number of chargers per depot or on-route charging station. In real-world practice, the load limit can also be represented as the maximum grid power output for simultaneous charging, per depot or on-route charging station. Therefore, equation (53) and (85) are updated with equation (101) and (102). That is, at each site, the aggregated power of all chargers cannot exceed the power limit (ψ_y^{Depot} or $\psi_p^{OnRoute}$). Power limits may vary by sites depending on the local electricity demand and grid network setup.

$$N_y U_{Depot} \leq \psi_y^{Depot} \qquad \forall\, y \in Y \tag{101}$$

$$\sum_{q \in Q_p} N_{p,q} U_q \leq \psi_p^{OnRoute} \qquad \forall\, p \in P \qquad (102)$$

6.2.3.4 Type of On-Route Chargers

The available chargers at charging station p can be of different types. The equations control for the feasible types of chargers, denoted as set Q_p, and control the number of chargers per type within its capacity ($\chi_{p,q}^{OnRoute}$). In practice, all chargers on a charging station are of the same type (multiple charging stations are constructed when different types of chargers are employed). To incorporate this additional control in the model, the binary variable ($H_{p,q}^{OnRoute}$) is added, which equals 1 if type q charger is built at charging station p, and its relationship with the number of chargers ($N_{p,q}$) is denoted in equation (103). Equation (104) denotes the constraint at that most one type of chargers can be built at station p.

$$N_{p,q} \leq \boldsymbol{M} H_{p,q}^{OnRoute} \qquad \forall\, p \in P, q \in Q_p \qquad (103)$$

$$\sum_{q \in Q_p} H_{p,q}^{OnRoute} \leq 1 \qquad \forall\, p \in P \qquad (104)$$

6.2.4 Implementation

6.2.4.1 Assumptions and Settings

The two proposed models are implemented for the local transit network. Energy use is estimated by implementing the energy prediction models proposed in Chapter 4. We

add weight penalty to the energy rates of battery-electric vehicles with larger battery capacities. The battery weight penalty is set as 10 kg/kWh, referring to previous studies described in Table 3. Schedules are based on the current MARTA's fleet operations as prescribed in the GTFS input file (see Scenario 1 in Section 5.2). On-route charging opportunity is considered feasible only if layover time between two consecutive revenue trips is five or more minutes. Buses with the same battery capacity are assumed to stay in the depot for the same amount of time ($TD_{b,i}^{f}$ or TD_{b}^{f}) to be fully charged. For simplification, depot charging duration is calculated as the amount of energy to be charged divided by the power of the depot charger.

Table 25 lists the parameter inputs, and these values will also be used in the following sections when applicable. In the depot-charging-only model, each tour can be served by vehicles with three battery capacities (200kWh, 300kWh, and 400kWh). In the depot and on-route charging model, each tour can be served by vehicles with four types of battery capacities (100kWh, 150kWh, 200kWh, and 400kWh). All the on-route charging stations can employ two types of chargers (200kW and 300kW). Operating time horizon is set as one year.

Table 25 – Parameter Values: Electrification Cost

Parameter	Values
Time slot (t_k)	5 minutes
Schedule adjustment: pre-revenue (TR_1)	10 minutes
Schedule adjustment: post-revenue (TR_2)	10 minutes
Frequency ($Freq_s$)	Weekday: 260, Saturday: 52.5, Sunday: 52.5
Vehicle spare ratio ($\eta 1$)	0.1
Depot charger spare ratio ($\eta 2$)	0

On-route fast charging penalty rate (σ_s)	\$0.01 per charge			
SOC range (SOC_{min}, SOC_{max})	Min: 0.2, Max: 1.0			
Operator salary rate (γ^f)	\$22.05/Hour across all vehicle types			
Battery-electric bus cost				
Battery capacity	Purchase (θ^f)	Maintenance (β^f)		
100kWh	\$700,000	\$0.30/mile		
150kWh	\$725,000	\$0.31/mile		
200kWh	\$750,000	\$0.32/mile		
300kWh	\$800,000	\$0.33/mile		
400kWh	\$850,000	\$0.34/mile		
Depot capacity				
Vehicle capacity (χ_y)	300 across all depots			
Vehicle capacity per type (χ_y^f)	300 across all vehicle types			
Charger capacity (χ_y^{Depot})	30 per depot			
Charger capacity				
On-route[1] ($\chi_{p,q}^{OnRoute}$)	5 per stop			
Depot (χ_y^{Depot})	30 per depot			
Depot plug-in charger cost				
Charger power (U_q)	Capital ($\mu 1_y$)	Maintenance ($\mu 1_y$)		
80kW	\$50,000	\$150/year		
Depot charging duration				
Battery capacity	100kWh	150kWh	200kWh	400kWh
Depot charging duration	1.25Hour	1.875Hour	2.5Hour	5Hour
On-route fast charging station cost				
Station location	Capital ($\tau 1_p$)	Maintenance ($\tau 2_p$)		
Within city	\$600,000	\$1,000/year		
Outside city	\$500,000	\$1,000/year		
On-route fast charger cost				
Charger power	Capital ($\epsilon 1_q$)	Maintenance ($\epsilon 2_q$)		
200kW	\$20,000	\$200/year		
300kW	\$50,000	\$300/year		
Energy cost (α^f)				
Diesel	\$2.3/DGE			
CNG	\$1.0/DGE			
Demand Charge				
Demand charge rate (φ)	\$10/kW per month			
Demand Interval (ϖt_k)	15 minutes			
Electricity Cost Rate Structure				
Day	Hour	Rate[2] ($\pi_{TC_{b,i}}/\pi_{T_{b,m,o}}$)		
Weekday, Weekends	1 A.M.- 5 A.M.	¢0.0000/kWh		
Weekday	5 A.M.-12 P.M.	¢4.0039/kWh		

Weekday	12 P.M.-8 P.M.	¢7.9086/kWh
Weekday	8 P.M.- 1 A.M.	¢4.0039/kWh
Weekend	5 A.M.- 1 A.M.	¢1.7731/kWh

[1] On-route charger is controlled by the number of chargers per type (χ_y^{Depot}, $\chi_{p,q}^{OnRoute}$), instead of total power limit (ψ_y^{Depot} and $\psi_p^{OnRoute}$)

[2] Georgia Power summer rates for electric transportation service (*Georgia Power, 2019*)

We implement the two cost models for 53 sets of selected tours. Theoretically, it is preferable to evaluate at the scale of a revenue route, i.e. to replace all the vehicles that serve one revenue route with battery-electric buses. However, this is not applicable for a large transit system like MARTA, because routes frequently interline with other routes. For example, a tour may consist of nine revenue trips on Route 1 and three revenue trips on Route 2, which means that the tour cannot be maintained if only Route 1 is electrified. Therefore, to make the tour sets more reasonable, we split the entire MARTA transit network into 53 sub-networks. A sub-network may include multiple routes, but between sub-networks there may be overlapping revenue routes. Detailed information for each sub-network is provided in Appendix D, Table 42. We apply the two cost models to each sub-network respectively.

6.2.4.2 Sub-network Electrification Example

We use one sub-network example (No.42 in Appendix D, Table 42) to describe the results in detail. The sub-network example consists of two revenue routes and four on-route charging station candidates. Two types of on-route charger (200kW and 300kW) are feasible at each charging station candidate. The daily number of tours is six, and the duration of each tour ranges from 18.1 to 20.7 hours. Layover duration for on-route charging ranges from 5 to 15 minutes. Table 26 shows the results of cost profiles of the two models. Even though on-route charging adds the construction costs for charging

stations and chargers, it still reduces the total cost because fewer buses are needed. For a larger network, on-route charging could be even more beneficial when sharing the charging facilities among more tours. In addition, demand charging can be distributed among more revenue tours.

Table 26 – Cost Profile of Example Sub-Network

		Depot Charging Only			Depot and On-route Charging	
	Total Cost	$11,939,107			$7,591,348	
Utility Usage	Depot Charging Cost	$82,535			$13,209	
	On-route Charging Cost	N/A			$44,042	
	Demand Charge Cost	$96,000			$60,000	
	On-route Charging Penalty	N/A			$2,028	
	Annual Energy Used	1,887,371kWh			1,414,247kWh	
Charger and Station	Charging Options	Depot			Depot	On-route
	Number of On-route Charging Stations	N/A			N/A	1
	Number of Chargers	10			6	1(200kW) 1(300kW)
	Capital Cost	$500,000			$300,000	$670,000
	Maintenance Cost	$1,500			$900	$1,500
Vehicle	Battery Capacity	200kWh	300kWh	400kWh	100kWh	400kWh
	Number of Vehicles	9	2	2	4	3
	Procurement Cost	$6,750,000	$1,600,000	$1,700,000	$2,800,000	$2,550,000
	Maintenance Cost	$156,533	$30,434	$35,043	$80,200	$950,910
	Operator Cost	$665,606	$156,007	$165,419	$481,625	$491,935

Figure 44 shows the energy profiles of two weekday tours. For simplicity, we use a straight line to show the energy use of each trip (we aggregate the energy use of all the micro-trips to calculate the energy use). For a revenue trip, a micro-trip is the operations between two consecutive stops. For a deadheading trip, a micro-trip is the operations of a roadway link. Tour 1 uses the 100kWh battery and is charged on-route for 13 times to maintain SOC levels. Tour 2 uses the 400kWh battery and is charged on-route for six

times. It takes a much longer time for Tour 2 to be charged at the depot because of the larger battery capacity. This is as expected as depot charging at midnight costs much less (in our case, it is free) than other time.

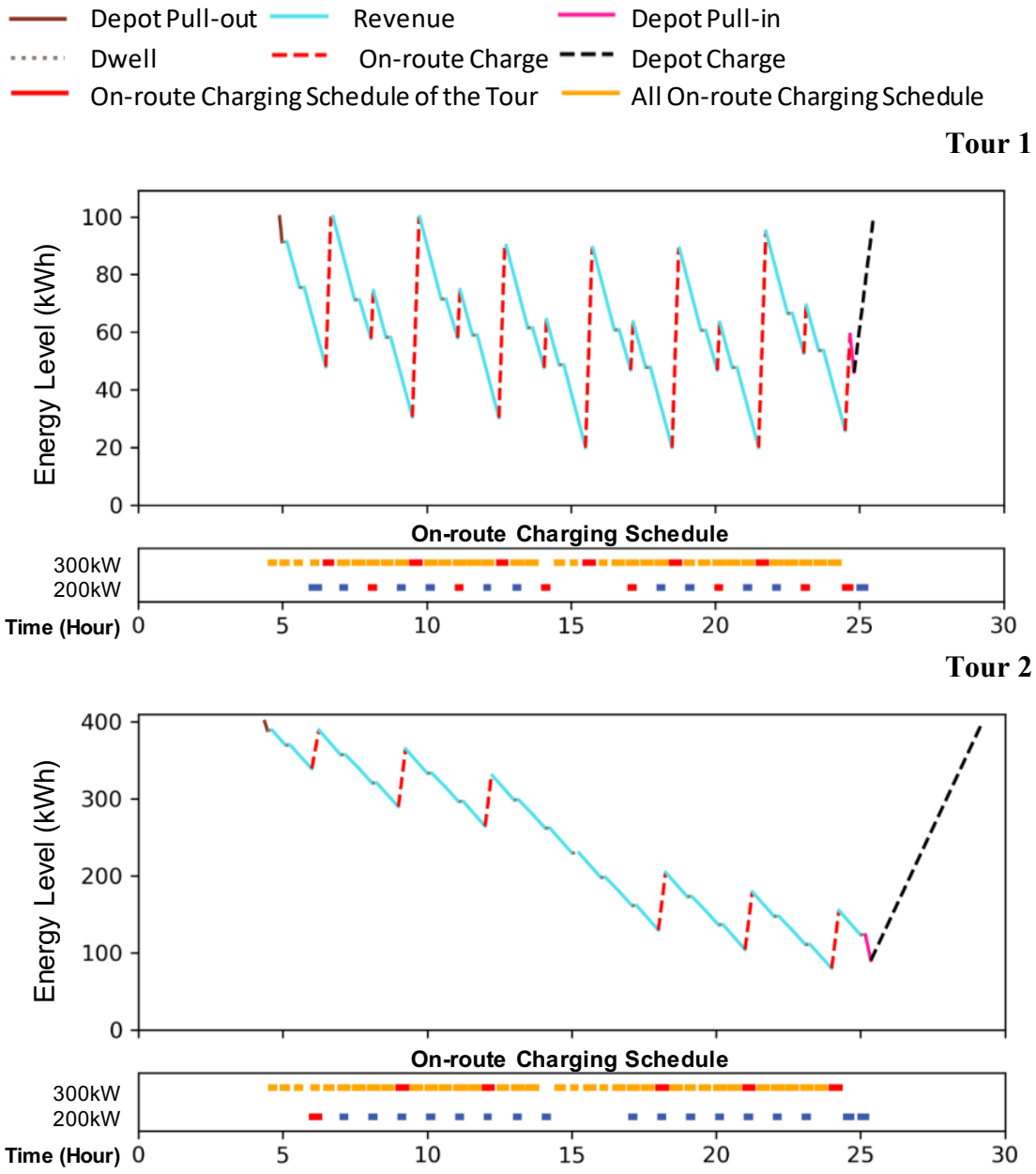

Figure 44 – Example Tour Energy Profiles

The annual energy use in the depot-charging-only model is 12,564 DGE more than the depot and fast charging model, which results in an additional electricity use cost of $25,284. This is due to the additional depot pull-in/pull-out operations when tour energy demand exceeds battery range limits. In this example, one original tour is split into two to seven sub-tours because energy demand of a tour ranges from 534kWh to 727kWh. Table 27 shows the energy rate, and unit utility cost (per kWh and per Mile). The energy rate in the depot-charging only model is higher because more tours are served with buses with 400kWh battery, and depot pull-in/pull-out operations are less energy-efficient than revenue operations because there is less energy recovered from regenerative braking. As for the utility cost per kWh without demand charge, i.e. the electricity usage cost rate, the depot-charging only model costs ¢0.32/kWh (7.4%) more than the depot and on-route charging model. This is related to the assumption that vehicles are fully charged at depot before being dispatched again. In the depot-charging-only model, a large amount of electricity is consumed at periods with high peak utility rates because buses are pulled back to depot and charged in the middle of the day. However, when on-route charging is available, vehicles are not required to get fully charged on-route as long as it satisfies the SOC limit, and thus more charging can occur overnight with low utility rates, as shown in Figure 44. If buses are charged only in depot, the peak demand power is 800kW and the cost of annual demand charge is $96,000. With the joint planning of depot and on-route charging options, the peak demand power is 500kW and the cost of annual demand charge is $60,000. Even though the total cost of demand charge is higher in the depot-charging only model, the gap of utility cost per kWh when considering demand charge is smaller between the two models, i.e. ¢0.15/kWh (1.8%). This is because the total energy use is

much higher for depot-charging, and thus when distributing among all the energy used, the unit utility cost is lower. When evaluating the unit utility cost on the per mile basis, the gap between the two models is increased to ¢1.6/mile (13.6%) and ¢1.9/mile (8.3%). The greater gap is related to the fuel efficiency difference between revenue and deadheading operations; that is, more deadheading trips are involved for when only charged at depot, and thus the overall fuel efficiency is lower.

Table 27 – Energy Use and Electricity Cost of Example Sub-Network

	Depot-charging Only	**Depot and On-route Charging**	**Percentage Difference**[1]
Average Energy Use Rate (kWh/mile)	2.7575	2.5741	-6.7%
Utility Cost per kWh w/o Demand Charge ($/kWh)	0.0437	0.0405	-7.4%
Utility Cost per kWh w/ Demand Charge ($/kWh)	0.0844	0.0829	-1.8%
Utility Cost per Mile w/o Demand Charge ($/mile)	0.1206	0.1042	-13.6%
Utility Cost per Mile w/o Demand Charge ($/mile)	0.2328	0.2134	-8.3%

[1] Percentage Difference $= \frac{(\text{Depot and Onroute} - \text{DepotOnly})}{\text{DepotOnly}} * 100\%$

6.2.4.3 Model Results for Electrifying All Sub-networks

Figure 45 shows the total cost (objective value) of electrifying each sub-network. Not surprisingly, the cost in the depot-charging-only model is higher than the depot and on-route charging model per sub-network. The electrification cost difference between the two models per sub-network ranges from 0.3 to 51.7 million USD. Figure 46 shows the

energy use of each sub-network. The energy difference between the two models ranges from 494 to 202,419 DGE per sub-network. In the depot-charging only model, fleet electrification can reduce life-cycle CO_2 emissions by 145-14,577 metric tonnes per sub-network, compared with the baseline fleets. In the depot and on-route charging model, CO_2 emissions can be reduced by 233-15,462 metric tonnes per sub-network. We see greater gaps between the two models when the sub-network has more revenue routes and longer distance traveled. This is because on-route charging stations and chargers are shared, and the charging facility cost per tour or per route is lower, when distributed among a larger network.

Detailed results are shown in the Appendix D. Table 43 lists the values of total cost and energy use of each sub-network. Table 44 lists the number of chargers and buses per type. We can see the advantage of joint decision-making through coordinating charging events and facility placement based on the number of electric vehicles and chargers. In the depot-charging-only model, the ratio of depot chargers to electric vehicles ranges from 1.0 to 3.0 with an average of 1.7. In the depot and on-route charging model, the ratio of charger to electric vehicle ranges from 1.2 to 3.8 with an average of 1.9 for depot-chargers, and ranges from 1.5 to 15.0 with an average of 5.7 for on-route chargers. The ratio of on-route charging stations to electric vehicles ranges from 1.5 to 9.0 with an average of 4.0. In addition, it is worthwhile to evaluate the pros and cons of procuring various battery capacities, which may reduce the total electrification cost. The number of sub-networks that use electric vehicles with mixed battery capacities are 50 and 27 in the depot-charging-only model, and the depot and on-route charging model, respectively.

Table 45 and Table 46 list the detailed cost profile of the two models. In the depot-charging-only model, the majority of the capital investment (vehicle and charging facility) comes from vehicle procurement, and the percentage ranges from 94% to 98% with an average of 96% per sub-work. In the depot and on-route charging model, the percentage of vehicle procurement of total capital investment ranges from 63% to 92% with an average of 83% per sub-network. Even though the on-route charging facility cost is much higher compared with depot chargers, the capital investment cost in the depot-charging-only model is still higher than the depot and on-route charging mode, and the difference ranges from 4% to 56% with an average of 30%. The results of utility cost imply the importance of considering demand charge when evaluating fleet electrification cost. The percentage of demand charge of the total utility cost ranges from 43% to 55% with an average of 51% per sub-network in the depot-charging-only model, and ranges from 38% to 76% with an average of 54% in the depot and on-route charging model.

Evaluating the monetary cost, energy use, and CO_2 emissions reductions will help agencies identify the most cost-effective routes to electrify. These results imply the importance of a thorough understanding of the costs and benefits of different charging options. Even though the cost of an on-route charging facility is around 10 times that of a depot charger, the cost is offset because fewer buses are required when energy can be sustained via on-route charging. In addition, cost metric components only include the initial cost and operating cost per year. In evaluating the life-cycle cost, the gap between the two models will be even larger because energy use in the depot-charging-only model is higher due to more frequent depot pull-in/pull-out trips.

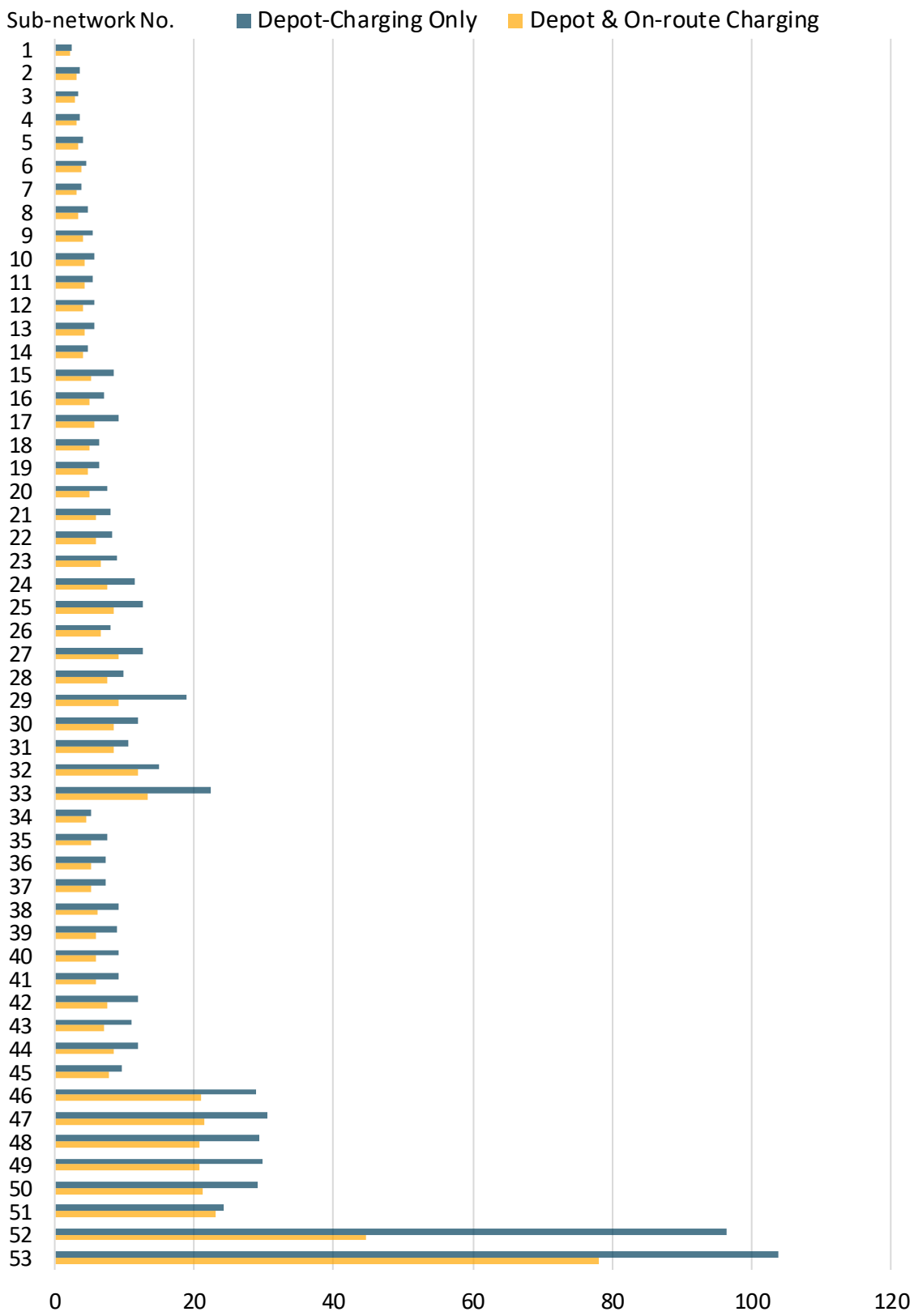

Figure 45 – Electrification Cost per Sub-Network (Millions of USD)

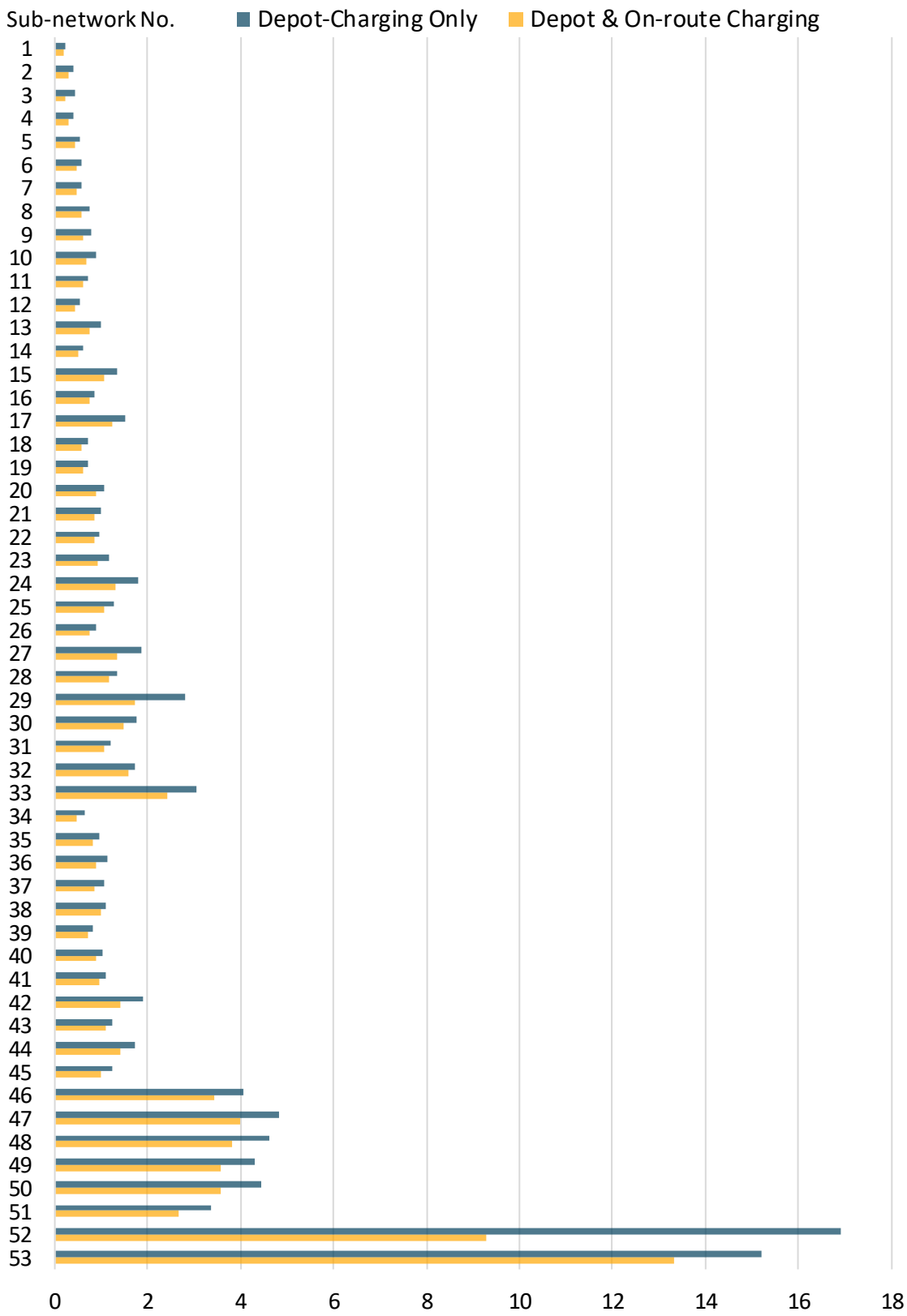

Figure 46 – Energy Use per Sub-Network (10^6 kWh)

6.3 Operation Optimization Model for Depot-Charged Electric Vehicle Sub-fleets

This model is designed to assess existing mixed fuel fleets with some battery-electric vehicles with depot chargers in place, where the desire is to minimize fleet-wide operating costs by properly assigning buses to tours and deciding when to charge the vehicles. The three cost metrics in Chapter 5 (life-cycle CO_2 emissions, operating monetary cost, and energy use) are also used here. The depot charging operations follow the same practice as described in Section 6.2.1.

6.3.1 Model Formulation

The decision variable in this model is binary variable W_b^f, for $\forall\, b \in B, f \in F_1 \cup F_2$, where W_b^f equals 1 if a type f vehicle is selected for tour b. We use type (f) to represent either vehicle type (fuel and age category) or battery capacity. Equation (105) denotes the objective function of this model, minimizing the fleet-wide operating cost evaluated for the three metrics. Equation (106) denotes the first metric, life-cycle CO_2 emissions (C_δ), calculated in a way similar to the models in Chapter 5. Emissions from electric and non-electric fleets are aggregated per sub-tour and tour, respectively. Equation (107) denotes the second metric, operating monetary cost (C_{op}), consisting of fuel/electricity, demand charge, vehicle maintenance, and operator. Different from the cost metric in Chapter 5, operator cost is added because additional depot pull-in/pull-out activities will result in longer operating duration and thus increase the operator labor cost. Equation (108) denotes the daily fuel cost ($C_{\alpha,s}$), calculated based on the amount of energy use (E_b^f and $E_{b,i}^f$) and energy cost rate (denoted as α^f for non-electric fleets, and $\pi_{TC_{b,i}^f}$ for

electric fleets). The energy cost rate of electricity usage is dependent on the time of the charging event. Equation (109) denotes the daily vehicle maintenance cost ($C_{\beta,s}$), calculated by multiplying distance traveled (D_b^f and $D_{b,i}^f$) by the vehicle maintenance cost rate (β^f). Equation (110) denotes the daily operation cost ($C_{\gamma,s}$), calculated by multiplying operation duration (T_b and $T_{b,i}^f$) by operator salary rate (γ^f). Equation (111) denotes the third metric (C_e), energy use, evaluated as DGE.

$$\min_{W_b^f} C_{\rho\in\{\delta,op,e\}} \tag{105}$$

$$C_\delta = \sum_{\forall s\in S}\sum_{\forall b\in B_s} Freq_s\left(\sum_{\forall f\in F_1} W_b^f E_b^f \delta^f + \sum_{\forall f\in F_2}\sum_{i\in I_b^f} W_b^f E_{b,i}^f \delta^f\right) \tag{106}$$

$$C_{op} = C_\varphi + \sum_{\forall s\in S} Freq_s\left(C_{\alpha,s} + C_{\beta,s} + C_{\gamma,s}\right) \tag{107}$$

$$C_{\alpha,s} = \sum_{\forall b\in B_s}\left(\left(\sum_{\forall f\in F_1} W_b^f E_b^f \varepsilon_{kWh2Gal}\alpha^f\right) + \left(\sum_{\forall f\in F_2}\sum_{i\in I_b^f} W_b^f E_{b,i}^f \pi_{TC_{b,i}^f}\right)\right) \tag{108}$$

$$C_{\beta,s} = \sum_{\forall b\in B_s}\left(\left(\sum_{\forall f\in F_1} W_b^f D_b^f \beta^f\right) + \left(\sum_{\forall f\in F_2}\sum_{i\in I_b^f} W_b^f D_{b,i}^f \beta^f\right)\right) \tag{109}$$

$$C_{\gamma,s} = \sum_{\forall b \in B_s} \left(\left(\sum_{\forall f \in F_1} W_b^f T_b \gamma^f \right) + \left(\sum_{\forall f \in F_2} \sum_{i \in I_b^f} W_b^f T_{b,i}^f \gamma^f \right) \right) \tag{110}$$

$$C_e = \sum_{\forall s \in S} \sum_{\forall b \in B_s} Freq_s \left(\left(\sum_{\forall f \in F_1} W_b^f E_b^f \varepsilon_{kWh2Gal} \right) + \left(\sum_{\forall f \in F_2} \sum_{i \in I_b^f} W_b^f E_{b,i}^f \varepsilon_{kWh2Gal} \right) \right) \tag{111}$$

Constraints related to service demand and vehicle availability are denoted in equation (112) through (119). Equation (112) denotes the constraint that each tour is served by one type of vehicle. Equation (113) denotes the number of type f vehicles from depot y that are in use at time slot t_k on service day type s. In equation (114), T_b^f denotes the set of in-use time slots of tour b if served with non-electric fleets, whereas $T_{b,i}^f$ is used for electric vehicle fleets, denoted in equation (62). Equation (115) denotes the vehicle availability constraint, i.e. at each time slot t_k, the supply for each type of vehicle is enough for the demand. Equation (116) denotes the constraint that at each depot, the total number of vehicles across all types should be enough for the in-use vehicles and spares. Equation (117) denotes the constraint that the number of vehicles at depot y cannot exceed its depot capacity (χ_y). Equation (118) denotes the constraint that the number of vehicles of type f cannot exceed the availability (χ^f). Equation (119) denotes the constraint that the number of type f vehicles at depot y does not exceed its capacity (χ_y^f). If the depot y does not have facilities to house type f vehicles, then χ_y^f is zero. In addition, the constraints related

to depot chargers are formulated in the same way as in the cost model (equations (50) through (53)). Note that χ_y^{Depot} in equation (53) represents the number of chargers already in place at depot y.

$$\sum_{f \in F_1 \cup F_2} W_b^f = 1 \qquad \forall b \in B \qquad (112)$$

$$w_{y,s,t_k}^f = \begin{cases} \sum_{\forall b \in B_{s,y}, t_k \in T_b^f} W_b^f \, , if \; f \in F_1 \\ \sum_{\forall b \in B_{s,y}, t_k \in T_{b,i}^f} W_b^f \, , if \; f \in F_2 \end{cases} \qquad \begin{matrix} \forall s \in S, y \in Y, \\ f \in F_1 \cup F_2, t_k \in T \end{matrix} \qquad (113)$$

$$T_b^f = \{t_{TO_b}, t_{TO_b+1}, \dots, t_{TI_b}\} \qquad \forall s \in S, y \in Y, f \in F_1, t_k \in T \qquad (114)$$

$$\max_{\forall s \in S, t_k \in T} w_{y,s,t_k}^f \leq w_y^f \qquad \forall y \in Y, f \in F_1 \cup F_2, \qquad (115)$$

$$\max_{\forall s \in S, t_k \in T} (1 + \eta 1) \sum_{\forall f \in F_1 \cup F_2} w_{y,s,t_k}^f \leq \sum_{\forall f \in F_1 \cup F_2} w_y^f \qquad \forall y \in Y \qquad (116)$$

$$\sum_{f \in F_1 \cup F_2} w_y^f \leq \chi_y \qquad \forall y \in Y \qquad (117)$$

$$\sum_{y \in Y} w_y^f \leq \chi^f \qquad \forall f \in F_1 \cup F_2 \qquad (118)$$

$$w_y^f \leq \chi_y^f \qquad \forall y \in Y, f \in F_1 \cup F_2 \qquad (119)$$

6.3.2 Implementation

The model is implemented in five scenarios. The current fleet composition of MARTA (Scenario 1 in Section 5.2) is used as the existing fleet. Electric vehicle fleets and charging facilities are shown in Table 28. The first three scenarios represent the early stage of fleet electrification, and the last two scenarios represent more mature fleets with 30 and 60 battery-electric vehicles in place. Per scenario, each of the three cost metrics is implemented individually to optimize transit operations of a whole year.

Table 28 – Parameter Values: Operation Optimization with Electric Vehicle Sub-Fleets Model

No.	Number of Electric Vehicle Fleets (χ^f)			Number of Chargers per Depot (χ_y^{Depot})
	200kWh	300kWh	400kWh	
1	4	4	4	2
2	0	0	10	2
3	5	0	5	2
4	10	10	10	4
5	20	20	20	6

Table 29 shows the cost reductions of each fleet electrification scenario, compared with the baseline fleet. The cost metric used in the objective function is highlighted in each column. In Scenario 1, introducing 12 battery-electric vehicles can reduce CO_2 emissions by up to 4.8%, operating cost by 2.6%, and energy use by 3.4%. However, the reductions achieved depend upon the optimization metric employed. When using energy use as the cost metric in the objective function, more tours are served by diesel buses than CNG because diesel buses have better fuel efficiency performance. However, unit fuel cost and CO_2 emissions are both higher for diesel buses, and thus the monetary cost and CO_2 emissions are increased. The gap among the first three scenarios are trivial. This is because

of the trade-offs between range and vehicle fuel efficiency. With a larger battery, the bus can operate for a longer distance, and thus saves energy use from depot pull in/pull-out. However, the weight penalty from the battery affects fuel efficiency performance and results in higher energy use.

In Scenario 4, the penetration of electric vehicle fleets is nearly tripled. However, cost reductions are tripled. This is because of the number of depot chargers are limited. If the number of chargers per depot is increased from 4 to 6 in Scenario 4, CO_2 emissions can be reduced to 126,470 metric tonnes, which is an addition of 1,027 metric tonnes (0.76%) than in Scenario 4. The results in Scenario 5 follows the same trend as in Scenario 4. The only exception is that when using energy use as the cost metric, we see reductions in CO_2 emissions, which is the opposite in the last 4 scenarios. This is because battery-electric buses have the advantages of both reducing energy use and life-cycle CO_2 emissions; with a high electrification rate, it can offset the life-cycle CO_2 emissions from diesels buses.

Table 29 – Cost Reductions: Operation Optimization with Electric Vehicle Sub-Fleets Model

No.		Mileage (1,000 Miles)		CO_2 Emissions (Metric Tonnes)		Monetary Cost (1,000 USD)		Energy Use (1,000 DGE)	
	Baseline	33,425		135,046		78,542		10,088	
	Cost Metric	**Diff***	**%****	**Diff***	**%****	**Diff***	**%****	**Diff***	**%****
1	CO_2 Emissions	14	0.04%	**-6,445**	**-4.77%**	-2,034	-2.59%	136	1.35%
	Monetary Cost	7	0.02%	-6,404	-4.74%	**-2,042**	**-2.60%**	143	1.42%
	Energy Use	14	0.04%	1,231	0.91%	1,178	1.50%	**-345**	**-3.42%**
2	CO_2 Emissions	7	0.02%	**-6,423**	**-4.76%**	-2,031	-2.59%	138	1.37%
	Monetary Cost	7	0.02%	-6,419	-4.75%	**-2,036**	**-2.59%**	139	1.38%
	Energy Use	8	0.03%	1,250	0.93%	1,181	1.50%	**-343**	**-3.40%**
3	CO_2 Emissions	14	0.04%	**-6,407**	**-4.74%**	-2,027	-2.58%	139	1.38%
	Monetary Cost	6	0.02%	-6,367	-4.71%	**-2,038**	**-2.60%**	147	1.45%
	Energy Use	15	0.04%	1,262	0.93%	1,183	1.51%	**-341**	**-3.38%**
4	CO_2 Emissions	35	0.10%	**-7,549**	**-5.59%**	-2,075	-2.64%	47	0.46%
	Monetary Cost	19	0.06%	-7,448	-5.52%	**-2,101**	**-2.68%**	59	0.59%
	Energy Use	33	0.10%	198	0.15%	1,159	1.48%	**-438**	**-4.34%**
	CO_2 Emissions	52	0.16%	**-8,603**	**-6.37%**	-2,119	-2.70%	-40	-0.39%

5	Monetary Cost	25	0.08%	-8,322	-6.16%	**-2,149**	**-2.74%**	-11	-0.11%
	Energy Use	54	0.16%	-792	-0.59%	1,141	1.45%	**-528**	**-5.23%**

* Diff=$Model - Baseline$

** %=$\frac{(Model-Baseline)}{Baseline} * 100\%$

6.4 Budget-Constrained Sub-fleet Electrification Optimization Model

This model solves the problem of "Under a fixed budget limit of fleet electrification, if we want to achieve the goal of maximizing the benefits of reducing life-cycle CO_2 emissions, how many vehicles (and their battery capacities) to purchase, which tour to electrify, where to build charger/charging stations, and when to charge vehicles." Two models are formulated, one with depot-charging-only option, and the other with both depot and on-route charging options.

6.4.1 Model Formulation - Depot Charging

This model is formulated based on the cost model in Section 6.2.1. The two decision variables are binary variable W_b^f, for $\forall\, b \in B, f \in F_2$, and integer variable N_y for $\forall y \in Y$. W_b^f equals 1 if the bus with battery capacity f is selected for tour b. N_y represents the number of chargers at depot y. Equation (120) denotes the objective function, to maximize the benefits of reducing life-cycle CO_2 emissions, calculated by aggregating the reductions of each electrified tour compared with the baseline. The life-cycle CO_2 emissions of an electric vehicle tour is the sum of each individual sub-tour. The baseline is the weighted sum of emissions across all existing vehicle types, and the weight is calculated as the number of vehicles per type in the existing fleet.

$$\max_{W_b^f, N_y} \sum_{\forall s \in S} \sum_{\forall b \in B_s} \sum_{\forall f \in F_2} Freq_s W_b^f \left(-\left(\sum_{i \in I_b} E_{b,i}^f \varepsilon_{kWh2MJ} \delta^f \right) + \left(\sum_{\forall f \in F_1} E_b^f \varepsilon_{kWh2MJ} \delta^f \left(\frac{\chi^f}{\sum_{f \in F_1} \chi^f} \right) \right) \right) \tag{120}$$

Equation (121) denotes the budget constraint, consisting of six cost components. Battery-electric vehicle investment (C_θ), depot charger investment and maintenance (C_μ), and demand charge (C_φ) are denoted in equation (36), (37), and (38), respectively. If electrifying a tour, the cost differences in terms of energy use, vehicle maintenance, and operation compared with the baseline are considered. The cost difference of energy use ($\Delta C_{\alpha,s}$) is denoted in equation (122). If tour b is served with a type f battery-electric vehicle, then its electricity usage cost is $\sum_{i \in I_b} E_{b,i}^f \pi_{TC_{b,i}^f}$, with electricity cost rate dependent on when the vehicle is charged. The baseline fuel cost is calculated as the weighted sum across all vehicle types in the existing fleet. Similarly, cost differences of vehicle maintenance ($\Delta C_{\beta,s}$) and operator ($\Delta C_{\gamma,s}$) are denoted in equation (123) and (124), respectively.

$$C_\theta + C_\mu + C_\varphi + \sum_{\forall s \in S} Freq_s \left(\Delta C_{\alpha,s} + \Delta C_{\beta,s} + \Delta C_{\gamma,s} \right) \leq \omega \tag{121}$$

$$\Delta C_{\alpha,s} = \sum_{\forall b \in B_s} \sum_{\forall f \in F_2} W_b^f \left(\left(\sum_{i \in I_b^f} E_{b,i}^f \pi_{TC_{b,i}^f} \right) - \left(\sum_{\forall f \in F_1} E_b^f \mu_{kWh2Gal} \alpha^f \left(\frac{\chi^f}{\sum_{f \in F_1} \chi^f} \right) \right) \right) \quad (122)$$

$$\Delta C_{\beta,s} = \sum_{\forall b \in B_s} \sum_{\forall f \in F_2} W_b^f \left(\left(\sum_{i \in I_b^f} D_{b,i}^f \beta^f \right) - \left(\sum_{\forall f \in F_1} D_b^f \beta^f \left(\frac{\chi^f}{\sum_{f \in F_1} \chi^f} \right) \right) \right) \quad (123)$$

$$\Delta C_{\gamma,s} = \sum_{\forall b \in B_s} \sum_{\forall f \in F_2} W_b^f \left(\left(\sum_{i \in I_b^f} T_{b,i}^f \gamma^f \right) - \left(\sum_{\forall f \in F_1} T_b \gamma^f \left(\frac{\chi^f}{\sum_{f \in F_1} \chi^f} \right) \right) \right) \quad (124)$$

Equation (125) denotes the constraint that each tour can be electrified with at most one vehicle type. $\sum_{f \in F_2} W_b^f$ equals 1 if tour b is electrified, and equals 0 otherwise. All other constraints related to service demand and depot charging are formulated in the same way as in the depot-charging cost model, described in Section 6.2.1 (equation (43)-(54)).

$$\sum_{f \in F_2} W_b^f \leq 1 \qquad \forall b \in B \quad (125)$$

6.4.2 Model Formulation - Depot and On-route Charging

This model is formulated based on the cost model in Section 6.2.2. The decision variables of this model are all the variables listed in Table 24. Equation (126) denotes the objective function, to maximize the benefits of reducing life-cycle CO_2 emissions, calculated by aggregating the CO_2 reductions of each tour. Per tour, the reduction is

quantified as the difference between if electrified (the first sum) and if using baseline (the second sum). $\sum_{\forall f \in F_2} W_b^f$ equals 1 if the tour is electrified.

$$\max_{W_b^f, N_y, N_p, N_{p,q}, V_{b,m,q,o}^f, X_{b,m,q,o}^f} -\left\{\sum_{\forall s \in S}\sum_{\forall b \in B_s} Freq_s \left(E_b + \sum_{\forall f \in F_2}\sum_{m=1}^{m_b-1}\sum_{o \in \{1,2\}}\sum_{\forall q \in Q_{p_{b,m,o}}} X_{b,m,o,q}^f U_q \right) \varepsilon_{kWh2MJ} \delta^f \right\} + \left\{\sum_{\forall s \in S}\sum_{\forall b \in B_s} Freq_s \left(\sum_{\forall f \in F_2} W_b^f \right) \left(\sum_{\forall f \in F_1} E_b^f \varepsilon_{kWh2MJ} \delta^f \left(\frac{\chi^f}{\sum_{f \in F_1} \chi^f} \right) \right) \right\} \quad (126)$$

Equation (127) denotes the budget constraint. Battery-electric vehicle investment (C_θ), depot charger investment and maintenance (C_μ), demand charging (C_φ), on-route charging station investment and maintenance (C_τ), on-route charger investment and maintenance (C_ϵ), and charging penalty ($C_{\sigma,s}$), are denoted in equation (36), (37), (38), (56), (57), and (61), respectively. Cost differences in terms of energy use, vehicle maintenance, and operation compared with the baseline, are denoted as $\Delta C_{\alpha,s}$, $\Delta C_{\beta,s}$, and $\Delta C_{\gamma,s}$ in equation (128), (129), and (130), respectively. The constraint of service demand, denoted in equation (125), still applies to this model. Other constraints related to vehicle availability, depot chargers, on-route chargers, energy flows, and charging events, are formulated in the same way as the cost model in Section 0.

$$C_\theta + C_\mu + C_\varphi + C_\tau + C_\epsilon + \sum_{\forall s \in S} Freq_s \left(\Delta C_{\alpha,s} + \Delta C_{\beta,s} + C_{\sigma,s} + \Delta C_{\gamma,s} \right) \leq \omega \quad (127)$$

$$\Delta C_{\alpha,s} = \sum_{\forall b \in B_s} \left(\left(E_b \pi_{TC_b} + \sum_{\forall f \in F_2} \sum_{m=1}^{m_b - 1} \sum_{o \in \{1,2\}} \sum_{\forall q \in Q_{P_{b,m,o}}} X^f_{b,m,o,q} U_q \, \pi_{T_{b,m,o}} \right) - \left(\sum_{\forall f \in F_2} W^f_b \right) \left(\sum_{\forall f \in F_1} E^f_b \varepsilon_{kWh2Gal} \alpha^f \left(\frac{\chi^f}{\sum_{f \in F_1} \chi^f} \right) \right) \right) \quad (128)$$

$$\Delta C_{\beta,s} = \sum_{\forall b \in B_s} \sum_{\forall f \in F_2} W^f_b \left(D^f_b \beta^f - \sum_{\forall f \in F_1} D^f_b \beta^f \left(\frac{\chi^f}{\sum_{f \in F_1} \chi^f} \right) \right) \quad (129)$$

$$\Delta C_{\gamma,s} = \sum_{\forall b \in B_s} \sum_{\forall f \in F_2} W^f_b \left(T_b \gamma^f - \sum_{\forall f \in F_1} T_b \gamma^f \left(\frac{\chi^f}{\sum_{f \in F_1} \chi^f} \right) \right) \quad (130)$$

6.4.3 Implementation

The model is implemented in a transit network consisting of all the tours from the Hamilton depot. Table 30 shows the information of the transit network, as well as the energy and operating cost in a year. In the depot-charging-only model, we use 400kWh battery-electric buses for fleet electrification. In the depot and on-route charging model, we use 200kWh battery-electric buses for fleet electrification. On-route chargers with 200kW power can be installed in all the 35 charging station candidates. The budget for fleet electrification is set as 20.0 million USD, and time horizon of operations is selected as a whole year.

Table 30 – Transit Network Information: Budget-constrained Fleet Electrification Model

Item	Value
Number of Revenue Routes	28
Number of Starting/Ending Stops	35
Number of Tours per Day	80 (Saturday), 74 (Sunday), 136 (Weekday)
Operating Duration (1,000 Hours)	634
Distance Traveled (1000 Miles)	9,122

Item	Value
Revenue Distance Traveled (1000 Miles)	8,431
Energy Use (1,000 DGE)	2,658
CO_2 emissions (Metric Tonnes)	35,591
Energy Cost (Million USD)	3.38
Maintenance Cost (Million USD)	3.09
Operator Cost (Million USD)	13.97
Revenue Route ID	93, 95, 42, 55, 78, 192, 79, 181, 155, 81, 82, 83, 84, 49, 195, 832, 178, 191, 183, 193, 194, 800, 162, 89, 189, 180, 172, 295

Figure 47 shows the results in terms of fleet-wide revenue distance traveled, life-cycle CO_2 emissions, and energy use. In the depot charging model, 1,129,525 revenue miles (13%) are electrified, reducing CO_2 emissions by 3,213 metric tonnes (9%) and energy use by 269,735 DGE (10%). In the depot and fast charging model, 1,841,492 revenue miles (22%) are electrified, reducing CO_2 emissions by 5,593 metric tonnes (16%) and energy use by 459,114 DGE (17%).

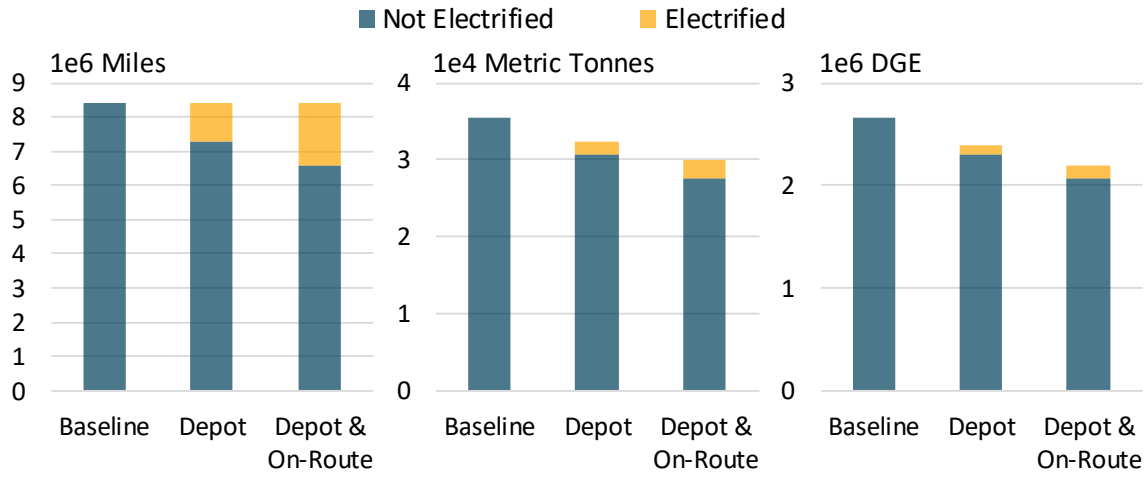

(a) Revenue Distance **(b) CO_2 Emissions** **(c) Energy Use**

Figure 47 – Fleet-wide Distance, Emissions, and Energy Use: Budget-constrained Fleet Electrification Model

Table 31 shows the cost profile of the two models. Even though the charging facili ty cost in the depot and on-route charging model is $2.93 million higher than that in the

depot-charging only model, it is offset by the low vehicle procurement cost, which is $2.2 million lower.

Table 31 – Operations and Cost Profile: Budget-constrained Fleet Electrification Model

		Depot-Charging Only	Depot and On-route Charging	
Total Cost (Million USD)		19.4	19.9	
Electrified Distance (1000 Miles)		1,290	1,960	
Electrified Revenue Distance (1000 Miles)		1,130	1,841	
Utility Usage	Depot Charging Cost	$146,562	$35,992	
	On-route Charging Cost	N/A	$162,261	
	Demand Charge Cost	$163,200	$192,000	
	On-route Charging Penalty	N/A	$9,337	
	Energy Cost Baseline	$461,679	$748,798	
	Electricity Used	3,533,876kWh	4,918,818kWh	
Charger and Station	Charging Options	Depot Charging	Depot Charging	On-route Charging
	Number of On-route Charging Stations	N/A	N/A	5
	Number of Chargers	17	20	9
	Capital Cost	$850,000	$1,000,000	$2,780,000
	Maintenance Cost	$2,550	$3,000	$6,800
Vehicle	Number of Vehicles	22	22	
	Procurement Cost	$18,700,000	$16,500,000	
	Maintenance Cost	$438,478	$627,072	
	Maintenance Cost Baseline	$413,740	$663,469	
	Operator Cost	$1,934,456	$3,228,233	
	Operator Cost Baseline	$1,928,523	$3,191,590	

6.5 Summary

In this chapter, three fleet electrification models are developed, targeted to solving three problems that transit agencies may face when adopting electric vehicle sub-fleets, especially at the early stage of fleet electrification. The fleet electrification cost model helps agencies estimate the cost of electrifying a sub-network. The operation optimization model helps agencies minimize the operating monetary cost, energy use, and life-cycle

CO_2 emissions with electric vehicle sub-fleets in place. The budget-constrained fleet electrification model helps agencies maximize the benefits of reducing CO_2 emissions. Each model is implemented in the local transit networks, with optimized decisions as well as cost profiles described in detail.

The main contributions of the proposed models, i.e. electrification cost model, operation optimization model for depot-charged electric vehicle sub-fleets, and budget-constrained sub-fleet electrification optimization model, are:

1) Vehicle energy use at the micro-trip level are accurately evaluated by incorporating vehicle specifications, operating and roadway characteristics. In particular, battery weight penalty is considered.
2) The proposed models output joint decisions in terms of fleet procurement, vehicle-to-tour assignment, facility location selection, and charging scheduling.
3) Fleet electrification cost is estimated in detail, including vehicle and facility capital investment, utility, vehicle maintenance, operator and etc.
4) Utility cost components include not only electricity usage, but also demand charging, which interacts with charging scheduling.
5) Both depot and on-route charging facilities can be shared among buses when available.
6) The operation optimization model uses three cost metrics, which provides a thorough understanding of pros and cons of fleet electrification.
7) The proposed models are readily available to be applied to local transit agencies, with the feasibility to be customized with fleet-specific characteristics.

The limitations of the models developed in this chapter that can be addressed in future work include:

1) The amount of energy charged per unit time interval is assumed to be linearly related to a fixed charging power. In fact, several phases of charging may be involved per charge.
2) Some impacting factors on electrification route selection are not considered, such as prioritizing the routes with the highest ridership, and ensuring all the communities have equal accessibility to access electric vehicle fleets.
3) Only starting/ending stops are used on-route charging facility candidates. In fact, charging facilities can be built at mid-stops of a route, especially at transit centers where buses dwell for a significant amount of time.
4) [Impact of temperature on vehicle fuel efficiency analysis is not incorporated. In fact, the A/C load under extreme weather conditions can greatly increase energy use.
5) We assume the overall budget can be distributed among capital investment, operator labor, and fuel. However, some sources of the funds can only be used for certain costs, and thus the total budget constraint will need to be split into several constraints to specify the funding source.
6) Spare ratio of chargers is set as zero, and thus the reliability of the electric bus system may be affected due to charging facility malfunctions. Dispatching a spare conventional diesel bus could be a viable option to solve this, but it is still worthwhile to evaluate whether or not the electric bus can be charged in other

facilities and the corresponding penalty in terms of vehicles scheduling adjustments and additional energy use.

7) We use the layover duration as the maximum charging duration per on-route charging event, which is an ideal condition. When delay or emergencies happen, the available charging duration may be reduced, and thus the amount of energy charged will be reduced. To address this problem, we may exclude a portion from the layover duration as the buffer time. The buffer time can be dependent on the time of day, stops, and routes, where a longer buffer time is given to the charging candidates where more frequent delays occur.]

CHAPTER 7. FLEET CONVERSION OPTIMIZATION UNDER ANNUAL BUDGET CONSTRAINTS

7.1 Model Overview

This chapter develops two models to optimize the conversion of large fleets to alternative fuels over time, under given capital purchase budget constraints. The goal is to minimize fleet-wide life-cycle CO_2 emissions or maximize the benefits of reducing life-cycle CO_2 emissions compared with baseline conditions. The proposed models are the extensions of the models in Chapter 6. The time horizon is extended to multiple years. The previous modeling efforts have demonstrated that battery-electric vehicles provide significant overall energy and emissions reduction benefits and fleet cost savings. Hence, the optimization models in this chapter will naturally push the fleet toward full electrification. However, the procurement and vehicle assignment decisions are not just battery-electric vehicles, but include all types of vehicles (along with their applicable costs, energy-use, and emission-reduction costs and benefits). Hence, it should not be surprising if the models do not recommend the electrification of the entire fleet.

The primary model outputs are presented in Table 32. Each model includes a scenario for depot-charging only, and a scenario of both depot and on-route charging. The first model, fleet conversion without considering salvage, focuses on the costs and benefits from adopting new alternative fuel fleets. Additional monetary cost and reductions of CO_2 emissions are compared with the baseline fleet, which assumes the traditional random bus-to-tour assignment in the existing fleet. The model decision outputs include procurement

of vehicle types and bus-to-tour assignment of the new fleets, as well as charging facility investments and scheduling as new electric vehicle fleets are introduced. Decisions are made each year within the planning time horizon. The second model fleet conversion model simultaneously considering salvage (fleet turnover), which extends the costs and benefits to the entire fleet. The model explicitly assesses fleet composition and bus-to-tour assignment of both the new and existing fleets (allows reconfiguration of the system and annual bus-to-tour assignments as the fleet is replaced), as well as charging facility investments and scheduling (if applicable) per year within the planning time horizon.

Table 32 – Model Overview: Fleet Conversion

	W/O Salvage		**W/ Salvage**	
Charging Option	Depot	Depot and On-route	Depot	Depot and On-route
Number of Vehicles per Type	Decisions	Decisions	Decisions	Decisions
New Fleet Bus-to-Tour Assignment	Decisions	Decisions	Decisions	Decisions
Existing Fleet Bus-to-Tour Assignment	NA	NA	Decisions	Decisions
Number of Depot Chargers	Decisions	Decisions	Decisions	Decisions
Depot Charging Schedule	Decisions	Decisions	Decisions	Decisions
Number of On-route Chargers	NA	Decisions	NA	Decisions
On-route Charging Schedule	NA	Decisions	NA	Decisions
Number of Vehicles Salvaged per Type	NA	NA	Decisions	Decisions

Table 33 shows the notations of the decision variables used in this chapter. Because this is a long-term scenario, we use z as year identifier and add the variable as a subscript

to each decision variable. The set of planning horizon is denoted as $z \in Z = \{1,2,\dots,\kappa\}$ where κ is the number of years in the plan. F_1 denotes the set of vehicle types in the existing fleet, and F_3 denotes the set of vehicle types in new fleets. F_3 may contain battery-electric vehicles and other types, such as CNG, hybrid-electric vehicles, and diesel vehicles. We use $F_3 \cap F_2$ to represent the set of new electric vehicle fleets (i.e. battery-electric vehicles), and $F_3 \backslash F_2$ to represent the set of new non-electric vehicle fleets.

Table 33 – Decision Variables: Fleet Conversion

Notation		Meaning
G_z^f	$\forall f \in F_1, z \in Z$	Number of salvaged vehicles variable Integer variable Cumulative number of type f vehicles that are salvaged up to year z
$H_{z,\lambda}$	$\forall \lambda \in \Lambda, z \in Z$	Vehicle salvage occurrence variable Binary variable 1 if at least one vehicle with salvage sequence λ is salvaged
$N_{p,z}$	$\forall p \in P, z \in Z$	On-route charging station variable Binary variable 1 if charging station exists at bus stop p in year z
$N_{p,q,z}$	$\forall p \in P, q \in Q_p,$ $z \in Z$	Number of on-route chargers variable Integer variable Number of type q chargers that exist at bus stop p in year z
$N_{y,z}$	$\forall y \in Y, z \in Z$	Number of depot chargers variable Integer variable Number of depot chargers that exist at depot y in year z
$V_{b,m,q,o,z}^f$	$\forall b \in B, z \in Z,$ $f \in F_3 \cap F_2,$ $m \in \{m,\dots,m_b\},$ $o \in \{1,2\}, q \in Q_{P_{b,m,o}}$	On-route charging event occurrence variable Binary variable 1 if charging event occurs when charged with type q charger, using charging option o, after finishing revenue trip m in tour b in year z
$W_{b,z}^f$	$\forall b \in B,$ $f \in F_1 \cup F_3, z \in Z$	Bus-to-tour variable Binary variable 1 if in year z, vehicle type f from new fleets (F_3) or existing fleets (F_1) is selected for tour b

Notation		Meaning
$X^{f}_{b,m,q,o,z}$	$\forall\, b \in B, m \in \{1, \dots, m_b\}$, $z \in Z, f \in F_3 \cap F_2$, $o \in \{1,2\}, q \in Q_{P_{b,m,o}}$	On-route charging duration variable Continuous variable Charging duration when charged with type q charger, using charging option o, after finishing revenue trip m in tour b in year z

Section 7.2 describes the model, fleet conversion without considering vehicle salvage. Section 7.3 describes the second model, fleet conversion with considering vehicle salvage. In each model, optimization equations are formulated and applied to the local network. Section 7.4 summarizes findings and limitations of the proposed models.

7.2 Fleet Conversion Model without Salvage

7.2.1 Model Formulation – Depot Charging Only

This model derives from the budget-constrained model presented in Section 6.4.1. The two decision variables are $W^{f}_{b,z}$ and $N_{y,z}$, representing the fleet-to-tour assignment of the new fleets and number of depot chargers per depot. Equation (131) denotes the objective function, to maximize the benefits of reducing life-cycle CO_2 emissions across all planning years (Z), calculated by aggregating the CO_2 emissions reductions of each tour (b) per year (z). The three sums in the equation denote the CO_2 emissions if served with new electric vehicle fleets ($\forall f \in F_3 \cap F_2$), new non-electric vehicle fleets ($\forall f \in F_3 \backslash F_2$), and the baseline fleet ($\forall f \in F_1$), respectively. The baseline fleet scenario includes random bus-to-tour assignments for all the existing fleets, calculated as the fleet-wide average weighted by the number of vehicles per type (f).

$$\max_{W_{b,z}^{f},N_{y,z}} \sum_{\forall z\in Z}\sum_{\forall s\in S} Freq_s \left\{ -\left\{ \sum_{\forall b\in B_s}\sum_{\forall f\in F_3\cap F_2} W_{b,z}^{f}\left(\sum_{i\in I_b} E_{b,i,z}^{f}\varepsilon_{kWh2MJ}\delta_z^{f}\right)\right\} \right.$$
$$-\left\{\sum_{\forall b\in B_s}\sum_{\forall f\in F_3\setminus F_2} W_{b,z}^{f}E_{b,z}^{f}\varepsilon_{kWh2MJ}\delta_z^{f}\right\} \qquad (131)$$
$$\left. +\left\{\sum_{\forall b\in B_s}\left(\sum_{\forall f\in F_3} W_{b,z}^{f}\right)\sum_{\forall f\in F_1} E_{b,z}^{f}\varepsilon_{kWh2MJ}\delta_z^{f}\left(\frac{\chi^{f}}{\sum_{f\in F_1}\chi^{f}}\right)\right\}\right\}$$

Equation (132) denotes the annual budget constraint, consisting of six cost components per year (z). In equation (133), $C_{\theta,z}$ denotes the new vehicle investment, calculated as the number of newly purchased type f vehicles ($w_z^f - w_{z-1}^f$) multiplied by the cost rate (θ_z^f). In equation (134), $C_{\mu,z}$ denotes the depot charger investment and maintenance cost. For depot y, the depot charging investment is calculated by multiplying the number of newly built chargers ($N_{y,z} - N_{y,z-1}$) by the charger cost rate ($\mu 1_{y,z}$), and the charger maintenance cost is calculated by multiplying the number of in-use chargers ($N_{y,z}$) by the charger maintenance cost rate ($\mu 2_{y,z}$). In equation (135), $C_{\varphi,z}$ denotes the cost of demand charge, calculated as the peak power ($U_{Peak,z}$) multiplied by the demand charge rate (φ_z). Daily cost differences in terms of energy use ($\Delta C_{\alpha,s,z}$), vehicle maintenance ($\Delta C_{\beta,s,z}$), and operator labor cost ($\Delta C_{\gamma,s,z}$) compared with the baseline fleet are denoted in equations (136) through (138). They are formulated such that when tours are served by new fleets, the cost difference is calculated as the difference between the new fleets and the baseline fleet. New electric vehicle fleets and new non-electric vehicle fleets are

aggregated separately, because tours are split into sub-tours for electric vehicle fleets due to range limitation.

$$C_{\theta,z} + C_{\mu,z} + C_{\varphi,z} + \sum_{\forall s \in S} Freq_s \left(\Delta C_{\alpha,s,z} + \Delta C_{\beta,s,z} + \Delta C_{\gamma,s,z}\right) \leq \omega_z \tag{132}$$

$$C_{\theta,z} = \sum_{\forall f \in F_3} \left(w_z^f - w_{z-1}^f\right)\theta_z^f \tag{133}$$

$$C_{\mu,z} = \sum_{\forall y \in Y} \left(\left(N_{y,z} - N_{y,z-1}\right)\mu 1_{y,z} + N_{y,z}\mu 2_{y,z}\right) \tag{134}$$

$$C_{\varphi,z} = U_{Peak,z} * \varphi_z \tag{135}$$

$$\begin{aligned}\Delta C_{\alpha,s,z} = &\left\{\sum_{\forall b \in B_s} \sum_{\forall f \in F_3 \cap F_2} W_{b,z}^f \left(\sum_{i \in I_b} E_{b,i,z}^f \pi_{TC_{b,i',z}^f}\right)\right\} \\ &+ \left\{\sum_{\forall b \in B_s} \sum_{\forall f \in F_3 \setminus F_2} W_{b,z}^f E_{b,z}^f \varepsilon_{kWh2Gal} \alpha_z^f\right\} \\ &- \left\{\sum_{\forall b \in B_s} \left(\sum_{\forall f \in F_3} W_{b,z}^f\right) \sum_{\forall f \in F_1} E_{b,z}^f \varepsilon_{kWh2Gal} \alpha_z^f \left(\frac{\chi^f}{\sum_{f \in F_1} \chi^f}\right)\right\}\end{aligned} \tag{136}$$

$$\begin{aligned}\Delta C_{\beta,s,z} = &\left\{\sum_{\forall b \in B_s} \sum_{\forall f \in F_3 \cap F_2} W_{b,z}^f \left(\sum_{i \in I_b} D_{b,i}^f \beta_z^f\right)\right\} + \left\{\sum_{\forall b \in B_s} \sum_{\forall f \in F_3 \setminus F_2} W_{b,z}^f D_{b,i}^f \beta_z^f\right\} \\ &- \left\{\sum_{\forall b \in B_s} \left(\sum_{\forall f \in F_3} W_{b,z}^f\right) \sum_{\forall f \in F_1} D_b^f \beta_z^f \left(\frac{\chi^f}{\sum_{f \in F_1} \chi^f}\right)\right\}\end{aligned} \tag{137}$$

$$\begin{aligned}\Delta C_{\gamma,s,z} = &\left\{\sum_{\forall b \in B_s} \sum_{\forall f \in F_3 \cap F_2} W_{b,z}^f \left(\sum_{i \in I_b} T_{b,i}^f \gamma_z^f\right)\right\} + \left\{\sum_{\forall b \in B_s} \sum_{\forall f \in F_3 \setminus F_2} W_{b,z}^f T_b \gamma_z^f\right\} \\ &- \left\{\sum_{\forall b \in B_s} \left(\sum_{\forall f \in F_3} W_{b,z}^f\right) \sum_{\forall f \in F_1} T_b \gamma_z^f \left(\frac{\chi^f}{\sum_{f \in F_1} \chi^f}\right)\right\}\end{aligned} \tag{138}$$

Equation (139) denotes the constraint that each tour can be served by at most one type of vehicle. $\sum_{f \in F_3} W_b^f$ equals 1 if tour b is served with new fleets, and 0 if served with baseline fleets. All other constraints related to service demand and depot charging are formulated similar to the depot-charging cost model, described in Section 6.2.1 (equations (43) through (54)). The minor updates to the structure are:

1) F_2 is updated with $F_3 \cap F_2$ to represent new electric vehicle fleets;
2) Each equation adds the lower subscript z to specify the year, and is extended to all time horizon;
3) Equation (44) is updated with equation (140) to represent the number in-use vehicle.

$$\sum_{f \in F_3} W_{b,z}^f \leq 1 \qquad \forall b \in B \tag{139}$$

$$w_{y,s,t_k,z}^f = \begin{cases} \sum_{\forall b \in B_{s,y}, t_k \in T_b^f} W_{b,z}^f, if\ f \in F_3 \backslash F_2 \\ \sum_{\forall b \in B_{s,y}, t_k \in T_{b,i}^f} W_{b,z}^f, if\ f \in F_3 \cap F_2 \end{cases} \qquad \begin{matrix} \forall s \in S, y \in Y, f \in F_3, \\ t_k \in T, z \in Z \end{matrix} \tag{140}$$

7.2.2 Model Formulation – Depot and On-route Charging

This model is built based on the budget-constrained model proposed in Section 6.4.2. The decision variables are all the variables in Table 33 except G_z^f and $H_{z,\lambda}$ because vehicle salvage is not specified in this model. Equation (141) denotes the

objective function, to maximize the benefits of reducing life-cycle CO_2 emissions. The three sums denote the life-cycle CO_2 emissions from new electric vehicle fleets ($\forall f \in F_3 \cap F_2$), new non-electric vehicle fleets ($\forall f \in F_3 \backslash F_2$), and the baseline fleet ($\forall f \in F_1$), respectively.

$$\max_{\substack{W^f_{b,z'} N_{y,z}, \\ V^f_{b,m,q,o,z'} X^f_{b,m,q,o,z'}, \\ N_{p,z}, N_{p,q,z}}} \sum_{\forall z \in Z} \sum_{\forall s \in S} Freq_s \left\{ -\left\{ \sum_{\forall b \in B_s} \left(E_{b,z} \pi_{TC_b,z} + \sum_{\forall f \in F_3 \cap F_2} \sum_{m=1}^{m_b - 1} \sum_{o \in \{1,2\}} \sum_{\forall q \in Q_{p_{b,m,o}}} X^f_{b,m,o,q,z} U_q \pi_{T_{b,m,o},z} \right) \varepsilon_{kWh2MJ} \delta^f_z \right\} \right.$$
$$- \left\{ \sum_{\forall b \in B_s} \sum_{\forall f \in F_3 \backslash F_2} W^f_{b,z} E^f_b \varepsilon_{kWh2MJ} \delta^f_z \right\}$$
$$\left. + \left\{ \sum_{\forall b \in B_s} \left(\sum_{\forall f \in F_3} W^f_{b,z} \right) \left(\sum_{\forall f \in F_1} E^f_b \varepsilon_{kWh2MJ} \delta^f_z \left(\frac{\chi^f}{\sum_{f \in F_1} \chi^f} \right) \right) \right\} \right\} \tag{141}$$

Equation (142) denotes the budget constraint per year (z). New vehicle investment ($C_{\theta,z}$), depot charger investment and maintenance ($C_{\mu,z}$), and demand charging ($C_{\varphi,z}$), are denoted in equations (133) through (135). On-route charging station investment and maintenance cost ($C_{\tau,z}$), on-route charger investment and maintenance ($C_{\epsilon,z}$), and charging penalty ($C_{\sigma,s}$), are denoted in equations (143) through (145). Daily cost differences in terms of energy use, vehicle maintenance, and operator labor cost compared with the baseline, are denoted as $\Delta C_{\alpha,s,z}$, $C_{\beta,s,z}$, and $C_{\gamma,s,z}$ in equations (146) through (148), respectively. Energy use of the electric vehicle fleets are formulated separately because the utility rate varies by time of the day.

$$C_{\theta,z} + C_{\mu,z} + C_{\varphi,z} + C_{\tau,z} + C_{\epsilon,z} + \sum_{\forall s \in S} Freq_s \left(\Delta C_{\alpha,s,z} + \Delta C_{\beta,s,z} + \Delta C_{\gamma,s,z} + C_{\sigma,s,z}\right) \leq \omega_z \tag{142}$$

$$C_{\tau,z} = \sum_{\forall p \in P} (N_{p,z} - N_{p,z-1})\tau 1_{p,z} + N_{p,z}\tau 2_{p,z}) \tag{143}$$

$$C_{\epsilon,z} = \sum_{\forall p \in P} \sum_{\forall q \in Q_p} (N_{p,q,z} - N_{p,q,z-1})\epsilon 1_{q,z} + N_{p,q,z}\epsilon 2_{q,z}) \tag{144}$$

$$C_{\sigma,s,z} = v_{s,z}\sigma_{s,z} \tag{145}$$

$$\Delta C_{\alpha,s,z} = \sum_{\forall b \in B_s} \left(\left(\sum_{\forall f \in F_3 \cap F_2} \sum_{m=1}^{m_b - 1} \sum_{o \in \{1,2\}} \sum_{\forall q \in Q_{p_{b,m,o}}} X^f_{b,m,o,q,z} U_q \pi_{T_{b,m,o},z} + E_{b,z}\pi_{TC_b,z} \right) + \left(\sum_{\forall f \in F_3 \setminus F_2} W^f_{b,z} E^f_{b,z} \mu_{kWh2Gal} \alpha^f_z \right) - \left(\sum_{\forall f \in F_2} W^f_{b,z} \right) \left(\sum_{\forall f \in F_1} E^f_{b,z} \mu_{kWh2Gal} \alpha^f_z \left(\frac{\chi^f}{\sum_{f \in F_1} \chi^f} \right) \right) \right) \right) \tag{146}$$

$$\Delta C_{\beta,s,z} = \sum_{\forall b \in B_s} \sum_{\forall f \in F_3} W^f_b \left(D^f_b \beta^f_z - \sum_{\forall f \in F_1} D^f_b \beta^f_z \left(\frac{\chi^f}{\sum_{f \in F_1} \chi^f} \right) \right) \tag{147}$$

$$\Delta C_{\gamma,s,z} = \sum_{\forall b \in B_s} \sum_{\forall f \in F_3} W^f_b \left(T_b \gamma^f_z - \sum_{\forall f \in F_1} T_b \gamma^f_z \left(\frac{\chi^f}{\sum_{f \in F_1} \chi^f} \right) \right) \tag{148}$$

The constraint of fleet-to-tour assignment of new fleets, denoted in equation (139), still applies in this model. Other constraints related to vehicle availability, depot chargers, on-route chargers, energy flows, and charging events, are formulated as they were in cost

model described in Section 6.2.2. The changes made are specifying the year z and changing the fleet set to $F_3 \cap F_2$.

7.2.3 Implementation

7.2.3.1 Settings and Assumptions

The proposed models in this chapter is implemented in the same MARTA transit network as used in Section 6.4.3, which includes all the tours that serve 28 revenue routes from the Hamilton depot. We implement the model for four scenarios, shown in Table 34. In Scenario 1 and 2, the new fleet set (F_3) only includes electric vehicles. In Scenario 3 and 4, the new fleet set (F_3) is expanded to not only the electric vehicle fleets, but also new CNG vehicles. The fleet composition of the baseline is selected as the Scenario 1 in Section 5.2. Parameter values of electric vehicle and non-electric vehicle fleets follow the same settings as Section 6.4.3 and Section 5.2 when applicable. We set the annual budget (ω_z) to \$3.0 million USD among all the scenarios.

Table 34 – Scenario Set-up: Fleet Conversion w/o Salvage

No.	Time Horizon	Vehicle Type of New Fleets	Charging Option
1	5	400kWh battery-electric	Depot-charging Only
2	5	200kWh battery-electric	Depot and On-route Charging
3	5	400kWh battery-electric, CNG	Depot-charging Only
4	12	400kWh battery-electric, CNG	Depot-charging Only

Within the planning horizon, the unit cost of each cost component varies due to inflation and potential impacts of technology development. We incorporate these factors into the vehicle procurement cost (θ_z^f), shown in Figure 48. The unit price of battery-

electric vehicles is assumed to drop by 5% annually from year 2-6, and then increases by 2% afterwards (discussed in Section 2.5.1). Because CNG vehicle technologies have been relatively mature and the unit price is assumed to increase by 2% annually. For simplicity, unit costs of other cost components, such as fuel and charging facility capital costs, are assumed to be the same over the planning horizon.

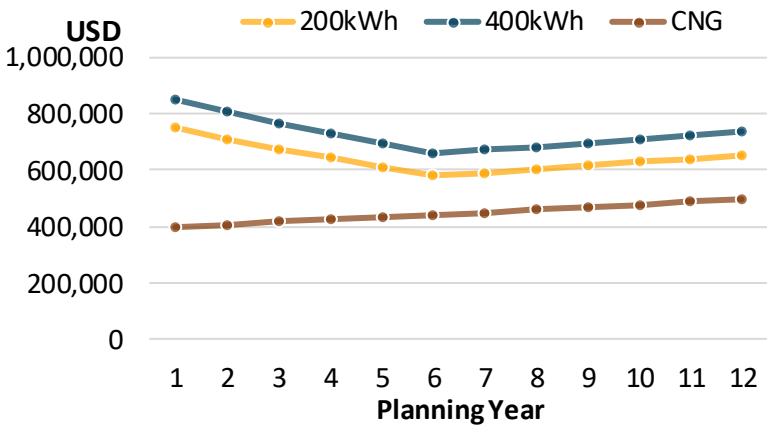

Figure 48 – Vehicle Procurement Cost by Year

7.2.3.2 Results

Scenarios 1 and 2: Five-Year Procurement Plan, New BEVs

In the battery-electric only five-year plan, total life-cycle CO_2 emissions are reduced by 7,290 metric tonnes (4.1%) in Scenario 1 and 9,021 metric tonnes (5.1%) in Scenario 2, compared with baseline. In Scenario 1, at the end of the planning horizon, 18 new battery-electric vehicles are procured in total, and 14 depot chargers are installed. Eight depot chargers are procured in the first two years, even though the fleet just has six battery-electric vehicles. Due to the budget constraint, the fleet cannot afford to procure additional vehicles but can afford to purchase additional chargers. Figure 49 shows the

CO_2 emissions reductions, number of vehicles procured, and distance traveled by the electric vehicle fleets per year.

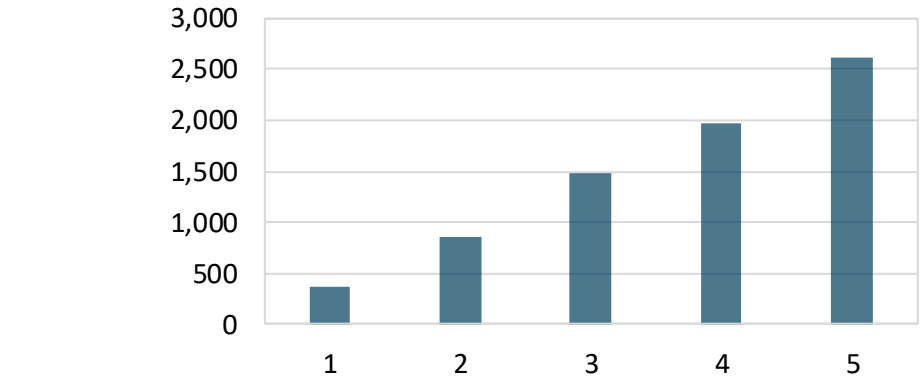

(a) Reductions of CO_2 Emissions (Metric Tonnes)

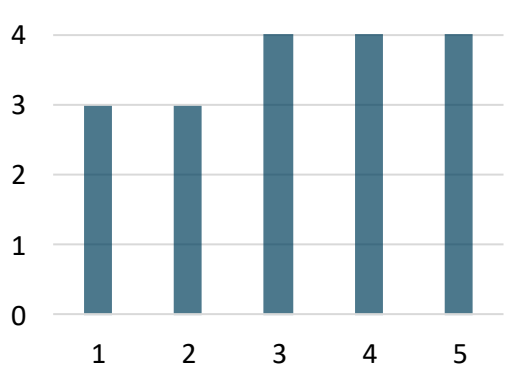

(b) Number of Vehicles Procured

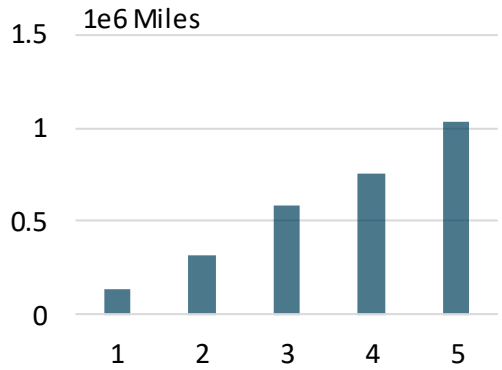

(c) Distance Traveled of New Fleets

Figure 49 – Results: Fleet Conversion without Salvage Model, Scenario 1

Scenario 3: Five-Year Plan, New BEV and CNG, Depot-Charging Only

In the battery-electric and CNG five-year plan, total life-cycle CO_2 emissions are reduced by 1,3464 metric tonnes (7.6%) compared with baseline. At the end of the planning horizon, 29 new CNG and four battery-electric vehicles are procured in total, and four depot chargers are installed. Figure 50 shows the CO_2 emissions reductions, number of vehicles procured, and the mileage traveled of the new fleets per year. Not surprisingly, in the "optimal" plan, no battery-electric vehicles will be procured until Year 5. This is because the price of a battery-electric bus is more than double that of its CNG counterpart

in Year 1. It is more cost-effective to procure two CNG vehicles than one battery-electric vehicles in terms of reducing life-cycle CO_2 emissions. However, in Year 5, the price of a battery-electric bus is only 60% higher. One thing interesting to mention is that the depot chargers are procured and installed in Year 4, even though the first battery electric buses are procured in Year 5; this takes advantage of the available budget increment in Year 4.

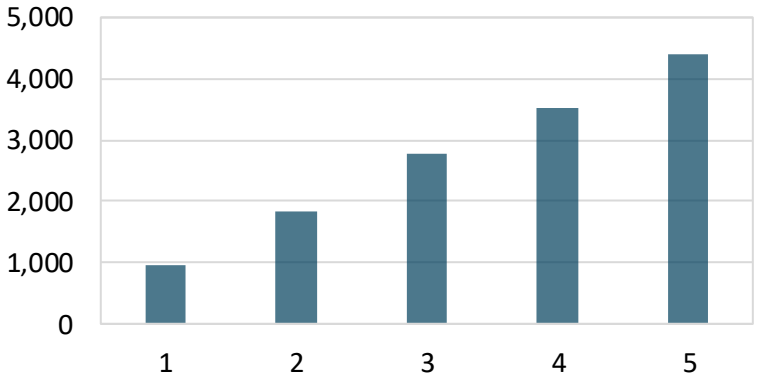

(a) Reductions of CO_2 Emissions (Metric Tonnes)

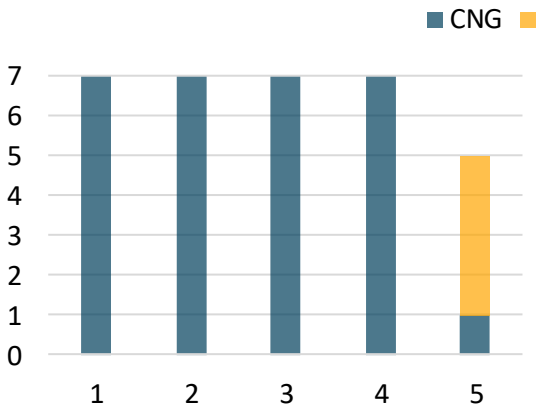

(b) Number of Vehicles Procured

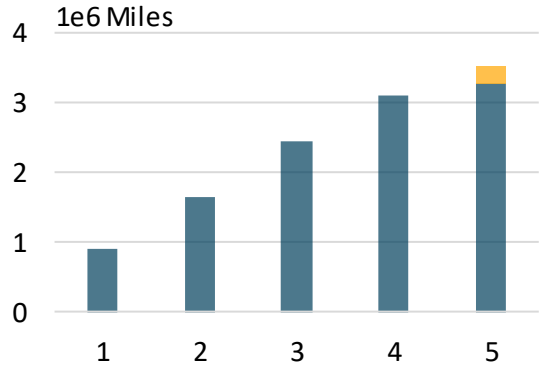

(c) Distance Traveled of New Fleets

Figure 50 – Results: Fleet Conversion without Salvage Model, Scenario 3

Scenario 4: 12-Year Plan, New BEV and CNG, Depot-Charging Only

In the 12-year plan, total life-cycle CO_2 emissions are reduced by 66,000 metric tonnes (15.4%) compared with baseline. At the end of the planning horizon, 63 new CNG and 14 battery-electric vehicles are procured in total, and 12 depot chargers are installed. Figure 51 shows the annual CO_2 reductions, number of vehicles procured, and the mileage traveled of the new fleets. As in Scenario 3, five depot chargers are installed one year before battery-electric vehicles are procured.

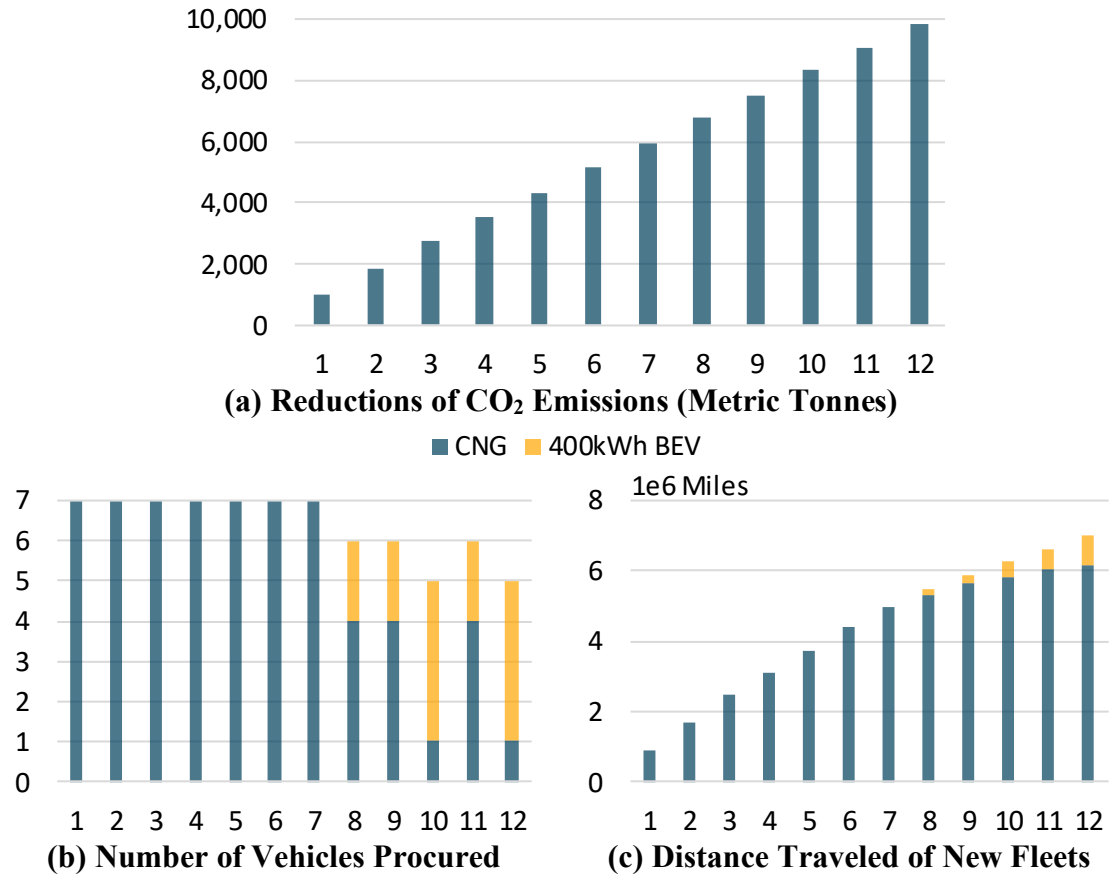

(a) Reductions of CO_2 Emissions (Metric Tonnes)

(b) Number of Vehicles Procured

(c) Distance Traveled of New Fleets

Figure 51 – Results: Fleet Conversion without Salvage Model, Scenario 4

7.3 Fleet Conversion Model with Salvage

7.3.1 Model Formulation – Depot Charging Only

The fleet conversion with salvage model extends the costs and benefits to the entire transit fleet, including the existing vehicles that will be replaced by the new vehicles that are procured. In addition to the two decision variables in Section 7.2.1, this model adds an integer variable G_z^f to represent the cumulative number of type f vehicles that are salvaged up to year z. In this model, we only salvage vehicles from the existing fleet (F_1). If the time horizon κ is longer than the life-span of new fleets, we can expand the available-to-salvage vehicle to the set of $F_1 \cup F_3$. To capture the fleets that are in-use and the fleets that are available to be salvaged, the bus-to-tour assignment among existing fleets are explicitly determined in the model outputs.

Equation (149) denotes the objective function, to minimize the fleet-wide life-cycle CO_2 emissions across all planning years (Z), calculated by aggregating the CO_2 emissions of each tour (b) per year (z). The first and second sum of the equation denote the CO_2 emissions if served with new fleets, and if with existing fleets, respectively.

$$\min_{W_{b,z}^f, N_{y,z}, G_z^f, H_{z,\lambda}} \sum_{\forall z \in Z} \sum_{\forall s \in S} Freq_s \left\{ \left\{ \sum_{\forall b \in B_s} \sum_{\forall f \in F_3 \cap F_2} W_{b,z}^f \left(\sum_{i \in I_b^f} E_{b,i,z}^f \varepsilon_{kWh2MJ} \delta_z^f \right) \right\} + \left\{ \sum_{\forall b \in B_s} \sum_{\forall f \in (F_3 \setminus F_2) \cup F_1} W_{b,z}^f E_{b,z}^f \varepsilon_{kWh2MJ} \delta_z^f \right\} \right\} \tag{149}$$

Equation (150) denotes the annual budget constraint, consisting of seven cost components. New vehicle investment ($C_{\theta,z}$), depot charger investment and maintenance ($C_{\mu,z}$), and demand charging ($C_{\varphi,z}$), are denoted in equations (133) through (135), respectively. In equation (151), $C_{v,s}$ denotes the value of the salvaged vehicles. Per vehicle

type f, its salvaged value is calculated as the number of vehicles that are salvaged (G_z^f) multiplied by the salvage cost rate (v_z^f). Equations (152) through (154) denote the daily fleet-wide cost in terms of energy use ($C_{\alpha,s,z}$), vehicle maintenance ($C_{\beta,s,z}$), and operator ($C_{\gamma,s,z}$). Costs are either aggregated by sub-tours or tours depending on whether they are served by electric vehicle or non-electric vehicle fleets.

$$C_{\theta,z} + C_{\mu,z} + C_{\varphi,z} - C_{\upsilon,z} + \sum_{\forall s \in S} Freq_s \left(C_{\alpha,s,z} + C_{\beta,s,z} + C_{\gamma,s,z}\right) \leq \omega_z \tag{150}$$

$$C_{\upsilon,z} = \sum_{\forall f \in F_1} G_z^f v_z^f \tag{151}$$

$$\begin{aligned} C_{\alpha,s,z} = &\left\{ \sum_{\forall b \in B_s} \sum_{\forall f \in F_3 \cap F_2} W_{b,z}^f \left(\sum_{i \in I_b^f} E_{b,i,z}^f \pi_{TC_{b,i',z}^f} \right) \right\} \\ &+ \left\{ \sum_{\forall b \in B_s} \sum_{\forall f \in (F_3 \setminus F_2) \cup F_1} W_{b,z}^f E_{b,z}^f \varepsilon_{kWh2Gal} \alpha_z^f \right\} \end{aligned} \tag{152}$$

$$\begin{aligned} C_{\beta,s,z} = &\left\{ \sum_{\forall b \in B_s} \sum_{\forall f \in F_3 \cap F_2} W_{b,z}^f \left(\sum_{i \in I_b^f} D_{b,i}^f \beta_z^f \right) \right\} \\ &+ \left\{ \sum_{\forall b \in B_s} \sum_{\forall f \in (F_3 \setminus F_2) \cup F_1} W_{b,z}^f D_{b,i}^f \beta_z^f \right\} \end{aligned} \tag{153}$$

$$C_{\gamma,s,z} = \left\{ \sum_{\forall b \in B_s} \sum_{\forall f \in F_3 \cap F_2} W_{b,z}^f \left(\sum_{i \in I_b^f} T_{b,i}^f \gamma_z^f \right) \right\} + \left\{ \sum_{\forall b \in B_s} \sum_{\forall f \in (F_3 \setminus F_2) \cup F_1} W_{b,z}^f T_b \gamma_z^f \right\} \tag{154}$$

The rest of the model is formulated in equations (155) through (171). Because all of these equations are based on the models described in the previous sections, we briefly describe them here. Equation (155) denotes the set of in-use time slots for tour b, if served

with existing fleets (F_1) or new non-electric vehicle fleets ($F_3 \backslash F_2$). Equation (156) denotes the set of in-use time slots for tour b, if served with new electrified fleets ($F_3 \cap F_2$). Equation (157) denotes the set of depot-charging time slots for tour b. Equation (158) denotes the constraint that each tour is served by one vehicle type. Equation (159) denotes the number of type f vehicles that are in-use at slot t_k on service day type s. Equation (160) denotes the constraint that for each depot y, the demand of each type of vehicles do not exceed the supply. Equation (161) denotes the constraint that for each depot y, the total number of available vehicles is enough for the in-use vehicles and the spares. Equation (162) denotes the constraint that the cumulative fleet size for each vehicle type f does not exceed depot capacity. Equation (163) denotes the fleet-wide demand for type f vehicles. Equation (164) denotes the constraint that the new fleet vehicles per type f are not salvaged. Equation (165) denotes the constraint that the number of existing fleets per type f does not exceed the number of the initial fleet, excluding the vehicles salvaged. Equation (166) denotes the vehicle demand for each depot y. Equation (167) denotes the constraint that for each depot y, the vehicle demand does not exceed the depot capacity, i.e. total number of vehicles that can be housed in the depot. Equation (168) denotes the depot charging demand of type f vehicles for each depot y. Equation (169) denotes the constraint that for each depot y, depot charger supply is enough for the demand and spares. Equation (170) denotes the constraint that the number of chargers built for each depot y does not exceed its supply. Equation (171) denotes the peak charging power.

$$T_b = \{t_{TO_b}, t_{TO_b+1}, \dots, t_{TI_b}\} \qquad \begin{matrix} \forall b \in B, \\ f \in F_1 \cup (F_3 \backslash F_2), i \in I_b^f \end{matrix} \qquad (155)$$

$$T_{b,i,z}^{f} = \{t_{TO_{b,i,z}^{f}}, t_{TO_{b,i,z}^{f}+1}, \dots, t_{TI_{b,i,z}^{f}+TD_{b,i,z}^{f}}\} \qquad \begin{matrix}\forall b \in B,\\ f \in F_3 \cap F_2, i \in I_b^f, z \in Z\end{matrix} \tag{156}$$

$$TC_{b,i,z}^{f} = \{t_{TI_{b,i,z}}, t_{TI_{b,i,z}+1}, \dots, t_{TI_{b,i,z}+TD_{b,i,z}^{f}}\} \qquad \begin{matrix}\forall b \in B,\\ f \in F_3 \cap F_2, i \in I_b^f, z \in Z\end{matrix} \tag{157}$$

$$\sum_{f \in F_1 \cup F_3} W_{b,z}^{f} = 1 \qquad \forall b \in B, z \in Z \tag{158}$$

$$w_{y,s,t_k,z}^{f} = \begin{cases} \sum_{\forall b \in B_{s,y}, t_k \in T_b} W_{b,z}^{f}, if\ f \in F_3 \backslash F_2 \\ \sum_{\forall b \in B_{s,y}, t_k \in T_{b,i}^{f}} W_{b,z}^{f}, if\ f \in (F_3 \cap F_2) \cup F_1 \end{cases} \qquad \begin{matrix}\forall s \in S, y \in Y, z \in Z,\\ f \in F_1 \cup F_3, t_k \in T\end{matrix} \tag{159}$$

$$\max_{\forall s \in S, t_k \in T} w_{y,s,t_k,z}^{f} \le w_{y,z}^{f} \qquad \forall\, y \in Y, f \in F_1 \cup F_3, z \in Z \tag{160}$$

$$\max_{\forall s \in S, t_k \in T} (1+\eta 1) \sum_{\forall f \in F_1 \cup F_3} w_{y,s,t_k,z}^{f} \le \sum_{\forall f \in F_1 \cup F_3} w_{y,z}^{f} \qquad \forall y \in Y, z \in Z \tag{161}$$

$$w_{y,z}^{f} \le \chi_y^f \qquad \forall y \in Y, f \in F_3 \tag{162}$$

$$w_z^f = \sum_{\forall y \in Y} w_{y,z}^{f} \qquad \forall f \in F_1 \cup F_3, z \in Z \tag{163}$$

$$w_{z-1}^{f} \le w_z^f \qquad \forall f \in F_3, z \in Z \tag{164}$$

$$w_z^f \le \chi^f - \sum_{\forall 1 \le z_i \le z} G_{z_i}^{f} \qquad \forall f \in F_1, z \in Z \tag{165}$$

$$w_{y,z} = \sum_{\forall f \in F_1 \cup F_3} w_{y,z}^{f} \qquad \forall y \in Y, z \in Z \tag{166}$$

$$w_{y,z} \leq \chi_y \qquad \forall y \in Y, z \in Z \qquad (167)$$

$$n^f_{y,s,t_k,z} = \sum_{\forall b \in B_{s,y}, t_k \in TC^f_{b,i}} W^f_{b,i,z} \qquad \forall s \in S, y \in Y, f \in F_3, t_k \in T, i \in I^f_b, z \in Z \qquad (168)$$

$$\max_{\forall s \in S, t_k \in T} (1 + \eta 2) \sum_{\forall f \in F_2} n^f_{y,s,t_k,z} \leq N_{y,z} \qquad \forall y \in Y, z \in Z \qquad (169)$$

$$N_{y,z} \leq \chi_y^{Depot} \qquad \forall y \in Y, z \in Z \qquad (170)$$

$$U_{Peak,z} = \max_{\forall s \in S, t_k \in T} \sum_{\forall y \in Y} \sum_{\forall t_k \in TU_k} n^f_{y,s,t_k,z} U_{Depot} \qquad \forall z \in Z \qquad (171)$$

The current model prioritizes the salvage of vehicles with the highest energy use and highest CO_2 emissions; however, it is possible to incorporate a variety of factors, such as vehicle age or vehicle state of repair into the salvage prioritization scheme if desired. Equations (174) through (175) denote the constraints about vehicle salvage sequence. $H_{z,\lambda}$ is a binary variable, which equals 1 if at least one vehicle with sequence λ is salvaged and 0 otherwise. The term ϕ_{λ_i} represents the number of vehicles with salvage sequence λ_i, and f_{λ_i} represents its vehicle type. The rationale is that no vehicles with salvage sequence λ can be salvaged, until all the vehicles with salvage sequence $\lambda - 1$ or below are salvaged first.

$$G_z^{f_\lambda} \leq \boldsymbol{M} H_{z,\lambda} + \sum_{\forall 1 \leq \lambda_i \leq \lambda - 1, f_{\lambda_i} = f_\lambda} \phi_{\lambda_i} \qquad \forall \lambda \in \Lambda, z \in Z \qquad (172)$$

$$G_z^{f_{\lambda-1}} \geq -\boldsymbol{M}(1 - H_{z,\lambda}) + \sum_{\forall 1 \leq \lambda_i \leq \lambda-1, f_{\lambda_i} = f_{\lambda-1}} \phi_{\lambda_i} \qquad \forall \lambda \in \Lambda, z \in Z \qquad (173)$$

Table 35 shows a salvage sequence example. The rule is to salvage older vehicles first, and if there are both diesel and CNG vehicles, salvage diesel vehicles first. For example, vehicles with sequence 2 or higher ($2 \leq \lambda$) will not be salvaged unless we salvage all the vehicles with sequence 1 ($\lambda = 1$). That is, if $G_z^2 > 0$, we need to ensure $G_z^1 \geq 20$. Vehicles with sequence 4 or higher ($4 \leq \lambda$) will not be salvaged, unless we salvage all the vehicles with sequence 1-3 ($1 \leq \lambda \leq 3$). That is, if $G_z^2 > 20$, we need to ensure $G_z^1 \geq 30$. Note that this is only one example of how to incorporate a salvage sequence into the model, the sequence table can be easily adjusted to fit agency-specific preferences and needs.

Table 35 – Salvage Sequence Example

Sequence ID (λ)	Vehicle Model	Vehicle Type (f_λ)	Number of Vehicles (ϕ_{λ_i})
1	Diesel, age=11	1	20
2	CNG, age=11	2	5
3	Diesel, age=10	1	10
4	CNG, age=10	2	25
5	CNG, age=5	3	10
6	Diesel, age=5	4	5

7.3.2 Model Formulation – Depot and On-route Charging

Following the same manner as the depot-charging only model presented in Section 7.3.1, the decision variables of the depot and on-route charging model are derived from the cost model described in Section 7.2.2. All the variables listed in Table 33 are used in this

model, the term z is added as a subscript to specify the year, and the set F_3 is used to represent the new fleets.

$$\min_{\substack{W^f_{b,z'},N_{y,z},G^f_z,H_{z,\lambda},\\ V^f_{b,m,q,o,z'},X^f_{b,m,q,o,z'},\\ N_{p,z},N_{p,q,z}}} \sum_{\forall z\in Z}\sum_{\forall s\in S} Freq_s \left\{\left\{\sum_{\forall b\in B_s}\left(E_{b,z}\pi_{TC_b,z} + \sum_{\forall f\in F_3\cap F_2}\sum_{m=1}^{m_b-1}\sum_{o\in\{1,2\}}\sum_{\forall q\in Q_{p_{b,m,o}}} X^f_{b,m,o,q,z}U_q\pi_{T_{b,m,o},z}\right)\varepsilon_{kWh2MJ}\delta^f_z\right\}\right.$$
$$\left. + \left\{\sum_{\forall b\in B_s}\sum_{\forall f\in(F_3\setminus F_2)\cup F_1} Freq_s W^f_{b,z}E^f_{b,z}\varepsilon_{kWh2MJ}\delta^f_z\right\}\right\} \tag{174}$$

Equation (175) denotes the annual budget constraint. Costs include new vehicle investment ($C_{\theta,z}$), depot charger investment and maintenance ($C_{\mu,z}$), and demand charging ($C_{\varphi,z}$), on-route charging station investment and maintenance ($C_{\tau,z}$), on-route charger investment and maintenance ($C_{\epsilon,z}$), charging penalty ($C_{\sigma,s}$), and vehicle salvage ($C_{\upsilon,s}$), appearing in equations (133) through (135), (143) through (145), and (151), respectively. Equations (179) through (181) denote the daily fleet-wide cost in terms of energy use ($C_{\alpha,s,z}$), vehicle maintenance ($C_{\beta,s,z}$), and operator labor ($C_{\gamma,s}$). Energy use of electric vehicle fleets are separately formulated because the utility rate for electricity use varies by time of the day.

$$C_{\theta,z} + C_{\mu,z} + C_{\varphi,z} + C_{\tau,z} + C_{\epsilon,z} - C_{\upsilon,z} + \sum_{\forall s\in S} Freq_s\left(C_{\alpha,s,z} + C_{\beta,s,z} + C_{\gamma,s,z} + C_{\sigma,s}\right) \le \omega_z \tag{175}$$

$$C_{\tau,z} = \sum_{\forall p\in P}(N_{p,z} - N_{p,z-1})\tau 1_{p,z} + N_{p,z}\tau 2_{p,z}) \tag{176}$$

$$C_{\epsilon,z} = \sum_{\forall p \in P} \sum_{\forall q \in Q_p} (N_{p,q,z} - N_{p,q,z-1}) \epsilon 1_{q,z} + N_{p,q,z} \epsilon 2_{q,z}) \tag{177}$$

$$C_{\sigma,s,z} = v_{s,z} \sigma_{s,z} \tag{178}$$

$$C_{\alpha,s,z} = \sum_{\forall b \in B_s} \left(\left(\sum_{\forall f \in F_3 \cap F_2} \sum_{m=1}^{m_b - 1} \sum_{o \in \{1,2\}} \sum_{\forall q \in Q_{p_{b,m,o}}} X^f_{b,m,o,q,z} U_q \pi_{T_{b,m,o},z} + E_{b,z} \pi_{TC_b,z} \right) + \left(\sum_{\forall f \in (F_3 \setminus F_2) \cup F_1} W^f_{b,z} E^f_{b,z} \varepsilon_{kWh2Gal} \alpha^f_z \right) \right) \tag{179}$$

$$C_{\beta,s,z} = \sum_{\forall b \in B_s} \sum_{\forall f \in F_1 \cup F_3} W^f_b D^f_b \beta^f_z \tag{180}$$

$$C_{\gamma,s,z} = \sum_{\forall b \in B_s} \sum_{\forall f \in F_1 \cup F_3} W^f_b T_b \gamma^f_z \tag{181}$$

The vehicle demand and depot charging equations formulated in the depot-charging-only model represented by equations (155) through (170) also apply to this model, with minor changes, as the original tour is maintained through on-route charging. Equations (156), (157), (159), and (168) are updated with equations (182) through (185). Equation (186) denotes the peak demand charge power. Other constraints related to on-route charging stations and chargers, energy flows, and charging events, are formulated similar to the cost model in Section 6.2.2 in equations (66) through (89). The changes made are specifying the year z and changing the fleet set to $F_3 \cap F_2$.

$$T^f_{b,z} = \{t_{TO^f_{b,z}}, t_{TO^f_{b,z}+1}, \dots, t_{TI^f_{b,z}+TD^f_{b,z}}\} \qquad \forall b \in B, z \in Z, f \in F_3 \cap F_2 \tag{182}$$

$$TC_{b,z}^{f} = \{t_{TI_b}, t_{TI_b+1}, \dots, t_{TI_b+TD_{b,z}^{f}}\} \qquad \forall b \in B, z \in Z, f \in F_3 \cap F_2 \qquad (183)$$

$$w_{y,s,t_k,z}^{f} = \begin{cases} \sum_{\forall b \in B_{s,y}, t_k \in T_b} W_{b,z}^{f}, if\ f \in F_3 \backslash F_2 \\ \sum_{\forall b \in B_{s,y}, t_k \in T_b^{f}} W_{b,z}^{f}, if\ f \in (F_3 \cap F_2) \cup F_1 \end{cases} \qquad \forall s \in S, y \in Y, z \in Z, f \in F_1 \cup F_3, t_k \in T \qquad (184)$$

$$n_{y,s,t_k,z}^{f} = \sum_{\forall b \in B_{s,y}, t_k \in TC_b^{f}} W_{b,z}^{f} \qquad \forall s \in S, y \in Y, f \in F_3 \cap F_2, t_k \in T, z \in Z \qquad (185)$$

$$U_{Peak,z} = \max_{\forall s \in S, t_k \in T} \sum_{y \in Y} \sum_{t_k \in TU_k} n_{y,s,t_k,z}^{f} U_{Depot} + \sum_{\forall b \in B_s, TU_k \cap T_{b,m,o} \neq \emptyset} \sum_{\forall p = P_{b,m,o}, q \in Q_p} V_{b,m,o,q,z} U_q \qquad \forall z \in Z \qquad (186)$$

7.3.3 Implementation

7.3.3.1 Settings and Assumptions

The transit network and parameter inputs are the same as the no-salvage models presented in Section 7.2.3. The additional settings related to vehicle salvage are shown in Table 36. The rationale is that older vehicles are salvaged first. Salvage value is set as $35,000 for diesel vehicles and $40,000 for CNG vehicles, around 10% of the new procurement price. Newly procured fleets are not salvaged in this model.

Table 36 – Fleet Composition: Hamilton Depot

Model Year	Number of Vehicles	Fuel, Age Group	Salvage Sequence
2008	5	Diesel, 1	1
2009	5	CNG, 1	2
2010	5	CNG, 1	3

Model Year	Number of Vehicles	Fuel, Age Group	Salvage Sequence
2013	10	CNG, 1	4
2013	40	Diesel, 1	5
2014	60	CNG, 2	6

For these case studies, we set the annual procurement budget (ω_z) to $25.0 million USD and apply the model to the same three five-year scenarios varying the battery size and depot vs depot plus on-route charging) presented earlier in Table 34.

7.3.3.2 Results

Scenario 1: Five-Year Plan, New BEV, Depot-Charging Only

The total amount of life-cycle CO_2 emissions across the planning horizon is 118,805 metric tonnes. The reduction achieved is 59,150 metric tonnes (33.2%) compared with baseline. At the end of the planning horizon, 31 battery-electric vehicles are procured in total, and 26 depot chargers are installed. Figure 52 shows the annual cost profiles, operations by fuel type, and fleet compositions. Annual procurement cost of battery-electric vehicles and chargers ranges from $4.3 to $4.8 million USD, covering around one fifth of the annual budget. With more battery-electric vehicles procured, the percentage of annual miles traveled from electric vehicle fleets increases from 3.5% in Year 1 to 20.4% in Year 5. However, the percentage of their energy use only increases from 0.9% to 6.0%, and CO_2 emissions only increase from 1.6% to 10.8 %. This is because battery-electric vehicles have the benefits of high fuel efficiency and low life-cycle CO_2 emissions; that is, for the same distance traveled, the energy use and CO_2 emissions are much lower for battery-electric vehicles compared with the other types of vehicles.

Fleet size increases from 125 in Year 0 (initial fleet) to 151 in Year 5. Five model year 2018 diesel vehicles are salvaged, and 31 new battery-electric vehicles procured. This is inconsistent with the general perception that vehicles are replaced on a one-to-one basis. This occurs for three reasons:

1) In adopting electric vehicle fleets, the in-use duration per vehicle is increases due to additional depot pull-in/pull-out operations and dwelling for depot charging. This increases the peak demand for vehicles, i.e. number of vehicles dispatched at the same time, from 112 to 122. Considering the spare ratio (0.1), the fleet-wide demand of vehicles increases from 124 in to 135.

2) The salvage sequence design limits the "available" vehicles to be salvaged. As new fleets are procured, the peak demand for the existing diesel vehicles drops from 28 in Year 1 to 11 in Year 5. The prioritized 5 diesel vehicles (λ=1) are salvaged first, but no additional diesel vehicles are available to be salvaged until the 10 older CNG vehicles (λ=2, 3) are salvaged under the rules of the scenario. However, the peak demand of existing CNG vehicles is 20, which means that no CNG vehicles are available to be salvaged.

3) The increased fleet size is still far below the depot capacity limit (χ_y=300), and the benefits from salvaging vehicles is trivial compared with fleet procurement. Therefore, even though the model "keeps" the inactive diesel vehicles, it does not impact the fleet conversion decisions in this case.

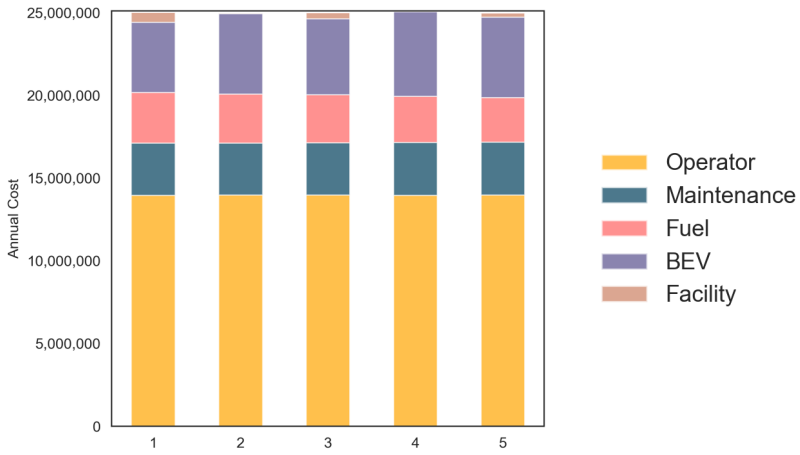

(a) Cost Components by Year

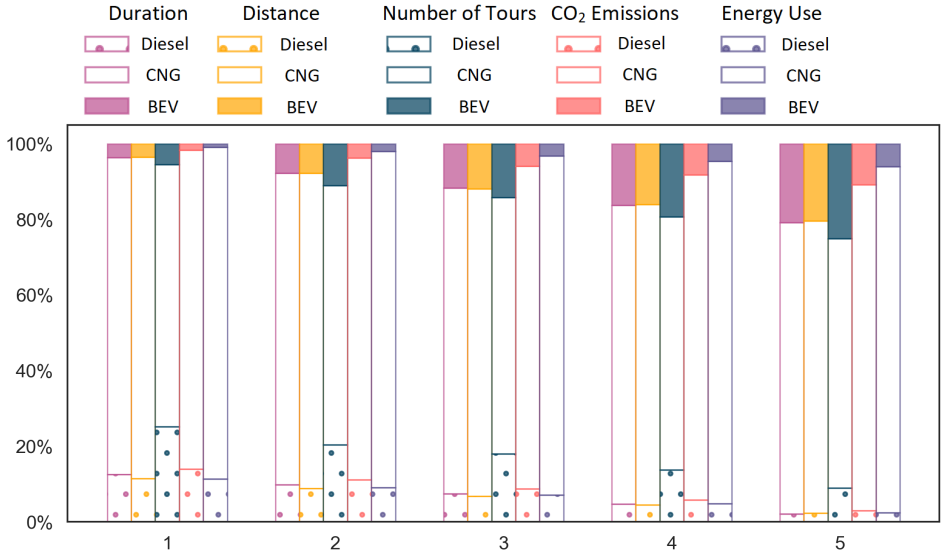

(b) Operations Percentages by Fuel Type, Year

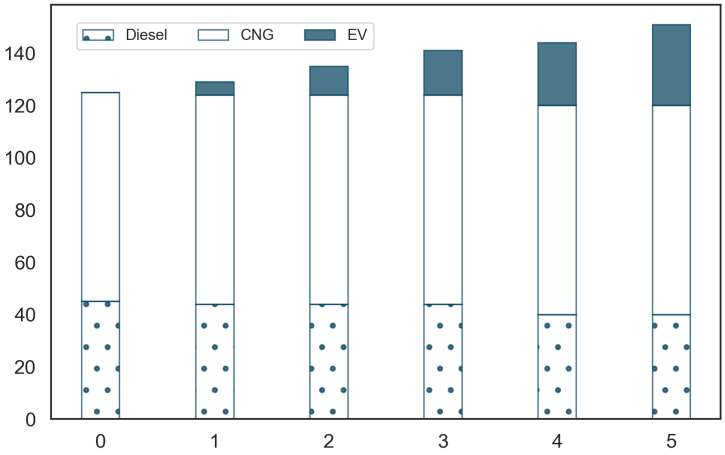

(c) Fleet Composition by Fuel Type, Year

Figure 52 – Results: Fleet Conversion with Salvage Model, Scenario 1

Scenario 2: Five-Year Plan, New BEV, Depot and On-route Charging

Total amount of life-cycle CO_2 emissions across the planning horizon is 117,848 metric tonnes and the reduction achieved is 60,107 metric tonnes (33.8%) compared with baseline. At the end of the planning horizon, 22 battery-electric vehicles are procured in total, and 17 depot chargers and 13 on-route charging stations are installed. Figure 53 shows the annual cost profiles, operations by fuel type, and fleet compositions. Annual procurement cost of battery-electric vehicles and chargers ranges from $4.3 to $5.4 million USD. We see a much higher cost associated with charging facilities, due to the higher unit cost of on-route charging stations compared with depot chargers. The percentage of electric vehicle fleets in terms of energy use and service is similar to the Scenario 1. With more battery-electric vehicles procured, the percentage of annual miles traveled from electric vehicle fleets increases from 2.1% in Year 1 to 23.1% in Year 5. However, the percentage of their energy use only increases from 0.5% to 6.4%, and CO_2 emissions only increase from 0.9% to 11.4 %. The trend of fleet composition is the same as Scenario 1, with five diesel vehicles salvaged.

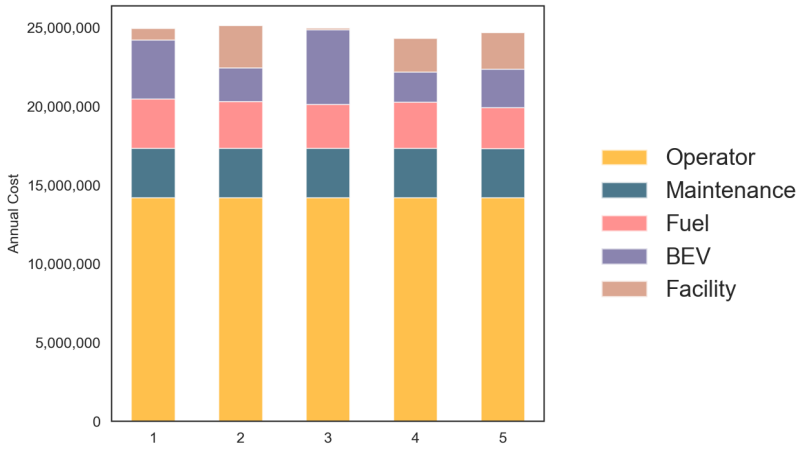

(a) Cost Components by Year

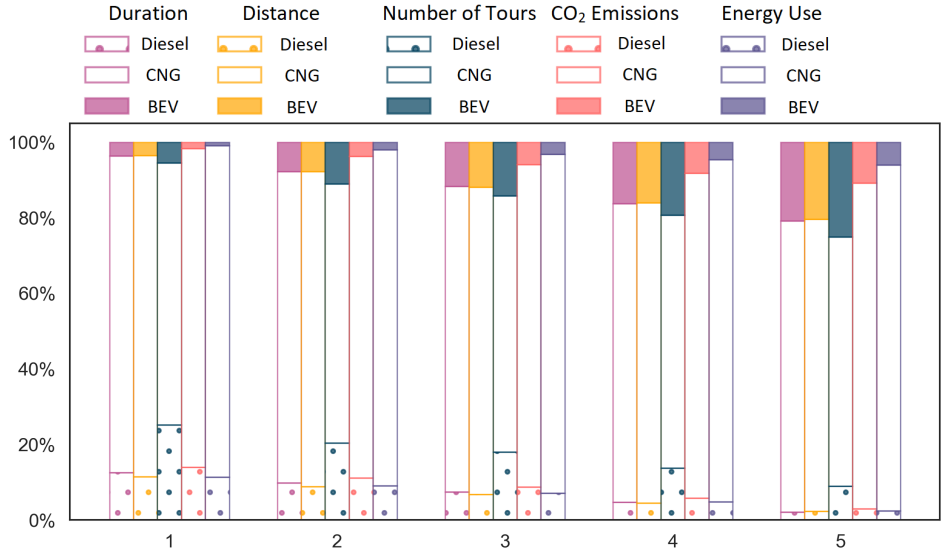

(b) Operations Percentages by Fuel Type, Year

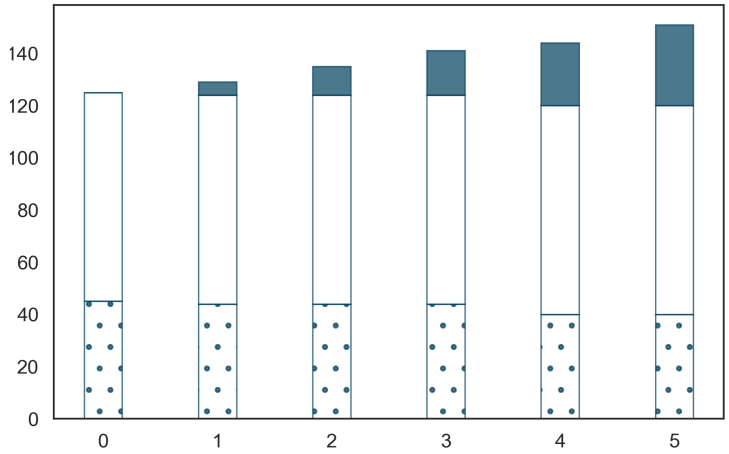

(c) Fleet Composition by Fuel Type, Year

Figure 53 – Results: Fleet Conversion with Salvage Model, Scenario 2

Scenario 3: Five-Year Plan, New BEV and CNG, Depot-Charging Only

Total amount of life-cycle CO_2 emissions across the planning horizon is 118,799 metric tonnes. Compared with the results in Scenario 1, adding the opportunity of procuring CNG vehicles only reduces CO_2 emissions by an additional 5.4 metric tonnes. At the end of the planning horizon, 2 new CNG and 30 battery-electric vehicles are procured in total, and 26 depot chargers are installed. Because the fleet procurement decisions differ by 1 battery-electric and 2 CNG vehicles, the results and trend in this scenario are similar to Scenario 1.

Figure 54 shows the annual cost profiles, operations by fuel type, and fleet compositions. Annual procurement cost of battery-electric vehicles and chargers ranges from $4.6 to $5.1 million USD. With more battery-electric vehicles procured, the percentage of annual miles traveled from electric vehicle fleets increases from 3.6% in Year 1 to 19.8% in Year 5, energy use increases from 0.9% to 5.8%, and CO_2 emissions increases from 1.7% to 10.5%. Fleet size increases from 125 in Year 0 (initial fleet) to 152 in Year 5. Five diesel vehicles with Model Year 2018 are salvaged, and 32 vehicles are procured. The trend results from the same three reasons outlined for Scenario 1: 1) increased peak demand due to dwelling for depot-charging; 2) the salvage sequence design limit; and 3) large depot capacity setting and trivial economic benefits from salvaging vehicles.

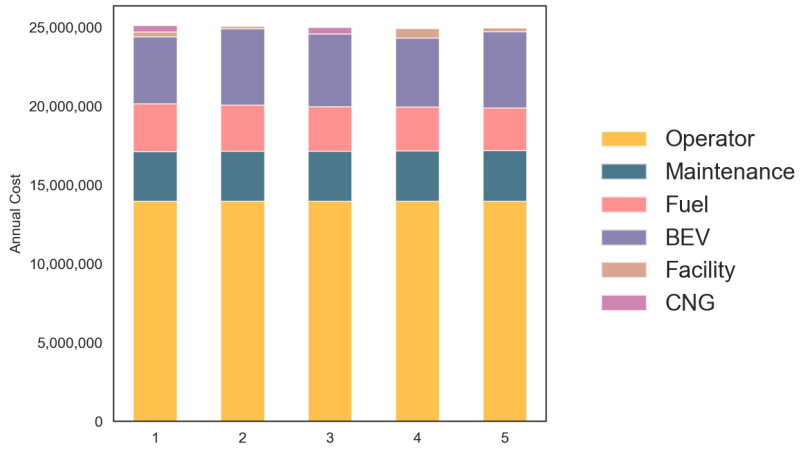

(a) Cost Components by Year

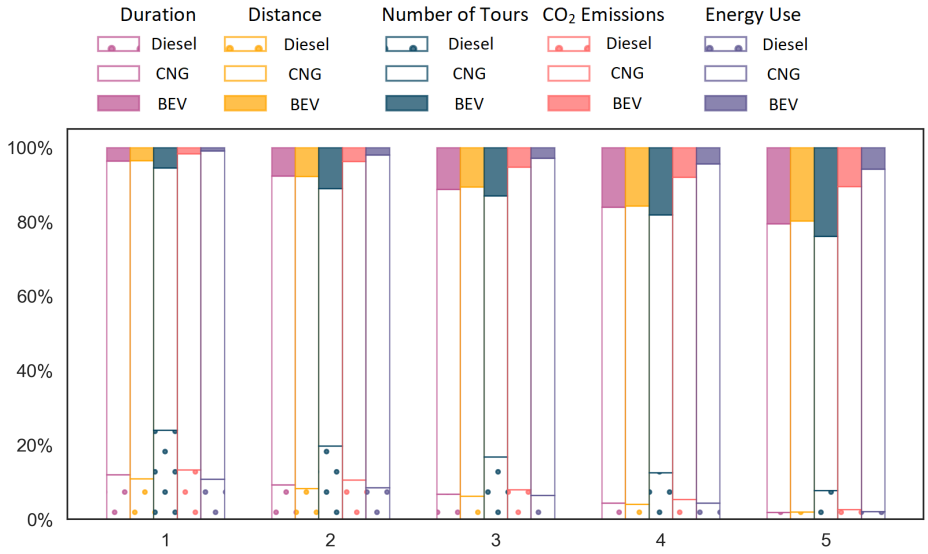

(b) Operations Percentages by Fuel Type, Year

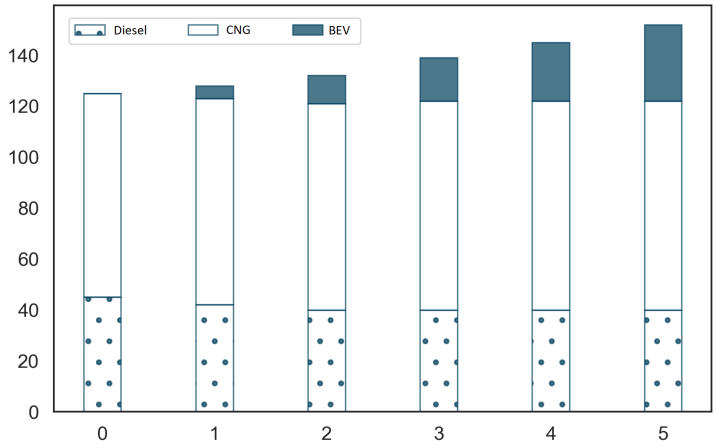

(c) Fleet Composition by Fuel Type, Year

Figure 54 – Results: Fleet Conversion with Salvage Model, Scenario 3

7.4 Summary

In this chapter, two new fleet conversion models extend the models previously presented in Chapter 6 to multi-year planning. Models optimize fleet procurement decisions across battery-electric vehicles and other alternative fuel vehicles. Each model is formulated and implemented for MARTA's existing local transit service.

It is worthwhile to evaluate the available charging options and different vehicle types. The case studies in Section 7.2.3.2 show that under the same annual budget limit, in five years, adopting depot-charged electric vehicles can reduce life-cycle CO_2 emissions by 4.1%. The emissions reduction can be extended to 5.1% if on-route charging option is also available, and can be extended to 7.6% if both CNG and depot-charged electric vehicles are both available. The case studies in Section 7.2.3.2 and 7.3.3.2 also show the advantage of long-term plan compared with one-time plan through allocating the limited budget "smartly". The fleet may wait and procure electric vehicles in later years when the vehicle procurement cost drops, and invest in facility when the fleet cannot afford to procure vehicles.

In addition to the contributions and limitations previously discussed in Section 6.5, the main contributions of the proposed models (fleet conversion without salvage and fleet conversion with salvage) are:

1) Vehicle procurement and salvage decisions are generated annually, which is closer to reality and easy for transit agencies to follow. While satisfying the constraints of annual budget, revenue service demand, charging facility and depot

capacity, the fleet turnover decisions can help agencies to achieve the optimal environmental performance.

2) The proposed models incorporate the trade-offs of high capital cost but low life-cycle CO_2 emissions for new electric vehicle fleets and non-electric vehicle fleets.
3) The proposed models support long term agency planning by allocating the limited funding among facility construction, vehicle procurement and maintenance, utility, and other cost components.
4) Decisions are made jointly among vehicle procurement and salvage, charging facility construction, and vehicle operations per year.
5) Transit agencies have the flexibility of specify their own inputs and remove/add constraints based on their own needs. The proposed models support sensitivity analysis on both constraints and cost parameter settings.

The limitations of the models presented in this chapter that can be addressed in future work include:

1) The models require detailed inputs for each cost components from transit agencies to generate solid results.
2) Life-spans for charging facilities are not currently included.
3) Alternative grant formulations for vehicle procurement and battery leasing are not currently included.
4) [We ignore the battery degradation as vehicle age. Battery capacity fades as more charging events occur, and some may even need to be replaced after several years.

5) We assume the ridership demand and revenue schedules remain the same over the planning horizon. In fact, the changes of ridership and revenue schedules closely relate to the decisions in terms of vehicle energy use and fleet procurement.]

CHAPTER 8. CONCLUSIONS

This study develops an analytical framework for optimizing public transit bus fleet conversion to alternative fuels, which will help agencies make sustainable transportation decisions. The alternative fuel options include CNG, hybrid-electric, and battery-electric vehicles. The framework allows transit agencies to develop reasonable estimations of changes in fuel use, operating cost, and life-cycle CO_2 emissions based on fleet-specific features, route characteristics, vehicle constraints, and on-road operating conditions. Agencies can then develop the most economically-efficient and energy-efficient plans to manage fleet turnover, vehicle-route assignment, vehicle-depot assignment, charger station/depot location selection, and charge scheduling. All these decisions can be generated simultaneously by applying the models developed in the framework.

One energy use prediction model is developed, to evaluate the fleet-wide energy use with mixed vehicle fuel technologies. Three sets of optimization models are formulated: 1) one set for operation optimization of existing mixed fuel fleets, 2) one set for fleet electrification, and 3) one set for long-term fleet conversion under budget constraints. All three modeling systems are designed to maximize the fuel-saving and emissions reduction benefits from alternative fuel fleets, while at the same time, satisfying fleet-specific constraints, such as budget, vehicle range limits, and depot capacity. Case studies are conducted by applying the models to the local transit service in Atlanta, Georgia.

8.1 Main Findings

The transit bus operation has trade-offs among life-cycle CO_2 emissions, monetary cost, and energy use. The case study results in Chapter 5 show that reductions among the three cost metrics are not concurrent when minimizing one cost metric than the other. This is consistent with the previous study by Ercan, et al. (*2015*), in which three standard operating cycles are used individually to represent the fleet-wide operations and four different cost metrics are used in the objective function. In this study, vehicles are specifically assigned to tours and trips, which provide a more accurate assessment of the cost reductions achieved through operating mixed fleet with alternative fuels.

The electrification cost model shows the advantages of joint decision making. Charging facility cost can be greatly reduced by the proposed models, through coordinating facility location selection, battery choice, and vehicle schedules. The results of the example case, described in Section 6.2.4.2, show that the system only requires 10 depot chargers to operate the 13 battery-electric buses in the depot-charging-only model. In the depot & on-route charging model, the system requires 6 depot chargers and 1 on-route charging station with 2 chargers to operate the 7 battery-electric buses. Across all the 53 sub-networks in Section 6.2.4.3, in the depot-charging-only model, the ratio of vehicle-to-charger ranges from 1 to 3, with an average of 1.7. However, charging facility is always oversized in previous fleet conversion optimization studies. Some assume equal number of vehicles and depot-chargers to ensure all vehicles can be charged overnight (*Ke, et al., 2016*). Some assume that all route termini have charging facility in place (*Li, et al., 2018a*).

The fleet conversion model shows the advantage of developing a long-term funding allocation plan among vehicle procurement and facility construction. The case study results in Chapter 7 show that it can be more cost-effective to construct charging facility first under limited annual budget, and not buy battery-electric vehicles until the procurement cost drops to a sweet spot.

8.2 Contributions

The Energy Use Prediction Model can reasonably assess fleet-wide energy use in a multi-depot transit network with mixed vehicle fuel technologies. It is impossible for transit agencies to collect the real-world energy consumption data of all vehicles among all bus routes, especially when the new vehicle technologies in place. Although energy use can be simulated based on vehicle specifications and operating cycles, it is too time-consuming to simulate every single trip, and is infeasible when simulation software and cycles are not available. However, the proposed prediction models enable transit agencies to conveniently estimate the fleet-wide energy use with reasonable accuracy. The major original modeling contributions include:

1) The explicit integration of energy use for both revenue and deadheading operations.
2) The incorporation of all main factors affecting vehicle fuel efficiency and performance as model features (roadways, vehicles, operations, and routes), which have not all been implemented at the same time in previous modeling work in the literature.

3) The implementation of model features that are very easy for agencies to collect or simulate.

The Mixed Fuel Fleet Optimization Model developed for this dissertation can help agencies achieve significant energy, emissions, and/or monetary cost savings over the short term by better managing the existing fleet. The primary contributions of this model include:

1) The fleet-wide energy use is assessed thoroughly by including revenue service, depot pull-in/pull-out, and interlining trips and by different service day types. In previous studies, energy use from deadheading operations are mostly omitted. Also, the differences across different service days are generally not explicitly modeled in the literature.
2) Operating costs are minimized by various model elements, including depot re-assignment, bus-to-tour assignment, and tour design.
3) The use of discretizing time to slots (in this and the more complex models that follow) enables the modeling of buses that serve multiple tours during the day, whereas previous studies assign buses to tours on a one-to-one basis.
4) Coupling the energy use difference of different fuel types with the time-space network makes it feasible to evaluate the potentials of re-chaining revenue trips into tours to maximize the fuel-saving benefits.
5) Three cost metrics, i.e. life-cycle CO_2 emissions, energy use, and monetary cost, are proposed. Decision-makers can compare the trade-offs among different objectives.

The Fleet Electrification Model can help agencies estimate fleet-wide cost of fleet electrification, and find the most cost-effective routes to electrify. The primary contributions of this model include:

1) Energy use of battery-electric vehicles is much more accurately assessed than in previous literature work. In particular, modal energy use and emissions rates, grade, and weight penalties associated with batteries and passenger load are factored in.
2) The proposed models output joint decisions in terms of fleet procurement, vehicle-to-tour assignment, facility location selection, and charging scheduling. Fleet electrification cost is estimated in detail, including vehicle and facility capital investment, utility, vehicle maintenance, operator labor, etc.
3) Utility cost for electricity is time-dependent, which is more realistic than previous studies because rates are generally low during off-peak periods. Most previous studies assume flat rate of electricity usage throughout the day. The variable electricity rate element allows the model to assess the trade-off between the lower cost from overnight depot-charging and additional deadheading cost.
4) Utility costs associated with demand charging is explicitly modeled, and interacts with charge scheduling and facility charger placement decisions. In previous studies, demand charge rates associated with peak 15-minute peak charging demands are either individually optimized without considering vehicle and facility decisions, or ignored in previous optimization models.
5) In the depot-charging-only model, the additional cost due to depot pull-in/pull-out operations from energy use and driving time are incorporated. Depot chargers

can be shared by buses when capacity is available; whereas, most previous studies have simply assumed one charger per bus.

6) In the on-route charging model, placement of multiple chargers at a single station, which lowers facility cost, and sharing of the chargers by vehicles, can be assessed for practical feasibility.

The Fleet Conversion Model can help agencies make long-term plans for transitioning to alternative fuels, especially with respect to maximizing the practical potential of fleet electrification. To the best of our knowledge, no previous studies jointly optimize fleet conversion with the option of electrified fleets as well as charging facility. The primary contributions of this model include:

1) The models incorporate the trade-offs of high capital cost but low life-cycle CO_2 emissions for new electrified fleets and non-electrified fleets.
2) The proposed models generate optimal long-term plans by allocating the limited funding among facility construction, vehicle procurement and maintenance, utility, and other cost components. Decisions are made jointly among annual vehicle procurement and salvage, charging facility construction, and vehicle operations.
3) Transit agencies have the flexibility of specify their own inputs and remove/add constraints based on their own needs. The proposed models support sensitivity analysis on both constraints and cost parameter settings.

All the proposed models can be readily implemented by local transit agencies, and can be easily customized with the agency's service details, fleet specifications, and on-road

operating characteristics. This study and the resulting models will assist policy-makers and transit planners by: 1) reducing technological uncertainties, 2) supporting operational and fleet management decision-making, 3) finding solutions to overcome fleet operation constraints, and 4) assessing the potential impacts of subsidies and incentives on life-cycle cost for alternative fuel vehicles.

8.3 Limitations and Future Research

Although the energy prediction model can achieve reasonable accuracy, there is still room to improve the model to reflect the real-world practice. First, some other impacting factors are not specifically considered in the model, such as ambient temperature, which will greatly impact the auxiliary loadings and thus fuel efficiency performance. Hanlin (*2016*) shows that the range can be reduce to half in the worst case in winter. Second, energy use is simulated by customizing one typical vehicle model for each fuel technology, and it is worthwhile to examine the variability among different models for the same fuel technology. For conventional vehicles, engine is the key impacting factor of fuel efficiency performance, and the technology has been more mature. For battery-electric and hybrid-electric vehicles, the control strategy manages generating, using, and saving energy, and thus brings the system complexity to a new arena. Different vehicle manufactures design their own competitive control strategies. To better capture this impact, we suggest collecting real-world fuel use data from different vehicle models in order to improve and validate the energy prediction model.

The three sets of optimization models analyze fleet-wide costs from various components, providing the flexibility for agencies to customize with their own

characteristics. In fact, the cost of each component may vary within a range, instead of a fixed value. For example, the unit vehicle maintenance cost varies by each vehicle, depending on its usage history. Also, there are still uncertainties in terms of alternative fuel technologies, which result in the uncertainties of the procurement cost. Therefore, it is necessary to conduct sensitivity analysis about the impact of different cost rates, ranging from the worst case to the best case, to give the agency a clear idea of how the rates will actually impact fleet conversion decisions.

Some additional constraints that can be incorporated to the optimization models to better meet the needs of transit agencies. First, the life-span of charging facility and electrified fleets are not considered, but this can greatly affect vehicle procurement salvage decisions. Since battery-electric vehicle technology is a new and growing field, there are not enough studies with enough longevity to accurately determine the lifespan of an electric bus fleet. However, there are some companies that can estimate the life of the batteries to their electric vehicles. Potkány, et al. (*2018*) conducted a lifetime cost study comparing diesel and electric buses that estimated the minimum lifespan for an electric bus to be 10 years. Some studies show that the course of the bus's life cycle is usually between 12 to 16 years (*U.S. PIRG Education Fund, 2018)*. Second, cost of new vehicle procurement is set as full market price in the optimization models, and it is worthwhile to add the option of reducing cost through subsidies and grants. The survey from NASEM (*2018*) reports that over 60% of the transit agencies use federal or state grants in the process of vehicle procurement. In addition, battery leasing options can also be factored in the models. Vehicle procurement cost accounts for one fifth of the total budget in the implementation results in Section 7.3.3.2, and this portion will differ once grants and subsidies are

incorporated. Third, vehicle-to-route assignment is based on the cost-minimal rule, and it is worthwhile to add some other factors when assigning routes. For example, some agencies may factor in ridership, accessibility and equity among different zones. [Fourth, the tour design model does not include any duration or mileage limits per tour. In fact, the tour duration closely relates to operator shifts, which may have maximum and minimum limits per shift.]

[The framework makes simplifications by ignoring the impacts from the following areas: 1) battery degradation as vehicle age, 2) seasonal impact on air conditioning load, 3) changes of passenger load and revenue schedules in the multi-year plan, 4) budget constraints from different sources, 5) spares of charging facilities, and 6) buffer time of on-route charging. For future studies, these areas can be explicitly tackled to make the framework more applicable to the real-world practice.]

[The framework incorporates 40-ft transit bus with fuel options including diesel, CNG, diesel hybrid electric, and battery electric. The framework does not include 1) articulated buses and vans, and 2) liquefied natural gas, biodiesel, fuel cell, and other alternative fuel types. If applying the framework to these vehicle types, we will need to develop corresponding energy use prediction models and some of the constraints will need to be adjusted. Hence the results and trends may be changed.]

The following projects, designed to further improve the four modeling frameworks, are highly recommended:

1) Expand efforts to collect and analyze real-world operations data with fuel use data to verify and improve the energy prediction model.

2) Conduct field research to assess the potential impact of environmental factors on energy use models, such as quantifying the impacts of ambient temperature and humidity on accessory load and therefore battery energy use.
3) Improving the optimization models by adding additional constraints, such as refined vehicle and charge facility life-spans, the impacts of grants for vehicle procurement and battery leasing options, and agency preferences for route selection (adding a human element to route constraints).
4) Conducting more detailed sensitivity analyses associated with the impact of electricity rates and energy efficiency on fleet-wide operating costs and potential reductions of energy use and emissions.

APPENDIX A.NOTATIONS

Table 37 – Indices

Notation	Meaning
b	Tour ID
f	Vehicle type
f_λ	Vehicle type in salvage sequence λ
i	Sub-tour
$l_{i,j}$	Trip identifier, from time-space node i to j
li	Roadway link identifier
m	Trip sequence ID
mi	Micro-trip identifier
m_b	Maximum trip sequence ID in tour b
o	On-route charging option: o=1 if charging before interlining; o=2 if charger after interlining
p	On-route charging station identifier
pi	Grade points identifier
$P_{b,m,o}$	On-route charging station identifier when the charging event occurs before trip m in tour b, using option o
q	On-route charger type
s	Service day type
ti	Timestamp in a micro-trip
y	Depot identifier
z, z_i	Year identifier
λ, λ_i	Salvage sequence identifier
ρ	Cost metric identifier
t_k	k^{th} time slot
λ	Salvage sequence identifier
$P_{b,m,o}$	Bus stop identifier when the charging event occurs before trip m in tour b, using option o
δ	Cost metric: life-cycle CO_2 emissions
op	Cost metric: operating cost
e	Cost metric: energy use

Table 38 – Decision Variables

Notation	Type and Meaning
$H_{p,q}^{OnRoute}$	Binary variable 1 if type q charger is built at on-route charging station p
$H_{z,\lambda}$	Binary variable 1 if at least one vehicle in sequence λ is salvaged at the start of year z
W_b^f	Binary variable 1 if tour b is served with a type f vehicle
$W_{b,y}$	Binary variable 1 if the vehicle which serves tour b is housed in depot y
$W_{b,y}^f$	Binary variable 1 if tour b is served with a type f vehicle and is housed in depot y
W_b^f	Binary variable 1 if tour b is served by a type f vehicle
$W_{b,z}^f$	Binary variable 1 if tour b is served by a type f vehicle in year z
N_y	Integer variable Number of chargers at depot y
$N_{y,z}$	Integer variable Number of chargers at depot y in year z
$X_{b,m,q,o}^f$	Continuous variable. Charging duration after finishing revenue trip m from block b, using charger type q, option o
$X_{b,m,q,o,z}^f$	Continuous variable. Charging duration after finishing revenue trip m from block b, using charger type q, option o in year z
$V_{b,m,q,o}^f$	Binary variable 1 if charging event occurs after finishing revenue trip m of block b, using charger type q, option o
$V_{b,m,q,o,z}^f$	Binary variable 1 if charging event occurs after finishing revenue trip m of block b, using charger type q, option o in year z
N_p	Binary variable 1 if on-route charging station is built at stop p
$N_{p,z}$	Binary variable 1 if on-route charging station is built at stop p in year z
$N_{p,q}$	Integer variable Number of on-route chargers with type q at stop y
$N_{p,q,z}$	Integer variable Number of on-route chargers with type q at stop y in year z
$H_{p,q}^{OnRoute}$	Binary variable 1 if charger type q is built at station p
G_z^f	Integer variable Number of type f vehicles that are salvaged at the start of year z

Table 39 – Sets, Parameters, and Other Variables

Notation	Type/Unit	Meaning
$A_{1,s,y}$	Set	Revenue trips on service day type s, served by vehicles from depot y
$A_{2,s,y}$	Set	Depot pull-in trips on service day type s from depot y
$A_{3,s,y}$	Set	Depot pull-out on service day type s from depot y
$A_{4,s,y}$	Set	Interlining trips on service day type s, served by vehicles from depot y
Avg_{Grade}	Rad	Average grade of a micro-trip
Avg_{Grade_neg}	Rad	Average negative grade of a micro-trip
Avg_{Grade_pos}	Rad	Average positive grade of a micro-trip
B	Set	All tours in the fleet
B_s	Set	Tours on service day type s
$B_{s,y}$	Set	Tours from depot y on service day type s
$Batt_b$	kWh	Initial energy level in tour b
BIN_{mi}	Set	STP bins in micro-trip mi
C_ρ	kWh/DGE/$	Fleet-wide cost, evaluated with metric ρ
$C^f_{l_{i,j},\rho}$	kWh/DGE/$	Cost of trip $l_{i,j}$ if served with type f vehicle, evaluated with metric ρ
$C^f_{m,\rho}$	kWh/DGE/$	Cost of trip m if served with type f vehicle, evaluated with metric ρ
$C^f_{m,e}$	DGE	Energy use of trip m if served with type f vehicle
$C^f_{m,\alpha}$	$	Energy cost of trip m if served with type f vehicle
$C^f_{m,\beta}$	$	Maintenance cost of trip m if served with type f vehicle
$C^f_{m,\delta}$	kg	Life-cycle CO_2 emissions of trip m if served with type f vehicle
$C^f_{m,op}$	$	Operating cost of trip m if served with type f vehicle
C_e	DGE	Fleet-wide energy use
C_{op}	$	Fleet-wide operating cost
C_δ	kg	Fleet-wide life-cycle CO_2 emissions
C_α	$	Fleet-wide energy cost
$C_{\alpha,s}$	$	Fleet-wide daily cost of electricity on service day type s
$C_{\alpha,s,z}$	$	Fleet-wide daily energy cost on service day type s in year z
$\Delta C_{\alpha,s,z}$	$	Cost difference of fleet-wide daily energy cost on service day type s in year z
C_β	$	Fleet-wide maintenance cost
$C_{\beta,s}$	$	Fleet-wide daily vehicle maintenance cost on service day type s
$C_{\beta,s,z}$	$	Fleet-wide daily vehicle maintenance cost on service day type s in year z
$\Delta C_{\beta,s,z}$	$	Cost difference of fleet-wide daily vehicle maintenance cost on service day type s in year z

Notation	Type/Unit	Meaning
$C_{\gamma,s}$	$	Fleet-wide daily operator cost on service day type s
$C_{\gamma,s,z}$	$	Fleet-wide daily operator cost on service day type s in year z
$\Delta C_{\gamma,s,z}$	$	Cost difference of fleet-wide daily operator cost on service day type s in year z
C_{δ}	kg	Fleet-wide life-cycle CO_2 emissions
$C_{\delta,s}$	kg	Daily life-cycle CO_2 emissions (kg) on service day type s
C_{ϵ}	$	Cost of on-route charger, including investment (with installment) and maintenance costs
$C_{\epsilon,z}$	$	Cost of on-route charger, including investment (with installment) and maintenance costs in year z
C_{θ}	$	Cost of the bus procurement
$C_{\theta,z}$	$	Cost of the bus procurement in year z
C_{μ}	$	Cost of depot charger, including investment and its maintenance costs
$C_{\mu,z}$	$	Cost of depot charger, including investment and its maintenance costs in year z
$C_{v,z}$	$	Value of salvaged vehicles in year z
$C_{\sigma,s}$	$	Daily charging penalty on service day type s
$C_{\sigma,s,z}$	$	Daily charging penalty on service day type s in year z
C_{τ}	$	Cost of on-route charging station, including capital investment (with installment) and maintenance
$C_{\tau,z}$	$	Cost of on-route charging station, including capital investment (with installment) and maintenance in year z
C_{φ}	$	Cost of demand charge
$C_{\varphi,z}$	$	Cost of demand charge in year z
$Ratio_{mi}^{f_{New}}$		Conversion ratio of micro-trip mi for vehicle f_{New}
$D_{b,i}^{f}$	Mile	Distance of a sub-tour (b,i)
D_{m}^{f}	Mile	Distance of trip m if served with a type f vehicle
D_{mi}	Mile	Distance of micro-trip mi
DD_{m}	Set	Deadheading micro-trip indices in trip m
Dur	Second	Duration of a micro-trip
$Dur_{mi,si}$	Second	Duration with STP bin=si in micro-trip mi
E_{b}^{f}	kWh	Energy use of tour b if served by a vehicle with battery capacity f
$E_{b,z}^{f}$	kWh	Energy use of tour b if served by a vehicle with battery capacity f in year z
$E_{b,z}$	kWh	Energy use of tour b if served by a vehicle with battery capacity f in year z
$E_{b,i}^{f}$	kWh	Energy use of sub-tour (b,i) if served with battery capacity f; Energy to be charged at depot after finishing sub-tour (b,i)

Notation	Type/Unit	Meaning
$E^{f}_{b,i,z}$	kWh	Energy use of sub-tour (b,i) if served with battery capacity f; Energy to be charged at depot after finishing sub-tour (b,i) in year z
$E_{b,0}$	kWh	Battery energy level after pulling out of depot in tour b
$E_{b,m}$	kWh	Battery energy level after finishing revenue trip m, before starting the trip $m+1$ in tour b
E_{b,m_b+1}	kWh	Battery energy level after pulling into depot in tour b
E^{f}_{m}	kWh	Energy use of trip m if served with a type f vehicle
$EA^{f_{Base}}_{mi}$	MJ	Energy use of micro-trip mi in the base scenario, modeled from Autonomie®
$EA^{f_{New}}_{mi}$	MJ	Converted energy use of micro-trip mi if served with a type f_{New} vehicle, based on the conversion ratio
$EC1_{b,0}$	kWh	Energy use of depot pull-out in tour b
$EC1_{b,m}$	kWh	Energy use of serving trip m in tour b
$EC1_{b,m_b+1}$	kWh	Energy use of depot pull-in in tour b
$EC2_{b,m}$	kWh	Energy use of serving trip m in tour b
$EM^{f_{Base}}_{mi}$	MJ	Energy use of micro-trip mi if served with the base vehicle, modeled using MOVES-Matrix
$EM^{f_{New}}_{mi}$	MJ	Energy use of micro-trip mi if served with the new vehicle, modeled using MOVES-Matrix
ER^{f}_{mi}	MJ/Mile	Energy rate of micro-trip mi if served with a type f vehicle
$ER^{f_{New}}_{si}$	MJ/Second	MOVES energy rate for vehicle type f_{New}, STP Bin=si
$ER^{f_{Base}}_{si}$	MJ/Second	MOVES energy rate for vehicle type f_{Base}, STP Bin=si
F_1	Set	Set of vehicle types of the baseline fleet
F_2	Set	Set of vehicle types of electrified fleets
F_3	Set	Set of vehicle types of new fleets
F_b	Set	Set of vehicle types that can serve tour b
$F_{l_{i,j}}$	Set	Set of vehicle types that can serve trip $l_{i,j}$
$Freq_s$		Number of days with service day type s in a year
$grade_{ti}$	Rad	Grade value of timestamp ti
I^{f}_{b}	Set	Sub-tour indices in tour b if served by a vehicle with battery capacity f
$l_{i,\cdot}$	Set	Set of trips that starts with time-space node i
$l_{\cdot,i}$	Set	Set of trips that ends with time-space node i
L^{D}_{b}	Set	Set of depot pull-in/pull-out trips in tour b
$L^{D}_{b,y}$	Set	Set of depot pull-in/pull-out trips in tour b if the vehicle is housed in depot y
L^{I}_{b}	Set	Set of interlining trips in tour b
L^{R}_{b}	Set	Set of revenue trips in tour b
$Links$	Set	Set of roadway links of a micro-trip
mph_{ti}	mph	Speed at timestamp ti
Num_{li}		Number of grade points from link li

Notation	Type/Unit	Meaning
SOC_{min}	%	Minimum limit of battery state-of-charge
SOC_{max}	%	Maximum limit of battery state-of-charge
P	Set	On-route charging stations (bus start/ending stops)
Q_p	Set	Charger types available at bus stop p
$Q_{P_{b,m,o}}$	Set	Charger types when the charging event occurs before trip m in tour b, using option o
R_m	Set	Micro-trip indices in revenue trip m
t_{TI_b}	Timestamp	Timestamp of depot pull-in for the bus serving tour b
$t_{TI_{b,i}^f}$	Timestamp	Timestamp of depot pull-in for the bus serving sub-tour (b,i) with battery capacity f
t_{TO_b}	Timestamp	Timestamp of depot pull-out for the bus serving tour b
$t_{TO_{b,i}^f}$	Timestamp	Timestamp of depot pull-out for the bus serving sub-tour (b,i) with battery capacity f
T	Set	All time slots
$T_{b,m,o}$	Set	On-route charging time slots of tour b, trip m, if using charging option o
T_b	Set	In-use time slots of tour b if served with a non-electrified vehicle
T_b^f	Set	In-use time slots of tour b if served with a vehicle with battery capacity f
$T_{b,i}^f$	Set	In-use time slots of sub-tour (b,i) if tour b is served with a vehicle with battery capacity f, used in the depot charging only model
$T_{b,i,z}^f$	Set	In-use time slots of sub-tour (b,i) if tour b is served with a vehicle with battery capacity f in year z, used in the depot charging only model
$T_{b,m,o}$	Set	On-route charging time slots if using option o, for revenue trip m in tour b
$T_{l_{i,j}}$	Set	In-use time slots of trip $l_{i,j}$
TC_b^f	Set	Set of depot charging time slots of tour b, used in the depot and on-route charging model
$TC_{b,i}^f$	Set	Set of depot charging time slots of sub-tour (b,i) if tour b is served with a vehicle with battery capacity f, used in the depot charging only model
$TC_{b,z}^f$	Set	Set of depot charging time slots of tour b, used in the depot and on-route charging model in year z
$TC_{b,i,z}^f$	Set	Set of depot charging time slots of sub-tour (b,i) if tour b is served with a vehicle with battery capacity f in year z, used in the depot charging only model
TD_b^f	Hour	Duration that the bus with battery capacity f stays at depot
$TD_{b,i}^f$	Hour	Duration that the bus with battery capacity f stays at depot after finishing sub-tour (b,i), used in the depot charging only model

Notation	Type/Unit	Meaning
$TE_{b,m}$	Timestamp	Timestamp when the trip m in tour b end
TI_b	Timestamp	Timestamp of depot pull-in for the bus serving tour b
$TI_{b,m,m+1}$	Hour	Duration of driving from the ending stop of trip m to the starting stop of trip $m+1$ in tour b
$TI_{b,i}^{f}$	Timestamp	Timestamp of depot pull-in for the bus serving sub-tour (b,i) with battery capacity f
TO_b	Timestamp	Timestamp of depot pull-out for the bus serving tour b
$TO_{b,i}^{f}$	Timestamp	Timestamp of depot pull-out for the bus serving sub-tour (b,i) with battery capacity f
TR_1	Hour	Maximum on-route charging duration of pre-revenue trips
TR_2	Hour	Maximum on-route charging duration of post-revenue trips
$TS_{b,m+1}$	Timestamp	Timestamp when the trip $m+1$ in tour b starts
S	Set	All service day types
U_{Depot}	kW	Power of depot plug-in charger
U_{Peak}	kW	Peak charging demand
$U_{Peak,z}$	kW	Peak charging demand in year z
U_q	kW	Power of type q on-route charger
Y	Set	All depots
α^f	\$/DGE	Energy cost rate of a type f vehicle
α_z^f	\$/DGE	Energy cost rate of a type f vehicle in year z
β^f	\$/Mile	Vehicle maintenance cost rate of vehicle type f
β_z^f	\$/Mile	Vehicle maintenance cost rate of vehicle type f in year z
γ^f	\$/Hour	Operator salary rate if driving a type f vehicle
γ_z^f	\$/Hour	Operator salary rate if driving a type f vehicle in year z
δ^f	kg/DGE	Life-cycle CO_2 emission rate of vehicle type f
δ_z^f	kg/DGE	Life-cycle CO_2 emission rate of vehicle type f in year z
δ_{CC}^{f}	kg/MJ	Carbon content of fuel from a type f vehicle
δ_{FP}^{f}	kg/MJ	CO_2 upstream emission rates per 1 MJ of fuel production, using fuel from a type f vehicle
δ_{OF}^{f}		Oxidation fraction of fuel from a type f vehicle
$\delta_{Upstream}^{f}$	kg/DGE	Upstream CO_2 emission rate of a type f vehicle
δ_{Onroad}^{f}	kg/DGE	On-road CO_2 emission rate of a type f vehicle
$\varepsilon_{kWh2Gal}$		Unit conversion factor from kWh to DGE
ε_{kWh2MJ}		Unit conversion factor from kWh to MJ
ε_{MJ2kWh}		Unit conversion factor from MJ kWh
$\epsilon 1_q$	\$	Cost of building a type q on-route charger, including capital investment and installment
$\epsilon 2_q$	\$	Maintenance cost of an type q on-route charger
$\eta 1$	%	Vehicle pare ratio

Notation	Type/Unit	Meaning
2	%	Depot charger spare ratio
θ^f	\$	Vehicle procurement cost with type f
θ_z^f	\$	Vehicle procurement cost with type f in year z
$\mu 1_y$	\$	Investment cost rate of charger at depot y
$\mu 1_{y,z}$	\$	Investment cost rate of charger at depot y in year z
$\mu 2_y$	\$	Maintenance cost rate of charger at depot y
$\mu 2_{y,z}$	\$	Maintenance cost rate of charger at depot y in year z
υ_z^f	\$	Salvage value of type f vehicle in year z
$\pi_{TC_{b,i}}$	\$/kWh	Electricity cost rate when charging the vehicle after sub-tour (b,i) at depot, used in the depot charging only model
$\pi_{TC_{b,i',z}^f}$	\$/kWh	Electricity cost rate when charging the vehicle after sub-tour (b,i), if served with a vehicle with battery capacity f at depot in year z, used in the depot charging only model
π_{TC_b}	\$/kWh	Electricity cost rate when charging the vehicle after tour b at depot, used in the depot and on-route charging model
$\pi_{TC_{b,z}}$	\$/kWh	Electricity cost rate when charging the vehicle after tour b at depot in year z, used in the depot and on-route charging model
$\pi_{T_{b,m,o}}$	\$/kWh	Electricity cost rate when on-route charging the vehicle after finishing trip m of tour b using option o, used in the depot and on-route charging model
$\pi_{T_{b,m,o},z}$	\$/kWh	Electricity cost rate when on-route charging the vehicle after finishing trip m of tour b using option o in year z, used in the depot and on-route charging model
σ_s	\$	On-route charging penalty rate on service day s
$\sigma_{s,z}$	\$	On-route charging penalty rate on service day s in year z
$\tau 1_p$	\$	Cost of building an on-route charging station at stop p, including capital investment and installment
$\tau 1_{p,z}$	\$	Cost of building an on-route charging station at stop p, including capital investment and installment in year z
$\tau 2_p$	\$	Cost of maintenance of an on-route charging station at stop p
$\tau 2_{p,z}$	\$	Cost of maintenance of an on-route charging station at stop p in year z
κ		Number of years in the planning horizon
φ	\$/kWh	Demand charge cost rate
χ		Maximum total number of vehicles
χ^f		Maximum number of vehicles of type f in the fleet
χ_y		Maximum number of vehicles housed in depot y

Notation	Type/Unit	Meaning
χ_y^f		Maximum number of vehicles of type f housed in depot y
χ_y^{Depot}		Maximum number of chargers at depot y
$\chi_{p,q}^{OnRoute}$		Maximum number of on-route type q chargers at stop p
ψ_y^{Depot}	kW	Power limit of depot charging at depot y
$\psi_p^{OnRoute}$	kW	Power limit of on-route charging at stop p
φ	\$/kW	Monthly demand charge rate
φ_z	\$/kW	Monthly demand charge rate in year z
ϖt_k	Hour	Demand interval, the duration used for calculating demand charge amount
ω	\$	Budget limit
ω_z	\$	Budget limit in year z
ϕ_{λ_i}		Number of vehicles in salvage sequence λ_i

APPENDIX B. MOVES

The VSP/STP equation:

$$VSP_t\ (STP_t)\ = \left(\frac{A}{M}\right) v_t + \left(\frac{B}{M}\right) {v_t}^2 + \left(\frac{C}{M}\right) {v_t}^3 + \left(\frac{m}{M}\right)(a_t + g * sin\,\theta_t) v_t \qquad (187)$$

Where:

v_t = velocity at time t (m/sec)

a_t = acceleration at time t (m/sec^2)

θ_t = road grade

g = graviational acceleration (9.81 m/sec^2)

m = vehicle mass (tonnes)

M = fixed mass factor for the source type (tonnes)

A = rolling resistance ($kW - sec/m$)

B = rotating resistance ($kW - sec^2/m^2$)

C = aeodynamic drag ($kW - sec^3/m^3$)

M in VSP = fixed mass factor (tonnes), used for light duty vehicles

M in STP = scaling factor from payload (tonnes), used for heavy duty vehicles.

Table 40 – MOVES VSP/STP Operating Mode Bins

Operating Mode ID	Operating Mode Description	VSP/STP (VSP_t, kW/tonne)	Speed (v_t, mph)	Acceleration (a, mph/sec)
0	Deceleration/Braking			$a_t \le -2.0$ or ($a_t < -1$ & $a_{t-1} < -1$ & $a_{t-2} < -1$)
1	Idle		$-1 \le v_t < 1$	Any
11	Coast	$VSP_t < 0$	$0 \le v_t < 25$	Any
12	Cruise/Acceleration	$0 \le VSP_t < 3$	$0 \le v_t < 25$	Any
13	Cruise/Acceleration	$3 \le VSP_t < 6$	$0 \le v_t < 25$	Any
14	Cruise/Acceleration	$6 \le VSP_t < 9$	$0 \le v_t < 25$	Any
15	Cruise/Acceleration	$9 \le VSP_t < 12$	$0 \le v_t < 25$	Any
16	Cruise/Acceleration	$12 \le VSP_t$	$0 \le v_t < 25$	Any
21	Coast	$VSP_t < 0$	$25 \le v_t < 50$	Any
22	Cruise/Acceleration	$0 \le VSP_t < 3$	$25 \le v_t < 50$	Any
23	Cruise/Acceleration	$3 \le VSP_t < 6$	$25 \le v_t < 50$	Any
24	Cruise/Acceleration	$6 \le VSP_t < 9$	$25 \le v_t < 50$	Any
25	Cruise/Acceleration	$9 \le VSP_t < 12$	$25 \le v_t < 50$	Any
27	Cruise/Acceleration	$12 \le VSP_t < 18$	$25 \le v_t < 50$	Any
28	Cruise/Acceleration	$18 \le VSP_t < 24$	$25 \le v_t < 50$	Any
29	Cruise/Acceleration	$24 \le VSP_t < 30$	$25 \le v_t < 50$	Any
30	Cruise/Acceleration	$30 \le VSP_t$	$25 \le v_t < 50$	Any
33	Cruise/Acceleration	$VSP_t < 6$	$50 \le v_t$	Any
35	Cruise/Acceleration	$6 \le VSP_t < 12$	$50 \le v_t$	Any
37	Cruise/Acceleration	$12 \le VSP_t < 18$	$50 \le v_t$	Any
38	Cruise/Acceleration	$18 \le VSP_t < 24$	$50 \le v_t$	Any
39	Cruise/Acceleration	$24 \le VSP_t < 30$	$50 \le v_t$	Any
40	Cruise/Acceleration	$30 \le VSP_t$	$50 \le v_t$	Any

APPENDIX C.UPSTREAM EMISSIONS

Table 41 – CO_2 Upstream Emissions (UEM, in grams) Per 1 MJ of Fuel Production

Year	Diesel[1]	CNG[1]	Electricity[1]
2019	13.6	9.27	130
2020	13.6	9.27	130
2021	13.6	9.27	130
2022	13.6	9.27	130
2023	13.6	9.27	130
2024	13.6	9.27	130
2025	13.4	8.97	110
2026	13.4	8.97	110
2027	13.4	8.97	110
2028	13.4	8.97	110
2029	13.4	8.97	110
2030	13.24	8.78	110
2031	13.24	8.78	110

[1]Default from North America (GREET)

APPENDIX D.FLEET ELECTRIFICATION RESULTS

Table 42 – Sub-network Information

No.	Number Counts			Annual Distance (1000's of Miles)	Revenue Route ID
	Revenue Routes	Start/Ending Stops	Tours		
1	1	2	365	77	823
2	1	2	625	116	162
3	1	1	625	109	800
4	1	2	730	117	899
5	1	1	730	175	832
6	1	3	730	191	4
7	1	2	730	183	172
8	1	3	730	246	195
9	1	2	1,095	245	93
10	1	2	1,095	274	42
11	1	3	1,095	236	50
12	1	2	1,095	168	27
13	1	2	1,095	317	194
14	1	2	1,250	208	74
15	1	2	1,460	424	66
16	1	2	1,460	308	26
17	1	2	1,510	513	180
18	1	2	1,615	222	809
19	1	2	1,615	230	816
20	1	2	1,615	340	32
21	1	3	1,980	343	68
22	1	2	1,980	321	95
23	1	2	2,500	376	49
24	1	2	2,605	502	83
25	1	2	2,605	412	110
26	1	4	2,655	299	6
27	1	2	2,975	504	39
28	1	3	3,020	471	55
29	1	3	3,020	648	196
30	1	2	3,385	593	71
31	1	4	3,540	412	12
32	1	2	4,580	631	117
33	1	2	4,640	1,071	201

No.	Number Counts			Annual Distance (1000's of Miles)	Revenue Route ID
	Revenue Routes	Start/Ending Stops	Tours		
34	2	3	1,460	200	25, 104
35	2	4	1,460	333	60, 153
36	2	6	1,460	371	856, 867
37	2	4	1,460	356	865, 850
38	2	3	1,825	394	1, 94
39	2	3	1,825	287	2, 102
40	2	3	1,825	354	14, 37
41	2	3	1,825	375	853, 813
42	2	4	2,190	549	81, 155
43	2	3	2,190	411	58, 40
44	2	4	2,710	574	9, 24
45	2	4	3,020	390	19, 103
46	3	7	6,930	1,367	15, 36, 107
47	3	6	7,760	1,624	82, 89, 189
48	4	7	6,720	1,607	78, 178, 191, 193
49	4	7	7,765	1,458	3, 51, 73, 165
50	5	8	7,395	1,438	79, 84, 181, 183, 192
51	6	10	9,170	1,043	30, 47, 124, 126, 132, 133
52	8	9	18,650	3,317	5, 85, 87, 140, 141, 143, 150, 185
53	15	21	31,245	5,363	8, 21, 34, 75, 86, 111, 114, 115, 116, 119, 120, 121, 123, 125, 186

Table 43 – Cost and Energy Use: Electrification Cost Model

No.	Depot-Charging Only		Depot and On-route Charging		Difference	
	Total Cost (Millions of USD)	Energy Use (1,000's of kWh)	Total Cost (Millions of USD)	Energy Use (1,000's of kWh)	Total Cost (Millions of USD)	Energy Use (1,000's of kWh)
1	2.50	211	2.20	192	0.29	19
2	3.54	385	3.10	299	0.44	86
3	3.33	427	2.87	239	0.46	188
4	3.64	384	3.08	302	0.55	82
5	3.95	529	3.24	431	0.72	98
6	4.36	577	3.77	460	0.59	117
7	3.76	577	3.14	451	0.61	127
8	4.68	730	3.26	563	1.42	168
9	5.50	765	4.08	612	1.42	153
10	5.66	880	4.24	683	1.43	197
11	5.48	696	4.30	601	1.18	95
12	5.63	526	4.03	449	1.60	77
13	5.55	993	4.23	762	1.32	231
14	4.61	600	3.91	498	0.70	102
15	8.37	1,323	5.18	1,055	3.18	268
16	7.11	860	5.00	736	2.11	123
17	9.08	1,519	5.66	1,236	3.41	283
18	6.26	696	4.87	569	1.39	126
19	6.26	698	4.81	595	1.44	103
20	7.50	1,062	5.02	873	2.49	188
21	7.88	978	5.88	840	2.00	138
22	8.14	940	5.76	845	2.38	96
23	8.96	1,174	6.53	935	2.43	239
24	11.53	1,775	7.46	1,288	4.07	487
25	12.51	1,261	8.32	1,072	4.19	189
26	7.87	885	6.47	742	1.40	143
27	12.69	1,876	9.05	1,351	3.64	524
28	9.73	1,331	7.52	1,153	2.22	178
29	18.88	2,800	9.20	1,724	9.68	1,076
30	11.94	1,756	8.34	1,477	3.60	279
31	10.59	1,202	8.34	1,058	2.25	144
32	14.95	1,711	11.90	1,581	3.05	130
33	22.46	3,040	13.30	2,406	9.16	634
34	5.25	644	4.55	478	0.70	166
35	7.53	969	5.18	824	2.35	145
36	7.37	1,119	5.06	895	2.31	224

No.	Depot-Charging Only		Depot and On-route Charging		Difference	
	Total Cost (Millions of USD)	Energy Use (1,000's of kWh)	Total Cost (Millions of USD)	Energy Use (1,000's of kWh)	Total Cost (Millions of USD)	Energy Use (1,000's of kWh)
37	7.22	1,070	5.06	854	2.16	216
38	9.08	1,109	6.12	981	2.96	128
39	8.95	821	5.94	719	3.01	101
40	9.09	1,020	5.98	877	3.11	142
41	9.08	1,107	5.93	943	3.14	165
42	11.94	1,887	7.59	1,414	4.35	473
43	11.03	1,248	7.07	1,079	3.96	169
44	11.82	1,719	8.49	1,410	3.33	309
45	9.55	1,232	7.75	977	1.81	254
46	28.87	4,041	20.93	3,429	7.94	612
47	30.43	4,814	21.42	3,991	9.00	823
48	29.29	4,597	20.81	3,828	8.48	769
49	29.86	4,300	20.63	3,575	9.23	725
50	29.19	4,433	21.29	3,581	7.90	852
51	24.11	3,362	23.08	2,664	1.02	699
52	96.41	16,918	44.69	9,296	51.72	7,622
53	103.97	15,220	78.13	13,328	25.83	1,892

Table 44 – Number of Vehicle and Chargers: Electrification Cost Model

No.	Depot-Charging Only				Depot and On-route Charging							
	Depot Chargers	Buses (kWh)			Depot Chargers	On-route Charging			Buses (kWh)			
						Stations	Chargers (kW)					
		200	300	400			200	300	100	150	200	300
1	1	3	0	0	1	1	1	0	1	1	0	0
2	2	2	2	0	1	1	1	0	3	0	0	0
3	2	4	0	0	1	1	1	0	3	0	0	0
4	3	2	2	0	2	1	1	0	3	0	0	0
5	4	0	2	2	2	1	1	0	3	0	0	0
6	3	5	0	0	2	2	2	0	3	0	0	0
7	4	2	2	0	2	1	1	0	3	0	0	0
8	3	1	2	2	2	1	0	1	1	2	0	0
9	5	4	2	0	3	1	1	0	4	0	0	0
10	4	2	2	2	3	1	0	1	4	0	0	0
11	5	4	2	0	3	1	0	1	1	2	1	0
12	5	2	2	2	3	1	1	0	4	0	0	0
13	4	4	0	2	3	1	0	1	1	2	1	0
14	3	3	0	2	2	1	1	0	4	0	0	0
15	6	1	8	0	4	1	0	1	2	3	0	0
16	4	6	2	0	3	1	0	1	5	0	0	0
17	6	1	9	0	3	2	1	2	1	4	0	0
18	3	5	0	2	3	1	1	1	5	0	0	0
19	3	4	2	1	3	1	1	0	5	0	0	0
20	5	0	6	2	3	1	1	1	2	3	0	0
21	4	7	2	0	4	1	0	1	6	0	0	0
22	5	6	0	3	4	1	1	0	6	0	0	0
23	7	7	3	0	4	1	2	0	7	0	0	0
24	7	10	3	0	3	1	2	0	8	0	0	0
25	7	8	4	2	5	1	2	0	9	0	0	0
26	5	7	2	0	3	1	2	0	6	1	0	0
27	9	10	2	2	4	1	2	0	9	1	0	0
28	7	10	0	1	4	1	1	1	3	4	1	0
29	12	1	3	16	4	2	0	2	2	4	2	1
30	8	6	5	2	4	1	3	0	9	0	0	0
31	7	10	0	2	4	1	0	1	6	0	2	1
32	11	11	5	1	5	2	2	2	10	3	0	0
33	15	23	0	3	4	1	2	3	8	7	0	0
34	3	3	3	0	2	1	1	0	5	0	0	0
35	7	4	2	2	4	1	0	1	5	0	0	0
36	6	6	0	2	4	1	0	1	5	0	0	0

No.	Depot-Charging Only				Depot and On-route Charging							
	Depot Chargers	Buses (kWh)			Depot Chargers	On-route Charging			Buses (kWh)			
						Stations	Chargers (kW)					
		200	300	400			200	300	100	150	200	300
37	5	6	2	0	4	1	0	1	5	0	0	0
38	5	6	2	2	5	1	0	1	1	5	0	0
39	7	8	2	0	5	1	1	0	6	0	0	0
40	6	6	2	2	4	1	2	0	6	0	0	0
41	5	6	2	2	4	1	2	0	6	0	0	0
42	10	9	2	2	6	1	1	1	4	0	0	3
43	7	6	2	4	5	1	0	1	1	6	0	0
44	7	8	3	2	6	2	0	2	5	3	0	0
45	6	9	2	0	3	2	1	1	7	1	0	0
46	16	19	11	2	11	4	1	4	13	8	0	0
47	22	15	10	8	10	3	0	4	12	4	3	3
48	18	18	6	8	11	5	5	3	16	2	1	1
49	16	21	10	2	9	2	3	2	18	3	1	0
50	19	16	11	5	10	5	3	3	13	6	1	1
51	14	17	6	4	9	4	6	1	18	2	2	3
52	71[1]	14	8	80	19	5	9	5	7	27	8	5
53	61[1]	46	41	26	40	10	15	8	55	23	3	2

[1] The demand of depot chargers exceeds the depot capacity, and thus re-reset the depot charger capacity to 80 to find the feasible solution.

Table 45 – Cost Profile: Depot-Charging Only

No.	Vehicle Purchase	Vehicle Maintenance	Operator	Depot Charger[1]	Electricity	Demand Charge
1	2,250,000	26,519	150,425	50,150	8,665	9,600
2	3,100,000	44,426	255,758	100,300	21,833	19,200
3	3,000,000	53,079	136,365	100,300	22,998	19,200
4	3,100,000	46,785	295,544	150,450	17,000	28,800
5	3,300,000	64,904	324,722	200,600	23,248	38,400
6	3,750,000	74,476	330,265	150,450	25,082	28,800
7	3,100,000	69,965	323,721	200,600	25,048	38,400
8	4,050,000	93,372	320,700	150,450	31,926	28,800
9	4,600,000	92,093	475,935	250,750	37,134	48,000
10	4,800,000	104,079	480,776	200,600	39,165	38,400
11	4,600,000	85,119	464,157	250,750	31,847	48,000
12	4,800,000	60,309	448,841	250,750	24,652	48,000
13	4,700,000	122,367	439,885	200,600	46,691	38,400
14	3,950,000	76,934	377,385	150,450	28,684	28,800
15	7,150,000	160,228	639,764	300,900	58,787	57,600
16	6,100,000	108,688	626,988	200,600	39,170	38,400
17	7,950,000	191,449	502,367	300,900	73,893	57,600
18	5,450,000	84,675	511,188	150,450	31,389	28,800
19	5,450,000	83,719	511,894	150,450	30,300	28,800
20	6,500,000	130,303	526,509	250,750	47,559	48,000
21	6,850,000	121,947	625,961	200,600	44,329	38,400
22	7,050,000	109,772	638,570	250,750	44,047	48,000
23	7,650,000	140,641	698,965	351,050	55,130	64,000
24	9,900,000	204,342	929,580	351,050	82,557	67,200
25	10,900,000	147,706	987,027	351,050	60,243	67,200
26	6,850,000	110,712	568,429	250,750	43,407	48,000
27	10,800,000	218,625	1,048,339	451,350	88,427	86,400
28	8,350,000	168,984	733,463	351,050	63,210	67,200
29	16,750,000	311,727	957,977	601,800	141,391	115,200
30	10,200,000	215,869	970,699	401,200	79,592	76,800
31	9,200,000	145,242	770,870	351,050	55,316	67,200
32	13,100,000	212,024	900,481	551,650	83,768	105,600
33	19,800,000	399,032	1,223,974	752,250	141,945	144,000
34	4,650,000	81,358	307,212	150,450	29,910	28,800
35	6,300,000	118,348	654,793	351,050	44,603	60,800
36	6,200,000	137,615	617,890	300,900	51,838	57,600
37	6,100,000	131,685	637,920	250,750	47,553	48,000
38	7,800,000	138,231	788,563	250,750	49,766	48,000

No.	Vehicle Purchase	Vehicle Maintenance	Operator	Depot Charger[1]	Electricity	Demand Charge
39	7,600,000	101,748	793,857	351,050	36,027	67,200
40	7,800,000	125,720	760,617	300,900	44,700	57,600
41	7,800,000	133,756	794,241	250,750	49,151	48,000
42	10,050,000	222,010	987,032	501,500	82,565	96,000
43	9,500,000	147,663	912,514	351,050	55,245	67,200
44	10,100,000	217,012	1,006,398	351,050	81,355	67,200
45	8,350,000	147,259	638,389	300,900	60,165	57,600
46	24,750,000	497,163	2,478,594	802,400	193,592	147,200
47	26,050,000	600,334	2,232,304	1,103,300	228,132	211,200
48	25,100,000	581,933	2,321,098	902,700	212,835	172,800
49	25,450,000	529,148	2,734,648	802,400	198,009	147,200
50	25,050,000	539,283	2,257,723	952,850	211,458	176,000
51	20,950,000	402,082	1,757,281	702,100	162,577	134,400
52	84,900,000	1,711,298	4,731,859	3,560,650	830,560	678,400
53	89,400,000	1,882,578	8,306,403	3,059,150	738,946	579,200

[1]includes both initial investment and maintenance of depot chargers

Table 46 – Cost Profile: Depot and On-route Chargers

No.	Vehicle Purchase	Vehicle Maintenance	Operator	Depot Charger[1]	On-route Charger[2]	Electricity	Demand Charge	Charging Events
1	1,425,000	23,795	148,474	50,150	521,200	7,769	24,000	480
2	2,100,000	34,853	254,174	50,150	621,200	13,790	24,000	620
3	2,100,000	32,707	127,311	50,150	521,200	11,673	24,000	474
4	2,100,000	35,196	290,288	100,300	521,200	12,609	24,000	813
5	2,100,000	52,466	319,226	100,300	621,200	18,044	24,000	1,037
6	2,100,000	57,289	325,481	100,300	1,142,400	19,507	24,000	1,079
7	2,100,000	55,038	321,840	100,300	521,200	19,607	24,000	902
8	2,150,000	75,793	317,940	100,300	551,300	24,546	36,000	704
9	2,800,000	73,562	478,184	150,450	521,200	25,867	28,800	1,340
10	2,800,000	82,153	484,635	150,450	651,300	29,467	36,000	1,330
11	2,900,000	73,791	464,496	150,450	651,300	25,828	36,000	730
12	2,800,000	50,408	457,056	150,450	521,200	18,724	28,800	1,058
13	2,900,000	99,248	459,939	150,450	551,300	33,060	36,000	673
14	2,800,000	62,329	372,589	100,300	521,200	22,123	33,600	1,068
15	3,575,000	130,343	644,021	200,600	551,300	43,774	38,400	1,429
16	3,500,000	92,319	638,580	150,450	551,300	31,833	36,000	1,330
17	3,600,000	158,990	499,738	150,450	1,122,800	55,411	72,000	2,021
18	3,500,000	66,639	509,867	150,450	571,500	25,659	44,000	1,033
19	3,500,000	68,985	511,384	150,450	521,200	26,017	33,600	1,215
20	3,575,000	104,451	528,854	150,450	571,500	37,597	48,000	1,178
21	4,200,000	102,829	645,450	200,600	651,300	36,990	45,600	1,330
22	4,200,000	96,321	662,630	200,600	521,200	37,577	38,400	1,829
23	4,900,000	112,749	690,182	200,600	541,400	42,804	40,000	2,044
24	5,600,000	150,613	916,635	150,450	541,400	54,488	48,000	2,486
25	6,300,000	123,554	1,009,953	250,750	541,400	46,897	49,600	2,314
26	4,925,000	90,160	577,815	150,450	641,400	34,239	52,800	1,397
27	7,025,000	151,667	1,025,358	200,600	541,400	57,152	51,200	2,569
28	5,750,000	145,514	750,014	200,600	571,500	53,297	45,600	1,642
29	6,650,000	204,192	882,766	200,600	1,102,600	78,990	76,000	1,980
30	6,300,000	177,925	976,697	200,600	561,600	62,721	60,800	3,168
31	6,550,000	125,769	796,370	200,600	551,300	48,064	64,800	1,392
32	9,175,000	190,769	982,043	250,750	1,143,000	75,299	80,000	2,625
33	10,675,000	325,540	1,143,922	200,600	692,300	106,844	156,000	3,666
34	3,500,000	60,092	303,125	100,300	521,200	21,743	43,200	918
35	3,500,000	99,850	654,735	200,600	651,300	35,490	38,400	1,403
36	3,500,000	111,219	617,164	200,600	551,300	39,639	38,400	1,293
37	3,500,000	106,675	624,009	200,600	551,300	36,792	38,400	1,351
38	4,325,000	121,983	780,063	250,750	551,300	41,372	48,000	1,345

No.	Vehicle Purchase	Vehicle Maintenance	Operator	Depot Charger[1]	On-route Charger[2]	Electricity	Demand Charge	Charging Events
39	4,200,000	85,964	802,820	250,750	521,200	30,597	48,000	1,408
40	4,200,000	106,277	752,395	200,600	641,400	37,026	38,400	1,845
41	4,200,000	112,426	797,536	200,600	541,400	40,190	40,000	2,168
42	5,350,000	176,110	973,560	300,900	671,500	57,251	60,000	2,028
43	5,050,000	127,184	898,614	250,750	651,300	47,472	48,000	1,355
44	5,675,000	174,641	1,002,937	300,900	1,202,600	61,247	72,000	2,163
45	5,625,000	117,522	652,883	150,450	1,072,500	46,081	79,200	1,663
46	14,900,000	415,959	2,534,803	551,650	2,225,400	155,236	144,000	5,123
47	16,100,000	503,152	2,253,197	501,500	1,704,200	180,447	176,800	5,395
48	14,250,000	490,726	2,340,249	551,650	2,856,900	170,864	144,000	6,685
49	15,525,000	440,226	2,758,471	451,350	1,163,200	153,933	132,800	6,947
50	15,050,000	439,954	2,264,147	501,500	2,716,500	162,627	148,000	5,847
51	18,100,000	319,267	1,769,535	451,350	2,175,500	129,598	134,400	4,237
52	34,725,000	1,044,566	4,331,520	952,850	2,938,300	423,441	260,000	12,149
53	59,125,000	1,633,635	8,543,836	2,006,000	5,715,400	617,332	470,400	22,600

[1]includes both initial investment and maintenance of depot chargers

[2]includes both initial investment and maintenance of on-route charging stations and chargers

REFERENCES

AFLEET Website. https://Greet.Es.Anl.Gov/Afleet_Tool. Accessed July 2019.

Atlanta Regional Commission (ARC). ARC Website. Http://Opendata.Atlantaregional.Com/. Accessed July 2019.

Barnitt, R., Chandler, K., 2006. New York City Transit (NYCT) Hybrid (125 Order) and CNG Transit Buses: Final Evaluation Results. Tech. Rep. NREL/TP-540-40125. National Renewable Energy Laboratory, U.S. Department of Energy.

Bellman, R. (1955). Equipment Replacement Policy. Journal of the Society for Industrial and Applied Mathematics, 3(3), 133-136.

Bi, Z., Keoleian, G. A., and Ersal, T. (2018). Wireless Charger Deployment for an Electric Bus Network: A Multi-Objective Life Cycle Optimization. Applied Energy, 225, 1090-1101.

Bi, Z., Song, L., De Kleine, R., Mi, C. C., and Keoleian, G. A. (2015). Plug-In Vs. Wireless Charging: Life Cycle Energy and Greenhouse Gas Emissions for an Electric Bus System. Applied Energy, 146, 11-19.

Bicer, Y., and Dincer, I. (2018). Life Cycle Environmental Impact Assessments and Comparisons of Alternative Fuels for Clean Vehicles. Resources, Conservation and Recycling, 132, 141-157.

Brown, G. G., Goodman, C. E., and Wood, R. K. (1990). Annual Scheduling of Atlantic Fleet Naval Combatants. Operations Research, 38(2), 249-259.

BYD Motors, Inc. (2015). BYD Announces 12 Year Battery Warranty. Http://Www.Mass

Transitmag.Com/Press_Release/12058920/Byd-Announces-12-Year-Battery-Warranty. Accessed July 2019.

Casale, M., and Mahoney, B. (2018). Paying for Electric Buses: Financing Tools for Cities and Agencies to Ditch Diesel.

Ceder, A. (2011). Public-Transport Vehicle Scheduling with Multi Vehicle Type. Transp. Res., Part C, 19 (3), 485−497.

Chandler, K., and Eberts, E. (2006). Washington Metropolitan Area Transit Authority: Compressed Natural Gas Transit Bus Evaluation. Tech. Rep. NREL/TP-540-37626. National Renewable Energy Laboratory, U.S. Department of Energy.

Chandler, K., and Eudy, L. (2008). Alameda-Contra Costa Transit District (AC Transit) Fuel Cell Transit Buses: Third Evaluation Report. Tech. Rep. NREL/TP-560-43545-1. National Renewable Energy Laboratory, U.S. Department of Energy.

Chandler, K., and Eudy, L. (2009a). Connecticut Transit (CTTRANSIT) Fuel Cell Transit Bus: Second Evaluation Report. Tech. Rep. NREL/TP-560-45670-1. National Renewable Energy Laboratory, U.S. Department of Energy.

Chandler, K., and Eudy, L. (2009b). Sunline Transit Agency Fuel Cell Transit Bus: Fourth Evaluation Report. Tech. Rep. NREL/TP-560-44646-1. National Renewable Energy Laboratory, U.S. Department of Energy.

Chen, Z., Yin, Y., and Song, Z. (2018). A Cost-Competitiveness Analysis of Charging Infrastructure for Electric Bus Operations. Transportation Research Part C: Emerging Technologies, 93, 351-366.

Chester, M. V., and Horvath, A. (2009). Environmental Assessment of Passenger Transportation Should Include Infrastructure and Supply Chains. Environmental Research Letters, 4(2), 024008.

Christofa, E., Pollitt, K., Chhan, D., Deliali, A., Gaudreau, J., and El Sayess, R. (2017). Zero-Emission Transit Bus and Refueling Technologies and Deployment Status.

Clark, N. N., Zhen, F., Wayne, W. S., and Lyons, D. W. (2007). Transit Bus Life Cycle Cost and Year 2007 Emissions Estimation (No. FTA-WV-26-7004.2007. 1).

Correa, G., Muñoz, P., Falaguerra, T., and Rodriguez, C. R. (2017). Performance Comparison of Conventional, Hybrid, Hydrogen and Electric Urban Buses Using Well To Wheel Analysis. Energy, 141, 537-549.

CPLEX Optimizer. https://Www.Ibm.Com/Analytics/Cplex-Optimizer. Accessed July 2019.

Daw, C. S., Gao, Z., Smith, D. E., Laclair, T. J., Pihl, J. A., and Edwards, K. D. (2013). Simulated Fuel Economy and Emissions Performance during City and Interstate

Driving for a Heavy-Duty Hybrid Truck. SAE International Journal of Commercial Vehicles, 6(2013-01-1033), 161-182.

Delaware Valley Regional Planning Commission (DVRPC). 2015. Vehicle Technology Analysis for SEPTA Routes 29 and 79. https://Www.Dvrpc.Org/Reports/13028.Pdf. Accessed July 2019.

Delgado, O. and Lutsey, N. (2015). Advanced Tractor-Trailer Efficiency Technology Potential In the 2020-2030 Timeframe. International Council on Clean Transportation, Washington, D.C.

Delgado, O., Miller, J., Sharpe, B., and Muncrief, R. (2016). Estimating the Fuel Efficiency Technology Potential of Heavy-Duty Trucks in Major Markets Around The World. International Council on Clean Transportation, Washington, D.C.

Delgado, O. and Li., H. (2017). Market Analysis and Fuel Efficiency Technology Potential of Heavyduty Vehicles in China. International Council on Clean Transportation, Washington, D.C.

Djiba, C. B., Balde, M., Ndiaye, B. M., Faye, R. M., and Seck, D. (2012). Optimizing Dead Mileage in Urban Bus Routes. Dakar Dem Dikk Case Study. Journal of Transportation Technologies, 2(03), 241.

Durango-Cohen, P. L., and Mckenzie, E. C. (2018). Trading Off Costs, Environmental Impact, and Levels of Service in the Optimal Design of Transit Bus Fleets. Transportation Research Part A: Policy and Practice. (114), 354-363 https://Doi.Org/10.1016/J.Tra.2018.01.030

Ercan, T., Zhao, Y., Tatari, O., and Pazour, J. A. (2015). Optimization of Transit Bus Fleet's Life Cycle Assessment Impacts with Alternative Fuel Options. Energy, 93, 323-334.

Eudy, L., and Jeffers, M. A. (2019). Foothill Transit Agency Battery Electric Bus Progress Report, Data Period Focus: Jul. 2018 through Dec. 2018 (No. NREL/PR-5400-72209). National Renewable Energy Lab. (NREL), Golden, CO (United States).

Eudy, L., and Jeffers, M. A. (2018a). Zero-Emission Bus Evaluation Results: County Connection Battery Electric Buses (No. NREL/TP-5400-72864). National Renewable Energy Lab. (NREL), Golden, CO (United States).

Eudy, L., and Jeffers, M. A. (2018b). Foothill Transit Agency Battery Electric Bus Progress Report, Data Period Focus: Jan. 2018 through Jun. 2018 (No. NREL/PR-5400-72207). National Renewable Energy Lab. (NREL), Golden, CO (United States).

Eudy, L., and Jeffers, M. (2018c). Zero-Emission Bus Evaluation Results: King County Metro Battery Electric Buses (No. FTA Report No. 0118). United States. Federal Transit Administration. Office of Research, Demonstration, and Innovation.

Eudy, L., and Jeffers, M. A. (2017). Foothill Transit Battery Electric Bus Demonstration Results: Second Report. https://Www.Nrel.Gov/Docs/Fy17osti/67698.Pdf. Accessed July 2019.

Eudy, L., Caton, M., and Post, M. (2014). Transit Investments for Greenhouse Gas and Energy Reduction Program: Second Assessment Report (No. FTA Report No. 0064). United States. Federal Transit Administration. Office of Research, Demonstration, and Innovation.

Farahani, R. Z., Miandoabchi, E., Szeto, W. Y., and Rashidi, H. (2013). A Review of Urban Transportation Network Design Problems. European Journal of Operational Research, 229(2), 281-302.

FTA, Federal Transit Administration (2018). Capital Leasing. https://Www.Transit.Dot.Gov/Funding/Funding-Finance-Resources/Capital-Leasing/Capital-Leasing. Accessed July 2019.

FTA, Federal Transit Administration (2016). Bus Testing: Establishment of Performance Standards, a Bus Model Scoring System, and Pass/Fail Standard and Other Program Updates. Available At: https://Www.Gpo.Gov/Fdsys/Pkg/FR-2016-08-01/Pdf/2016- 17889.Pdf. Accessed July 2019.

Feng, W., and Figliozzi, M. A. (2012). Bus Fleet Type and Age Replacement Optimization: A Case Study Utilizing King County Metro Fleet Data.

Fusco, G., Alessandrini, A., Colombaroni, C., and Valentini, M. P. (2013). A Model for Transit Design with Choice of Electric Charging System. Procedia-Social and Behavioral Sciences, 87, 234-249.

Gao, Z., Laclair, T., Ou, S., Huff, S., Wu, G., Hao, P., Boriboonsomsin, K., and Barth, M. (2019). Evaluation of Electric Vehicle Component Performance over Eco-Driving Cycles. Energy, 172, 823-839.

Gao, Z., Lin, Z., Laclair, T. J., Liu, C., Li, J. M., Birky, A. K., and Ward, J. (2017). Battery Capacity and Recharging Needs for Electric Buses in City Transit Service. Energy, 122, 588-600.

Gao, H. O., and Stasko, T. H. (2009). Cost-Minimizing Retrofit/Replacement Strategies for Diesel Emissions Reduction. Transportation Research Part D: Transport and Environment, 14(2), 111-119.

Georgia Power (2019). Electric Transportation Service Schedule: "ET-15". https://Www.Georgiapower.Com/Content/Dam/Georgia-Power/Pdfs/Business-Pdfs/Rates-Schedules/7.30-Et.Pdf. Accessed July 2019.

Goeke, D., and Schneider, M. (2015). Routing a Mixed Fleet of Electric and Conventional Vehicles. European Journal of Operational Research, 245(1), 81-99.

Göhlich, D., Kunith, A., and Ly, T. (2014). Technology Assessment of an Electric Urban Bus System for Berlin. WIT Trans. Built Environ, 138, 137-149.

Gong, J., and Wu, C. (2011). A Transit Fleet Replacement Model for Emissions Reduction. In Service Operations, Logistics, and Informatics (SOLI), 2011 IEEE International Conference, 22-25.

Gouge, B., Dowlatabadi, H., and Ries, F. J. (2013). Minimizing The Health and Climate Impacts of Emissions From Heavy-Duty Public Transportation Bus Fleets Through Operational Optimization. Environmental Science and Technology, 47(8), 3734-3742.

GTFS Website. https://Gtfs.Org. Accessed July 2019.

Guensler, R., Liu, H., Xu, Y., Akanser, A., Kim, D., Hunter, M. P., and Rodgers, M. O. (2017). Energy Consumption and Emissions Modeling of Individual Vehicles. Transportation Research Record, 2627(1), 93-102.

Guensler, R., Liu, H, Xu, X, Xu, Y., and Rodgers, M. (2016). MOVES-Matrix: Setup, Implementation, and Application. In 95th Annual Meeting of the Transportation Research Board. Washington, D.C.

Hao, X., Jin, W., and Wei, M. (2012). Max-Min Ant System for Bus Transit Multi-Depot Vehicle Scheduling Problem with Route Time Constraints. In Intelligent Control and Automation (WCICA), 2012 10th World Congress, 555-560.

Hartman, J. C. (1999). A General Procedure for Incorporating Asset Utilization Decisions into Replacement Analysis. The Engineering Economist, 44(3), 217-238.

Hartman, J. C. (2001). An Economic Replacement Model with Probabilistic Asset Utilization. Iie Transactions, 33(9), 717-727.

Hartman, J. C., and Tan, C. H. (2014). Equipment Replacement Analysis: A Literature Review and Directions for Future Research. The Engineering Economist, 59(2), 136-153.

He, X., Zhang, S., Ke, W., Zheng, Y., Zhou, B., Liang, X., and Wu, Y. (2018). Energy Consumption and Well-To-Wheels Air Pollutant Emissions of Battery Electric Buses under Complex Operating Conditions and Implications on Fleet Electrification. Journal of Cleaner Production, 171, 714-722.

Ho, S. H., Wong, Y. D., and Chang, V. W. C. (2014). Developing Singapore Driving Cycle for Passenger Cars to Estimate Fuel Consumption and Vehicular Emissions. Atmospheric Environment, 97, 353-362.

Hu, X., Murgovski, N., Johannesson, L., and Egardt, B. (2013). Energy Efficiency Analysis of A Series Plug-In Hybrid Electric Bus with Different Energy Management Strategies and Battery Sizes. Applied Energy, 111, 1001-1009.

Hung, W. T., Tong, H. Y., Lee, C. P., Ha, K., and Pao, L. Y. (2007). Development of a Practical Driving Cycle Construction Methodology: A Case Study in Hong Kong. Transportation Research Part D: Transport and Environment, 12(2), 115-128.

INSIA-UPM. (2010). Desarrollo De Una Metodología De Análisis Del Consumo Energético Y Las Emisiones Contaminantes Producidas Por El Transporte Público Urbano De Viajeros. Final Report. University Institute for Automobile Research (INSIA). Technical University of Madrid. Madrid, Spain (In Spanish).

J.B. Gallo, T. Bloch-Rubin, J. Tomić. (2014). Peak Demand Charges and Electric Transit Buses US DOT, Tech. Rep https://Calstart.Org/Wp-Content/Uploads/2018/10/Peak-Demand-Charges-And-Electric-Transit-Buses.Pdf. Accessed July 2019.

Jeong, S., Jang, Y. J., Kum, D., and Lee, M. S. (2018). Charging Automation for Electric Vehicles: Is a Smaller Battery Good for the Wireless Charging Electric Vehicles? IEEE Transactions on Automation Science and Engineering, (99), 1-12.

Jiménez, F., and Román, A. (2016). Urban Bus Fleet-To-Route Assignment for Pollutant Emissions Minimization. Transportation Research Part E: Logistics and Transportation Review, 85, 120-131.

Karabakal, N., Lohmann, J. R., and Bean, J. C. (1994). Parallel Replacement under Capital Rationing Constraints. Management Science, 40(3), 305-319.

Ke, B. R., Chung, C. Y., and Chen, Y. C. (2016). Minimizing The Costs of Constructing An All Plug-In Electric Bus Transportation System: A Case Study In Penghu. Applied Energy, 177, 649-660.

Keles, P., and Hartman, J. C. (2004). Case Study: Bus Fleet Replacement. The Engineering Economist, 49(3), 253-278.

Kliewer, N., Mellouli, T., and Suhl, L. (2006). A Time–Space Network Based Exact Optimization Model for Multi-Depot Bus Scheduling. European Journal of Operational Research, 175(3), 1616-1627.

Kunith, A., Mendelevitch, R., and Goehlich, D. (2017). Electrification of a City Bus Network—An Optimization Model for Cost-Effective Placing of Charging Infrastructure and Battery Sizing of Fast-Charging Electric Bus Systems. International Journal of Sustainable Transportation, 11(10), 707-720.

Lajunen, A. (2018). Lifecycle Costs and Charging Requirements of Electric Buses with Different Charging Methods. Journal of Cleaner Production, 172, 56-67.

Lajunen, A., and Tammi, K. (2016). Energy Consumption and Carbon Dioxide Emission Analysis for Electric City Buses. In Proceedings of the Electric Vehicle Symposium (EVS29), Montréal, QC, Canada (Pp. 19-22).

Li, L., Lo, H. K., Xiao, F., and Cen, X. (2018a). Mixed Bus Fleet Management Strategy for Minimizing Overall and Emissions External Costs. Transportation Research Part D: Transport and Environment, 60,104-118.

Li, H., Y. Wang, X. Xu, H. Liu, A. Guin, M.O. Rodgers, M. Hunter, J. Laval, K. Abdelghany, and R. Guensler (2018b). Assessing the Time, Monetary, and Energy Costs of Alternative Modes. 77th Annual Meeting of the Transportation Research Board. Washington, DC. January 2018.

Li, H., Liu, H., Xu, X., Xu, Y., Rodgers, M. O., and Guensler, R. L. (2016). Emissions Benefits from Reducing Local Transit Service Deadheading: An Atlanta Case Study. Transportation Research Board 95th Annual Meeting (No. 16-6385). Washington DC, United States.

Li, L., Lo, H. K., and Cen, X. (2015). Optimal Bus Fleet Management Strategy for Emissions Reduction. Transportation Research Part D: Transport and Environment, 41, 330-347.

Li, J. Q., and Head, K. L. (2009). Sustainability Provisions in the Bus-Scheduling Problem. Transportation Research Part D: Transport and Environment, 14(1), 50-60.

Liu, H., Guensler, R., Lu, H., Xu, Y., Xu, X., & Rodgers, M. O. (2019). MOVES-Matrix for High-Performance On-Road Energy and Running Emission Rate Modeling Applications. Journal of the Air & Waste Management Association, (Just-Accepted).

Liu, H., Li, H., Rodgers, M. O., and Guensler, R. (2018). Development of Road Grade Data Using The United States Geological Survey Digital Elevation Model. Transportation Research Part C: Emerging Technologies, 92, 243-257.

Lindgren, L. (2015). Full Electrification of Lund City Bus Traffic - A Simulation Study. Http://Lup.Lub.Lu.Se/Record/5470329

Lee, T. K., Adornato, B., and Filipi, Z. S. (2011). Synthesis of Real-World Driving Cycles and Their Use for Estimating PHEV Energy Consumption and Charging Opportunities: Case Study for Midwest/US. IEEE Transactions on Vehicular Technology, 60(9), 4153-4163.

Mahmoud, M., Garnett, R., Ferguson, M., and Kanaroglou, P. (2016). Electric Buses: A Review of Alternative Powertrains. Renewable and Sustainable Energy Reviews, 62, 673-684.

Markel, T., Brooker, A., Hendricks, T., Johnson, V., Kelly, K., Kramer, B., O'Keefe, M., Sprik, S., and Wipke, K. (2002). ADVISOR: A Systems Analysis Tool for Advanced Vehicle Modeling. Journal of Power Sources, 110(2), 255-266.

MARTA (2018). MARTA GTFS Data. https://Www.Itsmarta.Com/App-Developer-Resources.Aspx. Accessed November 2018.

MARTA (2019). MARTA Service Standards FY 2019. https://Www.Itsmarta.Com/Uploadedfiles/10.04.18_Servicestandardsfy19_Boardapproved.Pdf. Accessed July 2019.

Miller, A., H. Kim, J. Robinson, and M. Casale. (2018). Electric Buses Clean Transportation for Healthier Neighborhoods and Cleaner Air. https://Uspirg.Org/Sites/Pirg/Files/Reports/Electric%20Buses%20-%20National%20-%20May%202018%20web.Pdf. Accessed July 2019.

Mohamed, M., Ferguson, M., and Kanaroglou, P. (2018). What Hinders Adoption of The Electric Bus In Canadian Transit? Perspectives of Transit Providers. Transportation Research Part D: Transport and Environment, 64, 134-149.

NASEM, National Academies of Sciences, Engineering, and Medicine (2018). Battery Electric Buses—State of the Practice. Washington, D.C.: The National Academies Press. https://Doi.Org/10.17226/25061.

NTD, National Transit Database (2017). https://Www.Transit.Dot.Gov/Sites/Fta.Dot.Gov/Files/Docs/2017%20Glossary.Pdf. Accessed July 2019.

Ntziachristos, L., Gkatzoflias, D., Kouridis, C., and Samaras, Z. (2009). COPERT: A European Road Transport Emission Inventory Model. In Information Technologies in Environmental Engineering (Pp. 491-504). Springer, Berlin, Heidelberg.

Oakford, R. V., Lohmann, J. R., and Salazar, A. (1984). A Dynamic Replacement Economy Decision Model. IIE Transactions, 16(1), 65-72.

Ogle, J., Guensler, R., and Elango, V. (2005). Georgia's Commute Atlanta Value Pricing Program: Recruitment Methods and Travel Diary Response Rates. Transportation Research Record: Journal of the Transportation Research Board, (1931), 28-37.

Ostadi, A., and Kazerani, M. (2015). A Comparative Analysis of Optimal Sizing of Battery-Only, Ultracapacitor-Only, and Battery–Ultracapacitor Hybrid Energy Storage Systems for a City Bus. IEEE Transactions on Vehicular Technology, 64(10), 4449-4460.

Pagerit, S., Sharer, P., and Rousseau, A. (2006). Fuel Economy Sensitivity to Vehicle Mass for Advanced Vehicle Powertrains (No. 2006-01-0665). SAE Technical Paper.

Parthanadee, P., Buddhakulsomsiri, J., and Charnsethikul, P. (2012). A Study of Replacement Rules for A Parallel Fleet Replacement Problem Based On User

Preference Utilization Pattern and Alternative Fuel Considerations. Computers and Industrial Engineering, 63(1), 46-57.

Paul, T., and Yamada, H. (2014). Operation and Charging Scheduling of Electric Buses in a City Bus Route Network. In Intelligent Transportation Systems (ITSC), 2014 IEEE 17th International Conference. pp. 2780-2786. IEEE.

Pihlatie, M., Kukkonen, S., Halmeaho, T., Karvonen, V., and Nylund, N. O. (2014, December). Fully Electric City Buses-The Viable Option. In Electric Vehicle Conference (IEVC), 2014 IEEE International. pp. 1-8. IEEE.

Potkány, M., Hlatká, M., Debnár, M., and Hanzl, J. (2018). Comparison of the Lifecycle Cost Structure of Electric and Diesel Buses. NAŠE MORE: Znanstveno-Stručni Časopis Za More I Pomorstvo, 65(4 Special Issue), 270-275.

Qin, N., Gusrialdi, A., Brooker, R. P., and Ali, T. (2016). Numerical Analysis of Electric Bus Fast Charging Strategies for Demand Charge Reduction. Transportation Research Part A: Policy and Practice, 94, 386-396.

Rogge, M., Van Der Hurk, E., Larsen, A., and Sauer, D. U. (2018). Electric Bus Fleet Size and Mix Problem with Optimization of Charging Infrastructure. Applied Energy, 211, 282-295.

Rogge, M., Wollny, S., and Sauer, D. U. (2015). Fast Charging Battery Buses for the Electrification of Urban Public Transport—a Feasibility Study Focusing On Charging Infrastructure and Energy Storage Requirements. Energies, 8(5), 4587-4606.

Rothgang, S., Rogge, M., Becker, J., and Sauer, D. (2015). Battery Design for Successful Electrification in Public Transport. Energies, 8(7), 6715-6737.

Sebastiani, M. T., Lüders, R., and Fonseca, K. V. O. (2016). Evaluating Electric Bus Operation for a Real-World Brt Public Transportation Using Simulation Optimization. IEEE Transactions on Intelligent Transportation Systems, 17(10), 2777-2786.

Sharma, V., and Prakash, S. (1986). Optimizing Dead Mileage in Urban Bus Routes. Journal of Transportation Engineering, 112(1), 121-129.

Sinhuber, P., Rohlfs, W., and Sauer, D. U. (2010). Conceptional Considerations for Electrification of Public City Buses—Energy Storage System and Charging Stations. In Emobility-Electrical Power Train, 2010 (Pp. 1-5). IEEE.

Stasko, T. H., and Gao, H. O. (2010). Reducing Transit Fleet Emissions through Vehicle Retrofits, Replacements, and Usage Changes over Multiple Time Periods. Transportation Research Part D: Transport and Environment, 15(5), 254-262.

Stasko, T. H., and Gao, H. O. (2012). Developing Green Fleet Management Strategies: Repair/Retrofit/Replacement Decisions under Environmental Regulation. Transportation Research Part A: Policy and Practice, 46(8), 1216-1226.

Stevens, G., Wilson, A., Hammitt, J. K. (2005). A Benefit-Cost Analysis of Retrofitting Diesel Vehicles with Particulate Filters in the Mexico City Metropolitan Area. Risk Anal, 25(4), 883−899.

Suzuki, Y., and Pautsch, G. R. (2005). A Vehicle Replacement Policy for Motor Carriers in an Unsteady Economy. Transportation Research Part A: Policy and Practice, 39(5), 463-480.

Teoh, L. E., Khoo, H. L., Goh, S. Y., and Chong, L. M. (2018). Scenario-Based Electric Bus Operation: A Case Study of Putrajaya, Malaysia. International Journal of Transportation Science and Technology, 7(1), 10-25.

Tong, F., Hendrickson, C., Biehler, A., Jaramillo, P., and Seki, S. (2017). Life Cycle Ownership Cost and Environmental Externality of Alternative Fuel Options for Transit Buses. Transportation Research Part D: Transport and Environment, 57, 287-302.

USEPA, U.S. Environmental Protection Agency (2018). Greenhouse Gases Equivalencies Calculator - Calculations and References. https://Www.Epa.Gov/Energy/Greenhouse-Gases-Equivalencies-Calculator-Calculations-And-References. Accessed July 2019.

US EPA, U.S. Environmental Protection Agency. (2015). MOVES2014a. Available At: https://Www3.Epa.Gov/Otaq/Models/Moves/. Accessed July. 2019.

US PIRG Education Fund. (2018). Electric Buses Are Not Only Clean But Less Costly To Run. https://Www.Govtech.Com/Workforce/Electric-Buses-Are-Not-Only-Clean-But-Less-Costly-To-Run.Html. Accessed July 2019.

USGS, U.S. Geographical Survey (2016). Digital Elevation Models. Http://Nationalmap.Gov/Elevation.Html. Accessed July 2019.

Wang, H., and Shen, J. (2007). Heuristic Approaches for Solving Transit Vehicle Scheduling Problem with Route and Fueling Time Constraints. Applied Mathematics and Computation, 190(2), 1237-1249.

Wang, R., Wu, Y., Ke, W., Zhang, S., Zhou, B., and Hao, J. (2015). Can Propulsion and Fuel Diversity for The Bus Fleet Achieve The Win–Win Strategy of Energy Conservation and Environmental Protection? Applied Energy, 147, 92-103.

Wang, Y., Huang, Y., Xu, J., and Barclay, N. (2017). Optimal Recharging Scheduling for Urban Electric Buses: A Case Study in Davis. Transportation Research Part E: Logistics and Transportation Review, 100, 115-132.

Wei, M., Jin, W., Fu, W., and Hao, X. N. (2010). Improved Ant Colony Algorithm for Multi-Depot Bus Scheduling Problem with Route Time Constraints. In Intelligent Control and Automation (WCICA), 2010 8th World Congress. pp. 4050-4053. IEEE.

XGBoost Website. https://xgboost.readthedocs.io/en/latest/. Accessed July 2019.

Xu, Y., Li, H., Liu, H., Rodgers, M. O., and Guensler, R. (2017). Eco-Driving for Transit: An Effective Strategy to Conserve Fuel and Emissions. Applied Energy, 194, 784-797.

Xu, Y., Li, H., Liu, H., Rodgers, M.O., and Guensler, R. (2016). Eco-Driving for Transit. National Center for Sustainable Transportation. 2016.

Xu, Y., Gbologah, F. E., Lee, D. Y., Liu, H., Rodgers, M. O., and Guensler, R. (2015). Assessment of Alternative Fuel and Powertrain Transit Bus Options Using Real-World Operations Data: Life-Cycle Fuel and Emissions Modeling. Applied Energy, 154, 143-159.

Xu, Y., Lee, D. Y., Gbologah, F., Cernjul, G., Elango, V., Rodgers, M., and Guensler, R. (2013). Load-Based Life Cycle Greenhouse Gas Emissions Calculator for Transit Buses: An Atlanta, GA, Case Study. In Green Streets, Highways, and Development 2013: Advancing the Practice (Pp. 284-294).

Xylia, M., Leduc, S., Patrizio, P., Kraxner, F., and Silveira, S. (2017). Locating Charging Infrastructure for Electric Buses in Stockholm. Transportation Research Part C: Emerging Technologies, 78, 183-200.

Yoon, S., Rodgers, M. O., Pearson, J. R., and Guensler, R. (2004). Engine and Weight Characteristics of Heavy Heavy-Duty Diesel Vehicles and Improved On-Road Mobile Source Emissions Inventories: Engine Model Year and Horsepower and Vehicle Weight. Transportation Research Record, 1880(1), 99-107.

Yu, H., Tarsitano, D., Hu, X., and Cheli, F. (2016). Real Time Energy Management Strategy for a Fast Charging Electric Urban Bus Powered By Hybrid Energy Storage System. Energy, 112, 322-331.

Zegras, P. C. (2007). As If Kyoto Mattered: The Clean Development Mechanism and Transportation. Energy Policy, 35(10), 5136-5150.

Zhang, S., Wu, Y., Liu, H., Huang, R., Yang, L., Li, Z., Fu, L., and Hao, J. (2014). Real-World Fuel Consumption and CO2 Emissions of Urban Public Buses in Beijing. Applied Energy, 113, 1645-1655.

Zhou, B., Wu, Y., Zhou, B., Wang, R., Ke, W., Zhang, S., and Hao, J. (2016). Real-World Performance of Battery Electric Buses and Their Life-Cycle Benefits with Respect To Energy Consumption and Carbon Dioxide Emissions. Energy, 96, 603-613.

Zhu, C., and Chen, X. (2013). Optimizing Battery Electric Bus Transit Vehicle Scheduling with Battery Exchanging: Model and Case Study. Procedia-Social and Behavioral Sciences, 96, 2725-2736.